PB91-229229

EPRI
Electric Power
Research Institute

Proceedings: NSF/EPRI Workshop on Dynamic Soil Properties and Site Characterization
Volume 1

Proceedings: NSF/EPRI Workshop on Dynamic Soil Properties and Site Characterization
Volumes 1 and 2

Experts in geophysical sciences and earthquake engineering convened to evaluate state-of-the-art technology in geotechnical property characterization for earthquake-resistant design and analysis. Workshop areas discussed in this report will help focus and prioritize research on seismic hazard mitigation and seismic design improvement.

INTEREST CATEGORIES

EPRI R&D planning
Nuclear seismic risk,
  design, and qualification

KEYWORDS

Soils
Site characterization
Geotechnical engineering
Seismic effects

BACKGROUND   Earthquake experience shows that site geology and local soil properties exercise a decisive influence on seismic ground motions and structural damage potential. Progress has been made in measuring dynamic soil properties and understanding site characteristics. However, technologic limitations and resultant uncertainties have restricted the overall ability to confidently characterize a site for seismic design and analysis.

OBJECTIVES

• To discuss the current state of dynamic soil property measurement and site characterization for earthquake-resistant design and analysis.

• To explore ways to achieve necessary advances and identify research priorities.

APPROACH   Sixty-seven engineers, geologists, geophysicists, and seismologists from the United States and abroad participated in a two-day workshop November 9–10, 1989, in Palo Alto. State-of-the-art presentations focused on six previously selected technical topics, designed to help the National Science Foundation (NSF) and EPRI plan future research programs aimed at characterizing the dynamic material properties of sites for seismic design. Following these presentations, participants formed six panel groups to discuss the state of the art and to suggest research needs and priorities for each topic. The organizing committee met after the workshop to synthesize results and recommendations.

KEY POINTS   The workshop addressed six key technical topics, including low- and high-strain cyclic soil material properties, mechanisms for energy dissipation, spatial variability of soil properties, effect of site geometry and global characteristics, seismic arrays, and sloping ground sites. Experts determined that

• The highest priority research need industrywide is development and operation of field test sites for site soil characterization and method validation in seismically active areas.

• Other research needs exist in the following areas: technology enhancement of soil in situ and laboratory testing; investigation of physical-chemical processes affecting property changes; sensitivity evaluation of dynamic soil property variations; and improvements in data processing methods, field data interpretation techniques, and ground-response modeling procedures.

NOTICE

DISCLAIMER OF WARRANTIES AND LIMITATION OF LIABILITIES

Printed on Recycled Paper

ORDERING INFORMATION

Requests for copies of this report should be directed to Research Reports Center (RRC), Box 50490, Palo Alto, CA 94303, (415) 965-4081. There is no charge for reports requested by EPRI member utilities and affiliates, U.S. utility associations, U.S. government agencies (federal, state, and local), media, and foreign organizations with which EPRI has an information exchange agreement. On request, RRC will send a catalog of EPRI reports.

ABSTRACT

A 2-day workshop on dynamic soil properties and site characterization was held in Palo Alto, California, on November 9-10, 1989. The workshop was cosponsored by the National Science Foundation (NSF) and the Electric Power Research Institute (EPRI) under NSF Grant No. BCS-8916081 and EPRI RP810.

The primary purpose of the workshop was to bring together individuals with expertise in the areas of dynamic soil property measurement and site characterization to discuss the current state-of-the-art, to explore ways to achieve advances that are needed, and to identify research priorities. Participants included specialists in the fields of geotechnical and earthquake engineering as well as geologic, geophysicist and seismological sciences.

The workshop involved six state-of-the-art presentations dealing with dynamic soil properties and site characterization. Following the state-of-the-art presentations, the participants met in panel groups to discuss research needs for each of the research topics. Each panel prepared a report summarizing their views.

These proceedings contain the text of the state-of-the-art presentations as well as the panel reports.

FOREWORD

This report is the final product of a workshop on "Dynamic Soil Properties and Site Characterization," held in Palo Alto, California, November 9-10, 1989. The workshop was sponsored jointly by the National Science Foundation (NSF) and the Electric Power Research Institute (EPRI).

The need for a workshop on dynamic soil properties and site characterization was identified in late 1988 by NSF and EPRI during discussions about the state of the art in the areas of dynamic soil property measurement and site characterization. Both organizations identified technical limitations, and both organizations sought more effective ways to use their available funding to advance research in these areas. In view of the potential consequences of earthquakes in terms of loss of life and property damage, a review of geotechnical site characterization procedures seemed appropriate. This conclusion was strongly reinforced by the soil-related destruction from the Loma Prieta earthquake, which occurred just two weeks before the workshop.

The format for the workshop involved state-of-the-art presentations on six topics:

- Obtaining low- and high-strain cyclic material properties

- Mechanisms for energy dissipation and how they are dealt with

- Accounting for spatial variability

- Determining when site geometry and global characteristics are important

- Knowledge gained from arrays

- Treatment of sloping ground sites

The presentations were followed by concurrent panel discussions on each of the topics. Nearly 70 specialists from the United States and abroad with expertise in the fields of engineering and earth sciences attended the workshop. An attendee list is provided in Appendix A.

A proceedings containing the state-of-the-art presentations as well as panel reports for each of the six areas was prepared from the workshop. The organizing committee for the workshop was responsible for preparation of chapters 1 and 2, introduction and summary of research needs. Chapters 3 through 8 present the state-of-the-art reports and panel summaries for the specialized topics assigned to each workshop session.

Preceding page blank

v

Organizing Committee

Donald G. Anderson, Chairman
Y. K. Tang, Co-chair
Clifford Astill
John Christian
Ricardo Dobry
Jose Roesset
J. Carl Stepp
Kenneth Stokoe

ACKNOWLEDGMENTS

CONTENTS

Note: Appendices C, D and E are included in Volume 2 of this report

Preceding page blank

Damage During the Loma Prieta Earthquake

Damage During the Loma Prieta Earthquake

Chapter 1   INTRODUCTION

Chapter 1
INTRODUCTION

Ground shaking during earthquakes results from seismic waves that originate along a fault at some depth, and then travel upward and outward to the ground surface. The characteristics of the rupture, of the travel path, and of the near-surface geology units all influence the damage potential of shaking. Many earthquakes have shown in the past and Mexico City (1985), Armenia (1988), and Loma Prieta (1989) recently reminded us that the near-surface soil and/or rock can have a decisive influence on shaking and damage distribution for a given earthquake. Instrumental records on soft soil sites from some of these and other events show that the motions at certain frequencies can be amplified by an order of magnitude compared to rock sites nearby. Significant increases in duration of shaking have also been observed on soil. Widespread destruction and disruption can occur due to seismically induced ground failure.

PROPERTY MEASUREMENT AND SITE CHARACTERIZATION

The mechanisms for seismic wave propagation and the response of soil and buildings to wave propagation have been investigated for many years. Various methods of analysis and testing techniques are now available for estimating the level of ground shaking and the response of soil and soil-structure systems during forecasted earthquakes. The accuracy of those seismic response estimates is, however, controlled to a large extent by our ability to properly characterize the dynamic properties of the geologic materials at the site. Although some of these properties can be determined with relatively high levels of confidence, others cannot and further research is clearly needed.

CONSTITUTIVE MODEL REQUIREMENTS

For the purpose of analyzing ground response under seismic loading, the soil and/or rock ideally should be represented by constitutive equations that describe their behavior under all loading conditions and strains in a manner that very closely represents the real materials of rock, sand, silt, or clay under these conditions. Such a model would include a number of material constants determinable by laboratory or field tests. Some of the constants would indicate the nature of the material and its initial condition in the field; others would be its response to static and cyclic or dynamic loads. A particular cycle of stress or strain in such a mathematical model would give essentially the correct amount of energy dissipation or damping, the variation of response with strain level, and the strain accumulation, without special and separate formulation being required to describe such behavior. The model would be sufficiently complex so that boundary value problems involving the material would require calculation by computer. In the case of interest, the computer would require the capability of handling large strains, displacements, and non-Cauchy stresses. At present, we are far from developing such a system, but work is proceeding in that direction.

The penalties for a complex constitutive relation based on the physics and mechanics of the material behavior are the mathematical difficulties of the formulation, the effort and care needed in its implementation in a computer program, and the need to obtain experimentally a large number of parameters to fit the model. The advantages are that one relationship would cover a range of material behavior and that the material response to large strains or cyclic-load applications would follow naturally from the basic premises of the model.

Current practice involves simpler models of material behavior, generally based on empirical observations. For these models, certain types of laboratory or field tests are required from which the material properties are derived. Various simplifications are needed to represent the complicated behavior of the real soil. When a simple (the term is relative, since all the models under discussion have various degrees of complexity) model is employed, it has the advantage of being conceptually easier to grasp, and the operations of the representation under cyclic or dynamic excitation can be divided into physical steps corresponding to the perceived mechanical behavior of the medium. The penalties lie in the necessity for performing a large number of tests to determine the variables that are not implicit to the model. For example, one such approach may require a generalized bilinear or hyperbolic stress-strain behavior for the soil under study. The properties of slope (modulus) or peak value of this relationship are related to the ambient or changing effective stress in the field at different confining pressures. The relation of such a modulus to different strain levels has to be examined by dynamic tests which are typically applicable to different strain regimes. Damping may be included implicitly in such representation, but more commonly it is added as an explicit external variable which is determined by cyclic testing to different strain levels. Pore pressures which may be developed have to be evaluated with reference to cyclic laboratory tests on the soil at different void ratios, confining pressures, and other variables. Each representation bears its own burden.

In the absence of the "perfect" constitutive relationship, the consequence for site evaluation using simpler models is that the material properties to be measured in the field and laboratory depend on the model to be employed, and differ to some extent. Thus, in the text that follows, each recommendation related to dynamic soil property measurement and site characterization implies, at some level, a preconceived model for the representation of the anticipated ground response during the seismic event. If in fact, the possibilities of both large deformation and failure must be considered, more than one material or mechanical model is usually needed, and different tests and property evaluations must be performed for each mechanism.

MEASUREMENT UNCERTAINTIES

Despite many advances and developments that have occurred over the past decade in the areas of analysis and testing, helped by the rapid accumulation in recent years of instrumental recordings from strong motion networks and special arrays, significant uncertainties still exist in the general areas of dynamic soil property measurement and

site characterization. As discussed in the preceding section, these uncertainties are controlled in part by the need to account for the many interdependent variables in the determination of material properties for simpler soil models. This has led to the general view that the overall ability of the profession to confidently characterize a site or general area for seismic response analyses and design needs to be improved in order to achieve a satisfactory measure of earthquake hazards mitigation. In the absence of this confidence, current practice is to apply large ranges in material properties to account for measurement uncertainties. Eventually, this leads to excessive conservatism and unnecessary costs.

Improvement in measurement methods by itself will not necessarily result in a higher level of confidence in dynamic soil property measurement and site characterization. Improvements must go hand-in-hand with the development of new, more generalized constitutive models of the material response which can be used to explicitly interpret laboratory or field test results, or which can be used with laboratory or field test data to explicitly account for the physics and mechanics of soil property response.

NSF AND EPRI CONCERNS

During initial discussions between the National Science Foundation (NSF) and the Electric Power Research Institute (EPRI) in late 1988, it was realized that both organizations share similar concerns regarding the state of the art and its limitation in the areas of dynamic soil property measurement and site characterization for earthquake resistant design and analysis.

NSF's Earthquake Hazard Mitigation Program receives unsolicited proposals each year to conduct specific studies related to dynamic soil property measurement and site characterization. A number of important developments in the understanding or measurement of dynamic soil properties and site characteristics have been made over the past decade as a result of this program. However, NSF is seeking a more effective way to utilize the available funding to achieve a more focused research program toward earthquake hazard mitigation. Identification and prioritization of future research are needed.

EPRI has been sponsoring research related to seismic soil-structure interaction (SSI) for the last 10 years. In a recent investigation, the response of a site and two structures at Lotung, Taiwan, were monitored in detail during seismic events, and analytical predictions were compared with the recorded response. One of EPRI's purposes in the Lotung experiment has been to quantify uncertainties and reduce unnecessary conservatism in the seismic analysis and design of critical structures. However, results from the Lotung experiment show that characterization of strain-dependent soil properties is a weak link in the study. Data scatter and technology limitations have resulted in significant uncertainties, and further research is needed to reduce those uncertainties.

In viewing the potential consequences of earthquakes in terms of loss of life and property damage, it was concluded that a review of the state of the art in the areas of dynamic soil property measurement and site characterization was needed. This conclusion was strongly reinforced by the soil-related destruction from the Loma Prieta earthquake, which occurred just 2 weeks before the workshop was held.

STATEMENT OF NEED

As a means of satisfying the existing need to advance the state of the art and to identify and prioritize research requirements in the areas of dynamic soil property measurement and site characterization, a workshop was proposed jointly by NSF and EPRI in early 1989. Such a workshop seemed justified by a combination of needs:

- Continued progress in the area of analytical modeling, which places more rigorous needs for dynamic soil properties

- Continued development of networks and special arrays to collect information regarding soil response during earthquakes, with the corresponding need for more rigorous measurement of dynamic soil properties

- Continued progress in specific aspects of dynamic soil property measurement and site characterization

- Continued need for information about dynamic properties of soil and site characterization during the seismic analysis and design of critical structures, such as dams and nuclear power facilities

- Continued need to optimize the limited funds that can be directed towards research by either government agencies or private industry

To advance beyond the current approach to dynamic property measurements and site characterization, as well as to link this with the more general question of seismic soil response, it was concluded that some key questions which need to be addressed at this time are:

- How to obtain stress-strain relations *in situ* that are applicable to the characterization and prediction of ground response during seismic events?

- How to characterize, measure, and model analytically the effective damping of a site during an earthquake, including its material and radiation damping components?

- How to account for the spatial variability in dynamic properties for a given site?

1-4

- How to introduce site geometry and global characteristics in ground response estimates, including where one-dimensional site characterization is insufficient?

- How to link improvements in dynamic soil property and site characterization to optimum use of seismic networks and special arrays, including what has been learned from existing seismic networks and special arrays, and what should be our future strategy.

- How to characterize and evaluate sloping ground sites during earthquakes?

WORKSHOP OBJECTIVES

The objective of this workshop was to bring together individuals with knowledge and expertise in the field of geotechnical engineering and soil dynamics, as well as geological, geophysical, and seismological sciences, in order to discuss the current state of the art in the areas of dynamic soil property measurement and site characterization, to explore ways to achieve advances that are needed, and to identify research priorities, both immediate as well as over the next 10 to 20 years.

WORKSHOP PLANNING

The planning for this workshop began in late 1988. An organizing committee comprised of the following individuals was formed to plan the workshop:

- Donald G. Anderson of CH2M HILL as chairman

- Y. K. Tang of EPRI as co-chair

- Jose M. Roesset and Kenneth H. Stokoe of the University of Texas at Austin

- John Christian of Stone & Webster

- Ricardo Dobry of Rensselaer Polytechnic Institute

- Clifford J. Astill of NSF

- J. Carl Stepp of EPRI

The organizing committee decided that the format for the workshop would involve a series of state-of-the-art presentations during the first half day of the workshop. These

presentations would be followed by concurrent panel workshop discussions on six state-of-the-art topics. To maximize the interchange of information between panels, several plenary sessions also were scheduled during which panel leaders and recorders would give summaries of discussions that had taken place during their panel discussions. A copy of the agenda for the workshop is given in Appendix B.

Six state-of-the-art topics were identified. These topics, as well as the respective speakers for each topic, are listed below:

- "How Do We Obtain Low- and High-Strain Cyclic Material Properties?" State-of-the-art speaker: Professor Ricardo Dobry, Rensselaer Polytechnic Institute

- "What Are the Mechanisms for Energy Dissipation and How Are They Dealt With?" State-of-the-art speaker: Professor Jose Roesset, University of Texas

- "How Do We Account for Spatial Variability in Properties?" State-of-the-art speaker: Dr. Gary Olhoeft, United States Geological Survey

- "When Are Site Geometry and Global Characteristics Important?" State-of-the-art speaker: Dr. Walter Silva, Pacific Engineering and Analysis

- "What Have We Learned From Arrays?" State-of-the-art speaker: Dr. Brian Tucker, California Division of Mines and Geology

- "What Do We Do at Sloping Ground Sites?" State-of-the-art speaker: Dr. Gonzalo Castro, GEI Consultants

Approximately 75 individuals were invited to the workshop. These individuals represented a variety of backgrounds in the general areas of dynamic material property measurement and site characterization, including specialists in geology, seismology, geophysics, earthquake engineering, soil dynamics, and seismic field monitoring. Over 90 percent of the original invitees were able to accept the invitation. A list of participants is provided in Appendix A.

Each speaker was requested to prepare a state-of-the-art paper. Draft copies of five of the six were distributed to participants prior to the workshop. Workshop participants were requested to prepare a 2- to 3-page summary of views regarding research needs. These summaries were submitted to the state-of-the-art speakers prior to the workshop. The intent of the summaries was twofold: (1) to initiate thinking on the part of the attendee prior to arrival at the workshop and (2) to provide the state-of-the-art speakers with some indication of the different views of the workshop participants.

WORKSHOP PRODUCT

As part of the closing activities of the workshop, each workshop panel submitted a draft of its report. These summary reports, combined with the state-of-the-art reports, are presented as Chapters 3 through 8 in this document. The organizing committee was responsible for preparation of Chapters 1 and 2, INTRODUCTION and SUMMARY OF RESEARCH NEEDS.

A draft copy of the complete workshop report was sent to each workshop participant to obtain review comments on the report. To the extent possible, the review comments that were received have been included in the final report. Whereas comments have been solicited from a number of individuals, the document is by no means an accurate reflection of everyone's view on the needs for research and development in the areas of dynamic soil property measurement and site characterization. The workshop document should, therefore, be used as a guide towards the identification of possible research topics.

Ground Movement During the Loma Prieta Earthquake

Ground Movement During the Loma Prieta Earthquake

Chapter 2 SUMMARY OF RESEARCH NEEDS

Chapter 2
SUMMARY OF RESEARCH NEEDS

The preliminary product of the NSF/EPRI workshop was a series of draft panel reports prepared during the workshop to summarize each panel's views on the state of the art and the need for research in the areas of dynamic soil property measurement and site characterization. Following the workshop, the organizing committee reviewed these draft reports and grouped research needs in five areas of common concern or interest; i.e., panels addressed the same or similar research interests and needs, with details differing from one panel to the next. The five areas of common interest or concern involved:

- Development and operation of field test sites in seismically active areas

- Technology developments in the areas of in situ testing, laboratory testing, and ground response monitoring

- Fundamental studies of physical-chemical processes

- Sensitivity studies to evaluate the importance of dynamic soil property variation

- Analytical studies to develop improved data processing methods, laboratory and field data interpretation techniques, and ground-response modeling procedures

The first topic "Development and Operation of Test Sites" was identified by the organizing committee as being especially important and relevant to the objectives of the workshop. This topic has been given highest priority and is discussed in somewhat more detail. Following the discussion of test sites, a summary of research needs and interests in the other four areas is given. No priorities are assigned to these topics. This chapter concludes with a section that summarizes the need for additional research, for additional research funding, and for better communications.

DEVELOPMENT AND OPERATION OF TEST SITES

The topic "Development and Operation of Test Sites" was identified by the organizing committee as being of special importance and requiring a more detailed discussion. It was selected for more detailed discussion because:

- The topic was identified by all panels as one that will contribute to significant advances in the state of the practice in the areas of site characterization and soil property measurement.

- Information obtained from the development and operation of test sites will be of use to multiple disciplines, including geologists, geophysicists, seismologists, and engineers.

- The program will complement efforts already underway to identify sites for geotechnical experimentation (NSF, 1988).

- Finally, development and operation of test sites would likely require industry-wide support.

The last reason cited above is thought to be critical. Development and operation of tests sites will require significant planning, capital investment, and annual maintenance costs. It is unlikely that any single private organization or government agency presently has either the budget or staff to successfully operate the proposed test sites without significant contributions from other organizations. Consequently, development and operation of the test sites is expected to require an industry-wide cooperative effort.

PROGRAM DESCRIPTION

This industry-wide program would involve development and operation of two or more facilities, referred to as test sites, in seismically active areas. The objective of each site would be to provide a location where experiments related to site characterization and dynamic soil property measurement could be carried out over an extended period of time under the same general set of site conditions. The test sites would be characterized by certain geologic or topographic features; they would be thoroughly documented in terms of site characteristics; and they would be equipped with instruments on the ground surface and at depth that would allow measurements of ground motion, pore water pressure, etc., during seismic events.

A minimum of two sites is required to satisfy the need for experimentation and *in situ* simulation under different geologic and topographic conditions. These sites would have the following features:

- Geologic conditions at a particular site would be relatively consistent within a large area so that multiple experiments could be conducted by different investigators under similar geologic conditions.

- The sites would be located relatively close to a source of strong ground shaking so that high-amplitude, ground response information could be obtained in the same area where site characterization took place. This would allow results of experimental studies to be used in combination with measured ground response to test new methods of interpretation or analysis.

• The level of seismic activity should be high so that the seismic response information had a high probability of being collected over a several-year period. However, from a pragmatic standpoint, the possibility exists that the sites would have to be maintained over a longer time period before high-amplitude, seismic response data are obtained.

PROGRAM OBJECTIVES AND BENEFITS

The test site program would have two objectives. The primary objective would be to provide locations where different dynamic soil property measurement and site characterization procedures could be used or tested. The secondary objective would be to collect ground response information during seismic events.

Both objectives satisfy the basic need to improve the current levels of confidence in dynamic soil property measurement and site characterization procedures. As field and laboratory methods of dynamic soil property measurement and site characterization are compared and improved, the large level of uncertainty currently associated with the use of dynamic soil properties in design can be reduced, resulting in more economical designs.

PROGRAM PLANNING

Where practically feasible, the sites should have the following common features or goals:

• They should be tied in with new or existing strong motion seismic arrays to optimize planning, management, and maintenance.

• The sites should be located on loose, saturated, granular soil and soft clay to obtain data for a range of geologic conditions.

• The geometry should be well defined, and the test site area should be large enough to allow numerous experiments to be carried out.

• Soil sites should include sloping ground and have nearby rock outcrops.

• If possible, information on site characterization should be already available.

• The sites either should be available for non-earthquake-related studies or may be part of other projects involving earthquake or non-earthquake activities.

2-3

PROGRAM IMPLEMENTATION

The initial phase of the recommended program will likely require an expenditure of one-half million dollars or more per site. These costs are required to set up an organization for the coordination of the effort, to oversee initial site selection and exploration tasks, and to install a minimum set of ground response recording systems. The annual costs for maintaining a basic test site is expected to be in excess of $100,000. For planning purposes, the program should be funded to operate for a minimum of 5 years.

Because of the long-term use of the test sites, it will be necessary to select a single organization or agency to operate the test sites. The responsibilities of the organization or agency should be to control the type of, and documentation for, experiments carried out at the sites, to maintain the ground response instrumentation in an operational mode, and to process and distribute the data that are collected.

Coordination of such an effort could be most effectively handled by a public agency, such as the United States Geological Survey (USGS), the National Center for Earthquake Engineering Research (NCEER), or the California Division of Mines and Geology (CDMG). Other organizations, including universities and private companies, should have access to the site, as long as they have funding to carry out their work and as long as they have a well-defined work plan describing their objectives and scope of work.

TECHNOLOGY DEVELOPMENTS

Existing methods of *in situ* testing, laboratory testing, and ground response monitoring do not appear to be taking full advantage of data collection and processing capabilities that have become available over the last decade. Technology development in one or more of these areas should be carried out either to improve the accuracy of existing measurement techniques or to collect new information regarding soil behavior and soil property variation. As the accuracy is improved or better information is obtained, the large uncertainties often associated with soil property measurement and site characterization can be reduced. Especially important is the development of a technique(s) for measuring the soil strains and deformations during seismic loading.

In the area of *in situ* testing, the following technology developments are recommended:

- Nondestructive, nonintrusive (geophysical, electrical, seismic, radar, etc.) procedures for delineating subsurface stratigraphy in a rapid and accurate manner

- Nonlinear cyclic deformation and degradation characterization (stress-strain, volumetric change)

- Material damping and its variation with level of shearing strain

- *In situ* density variation and/or *in situ* measurement of steady state strength (S_{us}) in saturated, loose sand

- Standardization of *in situ* testing methods

In the area of laboratory testing, the following technology developments are recommended:

- Simple and inexpensive G_{max} test methods that can be used with (or during) other testing techniques (static and cyclic) to measure stiffness variation of material throughout the test, thereby providing a standard basis for comparing or extrapolating results during a test, between tests, and between the tests and the field

- Automated strain/stress path testing systems (biaxial)

- Procedures for reducing and/or correcting for sample and specimen disturbance

- Procedures for obtaining and testing representative samples of gravels

- Improved procedures for determining S_{us} and factors affecting S_{us}

- More accurate and consistent measurement of material damping at both low and high strain, as well as determining the effects of confining pressure (depth)

In the area of ground response monitoring during earthquakes, the following areas of technology development are suggested:

- Cyclic and permanent strain and deformation measurements

- Systems to monitor cyclic stress-strain response

- Six-component accelerometers

- Continuous monitoring of G_{max} during seismic events

- Pore pressure devices

- User friendly means to store, document and retrieve strong motion data

2-5

STUDIES OF PHYSICAL-CHEMICAL PROCESSES

A better fundamental understanding of physical-chemical processes affecting soil properties and their variation in time and space is needed. The intent of these studies should be to establish a more rational basis for including effects of geologic history such as aging, cementation, stress changes, and earthquake loading. A better understanding of physical-chemical processes may also serve as a basis for relating soil properties determined by indirect methods (for example, electrical and magnetic) with dynamic soil properties such as shear modulus and material damping.

Specific examples of research in these areas might involve

- Laboratory tests and associated micro-mechanical studies to investigate the basic particle-to-particle and chemical mechanisms controlling or influencing stress-strain behavior of soil, including methods for quantifying these effects through indirect chemical, electrical, or mechanical measurements

- Studies to determine the particle-to-particle and pore-fluid mechanisms that control material damping. This effort should assist in identifying appropriate laboratory and/or field procedures for determining damping

- Studies to quantify the effects of loading rate, temperature, and pore-fluid characteristics on stress-strain behavior of soil

- Procedures for estimating the change in seismic response of ground caused by changes in the physical-chemical consistency

- Methods for relating results of indirect field measurements, such as ground penetrating radar surveys, to the engineering properties of the soil

SENSITIVITY STUDIES

There seems to be a common concern that the practical significance of soil-property variation is not fully appreciated. This suggests that some details associated with dynamic soil property measurement and site characterization are likely being exaggerated in analytical studies, while other more critical details may be overlooked. Results of these sensitivity studies are needed to provide a basis for assigning research priorities in areas such as development of new testing methods or new studies of physical-chemical processes.

Their use should be encouraged especially:

- During the design of field exploration programs and field instrumentation for arrays

- To determine how accurate certain measurements must be for a particular application, as related to the type of site and type of structure

- To evaluate importance of 2- and 3-dimensional basin effects at short periods (<2 to 3 seconds) and at high levels of motion

ANALYTICAL STUDIES

Whereas significant advances have been made over the past decade in the area of analytical modeling, additional focused research needs still exist. This research should involve new data handling methods, improved modeling methods, and calibration and validation studies.

Some of the needs in the area of data handling include:

- Processing presentation involving 3-D color images

- Procedures for using and linking extremely large data sets

- Incorporation of probabilistic procedures (fuzzy sets, fractal chaos theory, etc.)

In the area of analytical modeling, a need exists for:

- Improved 1-, 2-, and 3-dimensional modeling, including consideration of limitations and sensitivity

- Improved nonlinear dynamic analysis techniques, including better treatment of material damping

- Numerical codes for addressing the effects of topography and the lateral changes in material properties, including damping and high strains

A critical consideration in the development or refinement of analytical models will be the need to calibrate or validate models using physical measurements made in the laboratory or field. Information collected at the proposed test sites offers one source of calibration data. Other information can be obtained through research programs involving instrumentation and response monitoring of soil or soil-structure systems in:

- Small-scale experiments, such as laboratory test devices, shaking table tests, foam-rubber models, and centrifuges

- Full-scale experiments involving the instrumentation of various rigid and flexible retaining walls, buildings (particularly embedded and pile-supported), pipelines and other buried structures, and embankments comprised of soil, rock, and solid waste materials

A key element of this latter requirement is the need for well-controlled blind predictions, where the response of the full-scale structure is monitored with a complete instrumentation array (accelerometers, pressure cells, and displacement transducers), and the predictions are made without prior knowledge of response (i.e., Class A or blind prediction).

REQUIREMENTS FOR FUTURE RESEARCH

Past expenditures for research in the areas of dynamic soil property measurement and site characterization have contributed to a better understanding of the interaction between soil and structures during seismic events. This better understanding has led to better design methods, which have reduced the risk to individuals living and working in seismically active areas. However, despite the profession's better understanding and better design methods, the consequences of earthquakes can still be devastating, as evidenced by the Loma Prieta earthquake in 1989.

NEED FOR ADDITIONAL RESEARCH

Earthquakes of sizes similar to or larger than the Loma Prieta earthquake occur throughout the world annually. Within the United States, they must be expected about every 10 years. Although many of these earthquakes will be located in remote areas, some will occur near population centers. Without changes in current design methods and land-use policies, the consequences of these earthquakes will likely be similar to or greater than those experienced during the Loma Prieta earthquake. Within the United States, the emotional damage and economic losses from events such as the Loma Prieta earthquake are considered to be unacceptable. This, by itself, suggests that additional research is needed in the area of earthquake engineering.

Several factors suggest that improved understanding and even better design methods, particularly in the areas of dynamic soil property measurement and site characterization, will be needed in the future. With growth, land will be developed in areas where there is a higher potential for large, earthquake-induced ground shaking. Growth will also likely occur in areas where soil is more susceptible to large displacements or even failure. Structures that are built on the ground will also become more complicated, thus requiring more detailed modeling of the soil-structure system to estimate response during seismic events. Given these conditions, it seems obvious that advances in the

state of the practice will be necessary to maintain even the current level of safety to individuals living or working in these areas.

The need for additional research is also related to the economics of design. In view of the various uncertainties that exist in the areas of dynamic soil property measurement and site characterization, a conservative approach is normally taken when selecting soil properties for seismic response studies. This generally leads to significant and perhaps excessive conservatism in the design, not only for structures constructed of soil but also within buildings, bridges, and other facilities constructed on or in the soil. Whereas conservatism may result in safety to those living and working in the facility, it also results in higher construction costs. At a certain point the economic viability of development becomes an issue.

NEED FOR ADDITIONAL FUNDING

The potential losses from earthquakes are staggering. The Loma Prieta earthquake, although somewhat removed from dense population, is reported to have resulted in close to $10 billion in losses. The damage at Stanford University alone exceeded by a factor of two the annual funding in the United States for earthquake research. If only a fraction of these losses could be reduced by research and development in the area of earthquake engineering, the investment would result in more than adequate payback.

The National Science Foundation (NSF) is the primary source of earthquake engineering research funding within the United States. As shown in Figure 2-1, NSF's funding has decreased steadily since 1978 so that it is now approximately 60 percent of its previous levels. Of NSF's current annual budget for earthquake hazards mitigation program (estimated to be on the order of $15 million per year), one third is currently assigned to the National Center for Earthquake Engineering Research (NCEER). The remaining annual budget can provide only minimal support within the various disciplines performing earthquake engineering research studies. In particular, the existing level of support appears to be insufficient to develop and maintain the two or more test sites recommended by the workshop. Such a commitment could only be made today at the expense of research in other areas unless the total level of support is increased.

Alternative sources of funding include government agencies other than NSF. A modest amount of research funding is available from federal, state, and local government agencies such as the United States Geological Survey, the United States Nuclear Regulatory Commission, and the California Division of Mines and Geology. With the general budget cutbacks over the past decade, these sources of research funding have also decreased. In some cases the government support is also being used internally. This suggests that the opportunity to achieve the goals listed above through this source of research support is currently limited.

Another source of research support is through private organizations such as large oil companies, construction firms, and non-profit research organizations. This source of

2-9

NEHRP Funding for Earthquake Science (constant FY90 dollars)

Figure 2-1. NEHRP Funding for Earthquake Science (AGU, 1990)

funding is relatively small and typically very task-oriented in the United States. In other countries such as Japan, a more active role in providing research support is taken by private organizations. However, until the benefits of investing in research are improved in the United States, little opportunity appears to be available to meet research goals through this funding source.

Given the current status of government and private research support, it seems apparent that additional funding provided by the existing sources and/or by new sources is necessary if earthquake design methods are to keep pace with the economic development of the United States. The economic losses that have occurred in past earthquakes and the losses that can be reasonably avoided in the future appear to provide justification for this additional funding needed.

NEED FOR BETTER COMMUNICATION

Whereas a need for additional research and a need for additional financial support in the areas of dynamic soil property measurement and site characterization appear to be justified, a need also exists for improved communication to maximize the benefit that is derived from future research. Improved communication is needed both within the scientific community and between the scientific community and public policy makers.

Improved communication within the scientific community is needed to promote education and technology transfer among engineers, geologists, geophysicists, and seismologists. Basic principles understood by one discipline are too often being neglected or misinterpreted by other disciplines. Training is also required to achieve more standardization in methods of testing and analysis. One of the methods for achieving this education and technology transfer is to support research programs which, by their nature, foster collaboration among different disciplines and different technical specialties within a discipline.

The engineering and scientific communities also need to do a better job of communicating technical issues and conclusions to groups preparing building codes and to those public officials who are responsible for zoning and implementation of seismic design procedures. Unless research results are actually used to improve codes that form the basis for practice, their benefits are not realized. Furthermore, unless the public is adequately educated about both the level of understanding and the risks of seismic design, the benefits of new developments in the state of the practice will also be limited.

Often there seems to be a lack of understanding and confidence between engineers and scientists who estimate the risk or response to seismic loading on the one hand, and public officials (politicians, city engineers, and zoning officials) who make decisions regarding where the public can live and work on the other. This lack of understanding and confidence seems to result for at least two reasons: (1) the economic consequences of the recommendation either from the standpoint of not being able to

develop land or the cost to construct completely safe facilities, and (2) the number of uncertainties cited by engineers and scientists when dealing with seismic design methods. The consequence of this lack of understanding and confidence is often un-willingness on the part of politicians, city engineers, and zoning officials to implement recommendations regarding appropriate zoning or design methods. The apparent solution to this problem is to reduce the uncertainty in current approaches to seismic response analyses and then to demonstrate to public officials that response predictions can and should be used to implement cost-effective, risk reduction.

REFERENCES

NSF. "Designated Sites for Geotechnical Experimentation in the United States." Proceedings of the Workshop at the University of New Hampshire, Jean Benoit and Pedro do Alba, eds., September 1988, 165 pages.

EOS Transactions, American Geophysical Union, Vol. 71, No. 14, April 1990, 369 pages.

State-of-the-Art Speaker — Professor Ricardo Dobry

Workshop Panel

Chapter 3   LOW- AND HIGH-STRAIN
CYCLIC MATERIAL PROPERTIES

Chapter 3
LOW- AND HIGH-STRAIN CYCLIC MATERIAL PROPERTIES[1]

Dynamic soil property and site characterization is normally assumed to mean determination of low- and high-strain cyclic properties of soil. This chapter presents a summary of procedures currently used *in situ* and in the laboratory for these determinations. The chapter also presents a summary of relevant observed cyclic properties of soil, and it provides recommendations for improvement and further research. The original state-of-the-art (SOA) report on this topic--previously distributed to the participants and presented at the opening session of the workshop--was prepared and presented by Dr. Ricardo Dobry, Professor of Civil Engineering at Rensselaer Polytechnic Institute. During the workshop, a panel of individuals with background and expertise in the area of low- and high-strain cyclic material property determination met and discussed the state of the art and then, as a group, modified the original SOA report prepared by Dr. Dobry. They included Ricardo Dobry (panel leader), Shobha K. Bhatia (panel recorder), C. H. Cramer, Robert Henke, Cornelius Higgins, Michele Jamiolkowski, Hon-Yim Ko, Richard S. Ladd, Shamsher Prakash, Anthony Saada, and Phillip C. Sirles. Other contributors to the document included C. Y. Chang, G. Wayne Clough, Keneth H. Stokoe II, Mladen Vucetic, and Jackson C. S. Yang. Ricardo Dobry coordinated the revisions and served as final editor to the document presented in this chapter.

SOA/PANEL REPORT

INTRODUCTION

There are several earthquake resistant design and analysis problems that require dynamic/cyclic soil properties and site characterization, including:

- Local site response and seismic wave propagation
- Liquefaction and densification of level or almost level sites
- Soil-structure interaction
- Geotechnical structure response (earth structures and engineered slopes)
- Slope stability
- Site improvement

---

[1] In this report, the word *cyclic* (soil properties) is used loosely to denote material stress-strain properties important in seismic site response. The words *dynamic* and *dynamic/cyclic* have also been used in the literature for the same purpose.

All these problems require the knowledge of cyclic soil properties defined and measured along characteristic loading paths of interest.

Each problem could be the subject of a separate workshop. This meeting focuses mainly on seismic wave propagation and local site response with some attention given to sloping ground response. Our panel on "Low- and High-Strain Cyclic Soil Material Properties" was directed in particular to local seismic site response.

Local site response is important by itself and is also a fundamental starting point for the other problems listed above. There is a mounting body of evidence from many earthquakes (including the 1985 event in Mexico City and the very recent 1989 Loma Prieta earthquake in the San Francisco Bay Area) that this is a very significant effect contributing to seismic damage. It is also clear that local site response prediction contains significant uncertainties, and soil properties are a major contributor to those uncertainties.

Cyclic soil properties, in conjunction with other factors such as the incoming earthquake waves, the surface topography, subsurface geometry and layering, and the impedance of the underlying rock, play an essential role in determining seismic site response. The two records on soil included in Figures 3-1 and 3-2 illustrate how important low- and high-strain soil properties can be in some cases. Figure 3-1 displays response spectra obtained on soft clay in Mexico City on September 19, 1985. The large peak of almost 1g at T $\approx$ 2 seconds was caused by site amplification and was associated with relatively low strains and an almost linear stress-strain response of the clay (Dobry and Vucetic, 1987; Seed et al., 1988). Figure 3-2 reproduces the two acceleration components measured on loose saturated sand at a site that liquefied in Niigata, Japan, on June 12, 1964. Starting at about 7 seconds, the period of motion suddenly lengthened and the accelerations subsequently dropped. Large strains and significant stress-strain degradation probably developed in the sand after 7 to 9 seconds.

Much experimental work as well as related analytical and case history studies has been done in the last 25 to 30 years on cyclic soil properties. This research has greatly improved our understanding of those properties and of the influence of a number of factors, including useful empirical correlations. Another important product has been the development of *in situ* and laboratory measurement techniques for site-specific determinations, including various seismic methods for measuring wave velocities in the field and the resonant column, cyclic triaxial, cyclic simple shear and cyclic torsional shear devices used in the laboratory. Publications containing surveys of work on cyclic soil properties include Seed and Idriss (1970), Hardin and Drnevich (1972a), Richart (1975), ASTM (1977), Woods (1978), Iwasaki et al. (1978), Hardin (1978), Stokoe (1980), Kokusho et al. (1980, 1982), Finn (1981), Prakash and Puri (1981), Ishihara (1985), ASCE (1985), Seed et al. (1986), Dobry and Vucetic (1987), Sun et al. (1988), and Vucetic and Dobry (1991).
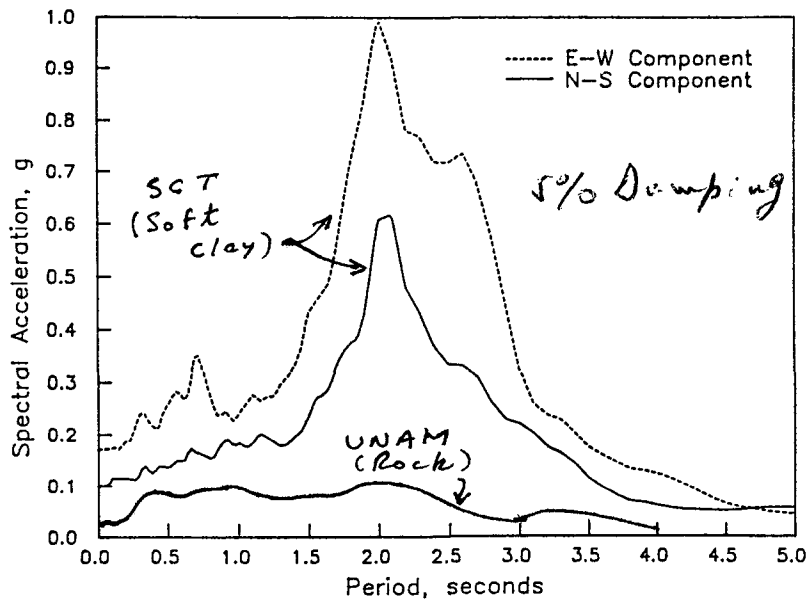
Figure 3-1. Acceleration Response Spectra Recorded On
Soft Clay At SCT Site, Mexico City, September
19, 1985 (Seed et al., 1988).

Figure 3-2.　Acceleration Records Measured On Loose Saturated
Sand, Niigata, Japan, June 12, 1964 (Ishihara, 1985; NRC, 1985).

However, as mentioned before, significant uncertainties associated with local site response still remain. One set of uncertainties is related to fundamental theoretical modeling aspects such as an understanding of the incident seismic wave field and the relative contributions and coupling between compressional (P), shear (S), and various types of surface waves. These uncertainties raise issues regarding the analytical and material soil models needed to predict site response and the types of tests that must be performed to determine the corresponding model parameters. As traditionally done in soil mechanics and soil dynamics applications (including nonearthquake problems such as blast and shock), soils must be characterized for load paths similar to those in the field. This is necessary because soils are not linear, elastic, and isotropic, nor are they elastic-plastic in the classical sense of metals. Therefore, the parameters and concepts we carry over from elasticity and classical plasticity (shear modulus, Poisson's ratio, constrained modulus, failure, surface, flow rule, etc.) are not universally applicable, and the values are not constant over arbitrary loading paths and for all strain levels. For example, Poisson's ratio is not, in general, constant with stress or strain level, and this should affect the interpretation of shear modulus from the Young's modulus measured in a standard triaxial test. To the extent that this sensitivity to load path occurs in seismic site response problems, our framework for future research must take it into account, including definition of load paths, general model requirements, and definition of new required testing and measuring techniques. Array studies including buried instruments and evaluation of measured site responses will be necessary to resolve some of these issues. Limited available data suggest that, at least in some important cases, local site response can be modeled in first approximation with vertically propagating uncoupled P and S waves, thus greatly simplifying the soil model and number of parameters required for the analyses.

A second set of uncertainties relates to applications of models to real predictions of *in situ* behavior during actual earthquakes. These uncertainties include inconsistencies in property parameters interpreted from different tests, difficulties in obtaining "undisturbed" samples, difference between properties measured in the laboratory and *in situ*, the absence of reliable *in situ* measurement techniques for cyclic soil properties at intermediate and large strains, some aspects of cyclic soil response and properties we still do not understand very well, and an absence of data on important soil types.

The solution to some of these problems and reduction of the associated uncertainties are made more urgent by the continued progress in analytical modeling with its more rigorous need for input soil parameters. On the other hand, the recent fast accumulation of earthquake records from seismic arrays in well-documented sites provides a powerful new tool to measure and investigate the soil properties of interest under actual earthquake conditions. The parallel development of centrifuge model testing including earthquake simulation capabilities also provides new opportunities for the investigation of cyclic soil properties in a simulated earthquake environment.

The following sections describe the scope of the issues addressed by this panel, present a short assessment of the state of the art of *in situ* and laboratory testing for

determining cyclic shear properties, summarize what we know about cyclic soil properties, and present recommendations for improvements and further research.

DEFINITIONS AND SCOPE

In one-dimensional (1D) site response analyses, horizontal soil layers of infinite extent are assumed to a certain depth, and the waves responsible for the horizontal ground motions are assumed to be vertically propagating plane shear waves (SH), as shown in Figure 3-3. In this model, vertical motions are caused by vertically propagating plane compressional waves (P). These seem to be reasonable first approximations at many sites where the near-surface soils play a primary role in determining ground response, including the Mexico City and Niigata cases previously described. One-dimensional analyses are also justified by the central role played by seismic shear stresses and strains in soil densification, pore pressure buildup, and liquefaction, which in turn affect the internal structure of the soil and modify its stress-strain response during the shaking, as in Figure 3-2. Therefore, this report focuses mainly on the cyclic soil properties needed for analyses of vertically propagating SH- and P-waves in horizontally layered soil profiles.

Any such site response calculation requires the mass density (ρ) of all soils involved, plus a cyclic stress-strain model with the corresponding soil parameters. For 1D vertical SH-wave analysis (one horizontal component of the ground acceleration), only the cyclic stress-strain behavior for one-dimensional shear acting on the horizontal plane is needed, as sketched in Figure 3-4. This behavior is highly nonlinear and inelastic (hysteretic), especially at high shear strains, and is the main subject of this report. For the more general case of two-dimensional (2D) SH-wave analysis involving both horizontal components, the cyclic behavior in 2D horizontal shear is required. A separate 1D P-wave analysis requires only the cyclic stress-strain behavior for constrained vertical compression (constrained modulus M and associated damping characteristics in constrained compression). On the other hand, a combined analysis including one or two horizontal components and the vertical component requires in principle a more complex nonlinear soil model, including the interaction between vertical compression and 2D horizontal shear (e.g., Ghaboussi and Dikmen, 1981). In equivalent linear site response calculations such as is done with program SHAKE, as well as in most nonlinear programs currently available, the three components of motion are analyzed separately (Schnabel et al., 1972; Richart, 1975; Lee and Finn, 1978).

Three important equivalent linear cyclic stress-strain properties for 1D shear are obtained from loop DECFD in Figure 3-5 (Seed and Idriss, 1970; Hardin and Drnevich, 1972a and b; Richart, 1975). The first is the secant shear modulus $G = G_s = \tau_c/\gamma_c$; the second is the material damping ratio $D = \Delta W/2\pi G\gamma_c^2$, where ΔW is the area within the loop; and the third is $G_{max} = G$ at very small strains ($\gamma_c \approx 10^{-4}$ percent). Both G and D vary with γ_c and they are the only stress-strain properties required for equivalent linear analyses. For nonlinear analyses, the backbone curve ACODB of Figure 3-5 is used instead (e.g., Richart, 1975), with appropriate rules (typically an extended Masing
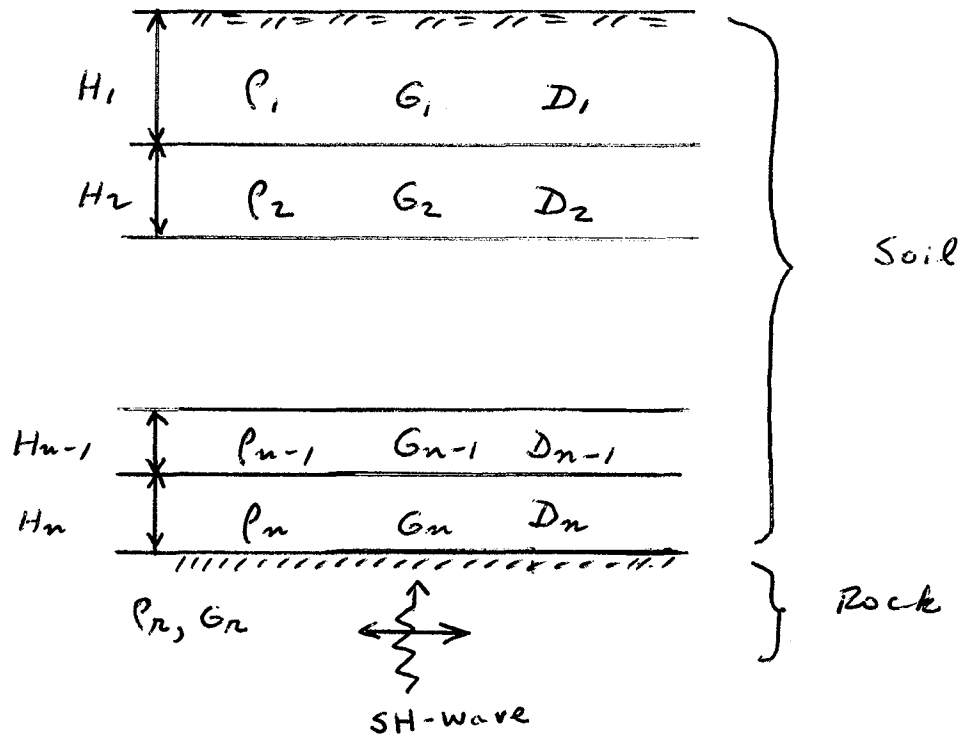
Figure 3-3.   One-Dimensional Site Response Analysis
For Vertically Propagating Plane SH Waves.

Figure 3-4.   Cyclic Stress-Strain Behavior of Soil For
One-Dimensional Shear.

Figure 3-5.   Backbone Curve and Hysteretic Loop in One-Dimensional Cyclic Shear.

criterion) specified for regular and irregular cyclic loading (Pyke, 1979; Vucetic and Thilakaratne, 1987; Vucetic, 1990). G_{max} is related to the shear wave velocity of the soil, V_s, through the expression $G_{max} = \rho V_s^2$. This is very convenient, as V_s can be measured in the field by geophysical seismic methods, thus avoiding the problem of sample disturbance often present in laboratory determinations.

The behavior of any soil under cyclic shear loading depends strongly on the level of cyclic strain induced in the soil. At very small strains the stress-strain response is linear and $G \approx G_{max}$. The upper limit of this range, which has been called "elastic threshold" is about 10^{-3} percent in sands and about 10^{-2} percent in normally consolidated clays of Plasticity Index, PI $\approx$ 50 (Lo Presti, 1987, 1989). At small strains the stress-strain response is still relatively linear, the value of G is only slightly lower than G_{max}, the material damping (D) is low, and there is very little or no stress-strain degradation or hardening with number of cycles. The upper limit of this range, which has been variously called " threshold strain" or "plastic threshold" is about 3 to 5×10^{-3} percent for gravels, near 10^{-2} percent for sands, and on the order of 10^{-1} percent for normally consolidated clays of high plasticity (Dobry et al., 1980, 1981, 1982; Hynes, 1988; Ladd et al., 1989; Bellotti et al., 1989; Lo Presti, 1987, 1989; Vucetic and Chu, 1990; Vucetic and Dobry, 1991). At intermediate strains above the plastic threshold the stress-strain response becomes strongly nonlinear, with much higher material damping and with considerable stiffness degradation or hardening caused by the cyclic unloading.

At large strains on the order of 1 percent to several percent, G is only a small fraction of G_{max}; the stress-strain response can change very dramatically in as little as one or two cycles; and the cyclic stress-strain behavior is controlled by factors other than G_{max}. These factors include mainly the degree of saturation of the soil, its contractive or dilative character, and its monotonic and cyclic shear strength characteristics. Therefore, in this strain range both G/G_{max} and D must be specified for site response analyses considering mainly the large strain behavior of the soil, including its monotonic shear strength (with due consideration to strain rate effects), rather than by a simple extrapolation of (or fitting an analytical model to) G/G_{max} and D curves determined at smaller strains. In both equivalent linear and nonlinear analytical methods, these large strain properties will determine the maximum level of acceleration to be computed at the ground surface of the soil profile, irrespective of input acceleration. Some nonlinear programs like DESRA (Lee and Finn, 1978) allow inputting the monotonic shear strength of the soil independently of G/G_{max}, and this strength acts as a cutoff for the acceleration.

Figure 3-6 includes some simplified calculations of maximum acceleration $(a_p)_{max}$ on soil for various assumed strength laws, showing that a very low $(a_p)_{max}$ will be calculated if a low strength is specified for the soil. How realistic are these low strengths and accelerations is a different issue. However, for very loose saturated sand deposits with shallow water table, observations by Ishihara (1985), exemplified by Figure 3-2, suggest that indeed there is an acceleration cutoff in these soils on the order of 0.2g or 0.3g.

(a)

LIMITING SURFACE ACCELERATIONS IN NONCEMENTED SHALLOW SOIL
(Vertically propagating, plane SH waves assumed)

a_p = Peak Acceleration

$z \lesssim 10m$

σ_v

τ_p

$\tau_p \approx \dfrac{a_p}{g} \sigma_v$ Peak Seismic Shear Stress

$S \approx b\bar{\sigma}_v$ Shear Strength of Soil

$\begin{cases} b \approx 0.3 \text{ for Soft Clay} \\ b \approx \tan 30° = 0.6 \text{ for Loose Sand} \end{cases}$

$(a_p)_{max}$ for $\tau_p = S$: $\dfrac{(a_p)_{max}}{g} = b \dfrac{\bar{\sigma}_v}{\sigma_v}$

Deep Ground Water Table: $\dfrac{\bar{\sigma}_v}{\sigma_v} = 1$

Shallow Ground Water Table: $\dfrac{\bar{\sigma}_v}{\sigma_v} \approx 0.5$

$\left. \right\}$ $\dfrac{(a_p)_{max}}{g} = (0.5 \text{ to } 1)b$

(b)

PREDICTED VALUES OF $(a_p)_{max}$ FOR SHALLOW SOIL ($z \lesssim 10m$)

Figure 3-6.   Limited Ground Surface Accelerations for Several Assumed Soil Shear Strengths.

Soil	b	$(a_p)_{max}$
Dry Loose Sand	0.6	0.6g
Saturated Loose Sand	0.6	0.3g (0.2g observed by Ishihara)
Soft, Normally Consolidated Saturated Clay	0.3	0.15 to 0.3g

- For larger soil depths, these $(a_p)_{max}$ increase due to soil flexibility: $\tau_p < \dfrac{a_p}{g} \sigma_v$

- Current 1D nonlinear site response programs specifying a shear strength for soil (i.e., DESRA) always compute $a_p \leq (a_p)_{max}$

The current state of the practice for site response evaluations of critical facilities includes obtaining G_{max} (and the associated constrained modulus at very small trains M_{max}) from both *in situ* measurements and laboratory determinations on small specimens, and the cyclic properties at larger strains such as G/G_{max} and D from the laboratory. For less critical structures and more limited budgets, very often some or all cyclic soil properties are estimated rather than obtained from measurements. This is done using our accumulated knowledge on the factors controlling G_{max}, M_{max}, G/G_{max}, D, etc., as well as published correlations between these cyclic properties and soil type, degree of saturation, effective confining pressure, and index properties such as penetration resistance, relative density, unconfined compressive strength, and plasticity index. Available *in situ* and laboratory techniques to conduct these measurements, as well as the most significant correlations for the cyclic soil properties, are discussed throughout the rest of this chapter.

IN SITU AND LABORATORY TECHNIQUES

A number of *in situ* and laboratory techniques have been developed to measure the cyclic soil properties of interest at small, intermediate, and large strains. Table 3-1 summarizes these techniques. For the purposes of the table, the separation between small[1] and intermediate strain behavior was assumed to be on the order of 10^{-2} percent, which is about right for granular soils and is a lower bound for cohesive soil. The determination of strength properties at large strains ($\gamma \geq 1$ percent) in Table 3-1 includes monotonic strength and regular static strength tests from triaxial and direct simple shear in addition to the cyclic tests listed.

Seismic Techniques

As revealed by Table 3-1, most of the *in situ* methods are seismic techniques (crosshole, downhole or uphole, seismic cone, and SASW), used mainly to determine G_{max} by measuring V_s. Similar seismic methods are used to determine V_p and $M_{max} = \rho V_p^2$, also at very small strains. There is a scarcity of *in situ* methods to reliably measure G at intermediate and large strains and D at any strain. Their development would be very desirable because of the difficulty of sampling and testing some soils in the lab (saturated sands, gravels), and also because of the uncertainty in the lab results because of sample disturbance in all soils. Four general types of seismic methods are used to determine dynamic properties of soil: crosshole, downhole/uphole, seismic cone, and spectral analysis of surface waves (SASW).

Crosshole. This *in situ* method is used mainly to measure V_s in a horizontal plane between boreholes (Figure 3-7) for horizontally propagating, vertically polarized S-waves (Hoar and Stokoe, 1977; Woods, 1978; Woods and Stokoe, 1985 and 1988). P-wave velocity (V_p) profiles can also be obtained using compressional source-receiver

---

[1] In Table 3-1, the small strain range has been defined to include both the very small and small strain ranges described in the previous section.

Table 3-1

DETERMINATION OF CYCLIC SOIL PROPERTIES IN SITU AND IN THE LABORATORY

Technique	Small Strains ($\gamma_c \le 10^{-2}\%$) G_{max}	G or G/G_{max}	D	Intermed. Strains ($10^{-2}\% \le \gamma_c \le 1\%$) G/$G_{max}$	D	Large Strain and Strength Properties ($\gamma_c \ge 1\%$)	Comments
In Situ:							
Crosshole	M	P	M				
Downhole/Uphole	M	P	M				
Seismic Cone	M	P	P				
SASW	P	M	P				
SB Pressuremeter	M	M	M	M	M	M	
Back Calculation from Arrays				M	M	M	
Laboratory:							
Bender Elements	M	M					
Resonant Column (RC)	M	M	M	M	M		Hollow–Cylinder Samples Desirable as γ_c Approaches 1% (RC and TS)
Cyclic TS	M	M	M	M	M	M	
Cyclic Triaxial:							
Conventional	M	M	M	M	M	M	
Modified			P	M	P	M	
Cyclic DSS	M			M	M	M	
Physical Modelling							
Triaxial Box	M	M	P				Univ. of Texas Low Level of Pressure
Large Shaking Tests (1g)	M	M	M	M	M	M	
Centrifuge Shaking Tests	M		M	M	M	M	

RC = Resonant Column
SB = Self Boring
TS = Torsional Shear
DSS = Direct Simple shear
SASW = Spectral Analysis of Surface Waves
Modified Cyclic Triaxial = Independent variation of axial and radial stresses, and special precautions are taken

M = Measurements have been reported
P = Measurements in principle possible, but no measurements have reported as yet (1989)

a.-PLAN VIEW
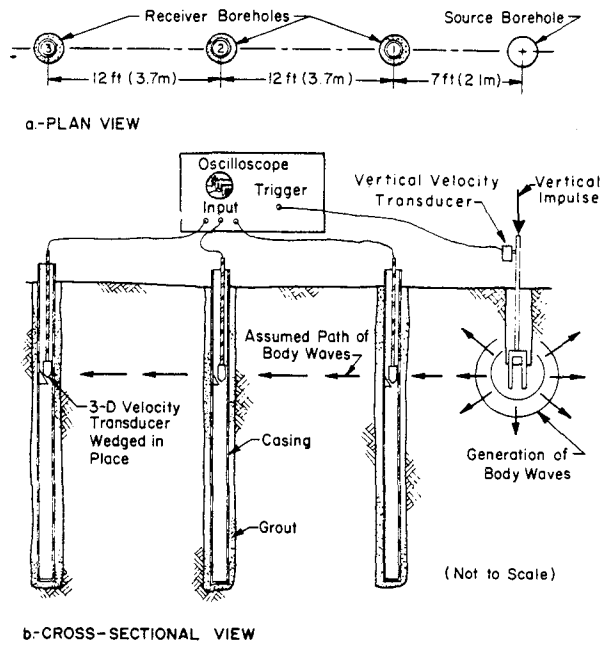
b.-CROSS-SECTIONAL VIEW

Figure 3-7.   Crosshole Seismic Method (Hoar and Stokoe, 1977).

Figure 3-8.   Crosshole and SASW Shear Wave Velocity Profiles,
Loose Saturated Sand Wildlife Site, Southern
California (Stokoe and Nazarian, 1985).

systems. These measurements lead to values of G_{max} and M_{max}. Field techniques and analysis methods have been standardized for measuring V_p and V_s through the establishment of an ASTM (1984) standard test procedure. For most investigations, three boreholes are required (typically separated by 3 to 5 meters), which minimizes timing errors and permits correction for refracted-wave arrivals caused by the presence of high-velocity layers above or below the source-receiver depth. Borehole deviation surveys must be performed within each drill hole to determine accurate distances between boreholes at all depths.

V_s profiles are typically obtained using the travel time of first arrivals (direct-wave arrival) and the results from borehole deviation surveying. Results for a loose, saturated, silty sand site are illustrated in Figure 3-8. The crosshole method is considered the most reliable *in situ* technique for determining V_s (and thus G_{max}) because of the small height of soil sampled at any depth and because it requires very little interpretation of the field data.

Evaluation of internal, material soil damping (D) at small strains may in principle be achieved through the use of spectral analysis of waveforms collected in the field (Redpath et al., 1982; Sirles, 1987; Mok et al., 1988) at successive distances from the source borehole. The problem is complicated by the inherent need to separate the radiation (geometric) damping from the material damping, as well as by the high rate of attenuation exhibited by many soil deposits.

Downhole and Uphole. Downhole measurement of V_p and V_s is usually conducted with a fixed-surface source and a downhole triaxial sensor moved to various measurement depths within the borehole at typical intervals of 5 to 10 feet. In uphole measurements the positions of the source and sensor are interchanged. The technique provides velocity averaged over the layers and therefore does not give the same detail as the crosshole method, especially when the soil wave velocities vary considerably between layers. Accuracy in the downhole technique has been improved by using a second fixed sensor at the top of the hole or near the source and by correcting for the source-receiver slant path near the top of the hole. Uncertainties in downhole measurement of V_p and V_s velocities can still be 10 percent or 20 percent (Hoar and Stokoe, 1977; Woods, 1978; Stokoe, 1980; Woods and Stokoe, 1985).

Downhole measurements of damping have been made at small strains (Redpath et al., 1982; Sirles, 1987). Spectral ratio techniques using two separated sensors have been the most successful; however, they also have uncertainties related to the field technique, sensor separation, and source spectra.

Lack of S-wave source repeatability, particularly when reversing S-wave polarity, affects the accuracy of downhole measurement of V_s, while a poorer generation of S-waves related to P-waves at very stiff sites degrades S-waves onset identification. The use of a repeatable source, such as proposed by Lui et al., 1988, would lead to more precise downhole V_s determinations and would assist in S-wave identification at very stiff sites.

Seismic Cone. The seismic cone has been used by several investigators (Campanella and Robertson, 1984; Robertson et al., 1986; Baldi et al., 1988; Jamiolkowski and Robertson, 1988). This method provides information on V_s and G_{max} in addition to regular static cone penetration resistance.

The seismic cone test configuration is shown in Figure 3-9. Basically, a cone penetrometer containing a triaxial receiver system is statically penetrated into the soil deposit. At the same time, downhole seismic tests are conducted by exciting sources on the ground surface in the vicinity of the cone. Wave velocities and moduli are inferred from the travel times of the waves between source and receiver. Information on soil strength is obtained from the cone penetrometer results. Figure 3-10 shows a comparison between results from downhole seismic cone and crosshole tests for a clay site in Norway.

The seismic cone method offers the capability of providing information on low strain behavior and strength characteristic at the same location. The limitations of the method include the inherent problems of cone penetrometer testing, that is, its lack of ability to test coarse-grained (gravel-type) soil deposits as well as those associated with downhole seismic testing as previously listed.

Spectral Analysis of Surface Waves (SASW). Stokoe and Nazarian (1985) have developed a surface wave method for monitoring G_{max} of the soil with depth without the use of boreholes. In this technique, two vertical transducers are placed on the ground surface at equal distances from an imaginary center line as shown in Figure 3-11. A vertical impulse is then generated on the ground surface at a distance which for the near receiver is approximately equal to the distance between receivers (Figure 3-11). Surface waves of the Rayleigh type are monitored as they propagate past the two transducers.

The depth of soil sampled with the SASW method is a function of the wave length generated, with low frequency waves sampling greater depths. This is related to the dispersion of surface waves in actual soil deposits, and it forms the basis of the SASW method (Rix and Stokoe, 1989; Rix et al., 1990). Dispersion means that the propagation velocity of surface waves is representative of the material stiffness over depths where there is significant particle motion. For example, a wave which has a wavelength λ_1, less than the thickness of the top layer in the profile shown in Figure 3-12a will exhibit a propagation velocity which is only dependent on the stiffness of that top layer (Figure 3-12b). On the other hand, the velocity of a surface wave which has a longer wave length $\lambda_2 > \lambda_1$, and thus has particle motions in all of these layers will be influenced by the stiffness of all layers (Figure 3-12c). Thus, by measuring the surface wave velocity over a wide range of wavelengths (frequencies), it is possible to assess the stiffness of the layers over a range of depths. The basic relationship between wave velocity, frequency, and wavelength is:

$$V_R = f \cdot \lambda \qquad (3\text{-}1)$$

Figure 3-9.   Seismic Cone Used in a Downhole Test
(Robertson et al., 1986).

Figure 3-10.   Seismic Cone and Crosshole Shear Wave
Velocity Profiles, Clay Site in Norway
(Robertson et al., 1986).

(a) General Configuration of SASW Tests

(b) Common Receivers Midpoint Geometry

Figure 3-11. Spectral Analysis of Surface Waves Test (Stokoe and Nazarian, 1985).

a. Material Profile   b. Shorter Wavelength, λ_1 c. Longer Wavelength, λ_2

Figure 3-12. Approximate Distribution of Vertical Particle Motion with Depth for Two Surface Waves of Different Wavelengths. (Rix et al., 1990).

3-16

where:

V_R = surface (Rayleigh) wave velocity

f = frequency, and

λ = wavelength

A series of receiver spacings is employed in testing one site. Initially, a close receiver spacing is used to sample the near-surface soils. Then the receiver spacings are increased about the imaginary center line as in Figure 3-11, so that deeper and deeper soils are sampled. For each receiver spacing, the source is located first to the left and then to the right of the receivers. With this approach, average values of wave propagation between the receivers are collected in an attempt to minimize problems with inhomogeneities between them. In this manner, a composite dispersion curve (V_R versus λ) is developed from all receiver spacings.

Once the dispersion curve has been developed for a site, it must be inverted. Inversion is the process of calculating the shear wave velocity profile from the dispersion curve. A theoretical dispersion curve is calculated from an assumed velocity profile and is then compared to the field dispersion curve. The assumed velocity profile contains a sufficiently large number of sublayers to define the *in situ* variation in stiffness with depth. The theoretical curve is calculated using a modified Haskell-Thomson matrix algorithm (Thomson, 1950; Haskell, 1953; Nazarian, 1984). The shear wave velocities and thicknesses of the sublayers in the assumed profile are adjusted by trial and error until a satisfactory match is obtained, at which time the final profile is assumed to represent the *in situ* profile. The computer programs used for this SASW inversion continue to be developed, and their availability is presently quite limited.

Stokoe and Nazarian (1985) and Rix and Stokoe (1989) report good correlation between results of SASW and crosshole measurements (Figure 3-8). However, Sirles (1987, 1988) reports some discrepancies in another case study. This seems to occur in layered soils with inclined boundaries or in heterogeneous soil deposits.

Self-Boring Pressuremeter (SBP)

A properly programmed unload-reload loop performed during a fully drained expansion of the self-boring pressuremeter test (SBP; see Wroth, 1982) in cohesionless soil is a promising technique for determining G at small and intermediate strains. There are two main reasons why one should refer to the unload-reload loop rather than to the initial monotonic expansion:

1.   Only for a fully drained unload-reload loop it is possible to relate the measured G to a specific cyclic strain (Figure 3-13).

Figure 3-13. G_{max} and G from Unloading - Reloading
Loops in Self Boring Pressuremeter Test
(Bellotti et al., 1989).

3-18

2. The experimental evidence suggests that an unload-reload loop is not very sensitive to the disturbance of the surrounding soil caused by the insertion of the self-boring probe.

This last feature inspires some hopes for the use of less sophisticated push-in and displacement pressuremeter probes for the assessment of G in granular soils from unload-reload loops.

In practice, the use of G obtained from the SBP test requires a link between the average mean effective stress p'_{av} and the average cyclic shear strain amplitude γ_{av} existing around the expanding cavity, which is assumed to be cylindrical in shape. Recommendations on how to determine p'_{av} and γ_{av} have been made by Robertson (1982), Robertson and Hughes (1986), and Bellotti et al. (1989). Byrne et al. (1990) showed that the corrected G for given p'_{av} and γ_{av} compares favorably with those measured in the laboratory at the same combination of void ratio, p' and strain level (Figures 3-14 and 3-15). The experience gained so far suggests that G can be inferred from an unload-reload loop performed during an SBP test for γ_{av} ranging between about 0.05 and 0.15 percent.

At least in principle, it is also possible to obtain the internal damping ratio D from the same SBP test's unload-reload loop (Dormieux and Canou, 1990). However, a more extensive use of the SBP for the assessment of both G and D is linked to the improvement of the existing equipment, especially as it relates to the measurement of the cavity strain (e_o). In fact, at present the measurement of e_o in the English version of the SBP, named Camkometer, is subjected to some uncertainties when this strain is less than about 0.1 percent. In this apparatus, the e_o is measured at the mid-height of the probe at three points along its perimeter, by means of three strain gauges instrumented with pivoting arms that exhibit some undesirable mechanical compliance; see Fahey and Jewell (1990). The other self-boring equipment available on the market, the French PAF, appears to be less suitable for the purpose under discussion. The instrument allows measuring only the volume of the liquid injected to the probe during expansion, from which the average volumetric strain (e_v) is inferred. This renders the measurements of the unload-reload modulus in the range of cyclic shear strain between 0.05 and 0.2 percent less reliable than in the case of the Camkometer probe.

Other Proposed *In Situ* Techniques for Intermediate and Large Strains

Other *in situ* test concepts have also been proposed that--though somewhat cruder than the methods described so far--do have the potential for evaluating shear behavior at intermediate to large strains. These proposed approaches involve applying a large strain boundary condition in the field, which propagates as a stress wave through the soil, with the wave motion measured at various distances from the source to evaluate its attenuation and time history variation. One technique that has been used in the defense community is the CIST (Cylindrical *In Situ* Technique, Bratton and Higgins, 1978). The CIST was designed to propagate a cylindrical compression wave into soil or

Figure 3-14. G/G_{max} From Self Boring Pressuremeter in Sand (Calibration Chamber, Bellotti et al., 1989).

Figure 3-15. G/G_{max} From Self Boring Pressuremeter in Sand from River Po Site, Italy (Bellotti et al., 1989).

rock. The test results were analyzed using iterative finite difference calculations, and the method was very effective in evaluating the uniaxial behavior, the *in situ* failure envelope, and the postfailure behavior.

Another version of CIST that has also been considered would use a cylindrical probe for creating large shear strains. It consists of a vertical, embedded corrugated pipe, perhaps filled with concrete supported on a compressible footing that is driven downward by a small explosive load (see Figure 3-16). The test will create a cylindrical SV wave that has a peak amplitude limited by the failure strain at the interface. For some time and distance, the motion will be close to one-dimensional cylindrical type. Later it will become two dimensional. In either case, this defines a situation susceptible to analysis with readily available finite difference or finite element codes.

Such an experiment obviously will be expensive and restricted to a shallow depth, but it can provide some baseline data on high-strain behavior for correlation with laboratory measurements.

Another interesting recent attempt in the same direction is the *in situ* cylindrical shear system (Henke and Henke, 1990). This device, penetrated carefully below the base of a borehole, enables the soil to be subjected to both impulse and cyclic torsional shear from which the dynamic and cyclic soil properties at intermediate and large strains are inferred.

Random Decrement Technique

The random decrement technique is a new method that has been recently proposed for inferring *in situ* damping and shear moduli of instrumented soil deposits at both low- and high-strain levels (Yang et al., 1989; Qi et al., 1989).

In the method, segments of the response of a system excited by random forces are ensemble averaged to form signatures that are representative of the free response of the system. Damping is then calculated from the decay of the free vibrations. Damping and shear moduli (shear wave velocities) are inferred for a range of strains by considering records from earthquakes of various magnitudes. For the damping, only the response (output) record is necessary; see Chapter 4.

The method offers advantages but also has limitations. The main advantage is that it is easy to use and requires ground motions recorded at only one location. The main limitations include: (1) the dynamic parameters determined are average properties over the entire soil profile, and (2) the damping determined includes both material and radiation contributions.

Figure 3-16. Schematic Representation of CIST Test (Higgins, 1989).

Backcalculation From Arrays

The rapidly increasing number of strong motion arrays deployed in soil deposits in Taiwan, Japan, Mexico, the United States, and other countries offers the possibility to backfigure cyclic soil properties directly from pairs of simultaneous earthquake records using a minimum of assumptions. This provides a new measuring tool for G_{max} as well as G and damping D versus strain.

Although backcalculations can be made in the time domain, it seems that the best results are obtained using similar frequency domain techniques and assumptions to those incorporated into program SHAKE (Schnabel et al., 1972). That is, if $F_s(\omega)$ is the complex Fourier spectrum of the "output" horizontal record (typically at the soil surface) and $F_r(w)$ that of the "input" record (on a rock outcrop or buried at a certain depth in the soil), the complex transfer function of the system, $H(\omega) = F_s/F_r$ depends only on the cyclic properties of the site and is independent of the input record. (This and other statements here are linked to the assumption of upward plane SH wave propagation and horizontally layered sites used in one-dimensional site response analyses.) That is, $H(\omega)$ depends only on the soil profile and properties of the layers above a buried "input" instrument, and also on the impedance of the rock for an outcrop instrument. In fact, if both the recorded and the future expected earthquakes induce similar levels of strain in the soil, the empirically measured $H(\omega)$ characterizes the site completely and can in principle be used to predict future site response without the need for cyclic soil measurements.

Figures 3-17 and 3-18 and Table 3-2 illustrate how the technique was used by Dobry (1988a) to obtain G_{max} and G/G_{max} with results obtained by two instruments during several earthquakes at the Lotung Array in Taiwan. The accelero-graphs were located at 0 and 6m depth in a saturated silt/sand site. Peak accelerations up to 0.21g were recorded at the ground surface, and they probably caused zero or moderate pore water pressure buildup in the soil. As shown in Figure 3-17, each surface record was divided in segments having different acceleration levels and thus inducing different levels of cyclic strain $\gamma_c \approx \gamma_p$ in the soil. Figure 3-17 plots the spectral ratios, $|H(\omega)|$, obtained in one event from seven segments ranging from $a_p = A_{max} = 0.01g$ to 0.13g (Chang et al., 1990).

Table 3-2 shows the calculations for G_{max} and G/G_{max}. For $a_p = 0.01$ to 0.02g, γ_p < 0.01 percent, the frequency of the peak of $|H(\omega)|$ is $f_{max} \approx 5.55$ Hz, which gives $G_{max} = 7.51 \times 10^5$ psf for the soil between 0 and 6m depth. This value of G_{max} is consistent with the shear wave velocities, V_{so} measured at the site with the crosshole technique. For higher accelerations corresponding to larger strains, the frequencies of the peaks are smaller than f_{max} because of the nonlinear soil response (see Figure 3-17), and the secant modulus G can be calculated from $G/G_{max} = (f/f_{max})^2$.

Figure 3-18 plots G/G_{max} obtained this way versus the shear strain in the soil, and compares it up to $\gamma_p \approx \gamma_c \approx 0.1$ percent with the standard band for sands proposed by

Table 3-2

BACK CALCULATION OF G_{max}, G/G max AND γ FROM LOTUNG RECORDS (DOBRY, 1988a)

Peak Shear Stress at 6m

$$\tau_p \approx a_p \, \rho \, z = (a_p/g) \, \sigma_v$$

$$\sigma_v \approx 1,250 \text{ psf}$$

$$\tau_p \approx 1,250 \, (a_p/g) \text{ psf}$$

Peak Shear Strain: $\quad \gamma_p = \tau_p/G$

$$\gamma_p = \frac{\tau_p}{G} = \frac{\tau_p}{G_{max} \cdot (G/G_{max})}$$

$$= \frac{1,250 \, a_p/g}{G_{max} \cdot (G/G_{max})}$$

$$G_{max} = \rho \, V_{so}^2 = 7.51 \times 10^5 \text{ psf}$$

$$\frac{G}{G_{max}} = (V_s/V_{so})^2 = (f/f_{max})^2$$

$$\therefore \quad \gamma_p = 1.67 \times 10^{-3} \frac{a_p/g}{(f/f_{max})^2}$$

with $\quad f_{max} = 5.55$ Hz

Figure 3-17. Surface Accelerogram and Spectral Ratio [H(ω)] Between 0m and 6m Depths for Several Time Windows, Lotung Array, Taiwan (Chang et al., 1990).

Figure 3-18. G/G$_{max}$ versus Strain, Back Calculated at Lotung Array and Band for Sands Determined in the Laboratory (Dobry, 1988a).

Seed et al. (1986), with good agreement. Therefore, the backcalculation technique allows measurement of G and G/G_{max} up to relatively high strain levels that are difficult to reach and/or interpret with current *in situ* seismic methods.

Indirect Measurements

Several *in situ* tests not directly aimed at measuring cyclic stress--strain properties--or giving results that at present are difficult to interpret--have been empirically correlated with V_s or G_{max}. They include the standard penetration test (SPT), the static cone penetration test (CPT), the Marchetti flat dilatometer test (DM), the electrical resistivity measured with a special probe, and others (e.g., Marchetti, 1980; Arulmoli et al., 1985). In what follows, a brief summary of these correlations is presented for the SPT and CPT, based on the following publications: Sykora and Stokoe (1983), Seed et al. (1983), Sykora and Koester (1988), Jamiolkowski and Robertson (1988), and Baldi et al. (1989, 1989a).

Table 3-3 and Figure 3-19 include several correlations between N (blows/foot) measured in the SPT and both G_{max} and V_s, proposed by several authors for sands, gravels, and other soils. As could be expected for such general correlations valid for different soil types obtained from different data bases, they differ considerably from each other (Sykora and Koester, 1988). A similar large scatter is present within a given data base, as illustrated by the correlation for granular soil in Figure 3-20 developed by Sykora and Stokoe (1983). The use of N_1--that is, of N corrected for effective overburden pressure--as proposed by Seed et al. (1983) does not improve the correlations (Sykora and Stokoe, 1983; Sykora and Koester, 1988).

On the other hand, the correlation improves considerably when restricted to one granular soil, as shown in Figure 3-21 for the Po River sand in Italy. Ghionna et al. (1989) explain this good correlation in a given cohesionless soil by the fact that both N and G_{max} are controlled to a large extent by the same two parameters: state of effective stresses and density of the soil. But even here a word of caution is necessary, in that geologic age effects may increase G_{max} more than N.

Similar correlations have been suggested between the point resistance q_c from the CPT and G_{max}. Figure 3-22 shows the correlation proposed by Baldi et al. (1989) for uncemented quartz sands, based on calibration chamber experiments and verified by a number of *in situ* measurements at four sites.

LABORATORY TECHNIQUES

Most of the information at intermediate and large strains can be currently provided only by the laboratory methods listed in Table 3-1. The main five techniques listed first in Table 3-1 are used at many laboratories, while the other three (triaxial box, large shaking table, and centrifuge shaking) are rather specialized and exist only at a few places. Although resonant column and torsional shear tests can be conducted at any

Table 3-3

CORRELATIONS BETWEEN N AND V_s

(SYKORA AND KOESTER, 1988)

Equation No.	Author(s)	Data Information	Soil Types Used	Reported Equation Shear Modulus, G, tsf	Reported Equation Shear Velocity, V_s, fps
1	Ohsaki and Iwasaki (1973)	200 sites in Japan; 220 sets of data	All	$G = 125 \, N^{0.78}$ (0.886)**	$V_s = 268 \, N^{0.39}$†
2	Ohsaki and Iwasaki (1973)	200 sites in Japan; 220 sets of data	Cohesionless	$G = 66.5 \, N^{0.94}$ (0.852)**	$V_s = 195 \, N^{0.47}$†
3	Ohta and Goto (1978a)	289 sets of data; Japanese soils	All	N.R.††	$V_s = 280 \, N^{0.341}$ (0.719)**
4	Ohta and Goto (1978b)	289 sets of data; Japanese soils	Sands	N.R.	$V_s = 290 \, N^{0.340}$
5	Ohta and Goto (1978b)	289 sets of data; Japanese soils	Gravels	N.R.	$V_s = 309 \, N^{0.340}$
6	Imai and Tonouchi (1982)	1,654 sets of data; Japanese soils	All	$G = 147 \, N^{0.68}$ (0.867)**	$V_s = 318 \, N^{0.314}$ (0.868)**
7	Seed, Idriss, and Arango (1983)	Unknown	Sands	$G = 65 \, N^{1.0}$	$V_s = 185 \, N^{0.5}$
8	Sykora and Stokoe (1983)	229 sets of crosshole data; throughout United States	Granular	N.R.	$V_s = 350 \, N^{0.27}$ (0.84)**

Note: * N = Standard Penetration Resistance N-value (blows/ft); not adjusted to a normalize energy efficiency.
** Regression correlation coefficient.
† Assumed, not reported; γ = 112.4 pcf, typical for Japanese sands (Ohsaki 1962).
†† N.R. = Not reported.

Figure 3-19.   Correlations Between N and V_s (Sykora and Koester, 1988).

Figure 3-20. Correlation Between N and V_s for Granular Soil (Sykora and Stokoe, 1983).

Figure 3-21. Measured and Predicted V_s Using Ohta and Goto Correlation N versus V_s for Sands, Po River Sand Sites (Baldi et al., 1989a)

3-28

	SITE	SOIL	G_0 SOURCE	BOREHOLE
△	VIADANA	MEDIUM SAND	CROSS-HOLE	4017
▲	VIADANA	MEDIUM SAND	SEISMIC CONE	4017
□	S. PROSPERO	MEDIUM SAND	SEISMIC CONE	16 17
●	GIOIA TAURO	SAND WITH GRAVEL	CROSS-HOLE	209 219

DEPTH BELOW G.L. CONSIDERED: 5.5 TO 43.5 m

Figure 3-22. Correlation Between CPT (qc) and G_{max} for Quartz Sands (Baldi et al., 1989, 1989a; see also Jamiolkoski et al., 1988).

strain, especially if hollow-cylinder specimens are used, most often resonant column determinations are performed at small strains and cyclic triaxial or DSS tests are done at intermediate and large strains. This may produce inconsistencies, as discussed later.

Cyclic Triaxial

Because of its widespread availability and great simplicity in testing procedures, cyclic triaxial tests are often used to evaluate the cyclic behavior of soils for design purposes. Triaxial tests can be conducted under cyclic stress- or strain-controlled conditions. Conventional cyclic triaxial strain-controlled tests have been used successfully by many researchers to evaluate dynamic properties (shear modulus and damping) of soil at intermediate strains ($\gamma_c > 10^{-2}$ percent, e.g., Ladd et al., 1989) but had not until recently been looked upon as a rational way to make reliable measurements at low strains. However, technical improvements in cyclic testing have resulted in reliable measurements of dynamic soil properties corresponding to strain amplitudes as small as the order of 10^{-3} or 10^{-4} percent in cyclic triaxial tests (Kokusho, 1980; Tatsuoka et al., 1984; Ladd and Dutko, 1985; Tatsuoka, 1988). Figure 3-23 shows a sketch of an improved cyclic triaxial device developed to obtain dynamic shear modulus and damping coefficients of clays and sands under cyclic loading for a wide range of strains between 10^{-4} percent and 1 percent (Kokusho, 1980). In this apparatus, the cap displacement is measured by means of a pair of two diametrically opposed proximity transducers. The ends are not lubricated so as to minimize the bedding error. Figure 3-24 shows some representative hysteresis loops obtained with both an improved cyclic triaxial device and with the conventional cyclic triaxial apparatus for various strain levels and numbers of cycles. The loops in Figure 3-24a are evidently smooth for all strain levels, while those in Figure 3-24b possesses bilinear characteristics at small strains. This indicates that the improved device is free from mechanical problems and thus can yield high-quality results at low strains (Kokusho, 1980). However, it should be remembered that even with the improved cyclic triaxial device, in the case of loose soil at large strains, failure takes place in the extension mode in a relatively early stage of the testing, and this leads to unreliable measurements of the dynamic properties of loose soils.

Figure 3-25 shows typical G/G_{max} and D versus γ_c curves obtained on saturated sand tested undrained at different void ratios using the improved cyclic triaxial device. The shear modulus measured at low strains (Figure 3-24a) obtained with the improved cyclic triaxial compares well with similar data obtained using the torsional shear device (Kokusho, 1980). However, the damping ratio measured by the improved cyclic triaxial apparatus was found to be smaller for a wide range of strains than those obtained by low frequency cyclic tests using the torsional or simple shear devices. It is believed that the improved triaxial test is frictionless, and hence the reliability of the damping ratio obtained from it may be greater.

Loading Piston
(Stroke ± 30mm)

Housing

Slide Ball Bearing

Bellow-phragm

Inner
Load Cell

High Sensitivity
Gap Sensor

Cap (φ50mm)

Lucite

Pedestal

Porepressure
Meter

UNIT : mm

Figure 3-23.   Improved Cyclic Triaxial Device (Kokusho, 1980).

(i) N=1 2 5 10   (ii) N=1 2 5 10

$\gamma = 7.8 \times 10^{-6}$ G=1550kgf/cm² $\gamma = 8.5 \times 10^{-5}$, G=1500kgf/cm²
h = 0.017

(iii) N=1 2 5 10

$\gamma = 8.4 \times 10^{-4}$, G = 960 kgf/cm²
h = 0.085

(iv) N=2 5 10

$\gamma = 3.97 \times 10$, G=355kgf/cm², h = 0.226

(a) TEST No.53, $\sigma_c = 2.0$ kgf/cm², e = 0.641

N=1~2 5~6 10~11   N=1~2 5~6 10~11

1~2 5~6 10~11

(i) $\gamma = 1.3 \times 10^{-5}$
G= 1120 kgf/cm²   (ii) $\gamma = 6.5 \times 10^{-5}$, G = 560 kgf/cm²

N=1.25 5 10

(iii) $\gamma = 4.3 \times 10^{-4}$, G = 340 kgf/cm²

(b)
GIFU SAND $\sigma_c' = 1.0$ kgf/cm², e=0.86
(1 kgf / cm² = 98 KN/m²)

Figure 3-24.   Measured Hysteresis Loops in Cyclic Triaxial Apparatus for: a) Improved Tests; and b) Conventional Tests (Kokusho, 1980).

Figure 3-25. Modulus for Damping Versus Cyclic Strain for $\overline{\sigma}_c = 1$ Kg/cm^2 and for Sand with Different Void Ratios (Kokusho, 1980).

Cyclic Torsional Shear and Resonant Column (RC)

Advantages and disadvantages of various testing devices capable of generating stress paths beyond those provided by the regular triaxial test have been discussed by Saada and Townsend (1981), Hight et al. (1983), Druevich (1985), and Alarcon et al. (1986, 1988). The hollow-cylinder configuration has been shown to be the most appropriate whenever both magnitude and direction of the principal stresses must be changed to accommodate a wide variety of stress paths. The subject of cyclic testing with thin long hollow cylinders was covered in detail by Saada (1985). More information on the device, its driving mechanisms, measuring units and data acquisition can be found in a state-of-the-art paper by Saada (1988).

From the point of view of uniformity of stress state within the specimen, the effect of the end platens is minimized by having a good length to diameter ratio (≥ 1.5) and a ratio of inner to outer diameter of about 0.7. The inner and outer pressures must be the same to maintain uniformity of the normal stresses. The thinner the cylinder, the more uniform are the shearing stresses. All stress and strain paths that can be used in the triaxial test can also be reproduced in the hollow-cylinder torsional shear device. In addition, the superposition of torsion allows one to rotate the principal stresses at will and to simulate some of the conditions present in the field. A drawback is that the coefficient $b = (\sigma_2 - \sigma_3)/(\sigma_1 - \sigma_3)$ cannot be changed without inclining the principal stresses on the axis of symmetry since $b = \sin^2\beta$ (Figure 3-26). A way around this restriction is to use different inner and outer pressures; however, this makes the normal stress distribution nonuniform within the specimen, and the test does not represent any more the state of stresses at a point.

The configuration of the thin hollow cylinder also lends itself well to resonant column tests and to slow cyclic stress-controlled or strain-controlled tests. Axial, torsional, and hydrostatic effects can be superimposed to produce any static or dynamic stress and strain paths. The controls can be pneumatic, hydraulic, or electronic; the latter is also used for data acquisition and processing. Measurements made inside the cell lead to higher accuracy.

Resonant Column. The resonant column, and in particular the "fixed-free" resonant column device, in conjunction with a thin long hollow cylinder has been used in both sands and clays to determine small strain properties. Axial moduli and damping ratios of the samples can be very accurately determined with this device at small strains. A frequency sweep can be made and nonlinearities (jumps) can be put in evidence even at small strains. In general, the measured G/G_{max} versus γ_c relation can be well represented by a Ramberg-Osgood equation. However, the use of the Ramberg-Osgood

Figure 3-26. System of Stresses for Hollow-Cylinder Torsional Test (Saada, 1985).

3-34

formulation for G/G_{max} in conjunction with the Masing assumption to predict the hysteresis loops usually does not represent well the values of damping ratio D at small cyclic strains.

Figure 3-27a shows a typical relation between shear modulus and strain and the corresponding Ramberg-Osgood constants. Figure 3-27b shows the damping ratio versus strain. Notice the damping at zero strain obtained by extrapolation. There seems to be some sort of a constant damping close to zero strain, which changes from clay to clay. The origin of this damping is not known.

Figures 3-28 and 3-29 show the result of frequency sweeps for a remolded and an undisturbed clay. The shapes of the curves indicate how the nonlinearities increase with strain. The dotted line joining the peaks gives G/G_{max} versus γ_c. Curves similar to those of Figure 3-29 have been generated for a variety of sands under different hydrostatic stresses (McNelis, 1987). Figure 3-30 shows differences between moduli G_{max} and E_{max} corresponding to isotropic and cross anisotropic clays. Such differences can be substantial (Saada, 1985). Figure 3-31 shows the normalized shear moduli of a dense sand under three different consolidation pressures. Figure 3-32 shows the normalized Young moduli of the same dense sand (McNelis, 1987).

The University of Michigan has developed a resonant column with strong magnets that give strains as high as 0.5 percent. At such large strains it could be advantageous to conduct very short time tests (a few bursts at a time) to avoid excessive modulus degradation. The resonant column is being used to conduct tests on both remolded and undisturbed samples. For the latter case, it is advised that the material be K_o-consolidated to the condition in the field. This would also help seat the sample.

Hollow-Cylinder Torsional Shear. The hollow cylinder torsional shear apparatus has been used routinely to study the behavior under large cyclic stresses and strains. For K_o-consolidated artificial clay in which the response in extension is different from compression, axial cyclic stresses result in loops displaced in the extension direction (Macky and Saada, 1984). On the other hand, under torsional cyclic loading, the loops are approximately symmetric. A combination of both axial and torsional cyclic effects results in different pore water pressure development and of degradation of the material's stress-strain response. The difference in phase between the axial and torsional stresses also affects the strains and pore pressures.

For sands, the stress path as well as the phase angle affects liquefaction (Gilbert and Donaghue, 1983). Whether the tests are conducted in stress-controlled or strain-controlled conditions, the buildup in pore water pressure results in both stiffness and strength degradation. Contractive sands liquefy. Dilative ones do experience an increase in pore water pressure and may liquefy momentarily but suffer limited (though sometimes large) strain. The hollow cylinder torsional device offers the possibility to study liquefaction and cyclic mobility under both simple shear and combined stress conditions, as illustrated by Figure 3-33. Figure 3-34 presents the modulus degradation

(a)

$$\frac{G'}{G'_{MAX}} = \frac{1}{1 + \alpha \left(\frac{\gamma_o}{10^{-4}} \frac{G'}{G'_{MAX}}\right)^{R-1}}$$

RAMBERG-OSGOOD

$\alpha = .033$
$R = 2.73$

A

$$\lambda = \lambda_{MIN} + \frac{\frac{2\alpha}{\pi}\left(\frac{R-1}{R+1}\right)\left(\frac{\gamma_o}{10^{-4}}\frac{G'}{G'_{MAX}}\right)^{R+1}}{\left(\frac{\gamma_o}{10^{-4}}\right)^2}$$

$\alpha = .0141$
$R = 2.214$
$\lambda_{MIN} = 1.440$

(b)

B

KAOLINITE ANISOTROPIC

$\overline{\sigma}_C = 40$ psi

$\gamma_{\theta z} \times 10^{-4}$

Figure 3-27.   Shear Modulus G/G_{max} and Damping λ Versus Cyclic Shear $\gamma_{\theta z}$ from Resonant Column Test, and Ramberg-Osgood Model (Bianchini, 1985).

Figure 3-28.   Frequency Sweep in RC Test on Remodeled Clay
(Bianchini and Saada, 1981).

Figure 3-29.   Frequency Sweep in RC Test on Undisturbed Clay
(Saada, 1988).

3-37

Figure 3-30.   Shear Modulus G_{max} and Young's Modulus E_{max} for Isotropic and Cross-Anisotropic Clays (Saada, 1985).

Figure 3-31. G/G_{max} versus γ_c of Dense Sand from RC Test for different Consolidation Pressures (Mc Nelis, 1987).

Figure 3-32. E/E_{max} versus γ_c for Same Dense Sand of Fig. 3-31 (Mc Nelis, 1987).

Figure 3-33. Cyclic Loading Conditions in Torsional Shear (Saada, 1985).

Figure 3-34. Modulus Degradation in Cyclic Triaxial Stress-Controlled Test in Clay (Saada, 1985).

Figure 3-35. Modulus Degradation in Cyclic Torsion Shear Stress-Controlled Test in Clay (Saada, 1985).

3-39

and movement of the hysteresis loops for a K_o-consolidated clay subjected to cyclic axial stress-controlled loading. Figure 3-35 shows the degradation under pure cyclic stress-controlled torsional loading of the same clay. Figure 3-36 shows the liquefaction of a sand tested in cyclic shear in strain-controlled condition.

In summary, the long and thin hollow-cylinder configuration, be it used in a resonant column or in a torsional shear device, offers excellent possibilities to study both small-strain and large-strain static and dynamic properties of soils. Its main drawback is related to sample preparation that requires great care. A discussion of moduli and damping ratios that can be obtained with this configuration is given in a later discussion.

Cyclic Direct Simple Shear (DSS)

Although there are several types of undrained or constant volume DSS tests, they all share the same basic characteristics: a horizontal cyclic shear stress or strain applied on a laterally confined saturated soil specimen with a constant (applied or assumed) total vertical stress, and zero vertical strain. The condition of zero horizontal strain simulates the field situation during vertically propagating plane SH waves. As the cyclic shear stress or strain is applied for a number of cycles, an excess pore water pressure develops. Errors because of system compliance are common to all undrained tests, with the magnitude of the compliance being primarily a function of the soil type. An alternative procedure for determining the undrained behavior of soil with reduced compliance is to conduct a constant volume test, where the change in the total vertical confining pressure needed to maintain constant volume is assumed to be equivalent to the change in pore pressure in the corresponding undrained test (Bjerrum and Landva, 1966; Finn et al., 1971).

Figure 3-37 includes the sketch of a simple shear apparatus, described by Finn et al. (1971), and later modified by Finn et al. (1977, 1978) to permit cyclic shear testing at constant volume. The two components of horizontal normal strain are identical to zero in this simple shear device, and the stiff pressure transducers mounted on one of the movable lateral boundaries allow measuring lateral stress during cyclic loading. In the Norwegian Geotechnical Institute (NGI) constant volume DSS tests, the lateral stresses can be measured by monitoring the electrical resistivity of the membrane wire reinforcement (Dyvik and Zimmie, 1982). A sketch of the typical NGI DSS test specimen setup is shown in Figure 3-38.

Measured stress-strain hysteresis loops are presented in Figure 3-39 for two DSS strain-controlled tests on normally consolidated and overconsolidated specimens of highly plastic marine clay samples. The degradation of shear modulus with increasing pore pressure can be evaluated from such data. Figure 3-40 includes a typical variation of secant shear modulus G with cyclic shear strain γ_c and with volumetric strain, for a clean silica sand, obtained in the DSS apparatus of Figure 3-37. It is common to use

Figure 3-36. Liquefaction of Saturated Sand in
Cyclic Torsional Shear Strain-Controlled Test (Saada, 1988).

Figure 3-37. Constant Volume Cyclic Direct Simple Shear Apparatus (Finn et al., 1978).

Figure 3-38. Norwegian Geotechnical Institute Direct Sample Shear Test Specimen Setup (Vucetic and Chu, 1990).

Figure 3-39. Typical Cyclic Stress-Strain Relationships from DDS Strain-Controlled Test on Clay (Vucetic, 1988).

Figure 3-40. Modulus Versus Cyclic Shear Strain for Various Volumetric Strains, DSS Tests in Sand (Bhatia, 1983).

DSS to study modulus and damping changes at intermediate and large strains in soft clay and sand. The measurements at low cyclic strains ($\gamma_c \leq 0.03$ percent) are generally questionable.

Wave Velocity Measurements in the Laboratory

Laboratory wave velocity measurements from directly monitoring the time required by the wave to travel a certain distance in the soil have been made for over three decades on both confined and unconfined test soil specimens. Most of these wave measurements have been compressional (P) with limited shear (S) wave applications, due to the difficulty in distinguishing between P and S waves. Because of the necessity of accurately determining S-wave velocities and thereby G_{max}, techniques were developed to generate and measure polarized S-waves where the reverse polarity could be checked, similarly to what is done with seismic techniques in the field.

Bender Elements. In this case, polarized S-waves are generated and measured by piezoceramic bender elements as described by Dyvik and Madshus (1985) and shown in Figure 3-41. They showed that when such elements were installed in a resonant column apparatus, G_{max} was basically the same by both techniques as demonstrated in Figure 3-42. They also indicated that bender elements can be incorporated into almost any testing device, such as cyclic triaxial or DSS, to provide direct measurement of G_{max} after any stress or strain history. Also, measurements of G_{max} in different tests and comparison with G_{max} measured *in situ* allow a direct method to evaluate sample disturbance effects.

Large-Scale Triaxial. A large-scale triaxial testing device for seismic wave propagation studies has been designed and constructed at the University of Texas at Austin (Kopperman et al., 1982; Stokoe et al., 1985). The device is used to load 7-foot cubes of dry sand under various states of triaxial stress with principal effective stresses ranging from 10 to 40 psi. Measurements of velocities of compression (P) and shear (S) waves propagating through the sand skeleton are performed with accelerometers and/or velocity transducers embedded in the sand. Wavelengths and frequencies are generally in the range of 0.5 to 1.5 feet and 500 to 1,500 Hz, respectively. Strains in the soil skeleton are less than 10^{-3} percent.

The large-scale triaxial device is simply a freestanding, heavily reinforced steel box as shown in Figure 3-43. Associated equipment is used to: (1) place sand into the device, (2) pressurize the sand mass to the desired stress state, (3) generate compression or shear waves in the sand, (4) monitor and digitally record these waveforms, and (5) monitor stress and strain throughout the sample during testing. A schematic drawing of the device and associated systems is shown in Figure 3-44.

Each wall of the triaxial device is designed to represent a principal plane so that axes perpendicular to the walls of the device represent principal directions. To permit independent control of the pressure in each of the three principal directions, confining

Figure 3-41. Setup for Incorporating Piezoceramic Bender Elements in the Resonant Column Apparatus (Dyvik and Madshus, 1985).

Figure 3-42. Comparison of G_{max} Measured by Resonant Column and Bender Elements (Dyvik and Madshus, 1985).

Figure 3-43.   Cut-Away, Isometric View of Large-Scale Triaxial Device (Stokoe et al., 1985).

Figure 3-44.   Schematic Diagram of Triaxial Device and Associated Systems (Stokoe et al., 1985).

pressures are applied to the soil mass using membranes placed on the inside walls of the device. With this system, either isotropic, biaxial, or true triaxial states of stress can be applied to the sand as shown in Figure 3-45.

Extensive testing has been performed under isotropic, biaxial, and triaxial states of stress. In each case, velocities of S-waves and P-waves propagating along all principal stress directions have been measured. Particle motions were always polarized along principal stress directions. Results from these tests lead to the following conclusions with regard to shear waves: (1) the effect of stress history on the values of S-wave velocities measured at the same current confining stresses is negligible, (2) the sand can be treated as a cross-anisotropic material under isotropic confinement because of structural anisotropy, with the horizontal plane being the plane of isotropy, (3) complete anisotropy results from coupling stress anisotropy and structural anisotropy, and (4) S-wave velocity and, hence shear modulus, depends about equally on the principal effective stresses in the directions of wave propagation and particle motion and is essentially independent of the third principal stress. One interesting observation from conclusion 4 with regard to field seismic tests is that, in level soil deposits, the velocity of SV-waves measured by the crosshole and downhole tests should be equal. Only the SH-wave velocity measured in the crosshole test should be different.

Physical Model Tests

Physical model tests are usually employed to simulate the response of the full scale prototype system and, as such, are not meant to be tests to obtain the fundamental stress-strain and strength properties of soil materials. However, physical model test results can be analyzed to backcalculate the soil parameters that contributed to the system response. Physical model testing is also useful in providing a validation of the analytical procedures that are used for predicting site response and, therefore, could provide a vital link between laboratory and field studies.

In order to obtain proper simulation of *in situ* conditions, physical model testing must replicate a key factor, the gravity-induced stresses, which governs the behavior of soils in the ground. Testing of small scale models under normal gravity cannot duplicate the overburden stress profile, whereas testing in the centrifuge allows this important factor to be properly simulated.

In recent years, the state of the art in centrifuge modeling has developed rapidly. Several viable techniques have been developed that allow the generation of simulated ground motion to be superposed on the steady-state acceleration in a rotating centrifuge, Figure 3-46 (Whitman and Arulanandan, 1985). Along with the development of an inflight seismic loading capability, research has also focused on reducing the container boundary effects by using an absorbing liner or by making the container from stacked rings, Figure 3-47 (Lambe and Whitman, 1985). Before these methods for

3-48

Note:
1. a is location of striking for compression waves
2. b and c are locations of striking for shear waves
3. clamping tool only used during sample construction; tool is removed during wave measurements.

Figure 3-45.   Clamping Tool and Excitation Port (Stokoe et al., 1985).

Figure 3-46.   Schematic of Centrifuge Model Test with Base Earthquake Excitation (modified from Whitman and Arulanandan, 1985).

Figure 3-47.   Schematic of Stacked-Ring Device for Simulating Column of Soil (Whitman and Arulanandan, 1985).

dynamic model testing can be universally applied to design, additional research is needed to delineate such problems as grain size effects, instrumentation, model construction techniques, and inflight soil property characterization.

One major issue that still must be clarified is the verification of the scaling relations to be used in extrapolating the model test results to prototype scale, particularly if the purpose of the centrifuge test is to directly simulate a prototype situation. Because the scaling relations that are usually associated with centrifuge testing (Table 3-4) imply a conflict between the $1/n^2$ time scale for diffusion phenomena (e.g., pore pressure dissipation) and the n-th scale model and gravity ratio, it has been suggested that a substitute pore fluid with a viscosity n times that of water be used in order to regain an identical time scale for the diffusion and dynamic phenomena. Obviously, the new problems created by the use of a substitute pore fluid need to be studied before the scheme can be accepted. In addition, the possible effect of the increased strain rate used in centrifuge testing needs to be examined carefully.

Irrespective of the validity of any scaling relation, a centrifuge model test can be viewed as an experiment in which a soil layer or structure is subjected to conditions closely approximating the field situation. The results from such a test provide the opportunity to validate any analysis that can be performed to match the test conditions. The accuracy of the analysis based on any theory depends on both the material property input and the numerical algorithm. Assuming the numerical algorithm is sufficiently robust, the material property description obtained from appropriate laboratory tests can be verified by comparing the numerical prediction with the centrifuge test measurements. Scale model testing is also a cost-effective means for validating designs, when compared with full-scale testing.

Advantages and Limitations of Laboratory Testing

The foremost advantage of performing laboratory cyclic testing is that stress history, stress path, and stress and strain levels can be controlled in most cases for both the static and cyclic parts of the test. Also, there is a large data base to check one's results and a testing program can be easily established to verify an analytical model.

The foremost limitation in performing laboratory tests is sampling/specimen disturbance, which affects the degree of *in situ* representativeness of the laboratory specimens. Also, the specimen tested is usually quite small (micro measurement versus macro application). Finally, there is the variability in test results between different test apparata, for which the causes are often not clearly understood. An example of this variability for damping ratio at small strains is presented in Figure 3-48. Causes for this variability between cyclic triaxial, DSS, resonant column, or torsional shear may include details of the testing or measurement technique, loading path, anisotropic soil, or other.

In general, different results are obtained for G_{max} when measured by different apparata/methods, with field results typically being the highest and laboratory results

Table 3-4

SCALING RELATIONS FOR GEOTECHNICAL CENTRIFUGE TESTS
(WHITMAN AND ARULANANDAN, 1985)

Quantity	Full Scale (Prototype)	Centrifugal model at n g's
Linear Dimension	1	$1/n$
Stress (Force/Area)	1	1
Strain (Displacement/Unit Length)	1	1
Density	1	1
Mass	1	$1/n^3$
Force	1	$1/n^2$
Displacement (Distance)	1	$1/n$
Velocity (Distance/Time)	1	1
Acceleration (Distance/Time^2)	1	n
Time		
in Dynamic Problems	1	$1/n$
in Diffusion Cases	1	$1/n^2$
in Viscous Flow Cases	1	1
Frequency		
in Dynamic Problems	1	n

Figure 3-48.   Example of Variability of Soil Damping Measured by Different Laboratory Techniques (Stokoe, 1989).

being lower in the following descending order: resonant column (fixed-free), resonant column (Hardin oscillator), torsional devices (hollow cylinder), torsional devices (solid cylinder), triaxial and direct simple shear. Some of these differences could be decreased, while at the same time producing an improved characterization of cyclic soil properties, by:

- Improved sampling techniques
- Improved testing techniques
- Corrections for equipment compliance
- Studying test variability

Improved Sampling Techniques. In general, they could readily be improved by use of detailed drilling specifications, experienced drillers and inspectors, and wider use of drilling mud and fixed-piston thin-walled tube samplers having a minimum O.D. of about 3 inches. Furthermore, the methodology developed by La Rochelle et al. (1981) for fine-grained soils needs to be further developed, while for coarse-grained soils the freezing methodology needs to be expanded (Osterberg and Varaksin, 1973).

Improved Testing Techniques. It has to be recognized and appreciated that testing is an art. It takes an artist to prepare the specimen, along with a specialized apparatus (which equipment manufacturers typically do not make), place it in the testing apparatus, and then when testing it to have an understanding of and to control all variables that affect the test results (time of consolidation, consolidation increments, size and rate of backpressuring, cell fluid, measurement devices, method of calculation and corrections, strain rate, equipment compliance, etc.). More emphasis must be placed on studying such effects and publishing them in appropriate journals such as ASTM's *Geotechnical Testing Journal* and its *Special Technical Publications*.

Certain test devices, like the triaxial, solid-cylinder resonant column, and direct simple shear, lend themselves to easy specimen preparation and minimal disturbance; while others, like the hollow-cylinder resonant column and torsional shear devices do not. However, the latter devices are superior in characterizing cyclic soil properties.

The SHANSEP methodology (Ladd and Foot, 1974), developed to characterize the static properties of fine-grained soils and reduce the effects of sampling and specimen preparation disturbance on such properties, has been applied to the characterization of cyclic properties of fine-grained soils by Dobry and Vucetic (1987), Vucetic and Dobry (1988), and Vucetic (1988, 1990). This approach needs to be developed further. Also, can a similar approach be developed for coarse-grained soils?

Corrections for Equipment Compliance/Friction. In the laboratory measurement of moduli and damping properties of soils, there will always be some equipment compliance/friction problem associated with:

- Membrane compliance

- Inappropriate coupling between test specimen and loading boundaries (platens)

- False deformations due to equipment compliance

- Friction

For cyclic triaxial testing, Kokusho (1980), Ladd and Dutko (1985), and Tatsuoka (1988) have shown how many of the above items can be accounted for up to a certain threshold. For example, Ladd and Dutko (1985) found that the moduli of the triaxial test equipment itself was in the order of 200,000 to 400,000 psi.

In resonant column testing, corrections for base impedance must be developed; while for torsional devices, compliance corrections have to be developed and applied. However, for direct simple shear devices, to completely account for false deformations and compliance is more difficult.

Studying Test Variability. Another testing limitation, which applies to both field and laboratory test methods, is a lack of precision and accuracy statements obtained from systematic round-robin testing programs involving several laboratories. Typically, based on limited data performed by a select group, it is assumed that our test methods are quite accurate for cyclic triaxial tests (Silver et al., 1976) and for resonant column tests (Drnevich, 1979). However, when a large round-robin testing program is performed involving many laboratories, as was done for relative density measurements (Tavenas et al., 1973), the results typically show a large variability. This large variability is most likely a result of the organizations performing the tests and not of the test method itself. This conclusion is based on the fact that when a single organization having many field laboratories (Bureau of Reclamation) performed a similar round-robin testing program, the variability was significantly reduced (Tiedemann, 1973).

The results of the above round-robin testing programs indicate that our test methods can be quite consistent when performed by selected organizations, but in the open market the test variability can be substantial. One organization that is actively working on developing test methods, along with precision and accuracy statements is ASTM, along with its subsidiary Standards Research Institute; these efforts should be encouraged and supported.

OBSERVED CYCLIC PROPERTIES OF SOILS

Results of laboratory testing programs such as described above provide an indication of what factors affect cyclic soil properties and dynamic soil behavior, including useful correlations, and suggest areas requiring further study.

G_{max}

Much work has been done in the last 30 years or so in which G_{max} (or V_s) has been measured *in situ* or in the laboratory, and has been correlated with a number of factors. It has been found that the most important factors affecting the value of G_{max} in uncemented soils are:

- Current state of effective stresses ($\bar{\sigma}_{ij}$)

- Current void ratio (e) or relative density (D_r)

- Overconsolidation ratio (OCR)

- Geological age of the deposit in the field or the time (t) since the end of primary consolidation (EOP) in the laboratory

Table 3-5 summarizes the influence of these and other factors on G_{max}, G/G_{max} and D where G and D correspond to strains ranging from small to intermediate ($\gamma \lesssim 1$ percent). Although Table 3-5 was originally developed by Dobry and Vucetic (1987) for normally consolidated and moderately overconsolidated clays, most of it also applies to other cohesive and granular soils.

Mainly on the basis of resonant column (RC) tests, Hardin (1978) developed the following empirical equation for clays, silts, and sands:

$$G_{max} = C \cdot F(e) \cdot (OCR)^k (\bar{\sigma}_o \cdot p_a)^{0.5} \qquad (3-2)$$

where:

$\quad C \quad =$ empirical constant equal to 625 according to Hardin (1978)

$\quad \bar{\sigma}_o \quad =$ mean effective stress $= (\bar{\sigma}_1 + \bar{\sigma}_2 + \bar{\sigma}_3)/3$

$\quad p_a \quad =$ atmospheric pressure

$\quad k \quad =$ exponent function of the plasticity index, PI $= I_p$ ($I_p = 0 \rightarrow k = 0$, $I_p = 100 \rightarrow k = 0.5$)

$\quad F(e) \quad =$ void ratio function assumed by Hardin (1978) to be equal to $(0.3 + 0.7\,e^2)^{-1}$

In a similar empirical expression developed by Seed and Idriss (1970) and Seed et al. (1986) for granular materials, e is replaced by relative density D_R and G_{max} is normalized with respect to $(\bar{\sigma}_o)^{0.5}$, leading to a set of modulus numbers K_{2max} which are function of D_r.

Table 3-5

EFFECT OF INCREASE OF VARIOUS FACTORS ON G_{max}, G/G_{max} AND DAMPING RATIO D OF NORMALLY CONSOLIDATED AND MODERATELY OVERCONSOLIDATED CLAYS (DOBRY AND VUCETIC, 1987)

INCREASING FACTOR	G_{max}	G/G_{max}	D
Confining Pressure $\bar{\sigma}_0$ (or $\bar{\sigma}_{vc}$)	Increases with $\bar{\sigma}_0$	Stays constant or increases with $\bar{\sigma}_0$	Stays constant or decreases with $\bar{\sigma}_0$
Void Ratio e	Decreases with e	Increases with e	Decreases with e
Geologic Age t	Increases with t	May increase with t	Decreases with t
Cementation c	Increases with c	May increase with c	May decrease with c
Overconsolidation OCR	Increases with OCR	Not affected	Not affected
Plasticity Index I_p	• Increases with I_p if OCR>1 • Stays about constant if OCR = 1	Increases with I_p	Decreases with I_p
Cyclic Strain γ_c	—	Decreases with γ_c	Increases with γ_c
Strain Rate $\dot{\gamma}$ (Frequency of cyclic loading)	Increases with $\dot{\gamma}$	• G increases with $\dot{\gamma}$ • G/G_{max} probably not affected if G and G_{max} are measured at same $\dot{\gamma}$	Stays constant or may increase with $\dot{\gamma}$
Number of Loading Cycles N	Decreases after N cycles of large γ_c but recovers later with time	Decreases after N cycles of large γ_c (G_{max} measured before N cycles)	Not significant for moderate γ_c and N

Figure 3-49. Effect of Confinement Time on G_{max} in Different Soils (Anderson and Stokoe, 1978).

Although the data base used for Eq. 3-2 had considerable scatter, it can be used for an approximate estimate of the lower bound of the *in situ* G_{max}. In general, Eq. 3-2 will tend to underestimate G_{max} because of the effect of geological age t, which is not considered in the equation. In fact, there is growing experimental evidence showing that G_{max} tends to increase with log t beyond primary consolidation, as shown in Figure 3-49 (Anderson and Stokoe, 1978). The rate of this increase, N_G, is more pronounced in normally consolidated clays, less in overconsolidated clays, and relatively small in sands.

Kokusho et al. (1982) published a correlation between N_G and the plasticity index I_p of the soil. Mesri and Castro (1987) and Mesri (1988, 1989) have linked N_G to the drained creep (or secondary compression) of the soil by means of the following empirical equation:

$$\frac{\Delta G}{G_{pmax}} = N_G \approx \exp(1.15 \frac{C_{\alpha e}/C_e}{C_r/C_c}) - 1 \qquad (3-3)$$

where:

ΔG = increase of G_{max} for cycle of log t

G_{pmax} = maximum shear modulus at the end of primary consolidation

$C_{\alpha e}$ = coefficient of secondary compression

C_c = compression index

C_r = recompression index

There are, however, indications that the influence of geological time on G_{max} in granular soil might be higher than inferred from laboratory tests. This can be explained by a number of phenomena such as:

- Cyclic prestraining due to seismic shaking (see Figure 3-50)

- Time-dependent increase in the horizontal stress

- Macrointerlocking of grains

- Macrointerlocking of grain surface roughness

Figure 3-50. G_{max} Versus Number of Cycles of Shear Prestraining, Hollow-Cylinder Torsional Shear Tests in Sand (Drnevich, 1967).

- Increase in the number and area of particle contacts due to diagenetic changes (see Figure 3-51)

- Bonding due to cementation

For more details see: Drnevich (1967), Tohno (1975), Finn (1979), Dusseault and Morgenstern (1979), Mesri and Castro (1987), Palmer and Barton (1987), Barton and Palmer (1989), Mesri (1989), and Schmertmann (1989). Most of these phenomena lead to an increase of either the effective stresses acting on the soil, the number of contacts per particle, or the area of the contacts between adjacent particles. Analytical studies in the area of micromechanics show that these are the main factors controlling G_{max} of granular media (Mindlin and Deresiewicz, 1953; Dobry and Ng, 1989).

An example of influence of the geological age on G_{max} as observed in the field is shown in Figure 3-52 (Jamiolkowski, 1989). This figure compares values of K_2 (see definition of K_2 in the figure) as inferred from V_s measured with the cross-hole technique in two sand and gravel deposits at the Messina Strait Crossing in Italy, where the construction of a 3,000-meter span suspended bridge is planned. Both deposits have very similar grading, mineralogical composition, and relative density. The only difference lies in the fact that at the anchor block location the soil deposit belongs to the Lower Pleistocene (500,000 to 1,000,000 years) while at the tower foundation site the upper 35 m of soil are of Holocene age (10,000 to 20,000 years). The observed difference in the K_2 values in the first 35 m can be attributed to the different ages of the soil.

Therefore, it seems clear that G_{max} measured in the laboratory can be significantly lower than those inferred from *in situ* measurements. In the case of cohesive soils this can be attributed to the disturbance of so-called "undisturbed" samples. For sands and gravels the common practice consists of laboratory testing of specimens reconstituted at the estimated *in situ* void ratio. In this case the difference between the laboratory and *in situ* measured values of G_{max} can be very high, generally increasing with the geologic age of the deposit.

Recent experience shows that much better agreement can be achieved in granular soils when laboratory tests are performed on undisturbed specimens obtained by freezing or impregnation techniques [see Figure 3-53 and Kokusho (1987)]. Relatively little is known about the factors influencing the values of G_{max} in gravels. This is also the case for partially saturated soils, important for soils above the water table, which have been investigated by Wu et al. (1984).

Regarding gravels, and given the inherent difficulty of testing them in the laboratory, the information available is mainly from *in situ* seismic tests (Seed et al., 1986; Stokoe et al., 1988; Jamiolkowski, 1989). The experimental evidence with respect to G_{max} in gravelly sites is still to some extent contradictory, indicating for comparable densities respectively higher and lower values in gravelly deposits as compared to sands. The general impression of the panel is that, at present, one has to assume that for a

Figure 3-51. Increase in Contact Area Between
Sand Particles Due to Diagenesis
(Dusseault and Morgenstern, 1979).

Figure 3-52.   Example of Influence of Geological
Age on G_{max} of Sand, Messina Strait Crossing-Sicilian Shore
(Jamiolkowski, 1989).

Figure 3-53.   Summary of Modulus Ratio, G_{OL}/G_{OF}, Versus
In-Situ Shear Modulus, G_{OF} (Kokusho, 1987).

comparable density and effective confining pressure the sand and the gravel deposits will have a similar value of G_{max}. In poorly graded gravelly soils in a loose state and with little sand, there are some preliminary indications that G_{max} values can occasionally be lower for gravels than for sands.

M_{max}

The compressional wave velocity (V_p), and thus also the constrained modulus at small strains $M_{max} = \rho V_p^2$, is controlled mainly by the degree of saturation of the soil. In fully saturated soil, V_p is close to or somewhat higher than the speed of sound in water ($\approx$ 5,000 ft/sec). However, when the saturation is not 100 percent, V_p decreases substantially as part of the wave energy starts propagating throughout the soil skeleton (Allen et al., 1980).

In an isotropic, homogeneous elastic medium, G_{max} and the small strain, maximum constrained modulus M_{max} are linked together by means of the following relationship:

$$M_{max} = \frac{2G_{max}(1 - \nu)}{1 - 2\nu} \qquad (3\text{-}4)$$

where ν is the Poisson's ratio of the soil.

In dry sands, Koppermann et al. (1982) has measured values of ν of the order of 0.1, much smaller than 0.3 or 0.4 typically recommended in the literature for dry and partially saturated soils. On the other hand, in a fully saturated soil, because of the high values of V_p and M_{max}, ν approaches 0.5 and the values of V_p and M_{max} calculated through Eq. 3.4 become very sensitive to the exact value of ν selected (for ν = 0.5, $M_{max} = \infty$ in Eq. 3.4). Therefore, if V_p or M_{max} is required in a saturated soil, ν should never be assumed, but, rather both G_{max} (or V_s) and M_{max} (or V_p) should be measured or estimated separately.

Anisotropic Behavior

Recent studies have shown that soils exhibit anisotropic behavior with respect to the seismic wave (V_s, V_p) velocities. The existing experimental evidence is mainly related to the propagation of seismic waves in dry sands performed in large-scale laboratory facilities such as described previously (Schmertmann, 1978; Kopperman et al., 1982; Stokoe et al., 1985; Baldi et al., 1990). These data show that, generally, sands exhibit cross-anisotropic behavior with respect to both V_s and V_p. The same tests as well as other laboratory tests (Roesler, 1979; Yu and Richart, 1984) indicate that seismic waves propagating along one of the principal stress directions depend almost exclusively on the stress components acting in the directions of wave propagation and of particle motion, being practically independent of the third out-of-plane principal stress component. This finding led to a reformulation of Eq. 3-2, which can be written in the following form:

Shear wave velocity:

$$V_s = F_s(e) \cdot C_s \cdot p_a^{(1-na-nb-nc)} \, \overline{\sigma}_a^{na} \cdot \overline{\sigma}_b^{nb} \cdot \overline{\sigma}_c^{nc} \qquad (3\text{-}5)$$

Compression wave velocity:

$$V_p = F_p(e) \cdot C_p \cdot p_a^{(1-na-nb-nc)} \, \overline{\sigma}_a^{na} \cdot \overline{\sigma}_b^{nb} \cdot \overline{\sigma}_c^{nc} \qquad (3\text{-}6)$$

Maximum shear modulus:

$$G_{max} = F_g(e) \cdot C_g \cdot p_a^{(1-2na-2nb-2nc)} \, \overline{\sigma}_a^{2na} \cdot \overline{\sigma}_b^{2nb} \cdot \overline{\sigma}_c^{2nc} \qquad (3\text{-}7)$$

Constrained modulus:

$$M_{max} = F_m(e) \cdot C_m \cdot p_a^{(1-2na-2nb-2nc)} \, \overline{\sigma}_a^{2na} \cdot \overline{\sigma}_b^{2nb} \cdot \overline{\sigma}_c^{2nc} \qquad (3\text{-}8)$$

where:

$\overline{\sigma}_a$ = effective stress in the direction of wave propagation

$\overline{\sigma}_b$ = effective stress in the direction of particle motion

$\overline{\sigma}_c$ = out-of-plane effective stress

p_a = atmospheric pressure

For compression waves, the directions of wave propagation and particle motion coincide, and thus $\overline{\sigma}_a = \overline{\sigma}_b$. Typically, for both V_s and V_p, na $\simeq$ nb = 0.09 to 0.13 and nc = 0.0 to 0.02.

Interpretation of the existing experimental data has led to the following preliminary conclusions for the small-strain anisotropy of artificially prepared sand specimens tested in the laboratory:

- Both G_{max} and M_{max} exhibit a weak dependence on the direction of the out-of-plane principal stress, which generally does not exceed ±15 percent (see Figure 3-54).

- This conclusion applies to both isotropically and anisotropically consolidated soil.

Very little information is available on the small-strain anisotropy of natural sand deposits. A rare example of such kind of information is reported in Figure 3-55.

3-65

Figure 3-54.   Effect of Stress Induced Anisotropy on Compressional Wave Velocity for Triaxial Confinement (Kopperman et al., 1982).

Figure 3-55.   Anisotropy of Shear Wave Velocity of a Natural Land
(Tanimoto, 1974).

Most systematic studies of G_{max} and M_{max} have been on uncemented sands, clays, and gravels. Relevant research on cemented sands has been conducted by Sitar (1979), Clough et al. (1981), Wang (1986), and Saxena (1987), showing the effect of cementation in increasing G_{max} (Figures 3-56 and 3-57). Information on calcareous sands, both onshore and offshore, has been reported by Dobry et al. (1988) and Nelson et al. (1989).

G/G_{max} and D Versus Strain

The curves of G/G_{max} versus cyclic strain γ_c and of material damping ratio D versus γ_c are used in the analyses together with G_{max} to define the stiffness and energy dissipation characteristics of the soil at different strain levels.

Figure 3-57 shows the influence of the plasticity index of the soil on the general locations of the curves for a wide assortment of soils ranging from clays to sands and gravels. Figure 3-57 was prepared by Vucetic and Dobry (1991), based on the previous study by Dobry and Vucetic (1987) supplemented by additional data; the chart for G/G_{max} in Figure 3-58a is essentially identical to that reported by Sun et al. (1988). Figure 3-58 shows that the transition from small to large strain behavior, associated, say, with $G/G_{max} \approx 0.8$, occurs in sands, gravels, and silts with no plasticity at strains of the order of $\gamma_c \approx 0.01$ percent and in clays of high plasticity at strains $\gamma_c \approx 0.1$ percent or larger. The small-strain behavior is quite linear, with G not very different from G_{max}, D small (D ≤ 5 percent) and essentially no change in G with number of cycles. As shown by the response of the high-plasticity Mexico City clay in the 1985 earthquake (see Figure 3-1), this linear, low-damping, small-strain seismic response of high plasticity clays can be very damaging to structures.

Figure 3-59 shows the influence of confining pressure on G/G_{max} for sands reported by Iwasaki et al. (1978). For most sands and gravels, the curve for G/G_{max} is close to those in Figure 3-58 corresponding to PI = 0 and falls within the range included in Figure 3-59. As the plasticity index increases above zero in Figure 3-58, the influence of confining pressure on the G/G_{max} curves becomes negligible (Sun et al., 1988). For a given soil, granular or cohesive, the G/G_{max} curve is typically quite stable and insensitive to wide variations in relative density or void ratio, stress history and OCR, static shear stress, and sample disturbance or method of sample preparation (Hardin and Drnevich, 1972a; Seed et al., 1986; Tatsuoka et al., 1979a, b). This justifies the current practice of combining G_{max} obtained from *in situ* measurements with G/G_{max} curves measured in the laboratory.

During cyclic loading at intermediate and high strains ($\gamma_c \geq 0.01$ percent in sands), the stiffness G of soils can change with number of cycles, and thus G/G_{max} also changes for an assumed constant G_{max}. In dry granular soils, the soil hardens and G/G_{max} increases (Finn et al., 1982), while in saturated sands and clays the soil degrades and G/G_{max} decreases (Dobry et al., 1982; Finn, 1985; Dobry and Vucetic, 1987). While the effect is not so pronounced in clays, it is very important in saturated sands (Figure 3-60), and

3-68

Figure 3-56.   Maximum Young's Modulus, E_{max}, Versus
Confining Pressure for Cemented Sands
(Clough et al., 1981).

Figure 3-57.   Shear Modulus in Cemented and Uncemented Sands
from Cyclic Triaxial and DSS Tests (Wang, 1986).

Figure 3-58.   Influence of Plasticity Index on Modulus and Damping
Curves of Saturated Soil (Vucetic and Dobry, 1991).

Figure 3-59.   Influence of Confining Pressure on the G/G_{max} Versus γ_c Curve for Sands (Iwasaki et al., 1978; reproduced by Seed et al., 1986).

Figure 3-60.   Stress-Strain Loops in DSS Contant Volume Cyclic Strain-Controlled DSS Test on Sand (Finn, 1985).

it can modify dramatically the response of a site as shaking progresses (see also Figure 3-2). In many saturated soils, the modulus degradation during strain-controlled cyclic loading can be approximated by $G_N = G_1 N^{-t}$, where G_1, G_N = modulus in cycle 1, N, and t = degradation parameter function of the cyclic sheer strain of the test (Idriss et al., 1978). Figure 3-61 illustrates the variation of t with γ_c and plasticity index, PI, of the soil (Tan and Vucetic, 1989).

Since the studies of Hardin (1965), Seed and Idriss (1970) and Dobry (1970), it is widely accepted that the nature of the material damping of soils is generally hysteretic rather than viscous, meaning that most of the energy loss is attributed to friction between the soil particles. Hence, both the modulus and damping ratio are almost constant at different frequencies. Many previous data have also shown that the damping ratio is strain-dependent because of this nonlinear hysteretic nature. If the soil damping were purely hysteretic, it would converge to zero at small strains. However, Saada and Macky (1985), Bianchini and Saada (1981), and Bianchini (1985) have suggested that D converges to some low value that is apparently larger than zero. These and other authors (Vucetic and Dobry, 1991) have found values of D ranging from about 0.5 percent to 5 percent at very small strains ($\gamma \simeq 10^{-4}$ percent). Further research is required to define the lower limit of damping for a variety of soils as well as the physical mechanism responsible for it.

Damping ratios of various soils have been measured in resonant-column, cyclic triaxial, cyclic simple shear, and torsional shear devices, and all data clearly indicated the strain dependency of the damping ratio. In clean sand there is some influence of confining pressure as well, while void ratio has a minimum effect (Tatsuoka et al., 1978). Figure 3-62 shows the experimental band of D for a variety of sands. For gravels, the damping ratio has been observed to depend not only on the confining stress but also on the shape of the grains (Kokusho et al., 1981). In cohesive soils, the plasticity index appears to appreciably affect the damping as shown in Figure 3-58, while confining pressure and overconsolidation ratio are not very important. In fact, Figures 3-58 and 3-62 illustrate a very important fact: that the main factor affecting the curve of D versus γ_c for most noncemented or collapsible soils, be they cohesive or granular, is its plasticity index (Dobry and Vucetic, 1987; Vucetic and Dobry, 1991). This suggests that the magnitude of the damping ratio at a given strain is determined to a large extent by the microstructure of the soil.

Figure 3-63 summarizes curves of D versus γ_c for various soils presented by Kokusho (1987). Standard deviations statistically derived from test data are shown as bands for three kinds of soils (sand, gravel, and clay). Cohesive soils having almost the same damping ratio as sandy soils at a low strain level can exhibit a remarkably lower damping ratio than sands at higher strains.

As discussed previously, *in situ* measurement of soil damping is much more difficult than that of shear modulus (see also Kokusho, 1987). There have been, however, a few cases in which *in situ* damping ratios were calculated from attenuation of propagating

Figure 3-61. Influence of Plasticity Index, PI, on Rate of
Cyclic Stiffness Degradation of Saturated Soils
(Tan and Vucetic, 1989).

Figure 3-62.   Measured Damping Ratios in Sands (Seed et al., 1986).

Figure 3-63.   Damping Ratios for Various Soils from Many Test Results (Kokusho, 1987).

waves in seismic surveys or vibrator tests. The internal damping ratio may be also measured in the field by low-frequency cyclic loading tests on the ground surface or in boreholes (Kokusho, 1987). Table 3-6 lists *in situ* damping ratios measured in various soils by Japanese workers with different methods. All data in Table 3-6 correspond to small strain levels of the order of 10^{-4} percent or less. These data are categorized and plotted in Figure 3-64. With few exceptions, the damping ratios of silts and clays are between approximately 1 to 3 percent, while those of sands are 1 to 5 percent. Higher damping values are evident for gravelly soils. Kokusho (1987) noted that the *in situ* damping is generally higher than the laboratory damping for sands and gravels and vice versa for clayey soils. The laboratory damping ratio of clayey soils may be somewhat decreased due to the long time consolidation effect, possibly becoming identical to or smaller than the *in situ* values. On the other hand, a close agreement has been found in Japan between *in situ* damping estimated by the optimization method applied to earthquake records and laboratory damping for the same soil. Further research is certainly required before more definite conclusions can be drawn on the relation between damping obtained *in situ* and in the laboratory for a variety of soils.

The statements made in this section about G/G_{max} and D, and especially the correlations with plasticity index in Figures 3-58 and 3-61, are valid for regular uncemented sands, silts, and clays. They are not necessarily true for cemented soils or for other soils having very sensitive structures such a quick clays or loess, or having different mineralogies like carbonated sands or calcareous soils, or for geologically very old or prestrained soils such as shown in Figures 3-50, 3-51 and 3-52. This is illustrated by the experimental results on a quick clay and on cemented sands reproduced in Figures 3-65 to 3-67. Not much is known about the G/G_{max} behavior of these other soils, and direct experimental determinations are recommended for site-specific studies.

Large Strain and Strength Properties

As mentioned previously, at large cyclic strains of the order of 1 percent or larger, the secant shear modulus G of the soil is only vaguely related to G_{max}. Therefore, at these large strains G needs to be specified independently for each soil based mainly on the strength response of the soil rather than extrapolated from an assumed G/G_{max} curve.

The specification of large strain soil properties--in the form of a G/G_{max} versus γ_c or of a τ_c versus γ_c backbone curve--determines the site response for very violent shaking and/or soft soil. It also determines the maximum acceleration that the soil is allowed to transmit during nonlinear site response calculations (Figure 3-6).

Much is known on the monotonic stress-strain behavior of soils at these large strains from static tests and static soil mechanics studies. This information can and should be used when specifying large strain properties for site response analyses. However, this static information needs to be modified to account for strain-rate effects (Figure 3-68) as well as for stiffness degradation during cyclic loading (Figure 3-60). In saturated

Table 3-6

DAMPING RATIOS OF VARIOUS SOILS MEASURED IN THE FIELD BY JAPANESE RESEARCHERS (KOKUSHO, 1987)

Damping ratio (%)	Soil	Shear wave velocity, V_s (m/sec.)	Depth (m)	Measuring method
6	Diluvial sand	260		Down-hole survey
2.5	Alluvial clay/silt	80 ~ 100		
10	Loam	150		
8	Mudstone	420	10 ~ 20	
5	Silt/sand	150 ~ 200	25 ~ 40	Down-hole survey
6	Clay core of dam	500	15	
8	Gravel	350	30	Vibrator test (S_H-wave)
6	Sandstone	800		
1 ~ 3	Ariake Clay			Vibrator test (Surface wave)
2	Alluvial silt	80 ~ 100	2 ~ 6	
5 ~ 7	Loam			Down-hole survey
1 ~ 3	Clay			
1 ~ 4	Sand		40 ~ 51	
1.5 ~ 2	Alluvial silt	160	14 ~ 28	
3.1	Alluvial sand	210	12 ~ 25	
0.3	Alluvial silt	140	25 ~ 35	
2	Alluvial clay	20 ~ 100	0 ~ 20	Optimization of earthquake records
2 ~ 5	Sand	120 ~ 400		
5	Gravel	300 ~ 600		

Note: Soil strain is in the order of 10^{-6} or less.

Figure 3-64. a) In-Situ Damping Ratios for Various Soils; and b) Comparison of In-Situ and Laboratory Damping Ratios (Kokusho, 1987).

Figure 3-65. Modulus and Damping Curves for Mexico City
Clay and a Canadian Quick Clay (Dobry, 1988, data
from Romo and Jaime, 1986, and Lefebvre, 1988).

Figure 3-66.　Damping Ratio Versus Cyclic Strain in Cemented and Uncemented Sands from Cyclic Triaxial and DSS Tests (Wang, 1986).

Figure 3-67.　Damping Ratio Versus Cyclic Shear Strain for Cemented and Uncemented Sand in Resonant Column Tests (Stokoe, 1989).

Figure 3-68.　Stress-Strain Curves from Static and Dynamic Monotonic Undrained Triaxial Tests on Saturated Clay (Dobry and Vucetic, 1988).

Figure 3-69.　Monotonic Undrained Triaxial Test on Contractive Loose Saturated Sand (Baziar, 1990).

soils, more research is needed on how to analytically model the contractive (Figure 3-69) or dilative (Figures 3-70 and 3-71) response of the material in site response analyses.

SUMMARY RECOMMENDATIONS BY PANEL

In what follows, eleven recommendations are presented for areas that require improvement and further research. They have been classified into seven highest priority and four high priority recommendations.

HIGHEST PRIORITY RECOMMENDATIONS

Arrays

The use of arrays to back-calculate and verify the cyclic properties of the soil from actual earthquake records is strongly recommended. Priority should be given to soft cohesive and loose saturated granular sites, as they have been shown to be most hazardous during earthquakes. However, sites more representative of "good" soil conditions such as medium dense or dense granular sites should also be considered. Both maximum use of records from existing arrays and the installation of new arrays at appropriate sites are recommended. In addition to aspects of arrays dealt within Chapter 7, specific attention and adequate support should be paid to their use in soil property determinations. This includes installing in the soil adequate specific instruments for this purpose in addition to strong motion accelerometers (devices for strain measurements, piezometers in saturated deposits, etc.), documentation of the site with soil exploration, *in situ* and laboratory static and cyclic determinations, and detailed backcalculations (such as shown in Figure 3-18) and site response studies once earthquake records are obtained.

In Situ Techniques

There is a considerable need to improve the existing techniques and/or to develop new ones for measuring the cyclic stress-strain properties of soils *in situ* at strain levels higher than 10^{-3} percent, thus extending our present capabilities beyond the measurement of G_{max} and confined compression modulus at small strains.

The standard existing techniques to obtain small strain cyclic properties are the seismic methods and especially the crosshole test. Efforts should continue to transmit enough energy with these tests to induce in the soil strains higher than 10^{-3} percent and to appropriately interpret the measurements.

Also, the pressuremeter test, and especially that performed using the self-boring device (SBP) deserve further attention. The unload-reload loops performed during a drained expansion test in sands seem to allow assessment of the secant shear modulus G at a

Figure 3-70.   Shear Strains and Pore Pressures During Undrained Cyclic Loading of Saturated Dilative Sand (Ishihara et al., 1975).

Figure 3-71.   Undrained Cyclic Stress-Strain Curves for Saturated Dilative Sand (Ishihara, 1985).

shear strain level ranging between about 0.05 and 0.5 percent. In principle, the unload-reload loop resulting from SBP tests could also allow for an assessment of the damping ratio D.

A more extensive use of the SBP test to assess G and D of granular soils will require further research oriented toward:

- A deeper insight into the problem of the average stress and strain level to which the soil is subjected around the expanded cavity

- Improvement of the precision of the cavity strain and pore pressure measured during the expansion test

- Comparison of G obtained from other *in situ* and laboratory tests with those resulting from the SBP tests, taking into account the influence of stress and strain level as well as possible anisotropy

The profession must also look for the development of new *in situ* techniques and related interpretation methods permitting us to evaluate G and D at intermediate and possibly large strains for a wide variety of soils. Interesting attempts in this direction are represented by proposed cylindrical probes and torsional shear systems.

Reconciliation of Laboratory Techniques

An important current problem is the discrepancy in the values of the secant shear modulus G and internal damping ratio D obtained with different laboratory techniques at both small ($\gamma \lesssim 10^{-3}$ percent) and intermediate ($10^{-2} \lesssim \gamma \lesssim 1$ percent) strains. This problem requires further research until consistency is achieved and a consensus is developed on the best way of determining these soil parameters in the laboratory for use in site response calculations.

Part of the differences in G values between various techniques may be due to actual differences in stiffness. This could be allowed if G_{max} were measured for each specimen (see recommendation below on "Simple Low Strain Technique for Laboratory") and the comparisons were made between values of G/G_{max} instead of between values of G. However, the problem obviously goes beyond that, and both G and D are affected by test conditions in ways that are poorly understood, but which most probably relate to different consolidation, boundary and loading conditions applied in the various tests, including different degrees of soil anisotropy.

The measurement of the maximum shear modulus G_{max} in horizontal-vertical planes can best be obtained from a resonant column test on a hollow cylinder excited in the torsional mode, or, alternatively, from piezoelectric elements. Similarly, the measurement of Young's modulus E_{max} is best obtained with axial excitation in the resonant column test. A carefully conducted triaxial test should also yield the same result.

It is assumed that the same levels of strain are measured in both torsional and triaxial tests with equivalent accuracy, which is feasible. For larger strains, it would be instructive to compare secant and tangent moduli obtained from slow cyclic tests conducted in the torsional and triaxial devices, as well as with moduli obtained with the resonant column. Since it is expected that the developing anisotropy and nonlinearity would be different in both cases, one should expect that the resulting stiffnesses might also be different.

Studies to Solve/Reduce/Correct for Sample and/or Specimen Disturbance

Every laboratory cyclic testing program should be concerned about how sample specimen disturbance affects the test results and how such disturbance can be eliminated. Cyclic shear modulus G is especially sensitive to this disturbance. If the disturbance is not eliminated, the variability of the test results can easily become unacceptably large.

A possibility that has been proposed and should be further explored is the use for cyclic loading of a methodology similar to SHANSEP, which has been applied systematically in the past to static analysis involving cohesive soils. Can this approach (requiring consolidating the soil to stresses higher than those *in situ*, and then correlating the cyclic properties with parameters such as confining pressure and overconsolidation ratio), be applied systematically to all or some of the cyclic properties of cohesive soils? When is it more appropriate to reconsolidate the specimens to the existing *in situ* stresses? Also, how can a related methodology be developed for sand?

For sampling disturbance, available field sampling techniques (block, freezing, large tube, etc.) should be reviewed and documented for each of the various soil types of interest (sands, sensitive clays, gravels, gravelly sands, etc.). This review could constitute a major effort; much of this information is buried deep within a number of Nuclear Regulatory Commission reports.

"Special" Soils

More experimental determinations and systematic studies are needed, both *in situ* and in the laboratory, on the cyclic properties of "special" soils.

A "special" soil is defined here as any soil which is not a fully saturated clay or a clean quartz sand, such as used in most systematic studies so far. Several of these "special" soils are, in fact, quite "general," as they are very important in many areas of the United States and around the world. Examples are: partially saturated soils; gravels; mixed soils, such as silty sands or clayey gravels; cemented sands; calcareous soils; loess and other collapsible soils; and quick clays.

Damping at Small Strains

The internal damping ratio D at small strains (10^{-4} percent or 10^{-3} percent) requires both theoretical and experimental clarification. We need to reassure ourselves that we are measuring the damping in the soil and not in the testing equipment. We also need to understand the physical origin of this small strain damping (is it viscous?) including studies at the microstructural level. The issue is important for two reasons. In non-linear analyses we have to add some damping at small strains to avoid instabilities, and we usually do it by adding an equivalent viscous damping at resonance, without really knowing what we are doing. The second reason is that D at 10^{-4} percent is an important contributor to D in a much wider strain range up to 10^{-2} percent or 10^{-1} percent, and in a soft site on hard rock the amplification of this shaking at resonance may depend strongly on this internal damping D, as shown by the 1985 earthquake in Mexico City.

Improve Modeling at Large Strains

In current nonlinear site response analysis, the cyclic behavior at large strains ($\gtrsim 1$ percent) and the cyclic stress-strain degradation of saturated soils are typically modeled with simple rules, including very often the specification of a maximum shear strength. Experimental and analytical studies should be performed to clarify the validity of these simple rules and their effect on site response. Special emphasis should be placed on their role in limiting the calculated ground surface accelerations, and the comparison of these predictions with observed acceleration values. In the case of saturated soils, different procedures and models should be developed for contractive and dilative soils, and attention should be paid to the changes in the shapes of backbone curve and hysteresis loops during degradation, as well as to the substitution of Masing criterion by more appropriate models when necessary. Both cohesive and granular soils, stiffness and damping aspects, and the effect of rotation of principal stresses, should be considered.

HIGH-PRIORITY RECOMMENDATIONS

Simple Low Strain Technique for Laboratory

Efforts to develop simple technique(s) for nondestructive measurement of G_{max} and other cyclic properties at small strains ($\gamma \simeq 10^{-4}$ percent or 10^{-3} percent) in the laboratory are recommended. A main objective should be to use the technique(s) on samples or specimens prior to (or during) static or cyclic tests such as consolidation, triaxial, simple shear, and torsional shear. In the case of torsional shear, use of the resonant column may be appropriate, while in other tests the use of piezoelectric elements (e.g., bender elements or other) may be the answer.

The technique(s) should be simple, inexpensive, easy to apply, easy to interpret, and adaptable to different laboratory tests. These measurements will provide the G_{max}

values needed to calculate G/G_{max} of the specimen when cyclic tests are conducted; will allow comparing G_{max} with *in situ* determinations, thus perhaps helping evaluate the effect of sample disturbance; will allow comparison of stiffness of different samples or specimens, thus helping evaluate spatial variability at the site; and will help quantify the change in small-strain stiffness during static or cyclic loading at high strains.

Laboratory and Field Testing Technology Transfer

The results of cyclic soil measurements in the field and in the laboratory are typically complex and can be easily wrong because of errors in the determinations or their interpretation. The person or group in charge of them must understand the basic concepts and objectives of the tests and must be properly trained in how to conduct and interpret them. Efforts should be made to assure that the accumulated experience in the art of correct testing procedures existing at a number of laboratories is disseminated and transferred to others. In addition to personal contacts and visits, this will require organized technology transfer efforts, such as seminars, short courses, publications, videos, etc.

Centrifuge Tests

Centrifuge model shaking tests--especially those simulating free-field conditions--are an available useful and cost-effective tool to study the response of soil deposits in the laboratory under simulated seismic excitation. Although not specifically designed to measure cyclic soil properties, these can be backcalculated from the tests in a way similar to records from arrays in the field. Centrifuge model testing can be especially useful to guide and validate nonlinear analytical predictions for liquefiable deposits, as well as for any deposit subjected to large seismic strains. In addition to generic centrifuge investigations, model tests can also be useful as part of specific array studies. Also, additional research is recommended on the effects of centrifuge test boundary conditions, scaling relations, and strain rate effects.

Micromechanical Studies

Further basic micromechanical studies are needed to provide a more fundamental understanding of the cyclic properties and behavior of soils. Numerical simulations of random arrays of elastic rough particles representing granular soils--and somewhat more complex models for cohesive soils--have proven effective and should continue being used for this purpose, utilizing methods such as the discrete element technique. This will help clarify the influence of various factors controlling the G_{max}, G/G_{max}, and D in the field and under various laboratory conditions. It will also help model the stress-strain behavior under complex stress and strain paths, including 2D and 3D cyclic loading at any strain level and for both drained and undrained conditions. Continuing development of the analytical techniques--as well as comparison with experimental results--are recommended to refine the simulations and increase their credibility.

Existing experimental techniques, such as fabric measurements in sands and other granular soils using thin sections and image analyzers, have also proven useful in providing valuable data to support and verify the numerical micromechanical simulations described above. These techniques should be further developed and used to improve our basic micromechanical understanding.

REFERENCES

A. Alarcon-Guzman, G. A. Leonards, and J. L. Chameau. "Undrained Monotonic and Cyclic Strength of Sands." Journal of the Geotechnical Engineering Division, ASCE, 114(10), 1988, pp. 1,089-1,109.

A. Alarcon-Guzman, J. L. Chameau and G. A. Leonards. "A New Apparatus for Investigating the Stress-Strain Characteristics of Sands." Geotechnical Testing Journal, ASTM, Vol. 9, No. 4, 1986, pp. 204-212.

N. F. Allen, F. E. Richart, Jr. and R. D. Woods. "Fluid Wave Propagation in Saturated and Nearly Saturated Sand." Journal of the Geotechnical Engineering Division, ASCE, GT3, March 1980, pp. 235-254.

D. G. Anderson, and K. H. Stokoe II. "Shear Modulus: A Time-Dependent Soil Property." Dynamic Geotechnical Testing, ASTM STP564, 1978, pp. 66-90.

K. K. Arulmoli, K. Arulanandan and H. B. Seed. "New Method for Evaluating Liquefaction Potential." Journal of the Geotechnical Engineering Division, ASCE 111(1), 1985, pp. 95-114.

ASCE. "Advances in the Art of Testing Soils Under Cyclic Conditions." Proceedings of a session sponsored by the Geotechnical Engineering Division in conjunction with the ASCE Convention in Detroit, Michigan, V. Khosla, ed., October 24, 1985.

ASTM. "Dynamic Geotechnical Testing." Special Technical Publication 654. M. L. Silver, and D. Tiedman, eds. A Symposium by ASTM Committee on Soil and Rock for Engineering Purposes, American Society for Testing and Materials, Denver, Colorado, June 28, 1977.

G. Baldi, V. N. Ghionna, S. Jamiolkowski, and D. O'Neill. "Seismic Tests on Ticino Sand in Calibration Chamber." Proceedings, IV Seminar on Research Involving Validation of In Situ Devices in Large Calibration Chambers, IGM, University of Grenoble, Grenoble, France, 1990.

G. Baldi, D. Bruzzi, S. Superbo, S. Battaglio and M. Jamiolkowski. "Seismic Cone in Po River Sand." Proceedings, ISOPT I, Orlando, Florida, 1988.

G. Baldi, M. Jamiolkowski, D. C. F. Lo Presti, G. Manfredini, and G. J. Rix. "Italian Experience in Assessing Shear Wave Velocity from CPT and SPT." Proceedings, XII ICSMFE, Rio de Janeiro, 1989.

G. Baldi, R. Bellotti, V. N. Ghionna, M. Jamiolkowski and D. C. F. Lo Presti. "Modulus of Sands from CPT's and DMT's." Proceedings, XII ECSMFE, Vol. 1, Rio de Janeiro, 1989a.

M. E. Barton, and S. N. Palmer. "The Relative Density of Geologically Aged British Fine and Fine-Medium Sands." Quarterly Journal of Engineering Geology, Vol. 22, 1989.

M. H. Baziar. "Permanent Deformations due to Seismically Induced Liquefaction." Dissertation to be submitted in partial fulfillment of the requirement for the degree of Doctor of Philosophy, Department of Civil Engineering, Rensselaer Polytechnic Institute, Troy, NY (in preparation), 1990.

R. Belloti, V. N. Ghionna, M. Jamiolkowski, and P. K. Robertson. "Design Parameters of Cohesionless Soils from In-Situ Tests." Submitted to Specialty Session on In-Situ Testing of Soil Properties for Transportation Facilities, sponsored by Committee A2L02 - Soil and Rock Properties, National Research Council, Transportation Research Board, Washington, January, 1989.

S. K. Bhatia. "The Verification of Relationships for Effective Stress Method to Evaluate Liquefaction Potential of Saturated Sands." Ph.D Thesis, Department of Civil Engineering, University of British Columbia, Vancouver, B.C., Canada, 1983.

G. Bianchini and A. Saada. "Effect of Anisotropy and Strain on the Dynamic Response of Clay Soil." Proceedings of the 10th International Conference on Soil Mechanics and Foundation Engineering, Stockholm, 1981.

G. Bianchini. "Evaluating Nonlinear Soil Behavior Using the Resonant Column." Proceedings of Advances in the Art of Testing Soils Under Cyclic Conditions, ASCE, 1985, pp. 197-231.

L. Bjerrum and A. Landva. "Direct Simple-Shear Test on a Norwegian Quick Clay." Geotechnique, Vol. 16, No. 1, 1966, pp. 1-20.

J. L. Bratton and C. J. Higgins. "Measuring Dynamic In-Situ Geotechnical Properties." Proceedings of the ASCE Geotechnical Engineering Division Specialty Conference on Earthquake Engineering and Soil Dynamics, Pasadena, California, June 19-21, Vol. I, 1978, pp. 272-289.

P. M. Byrne, F. M. Salgado and J. A. Howie. "Relationship Between the Unload Shear Modulus from Pressuremeter Tests and the Maximum Shear Modulus for Sand." Proceedings, III International Symposium on Pressuremeters, Oxford University, Oxford, U.K., 1990.

R. G. Campanella and P. K. Robertson. "Seismic Cone Penetrometer to Measure Engineering Properties of Soil." LIV Annual International Meeting and Exposition of the Society of Exploration Geophysicists, Atlanta, Georgia. 1984.

C.-Y. Chang, C. M. Mok, M. S. Power, Y. K. Tang, H. T. Tang, and J. C. Stepp. "Equivalent Linear Versus Nonlinear Ground Response Analyses at Lotung Experiment Site." Proceedings, Fourth National Conference on Earthquake Engineering, Palm Springs, California, Vol. 1, 1990, pp. 327-336.

H. H. Chu and M. Vucetic. Settlement of a Compacted Clay Under Cyclic Direct Simple Shear Loading. Research Report, Department of Civil Engineering, University of California, Los Angeles, 1990.

G. W. Clough, N. Sitar, R. C. Bachus, and N. Shafii Rad. "Behavior of Cemented Sands Under Static Loading." Journal of the Geotechnical Engineering Division, ASCE, Vol. 107, 1981, pp. 799-818.

G. W. Clough, J. Iwabuchi, N. Shafii Rad, and T. Kuppusamy. "Influence of Cementation on the Liquefaction of Sands." Journal of the Geotechnical Engineering Division, ASCE, Vol. 115, 1989, pp. 1102-1117.

R. Dobry. Damping in Soils: Its Hysteretic Nature and the Linear Approximation. M.I.T. Research Report, R70-63, January 1970.

R. Dobry, R. S. Ladd, F. Y. Yokel, R. M. Chung, and D. Powell. "Prediction of Pore Water Pressure Buildup and Liquefaction of Sands During Earthquakes by the Cyclic Strain Method." National Bureau of Standards Building Science 138, Washington, D.C., April 1982.

R. Dobry, D. J. Powell, F. Y. Yokel, and R. S. Ladd. "Liquefaction Potential of Saturated Sand--The Stiffness Method." Proceedings, VII World Conference on Earthquake Engineering, Istanbul, Turkey, September, Vol. 3, 1980, pp. 25-32.

R. Dobry, R. H. Stokoe II, R. S. Ladd, and T. L. Youd. "Liquefaction Susceptibility from S-Wave Velocity." Proceedings, Session on In Situ testing to evaluate liquefaction susceptibility, ASCE National Conv., St. Louis, Missouri, October, 1981.

R. Dobry and M. Vucetic. "Dynamic Properties and Seismic Response of Soft Clay Deposits." Proceedings, International Symposium on Geotechnical Engineering of Soft Soils, Mexico City, August 13-14, Vol. 2, 1987, pp. 51-87.

R. Dobry. "Geotechnical Aspects of Mexico City Response, or, Can it Happen Again at Other Soft Clay Sites." Presentation at EERI Annual Meeting, San Francisco, February 9, 1988.

R. Dobry. "Soil Effect on Strong Seismic Ground Motions: An Interdisciplinary Problem." Seminar presented at the Geophysical Institute, National University of Mexico, Mexico City, August 18, 1988a.

R. Dobry, T.-T. Ng, R. S. Ladd, and L. C. Reese. "Modelling of Pore Pressures and Shear Moduli in Calcareous Soils by Strain--Controlled Cyclic Triaxial Testing." Proceedings of the International Conference on Calcareous Sediments, R. J. Jewell and M. S. Khorshid, Eds., Perth, Australia, 1988.

R. Dobry, A.-W. Elgamal, M. H. Baziar, and M. Vucetic. "Pore Pressure and Acceleration Response of Wildlife Site During the 1987 Earthquake." Proceedings, Second U.S.--Japan Workshop on Liquefaction, Large Deformation and Effects on Buried Pipelines, Niagara Falls, New York, Sept. 26-29, 1989.

R. Dobry and T.-T. Ng. "Discrete Modelling of Stress-Strain Behavior of Granular Media at Small and Large Strains." Invited Paper, 1st U.S. Conference on Discrete Element Methods, Colorado School of Mines, Golden, Colorado, October 19-20, 1989.

L. Dormieux and J. Canou. "Determination of Dynamic Characteristics of a Soil Based on a Cyclic Pressuremeter Test." Proceedings, III International Symposium on Pressuremeter, Oxford, University, Oxford, U.K., 1990.

V. P. Drnevich. "Recent Developments in Resonant Column Testing." Richart Commemorative Lectures, R. D. Woods, ed., ASCE Convention, Detroit, Michigan, 1985, pp. 79-107.

V. P. Drnevich. "Effects of Strain History on the Dynamic Properties of Sand." Ph.D Dissertation, University of Michigan, Ann Arbor, Michigan, 1967.

V. P. Drnevich. "Results of Resonant Column Round Robin Testing Program." (Draft), ASTM Subcommittee D18.09, January 1979.

M. B. Dusseault, and N. R. Morgenstern. "Locked Sand." Quarterly Journal of Engineering Geology, Vol. 12, 1979.

R. Dyvik, and T. F. Zimmie. "Lateral Stress Measurements During Static and Cyclic Direct Simple Shear Testing." Proceedings of the 3rd International Conference on the Behavior of Offshore Structures, Cambridge, MA, August, Vol. 2, 1982, pp. 363-372.

R. Dyvik, and C. Madshus. "Lab Measurements of G_{max} Using Bender Elements." Proceedings, Advances in the Art of Testing Soils Under Cyclic Conditions, ASCE, V. Khosla, ed., 1985, pp. 186-196.

M. Fahey and R. J. Jewell. "Effect of Pressuremeter Compliance on Measurement of Shear Modulus." Proceedings, III International Symposium on Pressuremeters, Oxford University, Oxford, U.K., 1990.

W. D. L. Finn. "Role of Foundation Soils in Seismic Damage Potential." Proceedings, Third Canadian Conference of Earthquake Engineering, June, Montreal, Vol. 1, 1979, pp. 77-114.

W. D. L. Finn. "Liquefaction Potential: Developments Since 1976." Proceedings of the International Conference on Recent Advances in Geotechnical Earthquake Engineering and Soil Dynamics, St. Louis, Vol. II, April 26 through May 3, 1981, pp. 665-681.

W. D. L. Finn. "Aspects of Constant Volume Cyclic Simple Shear." Proceedings, Advances in the Art of Testing Soils Under Cyclic Conditions, ASCE, V. Khosla, ed., 1985, pp. 74-98.

W. D. L. Finn, D. J. Pickering, and P. L. Bransby. "Sand Liquefaction in Triaxial and Simple Shear Tests." Journal of the Soil Mechanics and Foundations Division, ASCE, 97(SM4), Proc. Paper 8039, April 1971, pp. 639-659.

W. D. L. Finn, and Y. P. Vaid. "Liquefaction Potential from Drained Constant Volume Cyclic Simple Shear Tests." Proceedings, 6th World Conference on Earthquake Engineering, New Delhi, India, January, Session 6, 1977, pp. 7-12.

W. D. L. Finn, Y. P. Vaid, and S. K. Bhatia. "Constant Volume Cyclic Simple Shear Testing." 2nd International Conference on Microzonation, San Francisco, California, November 26 - December 1, 1978.

J. Ghaboussi and S. U. Dikmen. "Liquefaction Analysis for Multidirectional Shaking." Journal of the Geotechnical Engineering Division, ASCE, Vol. 107, No. GT5, May 1981, pp. 605-627.

V. N. Ghionna, M. Jamiolkowski, G. J. Rix, and K. H. Stokoe II. "Initial Tangent Modulus of Sands from Penetration Tests," 1985.

P. Gilbert and R. Donaghe. "Cyclic Rotation of Principal Planes to Investigate Liquefaction of Sands." Miscellaneous Paper GL-83-24, WES, Vicksburg, Miss., 1983.

B. O. Hardin. "The Nature of Damping in Sands." Proceedings, ASCE, 91, No. SM1, January, 1965, pp. 63-97.

B. O. Hardin and V. P. Drnevich. "Shear Modulus and Damping in Soils: Measurements and Parameter Effects." Journal of the Soil Mechanics and Foundations Division, ASCE, 98(SM6), 1972a, pp. 603-624.

B. O. Hardin and V. P. Drnevich. "Shear Modulus and Damping in Soils: Design Equations and Curves." Journal of the Soil Mechanics and Foundations Division, ASCE, 98(SM7), July, 1972b, pp. 667-692.

B. O. Hardin. "The Nature of Stress--Strain Behavior for Soils." Proceedings of the Specialty Conference on Earthquake Engineering and Soil Dynamics, ASCE, Pasadena, Vol. 1, 1978, pp. 3-90.

N. A. Haskell. "The Dispersion of Surface Waves in Multilayered Media." Bulletin of the Seismological Society of America, Vol. 43, 1953, pp. 17-34.

W. Henke and R. Henke. In Situ Testing Procedure for Obtaining Dynamic and Cyclic Soil Properties. Report prepared for the National Science Foundation by Dynamic in Situ Geotechnical Testing, Inc., March 1990.

C. Higgins. Personal communication, 1989.

D. Hight, D. W. Gens and M. J. Synes. "The Development of a New Hollow Cylinder Apparatus for Investigating the Effects of Principal Stress Rotation in Soils." Geotechnique, Vol. 33, No. 4, December 1983, pp. 355-383.

R. J. Hoar and K. H. Stokoe, II. "Generation and Measurement of Shear Waves In Situ." Dynamic Geotechnical Testing, ASTM, STP 654, 1977, pp. 3-29.

M. E. Hynes. "Pore Pressure Generation Characteristics of Gravel Under Undrained Cyclic Loading." Ph.D. Thesis, Department of Civil Engineering, University of California, Berkeley, 1988.

I. M. Idriss, R. Dobry and R. D. Singh. "Nonlinear Behavior of Soft Clays During Cyclic Loading." Journal of the Geotechnical Engineering Division, ASCE, Vol. 104, No. GT12, December, 1978, pp. 1427-1447.

K. Ishihara, F. Tatsuoka, and S. Yasuda. "Undrained Deformation and Liquefaction of Sand Under Cyclic Stresses." Soils and Foundations, 15(1), 1975, pp. 29-44.

K. Ishihara. "Stability of Natural Deposits During Earthquakes." Proceedings of the Eleventh International Conference on Soil Mechanics and Foundation Engineering, San Francisco, 1985, pp. 321-376.

T. Iwasaki, F. Tatsuoka, and Y. Tagaki. "Shear Moduli of Sands Under Cyclic Torsional Shear Loading." Soils and Foundations, 18(1), 1978, pp. 39-56.

M. Jamiolkowski, and P. K. Robertson. "Closing Address. Future Trends for Penetration Testing." Geotechnology Conference on Penetration Testing in the UK, July 6-8, 1988, pp. 21-42.

M. Jamiolkowski. Personal communication, 1989.

M. Jamiolkowski, D. C. F. Lo Presti, G. Manfredini, and G. J. Rix. "Italian Experience in Assessing Shear Wave Velocity from CPT and SPT." XII ICSMFE, Rio de Janeiro, 1989.

T. Kokusho. "Cyclic Triaxial Test of Dynamic Soil Properties for Wide Strain Range." Soils and Foundations, 20(2), 1980, pp. 45-60.

T. Kokusho, V. Yoshida, and Y. Esashi. "Dynamic Properties of Soft Clay for Wide Strain Range." Soils and Foundations, 22(4), 1982, pp. 1-18.

T. Kokusho. "In Situ Dynamic Properties and their Evaluation." Proceedings, VIII ARCSMFE, Vol. 2, Kyoto, 1987.

S. E. Koppermann, K. H. Stokoe, II, and D. P. Knox. "Effect of State of Stress on Velocity of Low Amplitude Compression Waves Propagating Along Principal Stress Directions in Sand." Geotechnical Engineering Report, GR82-22, University of Texas, Austin, Texas, 1982.

C. C. Ladd, and R. Foott. "New Design Procedure for Stability of Soft Clays." Journal of the Geotechnical Engineering Division, ASCE, Vol. 100, No. GT7, 1974, pp. 763-786.

R. S. Ladd, and P. Dutko. "Small Strain Measurements Using Triaxial Apparatus." Proceedings, Advances in the Art of Testing Soils Under Cyclic Conditions, ASCE, V. Khosla (Ed.), 1985, pp. 148-165.

R. S. Ladd, R. Dobry, P. Dutko, F. Y. Yokel and R. M. Chung. "Pore-Water Pressure Buildup in Clean Sands Because of Cyclic Straining." Geotechnical Testing Journal, GTJODJ, 12(1), March, 1989, pp. 77-86.

P. C. Lambe and R. V. Whitman. "Dynamic Centrifugal Modeling of a Horizontal Dry Sand Layer." Journal of the Geotechnical Engineering Division, 111(3), March, 1985, pp. 265-288.

P. LaRochelle, J. Savrailh, F. Tavenas, M. Roy and S. Leroueil. "Causes of Sampling Disturbance and Design of a New Sampler for Sensitive Soils." Canadian Geotechnical Journal, Vol. 18, No. 1, 1981.

K. W. Lee and W. D. L. Finn. "DESRA-2, Dynamic Effective Stress Response Analysis of Soil Deposits with Energy Transmitting Boundary Including Assessment of Liquefaction Potential." Faculty of Applied Science, University of British Columbia, Vancouver, Canada, 1978.

G. Lefebvre. Personal communication, 1988.

D. C. F. Lo Presti. Personal communication, 1989.

D. C. F. Lo Presti. "Behavior of Ticino Sand During Resonant Column Tests." Ph.D. Thesis, Politecnico de Torino, Torino, Italy, 1987.

H.-P. Lui, R. E. Warrick, R. E. Westerlund, J. B. Fletcher, and G. L. Maxwell. "An Air-Powered Impulsive Shear-Wave Source with Repeatable Signals." Bulletin of the Seismological Society of America, 78(1), 1988, pp. 355-369.

T. Macky and A. Saada. "Dynamics of Anisotropic Clays Under Large Strains." The Journal of the Geotechnical Engineering Division, ASCE, Vol. 110, No. 4, April 1984.

S. Marchetti. "In Situ Tests by Flat Dilatometer." Journal of the Geotechnical Engineering Division, ASCE, GT3. 1980.

M. McNelis. "The Effect of Strain on the Dynamic Properties of Dry Sands." Thesis, submitted in partial fulfillment of the requirements for the degree of Master of Science in Civil Engineering, Case Western Reserve University, June, 1987.

G. Mesri and A. Castro. "$C\alpha/C_c$ Concept and K_0 During Secondary Compression." Journal of the Geotechnical Engineering Division, ASCE, 113(3), 1987, pp. 230-247.

G. Mesri. "The Fourth Law of Soil Mechanics The Law of Compressibility." Proceedings, International Symposium on Geotechnical Engineering of Soft Soils, Mexico City, Vol. 2, 1988.

R. Mesri. "Post Densification Penetration Resistance of Clean Sands." Personal communication to M. Jamiolkowski, 1989.

R. D. Mindlin and H. Deresiewicz. "Elastic Spheres in Contact Under Varying Oblique Forces." Journal Applied Mechanics, Trans. ASME, September 1953, pp. 327-344.

Y. J. Mok, I. Sanchez-Salinero, K. H. Stokoe, II, and J. M. Roesset. "In Situ Damping Measurements by Crosshole Seismic Method." Proceedings, ASCE Specialty Conference on Earthquake Engineering and Soil Dynamics II - Recent Advances in Ground Motion Evaluation, Park City, Utah, June 1988.

National Research Council. Liquefaction of Soils During Earthquakes, National Academy Press, Washington, D.C., 1985, pp. 240.

S. Nazarian. "In Situ Determination of Elastic Moduli of Soil Deposits and Pavement Systems by Spectral-Analysis-of-Surface-Waves Method." Ph.D. Dissertation, The University of Texas at Austin, 1984, pp. 453.

P. P. Nelson, K. H. Stokoe, II, and S. Nazarian. Engineering Characterization of Geotechnical Materials at a Potential Low-Level Radioactive Waste Disposal Site in Hudspeth County, Texas. Geotechnical Engineering Report GR89-4, (Draft), August, 1989.

J. O. Osterberg and S. Varaksin. "Determination of Relative Density of Sand Below Groundwater Table." Proceedings, Evaluation of Relative Density and Its Role in Geotechnical Projects Involving Cohesionless Soils, ASTM Special Technical Publication 523, E. T. Selig and R. S. Ladd, (Eds.), 1973, pp. 364-378.

S. N. Palmer and M. E. Barton. "Porosity Reduction, Microfabric and Resultant Lithification in UK Uncemented Sand." Diagenesis of Sedimentary Sequences, Marshall, J. D. (Ed.), Geological Society Special Publication No. 36, 1987, pp. 29-40.

S. Prakash and V. K. Puri. "Dynamic Properties of Soils from *In-Situ* Tests." Journal of the Geotechnical Engineering Division, ASCE, 107(GT7), July 1981, pp. 943-963.

R. Pyke. "Nonlinear Soil Models for Irregular Cyclic Loadings." Journal of the Geotechnical Engineering Division, ASCE, Vol. 105, No. GT6, June, 1975, pp. 715-726.

G. Z. Qi, J. C. S. Yang, A. J. Durelli and L. Esteva. "In-Situ Determination of the Strain Dependence of the Soil Dynamics Properties." Structural Dynamics and Soil Structure Interaction, A. S. Cakmak and I. Herrera, Eds., 1989, pp. 431-442.

B. B. Redpath, R. B. Edwards, R. J. Hale and F. Z. Kintzer. Development of Field Techniques to Measure Damping Values for Near-Surface Rocks and Soils. Report - URS/John A. Blume and Assoc., San Francisco, 1982, pp. 120.

F. E. Richart, Jr., J. R. Hall, Jr. and R. D. Woods. Vibrations of Soils and Foundations. Prentice Hall, Inc., Englewood Cliffs, New Jersey, 1970, pp. 414.

F. E. Richart. "Some Effects of Dynamic Soil Properties on Soil-Structure Interaction." Journal of the Geotechnical Engineering Division, ASCE, 101(GT12), 1975, pp. 1197-1240.

G. J. Rix and K. H. Stokoe II. "Stiffness Profiling of Pavement Subgrades." Transportation Research Record, Washington, D.C. (in press), 1989.

G. J. Rix, J. A. Bay and K. H. Stokoe, II. "Use of Seismic Tests to Assess *In Situ* the Properties of Portland Cement Concrete During Curing." Presented at the 1990 Annual Meeting of the Transportation Research Board, 1990.

P. K. Robertson. "*In-Situ* Testing with Emphasis on its Application to Liquefaction Assessment." Ph.D. Thesis, University of British Columbia, 1982.

P. K. Robertson, R. G. Campanella, D. Gillespie, and A. Rice. "Seismic CPT to Measure *In-Situ* Shear Wave Velocity." Journal of the Geotechnical Engineering Division, ASCE, 112(8), 1986, pp. 791-803.

P. K. Robertson and J.M.O. Hughes. "Determination of Properties of Sand from Self-Boring Pressuremeter Tests." Proceedings Symposium on the Pressuremeter and Its Marine Applications, Texas A&M, ASTM STP 950, 1986.

S. K. Roesler. "Anisotropic Shear Modulus Due to Stress Anisotropy." Journal of the Geotechnical Engineering Division, ASCE, 105(GT5), July 1979, pp. 871-880.

M. P. Romo and A. Jaime. Dynamic Characteristics of Some Clays of the Mexico Valley and Seismic Response of the Ground. Instituto de Ingenieria, Technical Report, Instituto de Ingenieria, (in Spanish), 1986.

A. Saada. "On Cyclic Testing with Thin Long Hollow Cylinders." Proceedings of Advances in the Art of Testing Soils Under Cyclic Conditions, ASCE meeting, Detroit, October 1985, pp. 1-28.

A. Saada and F. Towsend. "Strength Laboratory Testing of Soils." A State of the Art paper presented at the ASTM Symposium on the Shear Strength of Soils, June 25, 1980, Chicago, Illinois, ASTM, STP 740, 1981.

A. Saada and T. A. Macky. "Integrated Testing Properties of a Gulf of Mexico Clay." Strength Testing of Marine Sediments: Laboratory and In-situ Measurements, ASTM STP 883, 1985, pp. 363-380.

A. Saada. "Hollow Cylinder Torsional Devices, Their Advantages and Limitations." A State of the Art paper presented at the ASTM Symposium on Advanced Triaxial Testing of Soil and Rock, June 20, Louisville, Kentucky, ASTM, STP 977, 1988, pp. 766-795.

I. Sanchez-Salinero, J. M. Roesset, K. H. Stokoe II, S. H. H. Lee and Y. J. Mok. "Body Wave Velocities from Crosshole Tests Using Time and Spectral Analyses." Proceedings, 8th Euro. Conf. on Earthquake Engrg., Lisbon, Portugal, September, 1986.

S. K. Saxena. Mechanical Behavior of Cemented Sands. Illinois Institute of Technology, Report No. IIT-CE-8701, June 1987, pp. 172.

J. H. Schmertmann. Effect of Shear Stress on Dynamic Bulk Modulus of Sand. U.S. Army Engineering Waterways Experiment Station, Technical Report S-78-16, October 1978.

J. H. Schmertmann. "The Mechanical Aging of Soils." Draft of the 25th Terzaghi Lecture, 1989.

P. B. Schnabel, J. Lysmer, and H. B. Seed. SHAKE: A Computer Program for Earthquake Response Analysis of Horizontally Layered Sites. Report No. EERC/72-12, University of California, Berkeley, 1972.

H. B. Seed and I. M. Idriss. Soil Moduli and Damping Factors for Dynamic Response Analyses. Report No. EERC 70-10, Earthquake Engineering Research Center, University of California, Berkeley, California, 1970.

H. B. Seed, I. M. Idriss and I. Arango. "Evaluation of Liquefaction Potential Using Field Performance Data." Journal of the Geotechnical Engineering Division, ASCE, 109(3), 1983, pp. 458-482.

H. B. Seed, R. T. Wong, I. M. Idriss and K. Tokimatsu. "Moduli and Damping Factors for Dynamic Analyses of Cohesionless Soils." Journal of the Geotechnical Engineering Division, ASCE, 112(11), 1986, pp. 1016-1032.

H. B. Seed, M. P. Romo, J. I. Sun, A. Jaime and J. Lysmer. "The Mexico Earthquake of September 19, 1985--Relationships Between Soil Conditions and Earthquake Ground Motions." Earthquake Spectra, 4(4), 1988, pp. 687-729.

M. L. Silver, C. K. Chan, R. S. Ladd, K. L. Lee, D. A. Tiedemann, F. C. Townsend, J. E. Valera, and J. H. Wilson. "Cyclic Triaxial Strength of Standard Test Sand." Journal of the Geotechnical Engineering Division, ASCE, Vol. 102, GT5, May 1976, pp. 511-524.

P. C. Sirles. "Shear Wave Velocity and Attenuation Measurements in Liquefiable Soil Deposits in the Truckee Meadows, Reno, Nevada." M. S. Thesis, University of Nevada, Reno, 1987.

P. C. Sirles. "Evaluation of SASW and Crosshole Velocity Measurements Before and After Dynamic Compaction at Jackson Lake Dam, Wyoming." U.S. Bureau of Reclamation Report (unpublished), 1988.

N. Sitar. "Behavior of Slopes in Weakly Cemented Soils." Thesis presented in partial fulfillment of the Ph.D. degree, Stanford University, Stanford, California, 1979, pp. 165.

K. H. Stokoe II. "Field Measurement of Dynamic Soil Properties." Proceedings Second ASCE Conference on Civil Engineering and Nuclear Power, Vol. II, Geotechnical Topics, Knoxville, Tennessee, September 1980, pp. 15-17 and 7-1-1 to 7-1-31.

K. H. Stokoe II and S. Nazarian. "Use of Rayleigh Waves in Liquefaction Studies." in "Measurement and Use of Shear Wave Velocity for Evaluating Dynamic Soil Properties," Proceedings, Geotechnical Engineering Division, R. D. Woods, ed., ASCE, 1985, pp. 1-17.

K. H. Stokoe II, S. H. H. Lee and D. P. Knox. "Shear Moduli Measurements Under True Triaxial Stresses." Advances in the Art of Testing Soils Under Cyclic Conditions, V. Khosla, ed., ASCE, 1985, pp. 166-185.

K. H. Stokoe II, R. D. Andrus, G. J. Rix, I. Sanchez-Salinero, J.-C. Sheu and Y.-J. Mok. "Field Investigation of Gravelly Soils Which Did and Did Not Liquefy During the 1983 Borah Peak, Idaho, Earthquake." Geotechnical Engineering Report GR87-1, April, 1988.

K. H. Stokoe II. Personal communications, 1989.

J. I. Sun, R. Golesorkhi and H. B. Seed. Dynamic Moduli and Damping Ratios for Cohesive Soils. Report No. UCB/EERC-88/15, August, University of California, Berkeley, 1988.

D. W. Sykora and K. H. Stokoe II. Correlations of In-Situ Measurements in Sands with Shear Wave Velocity. Geotechnical Engineering Report GR83-33, The University of Texas at Austin, Texas, 1983.

D. W. Sykora and J. P. Koester. "Correlations between Dynamic Shear Resistance and Standard Penetration Resistance of Soils." Proceedings, Earthquake Engineering and Soil Dynamics II - Recent Advances in Ground--Motion Evaluation, Von Thun, J. L. (Ed.) ASCE. 1988.

K. Tamimoto. Preliminary Study of the Correlation of SPT N-values with the Velocity of Shear Waves in Sands of the Construction Engineering Research Institute Foundation. Report No. 16, pp. 103-111, Tokyo, Japan, 1974.

K. Tan and M. Vucetic. "Behavior of Medium and Low Plasticity Clays Under Cyclic Simple Shear Conditions." Proceedings of 4th International Conference on Soil Dynamics and Earthquake Engineering, Soil Dynamics and Liquefaction Volume, Mexico City, 1989, pp. 131-142.

F. Tatsuoka, T. Iwasaki and Y. Takagi. "Hysteretic Damping of Sands Under Cyclic Loading and its Relation to Shear Modulus." Soils and Foundations, 18(2), June 1978, pp. 25-40.

F. Tatsuoka, T. Iwasaki, S. Yoshida, S. Fukushima and H. Sudo. "Shear Modulus and Damping by Drained Tests on Clean Sand Specimens Reconstituted by Various Methods." Soils and Foundations, 19(1), March 1979, pp. 39-54.

F. Tatsuoka, S. Yamada and T. Sato. "Design and Manufacturing of Shear Testing Apparatuses for Soils. No. 6 - Methods of Controlling and Measuring Stress and Loads No. 3. Chishitsu-to-Chosa. Journal of Japanese Association of Geotechnical Consultants, No. 1984-1," 1984, pp. 56-62 (in Japanese).

F. Tatsuoka. "Some Recent Development in Triaxial Testing Systems for Cohesionless Soils." Advanced Triaxial Testing of Soil and Rock, STP 977, 1988, pp. 7-67.

F. A. Tavenas, R. S. Ladd, and P. La Rochelle. "Accuracy of Relative Density Measurements: Results of a Comparative Test Program." Proceedings, Evaluation of Relative Density and Its Role in Geotechnical Projects Involving Cohesionless Soils, ASTM Special Technical Publication 523, E. T. Selig and R. S. Ladd, (Eds.), 1973, pp. 18-60.

W. T. Thomson. "Transmission of Elastic Waves Through a Stratified Solid." Journal of Applied Physics, Vol. 21, 1950, pp. 89-93.

D. A. Tiedeman. "Variability of Laboratory Relative Density Test Results." Proceedings, Evaluation of Relative Density and Its Role in Geotechnical Projects Involving Cohesionless Soils, ASTM Special Technical Publication 523, E. T. Selig and R. S. Ladd, (Eds.), 1973, pp. 61-73.

T. Tohno. "Diagenesis and Mechanical Characteristics of Sediments." (In Japanese), Geological Journal, September 1975, pp. 547-559.

M. Vucetic. "Normalized Behavior of Offshore Clay Under Uniform Cyclic Loading." Canadian Geotechnical Journal. Vol. 25, No. 1, February 1988, pp. 33-41.

M. Vucetic. "Normalized Behavior of Clay Under Irregular Cyclic Loading." Canadian Geotechnical Journal, Vol. 27, February 1990.

M. Vucetic and R. Dobry. "Degradation of Marine Clays Under Cyclic Loading." Journal of the Geotechnical Engineering Division, ASCE, Vol. 114, No. 2, February 1988, pp. 133-149.

M. Vucetic and R. Dobry. "Effect of Soil Plasticity on Cyclic Response." Journal of the Geotechnical Engineering Division, ASCE, Vol. 117, No. 1, January, 1991.

M. Vucetic and V. Thilakarante. "Degradation of Clay Stiffness Under Irregular Cyclic Loading." Proceedings International Symposium on Geotechnical Engineering of Soft Soils, Mexico City, August 1987, pp. 155-162.

Y. D. Wang. "Investigation of Constitute Relations for Weakly Cemented Sands." Thesis presented in partial fulfillment of the Ph.D. degree, University of California, Berkeley, 1986, p. 293.

R. V. Whitman and K. Arulanandan. "Centrifuge Model Testing with Dynamic and Cyclic Loads." Proceedings, Advances in the Art of Testing Soils Under Cyclic Conditions," ASCE, V. Khosla, ed., 1985, pp. 255-285.

R. D. Woods. "Measurement of Dynamic Soil Properties." Proceedings of the ASCE Geotechnical Engineering Division Specialty Conference, Earthquake Engineering and Soil Dynamics. Pasadena, CA, June, Vol. 1, 1978, pp. 91-178.

R. D. Woods and K. H. Stokoe II. "Shallow Seismic Exploration in Soil Dynamics," Richart Commemorative Lectures, ASCE, Detroit, Michigan, R. D. Woods, Ed., 1985, pp. 120-156.

C. P. Wroth. "British Experience with the Self-Boring Pressuremeter." Proceedings, Symposium on the Pressuremeter and Its Marine Applications, Paris, 1982.

S. Wu, D. H. Gray and F. E. Richart. "Capillary Effects on Dynamic Modulus of Sands and Silts." Journal of the Geotechnical Engineering Division, ASCE, 110(9), 1984, pp. 1188-1203.

J. C. S. Yang, G. Z. Qi, V. Paulin and A. J. Durelli. "*In-Situ* Determination of Soil Damping in the Lake Deposit Area of Mexico City." Soil Dynamics and Earthquake Engineering, 8(1), 1989, pp. 43-52.

P. Yu and F. E. Richart, Jr. "Stress Ratio Effects on Shear Modulus of Dry Sands." Journal of the Geotechnical Engineering Division, ASCE, 110(3), March 1984, pp. 331-345.

State-of-the-Art Speaker — Professor Jose Roesset

Workshop Panel

Chapter 4   ENERGY DISSIPATION

Chapter 4
ENERGY DISSIPATION

The topic of energy dissipation is a key component to dynamic soil property and site characterization. As seismic waves travel through the ground and as structures respond to excitation from seismic waves, energy dissipation occurs. The amount of dissipation often determines the level of vibration at a location or within a structure. Given the critical nature of this topic, this chapter starts with a state-of-the-art report on energy dissipation that was prepared by Dr. Jose M. Roesset, Professor of Civil Engineering at the University of Texas, Austin. The state-of-the-art report is followed by a summary report prepared by a panel of individuals who met and discussed the topic of energy dissipation during the workshop. The panel included Jose Roesset (panel leader), Dick Woods (panel recorder), Bill Joyner, John Lysmer, Bob Pyke, Bruce Redpath, Ken Stokoe, Andy Veletsos, and Jackson Yang. The panel report includes a summary of research needs relative to the measurement of energy dissipation.

SOA REPORT

INTRODUCTION

The ability of a structure, a soil, or any physical system to dissipate energy while subject to vibrations is simulated in dynamic analyses through the introduction of damping terms (or a damping matrix). These terms are supposed to reproduce the physical process of energy dissipation, but they are often selected purely on a mathematical basis in order to obtain simple models that can be solved analytically. Most forms of energy dissipation are, in fact, associated with some type of nonlinear behavior, but they are normally modeled as linear terms. Moreover, most of our understanding on the effects is based on the consideration of single-degree-of-freedom systems. When this understanding is extrapolated to predict the response of actual multidegree-of-freedom systems, it is often assumed that the response variables of interest are controlled by one mode, typically the first mode of the system. This assumption is not always justified.

There are many aspects of damping, the way it is measured, and its analytical modeling that require a careful reevaluation. The purpose of this chapter on energy dissipation is to review some of the basic concepts, formulae, and procedures that are commonly used to determine values of damping experimentally as well as the ways in which these values are incorporated in dynamic analyses. It is hoped that this brief review will stimulate discussion and help to identify needed areas of research.

The determination of damping in the laboratory is normally performed using free vibration tests or cyclic (static or steady-state dynamic) tests. In the first case, damping is

determined from the decay of the amplitude of motion with time. In the second, it is obtained from the amplification curve (ratio of the dynamic displacement to the static one as a function of frequency), the difference in phase between the applied load and the displacement or the area of the loops relating force to displacement for a given frequency. In all cases, the computation of the damping is based on the implicit assumption that it is of a linear viscous nature.

The determination of damping in actual structures can be performed through free vibration tests, steady-state forced vibration tests, or from analysis of the motions recorded during actual earthquakes using system identification techniques. Various assumptions are also implicit in the procedures used to interpret the data and backfigure equivalent values of damping. The most common ones are that the structure has normal modes of vibration, that it behaves elastically, and that the damping in each mode is of a linear viscous nature.

In situ determination of damping in soil deposits can be attempted using geophysical methods (downhole, crosshole, spectral analysis of surface waves) imposing a dynamic excitation at one point and recording the resulting motions at one or more points within the soil mass or along the surface of the soil deposit. Damping can be estimated from the attenuation of the amplitudes of motion with distance or frequency or from the phases of the motions. An assumption has to be made as to the type of damping (linear viscous, linear hysteretic, or nonlinear). In addition, one must take into account the existence of energy dissipation due to spreading or radiation of the waves away from the source (radiation, spreading, or geometric damping). System identification techniques can also be used to determine damping values for soils when records of seismic motions are available at various depths within a soil deposit. In this case, however, one must make some assumptions not only with respect to the type of damping but also as to the types of waves (the usual assumption being that the earthquake is caused by vertically propagating shear waves).

In the following pages the behavior of various systems (linear viscoelastic, frictional, nonlinear) under free vibrations and steady-state forced vibrations is reviewed in some detail. The basis for the determination of damping values *in situ* with geophysical methods is then briefly outlined. Finally, some of the issues involved in the modeling of damping for dynamic analyses are discussed.

FREE VIBRATIONS OF A SINGLE-DEGREE-OF-FREEDOM SYSTEM

Linear Viscous System

The simplest mathematical model and the one most commonly used is that of a linear viscous dashpot with a resistance proportional to the rate of deformation (relative velocity between the ends of the dashpot). The equation of motion is then for free

$$Mü + cü + ku = 0 \qquad (4\text{-}1)$$

vibrations with the initial conditions $u(0) = u_0$ and $ü(0) = 0$ if u_0 is the initial displacement and the initial velocity is zero. M is the mass, k the stiffness of the spring, and c the constant of the viscous dashpot (Figure 4-1).

While the physical parameter involved in this model is the dashpot constant c, it is more common to represent damping by the fraction of critical damping

$$\beta = \frac{c}{c_{crit}} = \frac{c}{2\sqrt{kM}} = \frac{c}{2M\omega} = \frac{c\omega}{2k} \qquad (4\text{-}2)$$

where ω is the undamped natural frequency of the system $\omega^2 = k/M$. It should be noted that β is not only a function of c but also of k and M. Thus, the same dashpot will have different effects depending on the mass and stiffness of the system.

Calling $\omega_D = \omega(1-\beta^2)^{0.5}$, the damped natural frequency and T_D the corresponding damped period, the solution of Eq. 4-1 is written as

$$u = u_0 \, e^{-\beta\omega t} \left(\cos \omega_D t + \frac{\beta\omega}{\omega_D} \sin\omega_D t \right) \qquad (4\text{-}3)$$

Figure 4-2 shows the well-known variation of the displacement u with time for a system with $\beta = 0.1$ (10 percent of critical damping). The ratio of the peak amplitudes u_n and u_{n+1} at times $t_n = nT_D$ and $t_{n+1} = (n+1)T_D$ is

$$\frac{u_n}{u_{n+1}} = e^{2\pi\beta\omega/\omega_D} \qquad (4\text{-}4)$$

The logarithmic decrement is then

$$\Delta = \text{Ln} \, \frac{u_n}{u_{n+1}} = 2\pi\beta \, \frac{\omega}{\omega_D} \qquad (4\text{-}5)$$

Figure 4-1. Linear Viscous Single-Degree-of-Freedom System.

Free Vibration of a Elastic System

Figure 4-2. Free Vibrations of Linear Viscous System.

Thus,

$$\beta = \frac{\Delta}{2\pi} \frac{\omega_D}{\omega} = \frac{\Delta}{2\pi} \sqrt{1-\beta^2} \qquad (4\text{-}5a)$$

or

$$\beta = \frac{\Delta}{2\pi} \frac{1}{\sqrt{1+\left(\dfrac{\Delta}{2\pi}\right)^2}} \qquad (4\text{-}6)$$

For small values of β this expression is often simplified to

$$\beta \cong \frac{\Delta}{2\pi} \qquad (4\text{-}7)$$

For a system with linear viscous damping, the value of the logarithmic decrement Δ is a constant, independent of the cycle n.

The displacement from Eq. 4-3 is a decaying harmonic motion with period T_D. The peaks (maxima and minima) occur at times $t = nT_D/2$, but the zero crossings take place at

$$t = \left(\frac{2n-1}{4} + \frac{1}{2\pi} \phi\right)^{T_D} \qquad (4\text{-}7a)$$

where $\sin \phi = \beta$.

The velocity of the system is given by

Figure 4-3. Frictional Single-Degree-of-Freedom System

Free Vibration of a Frictional System

Figure 4-4. Free Vibrations of Frictional System

4-6

$$\dot{u} = -u_0 \frac{\omega^2}{\omega_D} e^{-\beta \omega t} \sin \omega_D t \qquad (4\text{-}8)$$

The zero crossings occur at $t = n\pi T_D$ but the peaks occur at times

$$t = \left(\frac{2n-1}{4} - \frac{1}{2\pi}\phi\right)T_D \qquad (4\text{-}8a)$$

The acceleration is

$$\ddot{u} = -\omega^2 u_0 e^{-B\omega t} \left(\cos\omega_D t - \frac{B\omega}{\omega_D} \sin \omega_D t\right) \qquad (4\text{-}9)$$

The zero crossings of the acceleration occur at the same time as the peaks of the velocity. Maxima and minima of the acceleration trace take place at

$$t = \left(\frac{2n-1}{4} + \frac{1}{2\pi}\phi'\right)T_D \qquad (4\text{-}10)$$

with $\sin \phi' = 1 - 2\beta^2$.

The traces of the displacement, velocity, and acceleration as functions of time are not therefore 90 degrees out of phase with each other, but the expression for the logarithmic decrement (Eq. 4-5) from the ratio of the amplitudes of two consecutive positive or negative peaks is valid for all three traces.

Linear viscous damping would be associated with the behavior of a linear viscoelastic material. For normal temperature ranges, the viscosity of soils or typical structural materials, such as steel or concrete, is very small. Viscous damping will also occur when a body moves in a fluid (drag forces). These forces are, however, nonlinear functions of the velocity.

4-7

Frictional Systems

Another relatively simple model is that associated with Coulomb friction. For a system consisting of a spring k and a mass M resting on a frictional surface (Figure 4-3), the equation of motion for free vibration is

$$M\ddot{u} + ku + R \text{ sign}|\dot{u}| = 0 \tag{4-11}$$

where R is the maximum friction force. While this is a nonlinear equation, it is very simple to obtain the analytical solution for each half-cycle of vibration. If the displacement u_0 is smaller than R/k, the system will remain at rest. For larger values of the initial displacement, u_0, the displacement, velocity, and acceleration are given by

$$nt < t < \frac{(2n+1)}{2}T \qquad u = \left(u_0 - (4n+1)\frac{R}{k}\right)\cos \omega t - \frac{R}{k}$$

$$\dot{u} = -\omega\left(u_0 - (4n+1)\frac{R}{k}\right)\sin \omega t$$

$$\ddot{u} = -\omega^2\left(u_0 - (4n+1)\frac{R}{k}\right)\cos \omega t$$

$$\tag{4-12}$$

$$\frac{(2n+1)}{2}T \le t \le (n+1)\,T \qquad u = \left(u_0 - (4n+3)\frac{R}{k}\right)\cos \omega t - \frac{R}{k}$$

$$\dot{u} = -\omega\left(u_0 - (4n+3)\frac{R}{k}\right)\sin \omega t$$

$$\ddot{u} = -\omega^2\left(u_0 - (4n+3)\frac{R}{k}\right)\cos \omega t$$

In contrast to the linear viscous system, the motion stops after a finite period of time, at $t = nT/2$ if $u_0 \leq (2n+1)R/k$. The positive peaks of the displacement occur at $t = nT$ and the negative peaks at $t = (2n+1)T/2$. The values of two consecutive positive peaks are

$$u_n = u_0 - 4n\frac{R}{k} \qquad (4\text{-}12a)$$

$$u_{n+1} = u_0 - 4(n+1)\frac{R}{k}$$

so that

$$u_n - u_{n+1} = 4\frac{R}{k} \qquad (4\text{-}13)$$

and

$$\frac{u_n}{u_{n+1}} = \frac{1}{1 - 4R/ku_n} \qquad (4\text{-}14)$$

The difference between two consecutive peaks with the same sign is thus a constant, and the envelope of the displacement is a straight line, as shown in Figure 4-4. The ratio of the amplitudes of two consecutive peaks is, on the other hand, variable, increasing with the number of cycles. The zero downcrossings of the displacement trace occur at

$$t = \frac{T}{2\pi} \cos^{-1} \frac{-1}{\dfrac{ku_0}{R} - (4n+1)} + nT \qquad (4\text{-}14a)$$

4-9

The zero upcrossings occur at

$$t = \frac{2n + 1}{2}T + \frac{T}{2\pi} \cos^{-1} \frac{-1}{\frac{ku_0}{R} - (4n + 3)}$$ (4-14b)

The velocity trace has zero crossings at $t = nT/2$ and peaks at $t = (2n+1)T/4$. The acceleration trace has peaks at $t = nT/2$ and zero crossings at $t = (2n+1)T/4$. The acceleration and velocity traces are therefore 90 degrees out of phase with respect to each other. The peaks of the velocity are 90 degrees out of phase with respect to the displacement peaks, but the zero crossings of the two traces have a variable phase difference.

It is interesting to consider, on the other hand, a system like that of Figure 4-5 representing a single-degree-of-freedom structure with a rigid, massless, foundation on a frictional surface. In this case, the spring force and the frictional resistance act in series rather than in parallel. If the initial displacement u_0 is smaller than R/k, the system will vibrate elastically without any damping. If u_0 is larger than R/k, there will be a displacement of the base $u_b = u_0 - R/k$. The system will then vibrate elastically, without any damping, around this displaced position (permanent set).

Inelastic Systems

Consider a mass resting on an elastic spring with an elastic, perfectly plastic force deformation relationship as shown in Figure 4-6. The free vibrations of this system are identical to those of the second frictional system of the previous section, replacing the friction force R by the yield force of the spring F_y. If the initial displacement u_0 is smaller than the yield displacement $u_y = F_y/k$, the system vibrates elastically without any damping. If u_0 is larger than u_y, the system vibrates again elastically around a permanent set $u_0 - u_y$.

For a more general inelastic system with a bilinear, trilinear, or curvilinear force deformation relationship, the response will be initially damped but may eventually become elastic.

STEADY-STATE VIBRATIONS OF SINGLE-DEGREE-OF-FREEDOM SYSTEMS

Linear Viscous Systems

Consider again the simple model of Figure 4-1 consisting of a mass M, a spring k, and a linear viscous dashpot with constant c. For a harmonic force of the form $F = P\sin\Omega t$,

Figure 4-5. Alternate Frictional Single-Degree-of-Freedom System.

Figure 4-6. Elasto-Plastic Force Deformation Relationship.

the steady-state response is given by

$$u = \frac{P}{k[(1 - \alpha^2)^2 + 4\beta^2\alpha^2]}[(1 - \alpha^2) \sin \Omega t - 2\beta\alpha \cos \Omega t] \qquad (4-15)$$

with $\alpha = \Omega/\omega$ the ratio of the frequency of the excitation to the natural frequency of the system (dimensionless frequency).

Alternatively,

$$u = \frac{P}{k[(1 - \alpha^2)^2 + 4\beta^2\alpha^2]} \sin (\Omega t - \phi) \qquad (4-16)$$

with

$$\tan \phi = 2\beta\frac{\alpha}{1-\alpha^2} = \frac{c\Omega}{k(1 - \alpha^2)} \qquad (4-17)$$

The ratio of the amplitude of the dynamic displacement to the static displacement $u_{st} = P/k$ is defined as the amplification function

$$A(\alpha) = \frac{1}{\sqrt{(1 - \alpha^2)^2 + 4\beta^2\alpha^2}} \qquad (4-18)$$

Figures 4-7a and 4-7b show the amplification function and the phase angle ϕ for a linear viscous system with $\beta = 0.1$ (10 percent of critical damping). The maximum amplification occurs at a dimensionless frequency $\alpha = (1-2\beta)^{0.5}$ and has a value $A_{max} = 1/[2\beta(1-\beta^2)^{-0.5}]$. At resonance $\alpha = 1$ and $A(1) = 1/2\beta$. The phase angle ϕ is equal to $\pi/2$ at resonance.

Several procedures are used in practice to determine the fraction of critical damping β from the amplification function and phase curve under steady-state vibration. Some of these are:

(a)   If the resonant frequency ω, corresponding to $\alpha = 1$, is determined from the phase curve (when the phase is equal to $\pi/2$), the damping could be

4-12

Amplification Factor for an Elastic System

Figure 4-7a. Amplification Function for Steady-State Vibration of Linear Viscous System.

Phase Angle for an Elastic System

Figure 4-7b. Phase Angle for Steady-State Vibration of Linear Viscous System.

determined from the phase angle ϕ at any other frequency as

$$\beta = \frac{1 - \alpha^2}{2\alpha} \tan \phi \qquad (4\text{-}19)$$

(b) Knowing again the natural frequency, the damping could be determined from the value of the amplification at resonance

$$\beta = \frac{1}{2A(1)} \qquad (4\text{-}20)$$

(c) Measuring any two frequencies α_1 and α_2 ($\alpha_1 > 1$ $\alpha_2 < 1$) at which the same amplification is obtained (intersection of the amplification curve with a horizontal line) and calling $1/\gamma$ the value of the amplification, α_1 and α_2 are the roots of

$$\alpha^4 - 2(1 - 2\beta^2)\, \alpha^2 + 1 - \gamma^2 = 0$$

$$\alpha_1^2 = 1 - 2\beta^2 + \sqrt{(1 - 2\beta^2)^2 - 1 + \gamma^2} \qquad (4\text{-}20a)$$

$$\alpha_2^2 = 1 - 2\beta^2 - \sqrt{(1 - 2\beta^2)^2 - 1 + \gamma^2}$$

and

$$\alpha_1^2 + \alpha_2^2 = 2(1 - 2\beta^2) \qquad (4\text{-}20b)$$

leading to

$$\beta = \sqrt{\frac{1}{2} - \frac{\alpha_1^2 + \alpha_2^2}{4}} \qquad (4\text{-}21)$$

Unfortunately, for small values of β, $\alpha_1^2 + \alpha_2^2$ will be very close to 2, and small errors in the determination of α_1 and α_2 will influence significantly the value of β. Selecting instead the values of α_1 and α_2 so that the amplification is

$$\frac{1}{\gamma} = \frac{1}{2\beta\sqrt{2}} = \frac{1}{\sqrt{2}A(1)} \qquad \text{(half power points)}$$

then

$$\frac{(\alpha_1 - \alpha_2)^2}{2} = 1 - 2\beta^2 - \sqrt{1 - 8\beta^2} \simeq 2\beta^2 \quad \text{or} \quad \beta \simeq \frac{\alpha_1 - \alpha_2}{2} \qquad (4\text{-}22)$$

Instead of using the amplification function, one can alternatively consider a plot of the dynamic applied force $F = P\sin\Omega t$ versus the displacement $u(t)$. Such plots are shown in Figures 4-8a, 4-9a, and 4-10a for a system with 10 percent critical damping. It can be seen that the figure is always an ellipse. For a dimensionless frequency less than 1 (excitation frequency smaller than the natural frequency of the system), the major axis of the ellipse has a positive slope. At resonance, the principal axes of the ellipse are horizontal and vertical. For frequencies larger than the fundamental frequency, the major axis has a negative slope.

The area enclosed by the ellipse is

$$W_1 = \pi\omega c u_{max}^2 \qquad (4\text{-}22a)$$

where u_{max} is the maximum amplitude of the dynamic displacement.

The dashpot constant can then be computed as

$$c = \frac{W_1}{\pi\Omega u_{max}^2} \qquad (4\text{-}23)$$

4-15

Normalized Frequency = 0.75

Linear system with 10% damping

a) Applied Force

Normalized Frequency = 0.75

Linear system with 10% damping

b) Resisting Force

Figure 4-8. Force-Displacement Relationship for Steady-State Vibration of Linear Viscous System.

4-16

Normalized Frequency = 1.

Linear system with 10% damping

a) Applied Force

Normalized Frequency = 1.

Linear system 10% damping

b) Resisting Force

Figure 4-9. Force-Displacement Relationship for Steady-State Vibration of Linear Viscous System.

Normalized Frequency = 1.5

Linear system with 10% damping

a) Applied Force

Normalized Frequency = 1.5

Linear system with 10% damping

b) Resisting Force

Figure 4-10. Force-Displacement Relationship for Steady-State Vibration of Linear Viscous System.

and the fraction of critical damping β is

$$\beta = \frac{1}{2}\frac{c\omega}{k} = \frac{\omega}{\Omega}\frac{W_1}{2\pi ku^2_{max}} \tag{4-24}$$

Calling $\Delta W = ku^2_{max}/2$, the strain energy associated with the maximum displacement is given by

$$\beta = \frac{\omega}{\Omega}\frac{W_1}{4\pi\Delta W} \tag{4-25}$$

and at resonance by

$$\beta = \frac{W_1}{4\pi\Delta W} \tag{4-26}$$

It should be noticed that the ellipses are plots of the dynamic force versus the dynamic displacement. If one were to plot instead the resisting force in the system $ku + c\dot{u}$ versus the dynamic displacement, the result would also be ellipses as shown in Figures 4-8b, 4-9b, and 4-10b for the same dimensionless frequencies. It is interesting to notice that these ellipses do not rotate with increasing frequency of excitation, but the main axis remains always (in these dimensionless plots) at 45 degrees. The area enclosed by this ellipse at resonance is again

$$W_2 = \pi c\Omega u^2 = \pi c\omega u^2_{max} \tag{4-26a}$$

so that

$$c = \frac{W_2}{\pi\Omega u^2 max} = \frac{\Omega W_2}{\pi\dot{u}^2 max} \tag{4-27}$$

4-19

and

$$\beta = \frac{W_2}{2\pi k u^2_{max}} = \frac{W_2}{4\pi \Delta W} \qquad (4\text{-}28)$$

On the other hand, a plot of the force in the spring ku versus u would be a straight line since the system is elastic.

One could obtain equally plots of the applied dynamic force P versus the velocity or the acceleration, depending on the quantity measured in an experiment. So, for instance, considering force versus velocity, one would obtain again ellipses, and the area enclosed would be

$$W_3 = \pi \Omega^2 c \dot{u}^2_{max} = \pi c \dot{u}^2_{max} \qquad (4\text{-}28a)$$

leading to

$$c = \frac{W_3}{\pi \Omega^2 u^2_{max}} = \frac{W_3}{\pi \dot{u}^2_{max}} \qquad (4\text{-}29)$$

and

$$\beta = \frac{\omega}{\Omega^2} \frac{W_3}{4\pi \Delta W} \qquad (4\text{-}30)$$

The energy dissipated by the viscous dashpot under a cycle of steady-state vibration with amplitude A is

$$E_d = {}_0\!\int^T c \dot{u} du = c\Omega^2 A^2 \frac{T}{2} = \pi \Omega c A^2 \qquad (4\text{-}30a)$$

or

$$E_d = \pi \Omega c u^2 \qquad (4\text{-}31)$$

This is the same as the area W_1 enclosed by the ellipse relating total applied force to displacement. It is also equal to the area W_2 enclosed by the ellipse relating resisting force ($c\dot{u} + ku$) to displacement at resonance (when the frequency of the excitation Ω is equal to the natural frequency of the system ω).

Frictional Systems

Consider again the system with Coulomb friction of Figure 4-3. If one assumes that a steady-state condition has been reached due to a force $F = P \sin\Omega t$, the displacement would be

$$\frac{(4n - 1)T}{4} < t < \frac{(4n + 1)T}{4} \qquad u = \frac{P}{k(1 - \alpha^2)} \sin \Omega t - \frac{R}{k}$$

$$\frac{(4n + 1)T}{4} < t < \frac{(4n + 3)T}{4} \qquad u = \frac{P}{k(1 - \alpha^2)} \sin \Omega t + \frac{R}{k} \qquad (4.32)$$

with discontinuities at $t = (2n\text{-}1)T/4$, and α the frequency ratio Ω/ω.

Omitting the points at which the discontinuities occur, the velocity and acceleration are given by

$$\dot{u} = \frac{P\Omega}{k(1 - \alpha^2)} \cos \Omega t$$

$$\ddot{u} = - \frac{P\Omega^2}{k(1 - \alpha^2)} \sin \Omega t \qquad (4.32a)$$

A plot of the applied force F versus the displacement u is a parallelogram with two horizontal sides. The area enclosed is $W = 4PR/k$.

At resonance, however, expressions (Eq. 4-32) are no longer valid. The displacement increases linearly with time and a steady-state condition cannot be reached. The

solution is analogous to that of an elastic system without any damping, although there is some energy dissipation due to friction.

For a displacement controlled steady-state vibration test, if the imposed displacement is of the form $u = A \sin\Omega t$, the force would be

$$\frac{(4n - 1)T}{4} < t < \frac{(4n + 1)T}{4} \qquad F = k(1 - \alpha^2)A \sin \Omega t + R$$

$$\frac{(4n + 1)T}{4} < t < \frac{(4n + 3)T}{4} \qquad F = k(1 - \alpha^2)A \sin \Omega t - R$$

(4.33)

A plot of the force F versus the displacement u would be again a parallelogram, but now with two vertical sides. The enclosed area is $W = 4RA$. At resonance, the parallelogram becomes a rectangle.

A frictional system like that of Figure 4-5, on the other hand, behaves like a nonlinear system with an elastoplastic spring, discussed next.

INELASTIC SYSTEMS

Figure 4-11 shows the amplification curve (maximum dynamic displacement divided by the static displacement) for an elastoplastic single-degree-of-freedom system, under a steady-state force $P = (3F_y \sin\Omega t)/4$ where F_y is the yield force of the spring. For very small or very large frequencies, the system remains elastic, and the displacement is the same as for an elastic system without damping. For intermediate frequencies, the system yields and vibrates around a displaced position corresponding to a permanent set. The top diagram in Figure 4-11 corresponds to the maximum displacement in the steady-state, including the permanent set. The bottom diagram, on the other hand, shows the amplitude of the vibration around the permanent set. It is clear that these amplification curves are different from those corresponding to a linear viscoelastic system.

Figure 4-12 shows the relation between the applied force and the displacement for three values of the dimensionless frequency $\alpha = \Omega/\omega$. The peak of the amplification curve occurs at a value of α of approximately 0.62. It can be seen that the force-displacement curves are again ellipses with similar behavior to those obtained for a linear viscoelastic system (notice, however, the existence of the permanent set). At frequencies close to the peak, the ellipse has horizontal and vertical principal axes. At the frequency of the peak response, the phase angle between the force and the displacement is also $\pi/2$. The relation between the resisting force and the displacement is, on the other hand, a parallelogram like the one shown in Figure 4-6. Under a displace-

Figure 4-11. Amplification Function for an Elastoplastic System.

Figure 4-12. Force Displacement Relationship for Steady-State Vibration of Elastoplastic System.

ment controlled steady-state test, the relation between force and displacement becomes again a parallelogram as shown in Figures 4-13a through 4-13c.

It has become customary to determine equivalent values of damping in laboratory experiments (using, for instance, cyclic torsional tests) by computing the area enclosed by the force-displacement loops. As shown above, these loops will be ellipses both for viscoelastic and nonlinear systems (as well as frictional systems of the second kind).

The value of the equivalent dashpot constant will then be given by Eq. 4-23 or 4-29, depending on whether displacement or velocity are measured. Eq. 4-23 is also used to compute an equivalent c from the static force-displacement relationship, as obtained in a cyclic triaxial test, by equating the area of the hysteresis loop of a nonlinear material to the energy that would be dissipated by a viscous dashpot (Eq. 4-31). To obtain equivalent values of the fraction of critical damping β, it is necessary, on the other hand, to select a value of k or of the maximum strain energy ΔW. Several different possibilities have been suggested. The one most commonly used in practice is the selection of the secant stiffness, corresponding to the maximum displacement (for a nonlinear system tested under force control, one must decide whether this is the maximum displacement, including the permanent set or the maximum amplitude of the vibration).

When attempting to simulate the dynamic response of nonlinear systems by equivalent linear viscoelastic systems, it is also customary to use an equivalent stiffness k_{eq} and c_{eq} using a Galerkin approximation. Then, for a steady-state harmonic motion of the form $u = A \sin\Omega t$, corresponding to a displacement controlled steady-state test

$$\int k_{eq} u \, du + \int c_{eq} \dot{u} \, d\dot{u} = \int F \, du$$

$$\int k_{eq} u \, d\dot{u} + \int c_{eq} \dot{u} \, d\dot{u} = \int F \, d\dot{u}. \tag{4-34}$$

This leads to

$$c_{eq} = \frac{\int F \, d u}{\pi \Omega A^2} = \frac{W}{\pi \Omega u^2_{max}} \tag{4-35}$$

Displacement Controlled Elastoplastic System

Figure 4-13a. Displacement Controlled Steady-State Vibrations of Elastoplastic System.

Displacement Controlled Elastoplastic System

Ductility = 3.   Frequency = 1.

Displacement Controlled Elastoplastic System

Ductility = 3.   Frequency = 1.

Figure 4-13b. Displacement Controlled Steady-State Vibrations of Elasticplastic System.

Displacement Controlled Elastoplastic System
Ductility = 3.   Frequency = 1.5

Displacement Controlled Elastoplastic System
Ductility = 3.   Frequency = 1.5

Figure 4-13c. Displacement Controlled Steady State-Vibrations of Elasticplastic System.

which coincides again with Eqs. 4.23 and 4.31 and

$$k_{eq} = \frac{\Omega}{\pi A} \ _0\!\int^T F \sin \Omega t \ dt \qquad (4\text{-}36)$$

It is interesting to notice that, although the formula used to compute the equivalent dashpot constant c_{eq} is the same in all cases, the interpretation of W is different. In some cases it is the area enclosed by the ellipse relating the total applied force P to the dynamic displacement, while in others it is the area of the hysteresis loop under a cyclic static load (with displacement control).

It is also important to remember that an equivalent linear viscoelastic system cannot reproduce all the details of the response of a nonlinear system. If one attempts to reproduce the amplitude of the vibration, the velocity, or the acceleration, the existence of a permanent set will not be reproduced (this may be important when assessing relative displacements between adjacent structures). If one attempts, on the other hand, to reproduce the maximum displacement, accounting for the permanent set, the amplitude of vibration, the velocity, and the acceleration will be misreproduced.

Linear Hysteretic Damping

The energy dissipated per cycle of vibration at a fixed displacement amplitude by a nonlinear system is normally independent of frequency. The energy dissipated by a viscous dashpot (Eq. 4-31) is, on the other hand, directly proportional to the frequency of vibration Ω. As a result, when Eq. 4-33 is used, the equivalent viscous dashpot would be inversely proportional to frequency. The equivalent fraction of critical damping β from Eq. 4-25 would also be inversely proportional to the frequency of vibration Ω and directly proportional to the equivalent natural frequency of the system. On the other hand, both terms would be a function of the amplitude of vibration u_{max}.

To simulate the behavior of a nonlinear system, it would thus be necessary to use a viscous damping inversely proportional to frequency and function of amplitude. This can be achieved by defining a damping ratio

$$D = \beta\frac{\Omega}{\omega} = \frac{W}{4\pi\Delta W} \qquad (4\text{-}37)$$

The equation of motion becomes then

4-29

$$\text{M\"u} + 2\frac{\text{Dk}}{\Omega}\text{\.u} + \text{ku} = \text{P } e^{i\Omega t} \qquad (4\text{-}37a)$$

and in the steady state if

$$u = A \ e^{i\Omega t} \qquad \text{\.u} = i\Omega A \ e^{i\Omega t} = i\Omega u$$

$$\text{M\"u} + 2iDku + ku = P \ e^{i\Omega t}$$

$$(4\text{-}37b)$$

or

$$\text{M\"u} + k(1 + 2iD)u = P \ e^{i\Omega t} \qquad (4\text{-}37c)$$

Under a steady-state harmonic motion, this type of damping can thus be simulated by using a complex stiffness of the form k(1+2iD). This is the so-called hysteretic or structural damping. When the variation of k and D with the amplitude of vibration is neglected, we have a linear hysteretic damping.

It should be noticed that the hysteretic damping ratio D would be equal to the fraction of critical damping at resonance. Figure 4-14 shows the amplification curve and the phase angle corresponding to a system with a hysteretic damping ratio D = 0.1. These graphs can be compared directly to those of Figure 4-7. These results can be obtained by replacing the terms $4\beta^2\alpha^2$ and $2\beta\alpha$ in Eqs. 4-14, 4-15, 4-16, and 4-17 by $4D^2$ and 2D, respectively.

Linear hysteretic damping is a mathematical abstraction intended to provide a simple model to reproduce an energy dissipation independent of frequency. It is only properly defined in the frequency domain (for steady-state vibrations), and when it used to obtain actual solutions in time, using a Fourier transformation, it violates the principle of causality, although this does not seem to be of any serious significance in most practical cases. Several attempts have been made to reproduce frequency independent damping through physical models, which would be valid in the time domain.

Variation of Damping With Strain Amplitude

Linear viscous damping is proportional to the frequency of vibration, but independent of amplitude. The hysteretic damping associated with the behavior of a nonlinear inelastic material (such as a soil) is, on the other hand, independent of frequency but a

Amplification Factor Elastic System with Hysteretic Damping

Phase Angle Elastic System with Hysteretic Damping

Figure 4-14. Amplification and Phase for Steady-State Vibration of Linear Hysteretic System.

4-31

function of the strain amplitude. Both of them are functions of the strain rate if the strain rate is defined as the product of the strain amplitude by the frequency for a harmonic motion.

To determine the variation of elastic moduli and damping with amplitude of motion (or level of strain), it is customary to conduct cyclic tests (static or dynamic) for different strain amplitudes. The results are then plotted typically, as shown in Figure 4-15. It is interesting to notice that, for very low levels of strain, the damping ratio remains constant with typical values between 0.005 and 0.02 (0.5 percent to 2.0 percent). Whether the damping at very low strains is due to some viscosity in the material or to frictional losses in the equipment is not clear and is a matter that deserves some investigation.

In Situ Measurement of Damping

Geophysical or seismic techniques, such as the crosshole method or the spectral analysis of surface waves, are being commonly and successfully used in practice to determine the elastic moduli of soils *in situ* (particularly the shear modulus) at low levels of strain. It is only recently, however, that efforts have been made to infer from the results of these tests values of material damping. This may be due in part to the fact that damping at low levels of strain is very small.

The common measure of attenuation used by geophysicists is the quality factor Q or its inverse, the dissipation factor. The definition of Q is

$$\frac{1}{Q} = \frac{E_d}{2\pi E} \tag{4-38}$$

where E_d is the amount of energy dissipated per cycle of harmonic vibration in a certain volume and E is the peak elastic energy stored in the same volume. Calling V the wave propagation velocity, f the frequency of the vibration (in cycles per second), and λ the wavelength = V/f, the dissipation factor can also be written as

Figure 4-15. Variation in Damping Ratio with Shearing Strain and Effective Confining Pressure of a Saturated Silty Clay.

Figure 4-16. Effective Damping for Various Forms of Damping Matrix.

$$\frac{1}{Q} = \frac{E_d}{2\pi E} = \frac{\alpha V}{\pi f} = \frac{\alpha \lambda}{\pi} \qquad (4\text{-}39)$$

where α is the attenuation coefficient.

It should be noticed that the expression for the dissipation factor (Eq. 4-38) is exactly the same as that used previously to define the damping ratio D multiplied by a factor of 2.

The basis of geophysical methods is the application of a dynamic excitation by a source placed at a point within the soil mass or on the surface of the soil deposit and the recording of the ensuing motions at one or more points (receivers). Values of the elastic moduli are obtained from the wave propagation velocities computed from the inter-arrival times of the motions at the various receivers or from the phase differences.

For a harmonic wave propagating in an infinite homogeneous medium, the variation of the amplitude of motion with distance A(r) can be expressed as

$$A(r) = S_0 \frac{1}{r} e^{-\alpha r} \qquad (4\text{-}40)$$

where r is the distance and α the attenuation coefficient because of material damping. This expression assumes that the attenuation of the amplitude is inversely proportional to distance, an assumption that is valid when the distance is several wavelengths (far field) but which would lead to errors in the near field.

The ratio of the amplitudes of the motions A_1 and A_2 recorded at two receivers at distances r_1 and r_2 is then

$$\frac{A_2}{A_1} = \frac{r_1}{r_2} e^{-\alpha(r_2 - r_1)} \qquad (4\text{-}40a)$$

leading to

$$\alpha = \frac{1}{r_2 - r_1} Ln \frac{A_1 r_1}{A_2 r_2} \qquad (4-41)$$

or

$$D = \frac{1}{2Q} = \frac{V}{2\pi(r_2 - r_1)f} Ln \frac{A_1 r_1}{A_2 r_2} = \frac{1}{2\pi f \Delta t} Ln \frac{A_1 r_1}{A_2 r_2} \qquad (4-42)$$

or

$$D = \frac{1}{\phi} Ln \frac{A_1 r_1}{A_2 r_2} \qquad (4-42a)$$

where Δt is the time interval between arrivals of the waves at the two receivers and ϕ is the phase difference (in radians) between the two recorded motions.

When the excitation is not harmonic but in the form of an impulse, it is necessary to decompose the recorded motions into their harmonics by means of a Fourier transform. Calling then $\phi(f)$ the phase of the cross spectrum in radians (or the difference between the phases of the two linear spectra), $A_1(f)$ the amplitude of the linear spectrum at the first receiver, and $A_2(f)$ the amplitude of the linear spectrum at the second receiver, the damping as a function of frequency is given by

$$D(f) = \frac{1}{\phi(f)} Ln(\frac{r_1 A_1(f)}{r_2 A_2(f)}) \qquad (4-43)$$

If one uses the autospectrum $U(f)$ instead of the linear spectrum at each receiver, $U(f) = A^2(f)$, and

$$D(f) = \frac{1}{2\phi(f)} Ln(\frac{r_1 U_1(f)}{r_2 U_2(f)}) \qquad (4-44)$$

The above expressions are based on the assumptions that the material damping is independent of strain amplitude for low levels of strain, that the receivers are placed at a sufficient distance from the source to make near-field effects negligible and have an attenuation because of radiation proportional to distance, and that the soil can be considered as a homogeneous full space. In addition, it is assumed that the motions can be accurately tracked at the two receivers.

In practice a number of complications may arise. If the source and receivers are placed at a distance that is not small in relation to their depth, free-surface boundary conditions will influence the records. If the soil properties are not homogeneous, additional reflections and refractions will take place. The attenuation of the amplitudes of motion also is affected by wave scattering around inclusions such as boulders in an alluvial deposit or by the presence of water in a soil that is not 100 percent saturated. The question then is whether these effects should be considered as part of the overall mechanism of energy dissipation without attempting to separate them. Finally, in order to obtain sensible results, it may be necessary to apply a time domain window to the records. A considerable amount of analytical and experimental work is still needed in order to refine and validate the procedure.

Modeling of Damping in Dynamic Analyses

Modeling of damping in discrete models of structures or soil deposits (using normal matrix structural analysis or finite elements) normally is performed by introducing a damping matrix C. When dealing with a mechanical system formed by springs and actual viscous dashpots, the assembly of the damping matrix is straightforward. In actual structures or soils the damping matrix represents only a mathematical means to reproduce some desired effects. It is normally selected so as to provide a system that has normal modes of vibration in the classical sense. This implies that the matrix C satisfies the orthogonality conditions

$$Q^T C Q = B \qquad (4\text{-}45)$$

where Q is the modal matrix containing the normalized mode shapes ($Q^T M Q = I$) as columns and B is a diagonal matrix. The ith diagonal element of B, b_{ii} then would be equal to $2\beta_i \omega_i$ if it is assumed that the damping β_i in each mode with natural frequency ω_i is of a linear viscous nature, and $2D_i \omega_i^2/\Omega$ if it is assumed to be linear hysteretic.

Eq. 4-45 can be satisfied by any matrix C of the form

$$C = M \Sigma a_n (k^{-1} M)^n \qquad (4\text{-}46)$$

or

$$C = M \Sigma b_n (M^{-1} K)^n \qquad (4\text{-}46a)$$

In the first case the term $b_{ii} = \Sigma a_n \omega^{-2n}$ and in the second $b_{ii} = \Sigma b_n \omega_i^{2(n+1)}$.

Particular cases which are often used in practice are:

1. $\qquad\qquad C = a_0 M$

    This is often referred to as mass proportional damping. The damping in each mode is then

$$\beta i = \frac{1}{2}\frac{a_0}{\omega_i} \text{ or } D_i = \frac{1}{2}\frac{a_0 \Omega}{\omega_i^2} \qquad (4\text{-}47)$$

    The physical model that would produce this damping matrix would have linear viscous dashpots with constants proportional to the values of the masses, connecting directly each mass to the base. The resisting forces in the dashpots would thus be proportional to the absolute velocity of each mass (relative velocity with respect to the base for the case of a base motion).

2. $\qquad\qquad C = b_0 k$

    This is often referred to as stiffness proportional damping. The damping in each mode is then

$$\beta_i = b_0 \omega_i/2 \text{ or } D_i = b_0 \Omega/2 \qquad (4\text{-}47a)$$

    The physical model would correspond to a system with linear viscous dashpots proportional to the stiffness of the springs connecting the masses (in the same way as the springs).

3. $\qquad\qquad C = a_0 M + b_0 K$

    This is often referred to as Rayleigh damping. It is a combination of the two previous models and produces a damping in each mode.

$$\beta i = \frac{1}{2}\frac{a_0}{\omega_i} + \frac{1}{2}b_0\omega_i \text{ or } D_i = \frac{1}{2}(\frac{a_0}{\omega i^2} + b_0)\Omega \qquad (4\text{-}47b)$$

    Figure 4-16 shows the variation of damping with frequency for each one of these models.

4.   An alternative to Eq. 4-46, if the mode shapes are known, is to form a damping matrix $C = MQBQ^TM$ where B is a diagonal matrix with the desired values $2\beta_i\omega_i$ or $2D_i\omega_i^2/\Omega$. If only some modes are specified, the Q and Q^T matrices will be rectangular. For lack of better knowledge, it is commonly assumed in practice that the damping is the same in all the modes.

In nonlinear dynamic analyses of structures, most of the energy dissipation will result naturally from the hysteretic behavior of the material. It is usual, however, to add a small amount of damping to account for energy dissipation at low levels of strain due to other causes. The damping matrix to simulate these losses is sometimes selected to be proportional to the mass matrix, the original (linear) stiffness matrix, the tangent stiffness matrix at each time or so as to provide an equal amount of damping in all the linear modes.

For linear dynamic analyses in the frequency domain, it is customary, on the other hand, to replace the damping matrix by a complex stiffness matrix, simulating in general frequency independent linear hysteretic damping. If all the members of the structure are assumed to have the same damping ratio D, then the complex stiffness matrix is of the form $K(1 + 2iD)$. However, the method allows one to consider materials with different damping ratios. It is sufficient in this case to multiply the stiffness matrix of each member by $(1 + 2iD)$, where D is the desired damping ratio for that element, then assemble the total stiffness matrix.

The form of the damping matrix used for the analyses (assuming that they all give the same amount of damping in the first mode) can influence global measures of response such as maximum displacements by 10 percent to 20 percent (which is often more than the variation caused by other effects, which are the subject of a considerable amount of attention and research). It will influence other response parameters, more affected by higher modes (and higher frequencies), by a much larger margin.

In continuous analyses of wave propagation in soil deposits, one could model the soil as a linear viscoelastic material. For a pure shear condition (shear waves propagating vertically), this implies a constitutive equation of the form $\tau = G\gamma + \eta\dot{\gamma}$ where η is the viscosity. A constant value of η would produce the same results as a stiffness proportional damping matrix in a discrete model. A value of η inversely proportional to frequency would yield, on the other hand, constant damping in all the modes. For analyses in frequency domain, the use of a complex modulus of the form $G(1 + 2iD)$ reproduces again frequency-independent linear hysteretic damping, equivalent to a viscosity inversely proportional to frequency.

The use of linear hysteretic damping may be adequate when studying the steady-state response at a specific frequency and adjusting the damping ratio as a function of amplitude. When considering, on the other hand, the response to a transient excitation, such as an earthquake, the use of a damping ratio independent of frequency often leads

to an excessive filtering of high-frequency components. As a result, site-specific motions computed at the free surface of a soil deposit using convolution analyses with an iterative linearized procedure tend to have a very small content of high frequencies (depending on the assumed depth of the soil deposit), and the motions computed at depth from a deconvolution analysis will eventually increase in amplitude and make the process unstable as the depth increases. These types of results are not consistent with those obtained from true nonlinear analyses or from experimental evidence on the frequency content of earthquake motions.

A second problem that deserves more consideration than it has received to date is the specification of damping ratios for two- or three-dimensional problems when involving not only the shear modulus but also Young's modulus or the bulk modulus. A solution often used is to assign the same amount of hysteretic damping to both elastic moduli. In more realistic analyses, the damping ratio is different for shear and compressional waves. This leads, however, to a further violation of the principle of causality. Although, apparently, the results are still reasonable, the fact that basic physical principles are not satisfied is unsettling. It should be noticed that similar questions must be raised as to the variation of the true elastic moduli with the level of strains in simulated nonlinear analyses.

Dynamic analyses in the frequency domain are particularly popular for soil structure interaction studies because of the frequency dependence of radiation damping. One has to deal in this case with the damping in the structure (which may be different for various parts of the structure), the internal damping in the soil due to some nonlinear behavior, and the damping due to radiation. The internal damping in the structure and the soil is often assumed to be of a hysteretic nature while the radiation damping is a more complicated function of frequency. In some cases, however, and particularly in simplified formulas to study soil structure interaction effects where the structure is modeled as a single-degree-of-freedom system, the structural damping is assumed to be of a linear viscous nature, which does not seem realistic.

Modeling of radiation damping in time domain analyses presents a particularly difficult problem. For surface foundations on an elastic half-space, Veletsos and Verbic obtained equivalent physical models that reproduce very accurately the frequency dependence of the radiation damping. For embedded foundations, Novak has proposed an approximation for the effect of embedment, replacing the lateral soil by springs and dashpots. For the case of a soil profile with properties varying with depth, and particularly for the case of a soil stratum of finite depth resting on much stiffer material, no such models are available. In this case, the fundamental frequency of the stratum the radiation damping will be very small.

In nonlinear soil structure interaction analyses in the time domain, modeling the soil typically with nonlinear finite elements, radiation damping is often ignored, moving the

lateral boundaries at a sufficient distance from the foundation and relying on the internal dissipation of energy to attenuate the amplitude of the waves.

PANEL REPORT

Following the state-of-the-art presentation, the topic of energy dissipation was discussed by a panel of experts. These experts considered the importance and state of the art of energy dissipation measurements. This information was then used as a basis for identifying research needs.

IMPORTANCE

The ability of a structure, a soil, or any physical system to dissipate energy while subject to vibrations is simulated in dynamic analyses through the introduction of damping terms. These terms are supposed to reproduce the physical process of energy dissipation, but they are often selected on a mathematical basis in order to obtain simple models that can be solved analytically. Most forms of energy dissipation are, in fact, associated with some type of nonlinear behavior, but they are normally modeled as linear terms. Moreover, most of our understanding of damping is based on the consideration of single-degree-of-freedom systems while, in reality, soil specimens used for laboratory tests are continuous multidegree-of-freedom systems.

Two types of damping are important in geotechnical engineering: material damping and radiation damping. The former refers to energy dissipation within a soil element and the second to dissipation of energy through wave propagation into regions outside the domain modeled or analyzed. This external region may be a semi-infinite region in the field or a testing apparatus.

Material damping is often important for soil systems that exhibit resonance frequencies within the frequency range of excitation. For such systems, low values of damping can often lead to large amplifications of the incident motions. This is especially true for relatively low levels of seismic excitation and thus low levels of strain in the soil.

At high levels of excitation, as the soil moves into the nonlinear range, the effective damping of soils can become very large and resonance phenomena become relatively less important. However, material damping may be even more important since it impedes wave propagation and can cause significant decay in motion amplitudes with respect to time and space. As a result, good quantitative data for material damping are an absolute requirement for accurate analysis of many seismic problems in geotechnical engineering.

Radiation damping can, in many cases, be handled quite well by analytical tools. However, it must be handled and this often requires that the damping properties of the

medium into which the radiation occurs be known. Hence, material damping may be important for accurate determination of the radiation damping.

Material damping may result from material properties such as viscosity or from the dissipation of energy by nonlinear behavior. Many of the problems encountered when nonlinear material damping is simulated in equivalent linear analyses could be solved by using appropriate nonlinear constitutive equations and performing true nonlinear analyses. It should be noticed, however, that additional positive or negative damping may be introduced by many analytical procedures currently used for solving nonlinear problems. This kind of damping is not generic to soil behavior, and its effect is to introduce errors on the high-frequency content of the computed motions.

STATE OF THE ART

Equivalent values of damping are determined in the laboratory from free vibration or cyclic (static or steady-state dynamic) tests. In the first case, damping is determined from the decay of the amplitude of motion with time. In the second, it is obtained from the amplification curve or the areas of the loops relating force to displacement for a given frequency.

In situ determination of damping in soil deposits has been attempted using geophysical methods (downhole, crosshole, spectral analysis of surface waves). A dynamic excitation is imposed at one point, and the amplitudes of the resulting motions are recorded at one or more points within the soil mass or along the surface of the soil deposit. From records of seismic motions, system identification techniques can also be used to determine effective damping values for soils. The bases and limitations of these methods are discussed briefly below.

Laboratory Measurement of Material Damping

Laboratory measurements of material damping have been performed for more than three decades. These measurements are normally conducted in conjunction with the measurement of soil stiffness, and generally the stiffness evaluation has been the issue of more concern. Both resonant column (in torsion or axial excitation) and slow cyclic methods (cyclic triaxial, cyclic simple shear) have been used to evaluate the material damping. When resonant methods are employed, damping is evaluated either from the free vibration decay curve or from the amplification curve. One assumes, then, a linear viscoelastic system or an equivalent linear system for measurements in the nonlinear range. When slow cyclic methods are employed, material damping is evaluated from the area of the hysteretic loops. In this case, a linear or equivalent linear hysteretic model is used to model the soil.

Resonant methods are used to measure material damping at strains ranging from less than 10^{-4} percent to slightly above 0.01 percent, depending on the equipment used and

the soil stiffness. Slow cyclic methods are used to measure material damping at strains above about 0.01 percent to 0.1 percent. In each method there is good repeatability in the measurements at a given strain level as long as large nonlinearities do not exist. However, oftentimes unreconciled differences between material damping values exist for the different methods. Furthermore, the general response of the soil begins to deviate from that predicted by the models as strain levels increase, especially at strain levels about 0.01 percent. Improved measurement techniques and better soil models are needed.

Field Determination of Damping by Seismic Methods

Downhole or crosshole measurements of compression and shear wave velocities to determine soil stiffnesses are now routine for geotechnical engineering applications. Measurement of material damping *in situ* using seismic methods is far from routine, but it is believed that such measurements can be developed into straightforward procedures that will be widely accepted for site characterization at least at low strain levels. Few efforts have been made in recent years to develop and apply seismic field methods to the determination of material damping in observational seismology, petroleum exploration, and geotechnical engineering.

Virtually all approaches to field determination rely upon the spectral analysis of seismic pulses as they propagate through the medium of interest. Typically, these measurements are made on a pulse as it travels downward from the surface (downhole) or as it propagates between an array of boreholes (crossholes). These seismic methods have been performed at low strain levels (10^{-5} percent to 10^{-4} percent) and rely upon computing the spectral ratio of a pulse recorded on at least two locations along its path. The objective is to quantify the attenuation of the pulse as a function of its frequency content; i.e., to measure the spectral decay over a known distance. The rate of attenuation with frequency is a function of the material damping of the medium. Although it is generally assumed that the rate of attenuation is proportional to frequency, because this has generally been observed over the earthquake motion bandwidth, this assumption is not required for data analysis, and tests of its validity are of interest in themselves.

It has been a frequent observation that downhole measurements of shear wave damping result in higher values than would be expected on the basis of (higher strain) resonant column tests on samples obtained from the same hole. It is apparent that these discrepancies warrant investigation.

Some limitations have been encountered in applying seismic field techniques that demonstrate the need for further research. There is no fundamental reason, however, why more energetic source (e.g., vibroseis) cannot be used at some sites (unpopulated areas) to allow measurements at higher strains. Downhole measurements in which the energy source is located on the ground surface near the collar of the hole can be

limited by the rapid attenuation of high frequencies in lossy near-surface layers. The signal thus becomes more monochromatic as it propagates downward, and consequently its spectral decay becomes more difficult to measure in the less attenuating, deeper materials. This limitation can be overcome by development of a downhole, horizontally polarized (SH) source, measuring the pulse as it travels upwards. Though not believed to be a major limitation, the possibility of frequency-dependent geometric spreading in certain layered media must be considered, and procedures to account for it must be developed.

Field Determination of Damping From Earthquake Records

As indicated above, field determination of damping using seismic methods is primarily used at present for low levels of strain. Equivalent or effective values of damping can be obtained for larger strain levels using the records of actual earthquakes and applying system identification techniques.

System identification techniques can be used to devise values of equivalent damping, using records of motions obtained at various depths (vertical arrays). A technique called the "random decrement technique" has been recently proposed to estimate *in situ* values of effective damping with only seismic records at the free surface and without any knowledge of the excitation input. The procedure is based on obtaining ensemble averages of various segments of the response of a system excited by random forces to form signatures that are representative of the free response of the system. Damping can then be calculated from the free decay history. The main advantages of this method would be its simplicity and the possibility of obtaining both an effective shear modulus and damping for different levels of strain, depending on the intensity of the motions. Several members of the panel had, however, strong reservations as to the validity or meaning of the results.

System identification techniques generally assume that the system has normal modes and that the damping in each mode is of a linear viscous nature (although no constraints are imposed on the variation of the damping with the modes). If the soil properties (modulus and damping) are determined from the motions at the free surface of the soil deposit and at a nearby outcropping of rock, an assumption must be made as to the type of waves and their angle of incidence. Normally vertically propagating shear waves are considered. When the properties are determined from the motions recorded at the surface and at various depths, although the same assumption must still be made, the effect of the angle of incidence of the waves is less important. In the random decrement technique, the value of damping obtained is a measure of the total effective damping in each mode, which includes an average value of the material damping over the soil profile plus any radiation effects. The remaining questions for the method to be useful are how to separate internal and radiation damping and how to assign damping values to the individual layers from the modal results.

RESEARCH NEEDS

Given the present state of the art and of the practice in the measurement and interpretation of damping values, the panel believes that it is necessary to:

- Develop an improved fundamental understanding of the basic mechanisms that contribute to material damping

- Develop an improved understanding of the variability of material damping values obtained by any one method (field or laboratory) and the discrepancies between the results provided by different methods to reconcile any differences

- Develop an improved understanding of the practical significance of the uncertainties involved in the characterization of damping and of the sensitivity of critical response parameters to the different mathematical models

To fulfill these three objectives, it is recommended to conduct research along three main lines.

Integrated Experimental Studies

A test site should be established that could be used for experimental studies and that could provide an opportunity for recording seismic motions. This site would be used for:

- Study of ground motions in order to back-calculate damping

- *In situ* measurement of soil damping

- Laboratory tests on soil samples to determine damping

- Development and calibration of new testing techniques (using forced vibrations, explosions, etc.) to determine values of damping under large strains

Clearly, values of modulus should also be obtained at the same time, and therefore these studies would apply equally to the low- and high-strain cyclic material properties studies.

The site should:

- Be conveniently accessible

- Be earthquake prone
- Have both rock and soil (saturated and unsaturated)
- Have good site information already available

It would be desirable if, in addition, it had:

- Some instrumental arrays already in place
- Some boreholes already available

Advantage should be taken of existing arrays such as those at Turkey Flat (near Parkfield, California) and at Lotung, Taiwan.

Development of Experimental Techniques

Field methods to determine values of damping *in situ* need a number of refinements and developments to overcome some of the present limitations. There is, for instance, a need to:

- Investigate the effects of casing and transducer coupling

- Develop good and reliable sources in general and a good downhole SH source, in particular

- Develop new techniques and instrumentation for field measurements of damping, particularly at large strain levels

- Develop methods for measuring at different strain levels two damping values for soil, one associated with shear deformation and the other one associated with compressional deformation

Analytical Studies

Several analytical studies are needed to help in the interpretation of the data obtained from laboratory or field tests and to incorporate these values into seismic analyses. It is necessary, in particular, to:

- Conduct analytical and numerical studies to investigate the sensitivity of key response parameters to the values of damping and the type of damping assumed in models

- Develop and evaluate nonlinear constitutive equations for soils and relate the parameters of these models to the quantities that can be measured in the laboratory, and preferably *in situ*

- Investigate the accuracy of nonlinear dynamic analyses, the importance of introducing fictitious damping in the numerical integration algorithms, and the existence of high-frequency components in the response. Moreover, results of nonlinear analyses must be validated by comparing them with actual data

- Develop analytical procedures to model the behavior of soil specimens in the laboratory tests to help in the interpretation of test data

In addition to these research topics, efforts should be made to make use of all the data already existing from instrumental arrays or to be generated in the future by existing or new arrays. Different system identification techniques could be applied to infer from these data equivalent values of damping at different sites. These values could then be compared to those obtained by other techniques. New arrays should be carefully designed and placed at carefully chosen locations to maximize the probability of obtaining the desired data. In this respect, it would be advisable to select any new array sites so as to obtain data from a sufficient number of different soil types.

PRIORITIES FOR RESEARCH

It is believed that significant progress in our understanding of damping can be achieved only with a broad front approach in which studies in the different areas discussed above are carried out simultaneously with a continuous exchange of information.

A considerable amount of earthquake damage has been associated with structures on soft soil deposits. Consequently, it would appear that higher priority should be given to the determination of material damping in this type of sites, particularly lacustrine alluvial and coastal soils with unconsolidated surface deposits where most of our urban and industrial centers are located.

CONCLUDING REMARKS

To achieve significant progress, it is necessary to coordinate research among engineers, geologists, geophysicists, and seismologists. To achieve better communications among these groups, there is a need to develop research programs that, by their own nature, would foster this collaboration. The test site studies that have been recommended are a good example of this type of program.

While there are many uncertainties in the determination of damping values and in the way these values are introduced into the analysis, there is already a substantial amount of knowledge that must be transmitted to the practicing earthquake engineer. An adequate educational or technology transfer program is needed to avoid the incorrect use of damping in practice.

State-of-the-Art Speaker — Dr. Gary Olhoeft

Workshop Panel

Chapter 5   SPATIAL VARIABILITY

Chapter 5
SPATIAL VARIABILITY

Considerable attention has been given over the past decade to determination of dynamic soil properties on a relatively localized basis. *In situ* tests are conducted in the immediate vicinity of the planned structure; laboratory tests are conducted on a limited number of soil samples obtained from boreholes drilled at the proposed site. Results of these tests can be very precise, indicating shear wave velocities to the nearest foot per second or the variation in shear modulus with shearing strain to less than a percent. However, these determinations, no matter how sophisticated or precise, represent information from a small fraction of the soil at the site. During the planning for this workshop, it was recognized that more attention had to be given to the spatial variability of soil properties in a region around a site to achieve adequate dynamic soil property measurements and site characterization. The state-of-the-art presentation for this topic was given by Dr. Gary Olhoeft, Research Scientist at the United States Geological Survey. Following Dr. Olhoeft's presentation, a report on the topic of spatial variability was prepared by a panel comprised of Gary Olhoeft (panel leader), John Christian (panel recorder), Roger Borcherdt, Wayne Clough, Fred Followil, Horisho Ito, Ann Keremedijian, Farrokh Nadim, Jerry Nelson, and Erik Vanmarcke.

SOA REPORT

INTRODUCTION

The measurement and description of spatial variability in soil are the characterization of geological heterogeneity. They are required in solving a variety of geological problems including mineral and petroleum exploration and development (Weber, 1986) and in geotechnical problems from agriculture to foundation engineering (Nielsen and Bouma, 1985; Peck et al., 1988). The necessity to characterize the stable existing soil is frequently coupled to that of finding out how it came to be that way and what might happen if something changed in the future (such as an earthquake or changing water levels). Thus, both spatial and temporal variability must be considered.

The measurement of soil properties in the laboratory and the field is readily performed with an array of existing geotechnical and geophysical tools (though not all practitioners know that these tools exist). What constitutes an adequate description (or parameterization) of soil spatial variability is more difficult and the subject of considerable current research. This discussion will focus on the geophysical methods of soil characterization.

GEOPHYSICAL METHODS

Available geophysical methods include electrical, electromagnetic, seismic, gravity, magnetic, radiometric, spectroscopic, and others, performed from satellite, aircraft, surface, and borehole platforms. All geophysical methods are based upon the measurements of a force or flux field. This field may be the natural flux of radiation from radioactive isotopes (radiometrics), sunlight reflecting from mineral surfaces (spectroscopy), variations in the earth's natural electrical, magnetic, or gravity fields, or fields induced by human activities (radio or sound waves). Variations in these fields occur for many reasons, including originating field stability and many sources of noise, and also from changes in physical or chemical properties in the earth.

Spatial variability within soil often occurs on small-length scales (meters to centimeters or smaller); therefore, only the highest resolution methods based upon the wave propagation will be discussed. These methods use electromagnetic (ground-penetrating radar or GPR) and elastic (seismic or acoustic) wave propagation to investigate the earth. Wave propagation through a material is described by velocity, attenuation and scattering properties of the material, and by the type, frequency, and orientation (polarization) of the propagating field. The resolution of wave propagation methods is determined by the distance scales over which material properties change compared to a wavelength of the propagating field. When the material properties change rapidly along the direction of propagation on distance scales that are short compared to the wavelength of the propagating field, the field is scattered (reflected, refracted, diffracted). Such scattering limits the depth of penetration of the propagating field (by randomly dispersing the energy in the field) but also provides the signals which are recorded to locate and describe the scatterers.

The velocity of electromagnetic wave propagation is controlled by the speed of light in a material, which is determined by the dielectric permittivity of the material. The dielectric permittivity is mostly a power law function of bulk density and fluid content, with secondary dependence upon frequency, temperature, and mineralogy (Olhoeft, 1987). The velocity of elastic wave propagation is controlled by the speed of sound in the material, which is determined by the elastic modulus. The elastic modulus is mostly a linear function of density, fluid content, and clay content, with secondary dependence upon frequency and temperature (Nur and Wang, 1988). The functional power versus linear dependence upon density causes the electromagnetic wave propagation techniques to be more sensitive to subtle changes in density and fluid content than the elastic wave methods.

The attenuation of electromagnetic wave propagation is determined by intrinsic electrical loss (fluid content and salt concentration), dielectric relaxation losses in water (fluid content), diffusion-limited dielectric relaxation losses in chemically surface-reactive colloidal-sized particles (mineralogical clay), and scattering losses (fracture or grain size distributions comparable to a wavelength; Olhoeft, 1984, 1987). The

attenuation of elastic wave propagation is controlled by the quality of grain-grain contacts, fluid movement, clay content, viscoelastic relaxation, and scattering losses (Nur and Wang, 1988). Dispersion describes the change in shape of a time-domain wavelet traversing through a medium with finite attenuation (hence, frequency-dependent velocity). Typically, higher frequencies are attenuated more than lower frequencies, resulting in broadening or spreading of the wavelet.

Electromagnetic wave propagation is the result of tightly coupled electric and magnetic fields propagating through a medium together. Elastic wave propagation is the result of particle motion along the direction of propagation (compressed or P-wave) or motion across the direction of propagation (shear or S-wave). While compressional and shear waves typically start together at a source, they do not propagate with the same velocities or orientations and thus, typically, separate in time as they propagate. Further, as they encounter changes in properties that cause scattering, mode conversions may occur which convert one form into another (a P-wave into an S-wave, for example).

CHARACTERIZATION OF SPATIAL VARIABILITY

Characterization of spatial variability with geophysical methods means determination of the three-dimensional distribution of locations where material properties change. Such determination is performed by launching a propagating wave and measuring how long it takes for a portion to return, and how much it is scattered and changed. By recording data at many locations, cross-sectional images of the subsurface are obtained. The time delay for a portion of the propagating field to return indicates depth to a scatterer. The amplitude of the portion returned indicates the contrast in physical properties at the scatterer. The change in shape of the return (wavelet dispersion) indicates frequency dependence of velocity and attenuation, or due to scatterers (ultimately yielding scatterer size distributions).

With ground penetrating radar, this is performed by towing a radar antenna across the surface of the earth. Seismic methods require closer coupling to the earth and are performed by physically impacting the ground to produce an elastic wave that is received at geophones which must be in physical contact with the ground. This means that seismic data are acquired by stopping and starting at discrete locations while the radar data are acquired continuously. In practice, the starting and stopping cause the seismic data acquisition to be costlier and with fewer horizontal locations than the ground penetrating radar.

Ground-penetrating radar cross sections typically have horizontal resolutions of centimeters. Seismic methods rarely have horizontal resolutions of less than a meter. In both methods, vertical depth of penetration and resolution are a function of wavelength of propagating wave in the material. At a frequency of 100 MHz, ground-penetrating radar has a resolution of about 10 centimeters with a depth penetration of about

40 meters in 1,000 ohm-m sandy soils. At a frequency of 1,000 MHz, the resolution is about 1 cm with a depth of penetration of about 4 meters. The resolution increases with increasing frequency (decreasing wavelength) but the depth of penetration decreases with increasing frequency (because of increased scattering if not additional attenuation mechanisms).

For loose sandy soils, meter or better resolution requires wave propagation frequencies in the acoustic (10 kilohertz) range for elastic waves and in the radiowave (10 to 100 megahertz) range for electromagnetic waves. These frequencies are determined from the required resolution (hence wavelength) and the velocity of propagation in the material. However, in their respective frequency ranges for the required resolution, the sandy soil with loose particle-particle contacts produces high attenuation to acoustic wave propagation while the electromagnetic waves propagate in an attenuation window (minimum loss). Thus, ground-penetrating radar produces the highest resolution cross-sectional images of sandy soil heterogeneity. This is true for sandy soil, dry or saturated with fresh water, in the absence of clay minerals and salt water (Wright et al., 1984).

If the soil contains clay minerals (not just engineering-size fraction clay, but mineralogical clay such as montmorillonite), then the situation reverses. The clay (depending upon distribution and morphology) usually improves particle bonding, increasing the utility of the elastic wave methods (Hasbrouck, 1987). At the same time, the chemically reactive surfaces of the colloidal-sized clay particles produce a dielectric relaxation loss mechanism that dramatically attenuates electromagnetic waves.

Thus, the seismic and radar methods are very complementary, with one able to acquire information where the other fails. The radar always has higher resolution and is less expensive to operate than the seismic, but it does not always work--nothing works all the time. For an example of some of the required information in choosing the appropriate geophysical technique, see Olhoeft (1988c; tailored for EPA Superfund site problems).

DATA INTERPRETATION

Once the appropriate technique has been used to acquire data to produce a cross section, interpretation begins. Interpretation may proceed qualitatively on the raw data, or the data may be computer processed to correct for acquisition biases, to improve visibility of some feature, or to acquire a quantitative interpretation of particular features. In these, each technique has further strengths and weaknesses.

Ground-penetrating radar (GPR) has not only the highest resolution but also the highest sensitivity to detect subtle changes in soil stratigraphy represented in changes of bulk density and water content. GPR can produce cross sections that show such stratigraphic features as eolian dune foresets and thin beds of till in sand and can distinguish

between clay through gravel particle size distributions. GPR can see down to, but not through, mineralogical clay horizons. Often the raw data cross-sectional images may be used to identify sedimentological structure and, thus, the processes which created the sediments and soils (Allen, 1984). GPR also detects many hydrological features such as the surface between the unsaturated and water-saturated zones (the water table), rainfall wetting fronts, and other changes in water content. From these, other properties may be inferred, such as the vertical transmissivity from repeated GPR measurements with time of a rainfall wetting front as it sinks in or estimates of hydrological dispersivity from correlations of length scales in the GPR cross sections (Rehfeldt et al., 1989; Olhoeft et al., 1988). For further details and examples about ground-penetrating radar, see Olhoeft (1988b), Lucius et al. (1990), and Duke (1990).

Figure 5-1 is an example of ground penetrating radar data acquired between Ashumet Pond (at left edge) and John's Pond (at right edge) on Cape Cod, Massachusetts. Ashumet Pond has been contaminated by the subsurface outflow of sewage settling ponds for nearly 50 years and has an average elevation about 2 meters higher than John's Pond. The intervening material is coarse sand, which should allow ready transport of water down gradient to John's Pond. Yet, John's Pond is not contaminated. Why not? The radar record clearly shows the water table between the two ponds, including a mound that must divert direct flow from one pond to the other. The mound may be due to enhanced recharge or other unknown reasons. The freshwater in this area is entirely due to rain recharge, forming a fresh water lense floating on the sea water intrusion. Details are also clearly visible in the water table structure. The region labelled "isotropic" is where the water table crosses downward dipping soil stratigraphic horizons without change. The region labelled "anisotropic" is where the water table follows the stratigraphy (where it is easier to flow along that across the bedding). W1 and W2 are wetting fronts from rainfalls 2 days and 4 days before, respectively. WW is a drawdown surface from a seasonal water well. SS1, SS2, and SS3 are examples of higher porosity stratigraphic reflectors. The data roughly has 10 to 20 centimeters resolution to a depth of 20 meters limited by the frequency of the radar system and the resultant wavelength in the ground. Higher frequency radar systems have higher resolution, but less depth of penetration--900 MHz would have 1 to 2 centimeters resolution, but only about 4 meters of penetration.

In contrast, the elastic wave propagation methods are less sensitive than GPR to changes in soil density and moisture content, but they directly measure soil particle movement (and sometimes water movement), to which GPR is insensitive. High-resolution seismic data may also be interpreted with little or no processing to observe stratigraphy and hydrology (Haeni, 1986; Steeples and Miller, 1990). The problems of quantitative interpretation of elastic wave data begin in the data acquisition process where coupling of the measurement device to the ground is a severe problem and often an unknown variable. However, when done properly, quantitative interpretation may yield dynamic properties of soils directly (Stokoe, 1980; Stokoe and Nazarin, 1985; Schuster et al., 1990).

Figure 5-1. The black and white drawing is the key to the color portion of this figure. The top half is the raw ground penetrating radar data, acquired using 80-Mhz center frequency antennas. The bottom half is the same data corrected for topography, distortions caused by variations in vehicle speed, and enhanced with an adaptive deconvolution filter. The overlay is a 30-meter horizontal by 30-meter vertical grid. See text for further details and discussion.

TECHNOLOGY NEEDS

The preceding brief discussion of wave propagation methods for spatial characterization of soils is meant to demonstrate that some measurement technology exists. Not all desirable material properties can be measured with existing technology, indicating directions for new technology development. However, the bigger problems of spatial characterization of soils lie in the areas of education and technology awareness, of adequate levels of characterization, and of meaningful methods to parameterize and describe geological heterogeneity.

Of the two geophysical methods discussed, seismic methods are more widely known than is ground-penetrating radar. However, even the seismic methods outlined above and in the references are not widely practiced but are examples of state-of-the-art research. In most site characterization efforts, the first technique normally selected for use involves drilling and soil sampling. However, a better approach would be to use noninvasive geophysics, which as raw data can, at a minimum, outline areas of differences for later investigation by drilling and sampling. With minimal interpretation and uncertainty, the geophysical data can also outline areas of differences with depth to give a three-dimensional drilling guide. When geometrically correct cross sections are produced, the geophysical data can interpolate between boreholes and see length scales larger than core samples but smaller than inter-borehole spacings. When proper quantitative interpretation of the geophysical data is performed, material physical properties may be determined without uncertainty associated with drilling and sampling disturbances. The fact that these things are not often done is indicative of the need for education and making practitioners aware of the available state-of-the-art technologies.

Also of interest to practitioners and an area of active research is the question, "How much data and detail are enough?" A 30-meter cube of soil fully characterized at 1-cm resolution for one property measurement at 8 bits of accuracy is 27 gigabytes of data. Commercial ground-penetrating radar systems can generate nearly a gigabyte of data in one working day. Obviously, that data density is not required to simply locate the water table, but it may be required to model the consequences of a point source contaminant spill at the surface. How can we tell when sufficient data have been acquired for a given problem?

Another active area of state-of-the-art research is the problem of parameterizing geological heterogeneity. With the availability of instruments that produce gigabyte data sets, the necessity to statistically describe geological heterogeneity, and the requirement to manipulate the data quantitatively, human interpretation requires computer assistance. Such assistance is becoming available to guide the choices in characterization measurements (Olhoeft, 1988c), and it needs to be developed and tested to assist quantitative interpretation and modeling. The choices of statistical descriptions and modeling need further exploration--do we need (and can we get) deterministic model

predictions, or are stochastic forecasts acceptable? What about situations that depend not on the modal (central) portion of the statistics but the extreme (such as threshold phenomena or 100-year floods)? Many current computer models are approximations, frequently involving simplification to one- or two-dimensional situations. Few three-dimensional models exist. How do we know what is good enough?

PANEL REPORT

The panel members considered the following topics during their discussions: importance of spatial variability, research needs, and technology transfers.

IMPORTANCE

Figures 5-2 and 5-3 (Borcherdt et al., 1989, and Maley et al., 1989) show dramatically the effects of spatial variability in dynamic soil properties during the October 17, 1989, Loma Prieta earthquake. The figures illustrate the widely varying response to the earthquake excitation for five sites located on soft San Francisco Bay clays compared to three sites on rock. Similar variability is observed in patterns of damage recorded in other earthquakes (e.g., Mexico City). Such wide variability in dynamic soil response is not unexpected, but the explanations for such widely varying dynamic response are not fully understood, suggesting many areas for further research.

RESEARCH NEEDS

Spatial variability in dynamic soil properties may result from differences in the way properties or processes are distributed in space or in time. Such distributions are complex and are neither easily described nor readily parameterized. Technology has evolved to the point where such systems may be measured and documented to high degrees of accuracy and resolution, but many questions remain. Are the correct parameters being measured? What are the scales over which they need to be measured? What methods are needed to describe them? How are different scales related? Is there an orientation to the scale (e.g., vertical versus horizontal)? What is the relation of scale to dimension and geometry? How are models tied to measurements? What is the required level of characterization required for adequate prediction of site response? Are available technologies being fully utilized? What transfer mechanisms are required to ensure passage and translation of useful technologies between diverse disciplines?

Scales

It must be recognized that many different spatial and temporal scales are required to characterize the problem of dynamic soil response for earthquake-resistant design. There is the spatial scale of the problem (buildings on a site), and there is the scale of measurements (core samples through regional seismometer arrays). Some properties

Figure 5-2. Effects of Spatial Variability in Dynamic Soil Properties on Acceleration Records during Loma Prieta Earthquake.

Figure 5-3. Effects of Spatial Variability in Dynamic Soil Properties on Attenuation Curves for Loma Prieta Earthquake.

measurements (core samples through regional seismometer arrays). Some properties and processes occur over time scales that are short (frequency- or rate-dependent properties, such as dissipation; processes such as elastic wave propagation), while others occur over geological-evolutionary times (e.g., cementation), and some may even indicate memory effects (e.g., deformation is history dependent). The scale capable of being modeled with existing computer hardware and software may differ from the scale of true variability in the earth, which we may never know but only approximate. Lastly, some properties are scale invariant (e.g., porosity) while others are strong functions of scale (e.g., strength). Small rocks are very strong, decreasing in strength with increasing size.

Measurement and Statistics

The ability to describe complex media and parameterize them lags behind the ability to measure such media. It is possible to produce gigabyte, megapixel images with centimeter accuracy over distances of hundreds of meters, but this may miss the large features of the problem. Research is needed on the utility of such measurements, as current numerical models have difficulties with nodes or elements exceeding 10,000.

Measurements show that the earth rarely is simple. Yet, to simplify models, assumptions are commonly made about homogeneity, isotropy, dimensionality, geometry, linearity, reversibility, elasticity, and other things that measurements show not to be true. How do we describe and utilize such measurements? Some descriptions (such as fractal pore and fracture morphologies) are beginning to change effective medium models of random media. How do we use them to change the statistical input to deterministic/probabilistic/possibility models? Can chaos theory be used to describe or predict the location and timing of critical cusp phenomena, such as slope failure or sand boils?

Methods of classical statistics are generally inappropriate for analyzing and describing spatial variability of soil properties. Classical statistics assume statistical independence between observations while soil exhibits structure and correlation over various scales. It is essential to describe and quantify the lack of spatial independence, usually with correlation length functions but sometimes with other statistical methods. The assumptions made about statistics can strongly bias the interpretation of measurements and models. Averages, means, and least-squares fitting are inappropriate in systems where the extreme value of a soil property may control catastrophic failure under dynamic loading. The use of fractals, chaos theory, possibility theory (fuzzy sets), nonparametric statistics, and other methods need to be explored (Alexander, 1986; Katz and Thompson, 1985; Vanmarcke, 1977, 1983; Wong, 1987).

Analytical Models

Understanding the variability in dynamic soil response requires the use of models as well as measurements. Many models have been built with assumptions that are given the best practically available, though known to be inaccurate, approximations of reality, or that have not been adequately tested for lack of data or for lack of ways to tie the models to available data. The present state-of-the-art is to use one-dimensional soil models to account for vertical variation. One-dimensional models are known to be inadequate in certain situations, and two- or three-dimensional models should be developed.

All models available today for earthquake design and analysis are based on a deterministic representation of soil properties. Although the technology for performing static analysis with probabilistic representation of static soil properties is currently under development (stochastic finite element; Vanmarcke, 1977), extending this technology to possibilistic (fuzzy set theory) and dynamic problems (e.g., earthquake response) is by no means straightforward (Nadim et al., 1989). There is an urgent need to develop dynamic analysis techniques that are capable of handling a soil profile, section, or volume element that is defined as a random field (e.g., statistically; Vanmarcke, 1983).

Soil properties are inherently nonlinear, even at small loading levels. Measurements of nonlinear behavior exist, but nonlinear models that are capable of handling spatially variable nonlinear soil properties need to be developed. Once a numerical model exists, sensitivity studies of the model need to be performed in order to identify the parameters or processes that control the model results. The sensitivity analysis is a key tool in determining what parts of the model require accurate measurement inputs and extended computational accuracy, or may be safely neglected through approximate measures. Ideally, the numerical models that are developed should be user-friendly and be available to practicing engineers and students. Expert systems should be developed to aid in the interpretation of the model output and guide the user in preparing input for and running of the model.

Numerical models should be carefully tested for parametric sensitivity and validated against known physical examples (from physical models or case histories) to ensure a high degree of confidence in the use of the models for predictive purposes. Such testing may result in knowledge about the required level of characterization for a site. Overcharacterization is an unnecessary expense while undercharacterization may result in inaccurate prediction and unacceptable risk (Figure 5-4). Many well-established design procedures have been deliberately constructed to give adequately conservative results on the basis of relatively simple site descriptions. Others are mandated by regulatory requirements. Many of these are not adequately tested (nor are they even testable) before an earthquake occurs. Difficulties also arise due to conflicts in available data sets. How much further effort is required to reduce or eliminate those

Top diagram labels: Site Complexity (y-axis), MODEL DETAIL (x-axis), Model Comprehensibility. Zones: Unreliable Results, Expert Advise Needed, Satisfactory, Zone, Models Struggle, Nonsense, Data Density.

Bottom diagram labels: Site Complexity (y-axis), MODEL DETAIL (x-axis), Model Performance Zones. Zones: Unreliable Results, Expert Advise Needed, Satisfactory, Zone, Models Struggle, Nonsense, Data Density.

Figure 5-4.   Relation Between Site Complexity and Detail of Numerical Model.

conflicts? What are the acceptable levels of uncertainty (and how are they determined) from conflicts in measured data or competing models?

Needed Technology

The existing technology for determining spatial variability is reasonably well developed, particularly where certain parameters are concerned. For example, procedures to determine the maximum shear wave velocity, and hence the maximum shear modulus, are readily available and economic to perform. However, in other areas, the state of the art is primitive. Problems exist in terms of the complete absence of a method to make certain measurements, existing methods that are not economic (and thus not routinely available), or inadequate software to process or display the results.

Examples of missing technology that is badly needed include:

- *In situ* measurements of modulus degradation with strain

- Sampling of gravelly soil

- Methods to locate cracks and high porosity in soil

- *In situ* stress-strain determination in soil (well developed in rock but not soil)

Examples of existing tools to solve problems where the existing technology is uneconomic include:

- Techniques to rapidly profile the ground in urban areas with density, rubble, or utility concentrations that interfere with existing remote sensing methods

- Procedures for undisturbed sampling of loose sand

- Methods to allow accurate, quantitative determination of local stiffness of soil

Examples of needed software development include:

- Integrated graphics to compare subsurface database and model results

- Statistical processing methods to sort large amounts of data and assess what fraction of soil is at a level to lead to general failure

•   Linkage programs between remote sensing data sets, analytical tools, and models to result in engineering risk assessments

With the improvement of ground characterization methods will come a need to improve data display and automatic interpretation procedures. Expert approaches may offer an appropriate avenue to automatic interpretation not only of massive data sets, but also between isolated data notes (e.g., cone profiles), and to cross correlate between information from surface geophysics (e.g., ground penetrating radar), borehole logs, and other measurements. Expert systems should be developed for different types of geologic regimes.

Research in all areas is needed to address definitions of spatial variability. The issues at hand relate not only to the appropriate level of resolution of parameters but particularly to how to cover an area, both quickly and economically. Refined knowledge of a few parameters does not necessarily translate into knowledge of spatial variability. The average project allows only a limited budget for fieldwork, and it is important that the exploration project is efficient and economic over as wide an area as possible.

Other Research Needs

Most of the emphasis of dynamic soil research to date has been on physical mechanisms. There are whole classes of chemical problems that need research, such as the effects of varying mineralogy, water content and chemistry, stress corrosion, cementation, and soil alteration. Coupled processes and correlated properties also need further research. Many processes are treated as if they were the result of independent forces and flows, when numerous examples of coupled processes are known. More research is needed in areas of coupled chemical-hydraulic-mechanical-electrical-thermal systems, such as dissipation/attenuation, osmosis, liquefaction, and others (Olhoeft et al., 1987).

In general, many of the problems of variability in the dynamic response of soils may be addressed only by field studies. We have many pictures of sand boils that show what they look like in plan view, but what does a sand boil look like in cross section? Why here instead of there? The only way to know the required level of characterization of such variability is to over measure and over study a field site in excessive detail with multiple disciplines. Then the results of the study can back off and specify the required level of characterization for various purposes--site characterization, regulatory approval, predictive modeling, etc.

TECHNOLOGY TRANSFER

Methods for characterization of sites tend to be derived from two fields: geotechnical engineering and geophysics. The geotechnical approach is generally focused toward a site-specific, even location-specific, orientation. Thus, a cone penetration test provides data with depth for 4 cm-diameter spot of soil. The geophysical approach provides

information on a larger scale, noninvasively, continuously, and in three dimensions. In the past, this often aggregated site properties; e.g., modulus from a seismic wave study. However, with the introduction of ground-penetrating radar, very specific information can be obtained on details of soil stratigraphy.

Recent advances have occurred in terms of site characterization in both geotechnical engineering and geophysics. Unfortunately, the lack of adequate technology transfer has limited the use of new methods outside the specialty environs. There is a strong need to have mechanisms that would promote transfer of the available technology. With implementation of technology transfer, there will also exist needs to capitalize on the merging of the results and verification of the different technologies.

An effective means of promoting technology transfer is through faculty development programs. These could come in the form of intensive workshops or short courses where equipment and data processing tools could be demonstrated. The educational processes would be enhanced if the workshops could take place at the location of a well-documented experimentation field site. Such a site would have available reports on stratigraphy, soil or rock parameters, ground water regime, and even past seismic performance. Faculty and students could undertake hands-on experiments with various new exploration tools and have immediate confirmation of the accuracy of the findings as well as their physical meaning.

It is important to note that technology transfer offers a means to attain quick return for a relatively small investment. For example, if ground-penetrating radar can rapidly determine soil stratigraphy at a site where liquefaction has occurred, it may serve as a singular tool in helping to understand why one site liquefies while an immediately adjacent one does not. Further, this approach might well prove to have a substantial impact on commercial and regulatory geotechnical site assessments.

REFERENCES

S. Alexander. "Fractal Surfaces: In Transport and Relocation in Random Materials," J. Klafter, R. J. Rubin, and M. F. Shlesinger, eds., World Scientific, Singapore, 1986, pp. 59-71.

J. R. L. Allen. " Sedimentary Structures, Their Character and Physical Basis." Elsevier, Amsterdam, 1984, 663 pages.

R. D. Borcherdt, N. C. Donovan, B. A. Bolt, D. Boore, M. Celebi, D. Eberhart-Phillips, T. Hall, S. F. Hough, A. F. Shakal, and R. V. Sharp. Geoscience Investigations of the Earthquake of October 17, 1989, Near the Summit of Loma Prieta in the Southern Santa Cruz Mountains: EERI Geoscience Recon. Team Report, November 8, 1989, 16 pages + 12 figures.

S. Duke. "Calibration of Ground Penetrating Radar and Calculation of Attenuation and Dielectric Permittivity Versus Depth," M.Sc. Thesis, Dept. of Geophysics, Colorado School of Mines, Golden, Colorado, 1990, 236 pages.

F. P. Haeni. Application of Seismic-Refraction Techniques to Hydrologic Studies. U.S. Geological Survey Open File Report 84-746, 1986, 144 pages.

W. Hasbrouck. "Hammer-Impact, Shear-Wave Studies." In Shear-Wave Exploration, S. Danborn, and S. N. Domenico, eds., Geophysical Developments No. 1, Tulsa, Soc. Explor. Geophys., 1987, pp. 97-121.

A. J. Katz, and A. H. Thompson. Fractal Sandstone Pores: Implications for Conductivity and Pore Formation. Phys. Rev. Lttrs., v. 54, 1985, pp. 1325-1328.

R. W. Knapp and D. W. Steeples, "High-Resolution Common-Depth-Point Seismic Reflection Profiling: Field Acquisition Parameter Design," Geophysics, v. 51, 1986a, pp. 283-294.

——————. "High-Resolution Common-Depth-Point Seismic Reflection Profiling: Instrumentation," Geophysics, v. 51, 1986b, pp. 276-282.

R. W. Lankston, "High-Resolution Refraction Seismic Data Acquisition and Interpretation," In Geotechnical and Environmental Geophysics, Vol. 1, Review and Tutorial, S. H. Ward, ed., Tulsa, Soc. Explor. Geophys., 1990, pp. 45-73.

Third International Conference On Ground Penetrating Radar, U.S. Geological Survey Open File Report 90-414, J. E. Lucius, G. R. Olhoeft, and S. K. Duke, eds., 1990, 94 pages.

R. Maley, A. Acosta, R. Ellis, E. Etheredge, L. Foote, D. Johnson, R. Porcella, M. Salsman, and J. Switzer. U.S. Geological Survey Strong Motion Records from the Northern California (Loma Prieta) Earthquake of October 17, 1989, U.S.G.S. Open-File Report 89-568, 1989, 85 pages.

R. D. Miller, D. W. Steeples, J. A. Treadway, and S. Hinschberger. "Seismic Survey Over a Topographic Scarp in the Snake River Plain, Idaho," Seismol. Soc. Am. Bull., v. 78, 1988, pp. 299-307.

R. D. Miller, D. W. Steeples, R. W. Hill Jr., and B. L. Gaddis. "Identifying Intra-Alluvial and Bedrock Structures Shallower Than 30 Meters Using Seismic Reflection Techniques." Geotechnical and Environmental Geophysics, v. 3, Geotechnical, S. H. Ward, ed., Tulsa, Soc. Explor. Geophys., 1990 pp. 89-97.

P. B. Myers, R. D. Miller, and D. W. Steeples. "Shallow Seismic-Reflection Profile of the Meers Fault, Comanche County, Oklahoma." GRL, v. 15, 1987 pp. 749-752.

F. Nadim, L. Haarvik, H. Nordal, and O. T. Gudmestad. "Analysis of Earthquake Response at a Site With Uncertain Properties." In Proceedings, 5th Int'l. Conf. on Structural Safety and Reliability (ICOSSAR '89), San Francisco, CA, August, 1989.

"Soil Spatial Variability." Proceedings of a Workshop of the ISS and SSSA, D. R. Nielsen and J. Bouma, eds., 1985, 30 Nov.-1 Dec., Las Vegas, 1984, 243 pages.

"Seismic and Acoustic Velocities of Reservoir Rocks, V. 1, Experimental Studies." Geophysical Reprint Series, No. 10, Tulsa, Soc. Explor. Geophys., A. Nur, and Z. Wang, eds., 1988, 405 pages.

G. R. Olhoeft. "Applications and Limitations of Ground Penetrating Radar: In Expanded Abstracts." 54th Ann. Int. Meeting and Expo. of the Soc. of Explor. Geophys., Atlanta, Georgia, 1984 pp. 147-148.

————. "Electrical Properties from 10^{-3} to 10^9 Hz, Physics and Chemistry: In Physics and Chemistry of Porous Media II." AIP Conference Proceedings, 154, J. R. Banavar, J. Koplik, and K. W. Winkler, eds. NY, Am. Inst. Physics, 1987, pp. 281-298.

————. "Interpretation of Hole-To-Hole Radar Measurements." In Third Techn. Symp. on Tunnel Detection, January 12-15, 1988, Golden, Colorado, 1988a, pp. 616-629.

————. "Selected Bibliography on Ground Penetrating Radar." In Proceedings of the Symp. on the Appl. of Geophysics to Eng. and Environ. Problems, March 28-31, 1988, Golden, Colorado, 1988b, pp. 462-520.

—————————. Geophysics Advisor Expert System, U.S. Geological Survey Open-File Report 88-399, 1988c, floppy disc.

—————————. "Geophysical Characterization of Hazardous Waste Sites." In Abstracts, 28th Int'l. Geol. Congress, Washington, D.C., July 9-19, 1989, v. 2, pp. 545-555.

G. R. Olhoeft, G. D. Callahan, W. D. Carrier III, D. Langmuir, H. W. Olsen, V. Rajaram, and J. E. Rhoderick. Annual Review of U.S. Progress in Rock Mechanics--Coupled Processes. Washington, D.C., Nat. Acad. Press, 1987, 36 pages.

G. R. Olhoeft, J. E. Lucius, and R. M. Bochicchio. "Scales of Length and Connectivity from Ground Penetrating Radar." In U.S. Geological Survey Toxic Substances Hydrology Program--Proceedings of the Technology Meeting, Phoenix, Arizona, September 26-30, 1988, USGS WRI-88-4220, 1988, p. 555.

A. Peck et al. "Consequences of Spatial Variability in Aquifer Properties and Data Limitations for Groundwater Modeling Practice." IAHS, Oxfordshire, 1988, 271 pages.

S. E. Pullan and J. A. Hunter. "Delineation of Buried Bedrock Valleys Using the Optimum Offset Shallow Seismic Reflection Technique." In Geotechnical and Environmental Geophysics, v. 3, geotechnical, S. H. Ward, ed., Tulsa, Oklahoma, Soc. Explor. Geophys., pp. 75-87.

K. R. Rehfeldt, L. W. Gelhar, J. B. Southard, and A. M. Dasinger. Estimates of Macrodispersivity Based on Analyses of Hydraulic Conductivity Variability at the MADE Site. Palo Alto, EPRI interim report EN-6405, 1989, var. pag.

G. Schuster, H. Benz, M. Murphy, J. Hill, C. Sikorski, and C-W. Tsay. "Prediction of Seismic Ground Amplification by Forward Modeling Techniques." In Geotechnical and Environmental Geophysics, v. 3, Geotechnical, S. H. Ward, ed., Tulsa, Oklahoma, Soc. Explor. Geophys., 1990, pp. 1-21.

D. W. Steeples and R. D. Miller. "Seismic Reflection Methods Applied to Engineering, Environmental, and Groundwater Problems." In Proceedings of the Symp. on the Appl. of Geophysics to Eng. and Environ. Problems, March 28-31, 1988, Golden, Colorado, 1988 pp. 409-461.

—————————. "Seismic Reflection Methods Applied to Engineering, Environmental, and Groundwater Problems." In Geotechnical and Environmental Geophysics, v. 1, review and tutorial, S. H. Ward, ed., Tulsa, Oklahoma, Soc. Explor. Geophys., 1990, pp. 1-30.

K. H. Stokoe II. "Field Measurement of Dynamic Soil Properties." In Proceedings 2nd ASCE Conf. on Civil Eng. and Nuclear Power, v. 2, September 15-17, Knoxville, Kentucky, 1980 pp. 7-1-1 to -31.

K. H. Stokoe II and S. Nazarin. "Use of Rayleigh Waves In Liquefaction Studies." In Measurement and Use of Shear Wave Velocity for Evaluating Soil Dynamic Properties, R. D. Woods, ed., Proc. Geotech. Eng. Div. ASCE, 1985, pp. 1-17.

E. H. Vanmarcke. "Probabilistic Modeling of Soil Profiles." Journal of the Geotechnical Engineering Division, v. 103, 1977, pp. 1227-1246.

E. H. Vanmarcke. Random Fields: Analysis and Synthesis. Cambridge, MA, MIT Press., 1983.

J. S. Y. Wang. T. N. Narasimhan, and C. H. Scholz. "Aperture Correlation of a Fractal Fracture." JGR, v. 93, 1988, pp. 2216-2224.

K. J. Weber. "How Heterogeneity Affects Oil Recovery." In Reservoir Characterization, L. W. Lake and H. B. Carroll Jr., eds., NY, Academic Press, 1986, pp. 487-544.

P-Z Wong. "Fractal Surfaces in Porous Media." In Physics and Chemistry of Porous Media II, AIP Conf. Proc. 154, J. R. Banavar, J. Koplik, and K. W. Winkler, eds., NY, Am. Inst. Physics, 1987, pp. 304-0318.

D. L. Wright. G. R. Olhoeft, and R. D. Watts. "Ground-Penetrating Radar Studies on Cape Cod." In Surface and Borehole Geophysical Methods in Groundwater Investigations, D. M. Nielsen, ed., NWWA, Worthington, Ohio, 1984, pp. 666-680.

State-of-the-Art Speaker — Dr. Walter Silva

Workshop Panel

Chapter 6   SITE GEOMETRY AND GLOBAL CHARACTERISTICS

Chapter 6
SITE GEOMETRY AND
GLOBAL CHARACTERISTICS

A number of issues related to site geometry and global (area) response are thought to be important to the evaluation of dynamic soil properties and site characterization. These include topics such as topography effects, near-surface scattering and attenuation of energy, and specification of strong ground motions. The contributions of these effects at a site will possibly determine the need for or accuracy of dynamic soil properties and site characterization information. The general topic of site geometry and global effects, with particular emphasis on specification of site-dependent strong ground motion, was reported and presented by Dr. Walter J. Silva, Senior Seismologist at Pacific Engineering and Analysis. Following Dr. Silva's presentation, a panel comprised of Walt Silva (panel leader), John Schneider (panel recorder), John Anderson, Terry Barker, Jacob Philip, Al Rogers, Wood Savage, Ray Seed, and Paul Somerville reviewed the state of the art (SOA) in the area of site geometry and global effects. Results of their panel discussions were used to prepare a panel report with recommendations for research.

SOA REPORT

INTRODUCTION

Local geologic conditions have long been recognized to have a dominant effect upon strong ground motions (Hayashi et al., 1971; Mohraz, 1976; Seed et al., 1976). For example, Figure 6-1 shows average spectral amplifications (response spectral acceleration divided by peak acceleration) computed from recordings made on rock and soil sites at close distances to earthquakes in the magnitude range of about 6 to 7. The differences in spectral shapes are significant and depend strongly upon the general site classifications. These variations in spectral content represent average site-dependent ground motion characteristics and result from vertical variations in soil material properties (1-D effects).

Due primarily to the limited number of records from earthquakes of different magnitudes, spectral content in terms of response spectral shapes, was interpreted not to depend upon magnitude or distance, but rather to be primarily affected by the stiffness and depth of the local soil profile. With an increase in the strong motion data base, it has become apparent that spectral shapes depend strongly upon magnitude as well as site conditions (Joyner and Boore, 1982, Idriss, 1985; Silva and Green, 1989) and that site effects extend to rock sites as well (Boatwright and Astrue, 1983; Campbell 1981, 1985, 1988; Cranswick et al., 1985; Silva and Darragh, 1989).

Figure 6-1. Average 5% damping response spectral shapes (Sa/a) computed from motions recorded on different soil conditions (after Seed et al., 1976).

Examples of differences in spectral content largely attributable to one-dimensional (1-D) site effects at rock sites can be seen in comparisons of spectral amplifications computed from motions recorded in both active and stable tectonic regions (Silva and Darragh, 1989). Figure 6-2 shows average spectral shapes computed from recordings made on rock at close distances to large and small earthquakes (Table 6-1). For both magnitudes (moment magnitude M 6.4 and 4.0), the motions recorded in eastern North America (ENA), a stable tectonic region, show a dramatic shift in the maximum spectral amplifications toward shorter periods compared to the western North American (WNA) motions. These differences in spectral content are significant and are interpreted as primarily resulting from differences in the shear-wave velocity and damping in the rocks directly beneath the site (Boore and Atkinson, 1987; Toro and McGuire, 1987; Silva and Green, 1989; Silva and Darragh, 1989). Also evident in Figure 6-2 is the strong magnitude dependency of the response spectral shapes. The smaller earthquakes show a much narrower bandwidth. This is a consequence of lower corner frequencies for smaller magnitude earthquakes (Boore, 1983; Silva and Green, 1989; Silva and Darragh, 1989).

The difference in spectral content resulting from soil site effects, as shown in Figure 6-1, and from path or rock site effects, as shown in Figure 6-2, is dramatic and illustrates the degree to which 1-D site conditions (vertical variations in dynamic material properties) control strong ground motions. Superimposed upon these effects, for linear systems, are the effects of lateral heterogeneities upon strong ground motion. Such laterally varying structures as surface topography, dipping interfaces, and changes in material properties contribute two-and three-dimensional (2-D and 3-D) aspects to ground motion specification. These non-homogeneous effects, resulting from scattering, focusing, and mode conversions are present at all sites to some extent. In some cases, these effects can significantly alter the spectral content of ground motions as well as increase the duration of strong shaking.

Such factors as earthquake size as well as 1-D, 2-D, and 3-D geologic site structure contribute significant effects to strong ground motions in terms of absolute levels and spectral content. As a result, it is necessary to separate these effects and assess their individual contributions in terms of degree of influence, ranges in applicability, and predictability.

In the following sections, single- and multidimensional geological structures relevant to categorizing geologic structural effects on ground motions are defined in general terms. The degree of such effects and ranges in applicability will also be discussed. Following that, the Band-Limited-White-Noise (BLWN) ground motion model employing a single-corner-frequency, constant-stress-drop source spectrum will be introduced. This model naturally separates source, propagation path, and site effects with physically simple parameters and is useful when isolating factors controlling 1-D aspects of site response at rock and at soil sites. Subsequently, applications to rock and soil sites are

Figure 6-2. Average 5% damping response spectral shapes (Sa/a) computed from motions recorded on rock sites at close distances to M=6.4 earthquakes (top figure) and M=4.0 earthquakes (bottom figure). In each figure the solid line corresponds to motions recorded in WNA, dashed line to motions recorded in ENA. (See Table 1 for a list of earthquakes, sites, distances, and average peak accelerations).

Table 6-1
EARTHQUAKES AND STATIONS USED FOR WNA AND ENA COMPARISONS

Earthquake	Date	Magnitude ML	M	Source Depth (km)	Epicentral Distance (KM)	Station	USGS No.	Reprocessed Average Horizontal Peak Acceleration (g)
San Fernando	71209	6.4	6.6	8.4	23.0	Lake Hughes 12	128	0.316
					26.3	Lake Hughes 9	127	0.147
					27.3	Lake Hughes 4	126	0.184
					33.8	Griffith Park	141	0.185
					36.1	Seis. Lab.	266	0.151
					43.2	Santa Anita	104	0.194
Nahanni	851223	6.4(m$_b$)	6.8[a]	18.0	8.0	Site #1		1.176
					9.0	Site #2		0.450
					20.0	Site #3		0.202
Coalinga Aftershocks								
A	83050322	3.8		7.64	8.54	LLN		0.0053
D	83050700	3.9		8.92	8.39	LLN		0.0189
K	83051013	3.9		4.79	12.46	LLN		0.0036
K3	83051405	3.9		11.18	5.56	VEW		0.0269
M	83051414	3.9		9.15	4.94	LLN		0.0084
New Brunswick	820331	4.01[b]		5[c]	4	Mitchell Road		0.20

[a]After Choy and Boatwright (1988).
[b]After Boore and Atkinson (1987).
[c]After Toro and McGuire (1987).

presented,and an assessment is made as to the degree to which single and multidimensional geological structures affect strong ground motion. Lastly, recommendations are presented to help improve the predictability of these effects.

GEOMETRICAL SITE EFFECTS DEFINITIONS AND SENSITIVITIES

For the purpose of discussion, some very general definitions of non-homogeneous geologic conditions are useful. Figure 6-3 shows a sketch that outlines idealized 2-D structures depicting topographic as well as alluvial valley features. Site 1 illustrates mountain or ridge topographic features, recognizing that the effects pertain to sides and bases of elevated structures as well as to the crests. Site 2 represents mountain base or valley rock outcrop conditions. Sites 3, 4, and 5 represent alluvial valley sites. Site 3 may represent a valley edge site while sites 4 and 5 are intermediate and valley center sites.

Topographic Effects

Topographic effects are a result of a focusing of energy near ridge crests and the interaction of the primary (incident) wavefield with outgoing scattered surface waves (Bard, 1983). The resulting total wavefield shows broad-band amplifications at ridge crests and is most pronounced for wavelengths that correspond roughly to the width of the structure (2L in Figure 6-3). Along the slopes and at the bases of elevated geologic structures, the interaction of the primary field with the scattered fields results in complicated patterns of amplification and deamplification. This varying pattern is associated with rapidly varying phase and may be expected to give rise to differential motions, which could be of concern to extended structures.

An example of computed ridge effects is shown in Figure 6-4. The ridge structure shown has a shape ratio of 0.4 and the amplifications, relative to a homogeneous half-space, for sites 1-6 moving from crest to base are shown above the feature. In the amplification factors shown, the dimensionless frequency is the ridge width (2L) to wavelength ratio. Figure 6-4 clearly shows broad amplifications occurring at the ridge crest (site 1) with a value near 1.5 for wavelengths comparable to the ridge width. As the site locations move down the slope to the base, the interference patterns appear in the amplification factors and show oscillating patterns ranging from amplification to deamplification.

The computed value of the amplification at the crest is generally less than about 1.5 while the deamplification at the base for the same dimensionless frequency (around 1) is not less than about 0.75. The resulting crest-to-base amplification would then be about 2 and would not exceed 3. While these results are only appropriate for a shape ratio of 0.4 and effects computed for other ratios show somewhat larger amplifications and deamplifications, they do serve to illustrate the general underprediction of

6-6

Figure 6-3. Sketch of idealized two-dimensional features that result in topographical and alluvial valley effects on strong ground motion. Site 1 depicts elevated topography with a shape ratio given by h/l. Site 2 represents mountain base or valley rock outcrop conditions. Sites 3, 4, and 5 are alluvial valley sites representing valley edge, intermediate, and center locations, respectively.

Figure 6-4. SH Fourier transfer functions to homogeneous halfspace outcrop motions computed at six sites for an isolated, homogeneous ridge. The shape ratio is 0.4 and the dimensionless frequency is the ratio of the structure width (2L) to wavelength (after Geli et al., 1988).

observed crest-to-base ratios. Observed amplifications range from about 2 to 20 in the spectral domain (Fourier and response) (Bard, 1983) and can be as high as 30 (Davis and West, 1973).

In the time domain these amplifications generally are observed to range up to about 5 (Griffiths and Bollinger, 1979). Predicted values of ridge-to-base amplifications generally are much less than these and range from 3 to 4 in the spectral domain to less than 2 in the time domain (Geli et al., 1988). The differences, between predicted and observed crest-to-base topographical effects are up to about 10, which is a factor of 3 higher than the predicted total effect. Causes of this significant underestimate are related to the influence of 3-D effects as well as ridge-ridge interactions (Geli et al., 1988).

The lateral dimensions of geologic structures that may impact strong motion depends upon frequency through wavelength. If the bandwidth of interest to engineered structures is taken as 5 sec. to 25 Hz and assuming the shear-wave velocities near the earth's surface range approximately from 1 to 3 km/sec. for soft and hard rocks respectively (Silva and Darragh, 1989), the corresponding range in wavelength is 40 m to 5 km and 120 m to 15 km, respectively. Topographical irregularities of dimensions near to this range may then exert considerable influence upon corresponding ground motions depending upon the shape ratios (Geli et al., 1988).

Alluvial Valley Effects

Consideration of ground motions in alluvial valleys is fundamentally an assessment of departures in response from the classical 1-D model of vertically propagating plane shear-wave (Seed and Idriss, 1969; Schnabel et al., 1972). The main effect of the curvature of the sediment-basement interface is the generation of surface waves and trapped body waves that propagate in the alluvium and superpose with the vertically-propagating shear waves. This results in an amplification of motion as well as increased duration over 1-D soil effects alone.

Observations suggest that the simple 1-D model works well at and near the valley center in predicting the effect of the valley response to outcrop motions (King and Tucker, 1984) (sites 4 and 5 in Figure 6-4). This observation is also predicted in modeling (Bard and Gariel, 1986) which, as one may expect, is more appropriate for shallow and wide valleys than for deep and narrow valleys. Edge effects, associated with rapid changes in soil thickness may give rise to the local generation of short period surface waves which, because of material damping, do not significantly alter the spectral content of motions some distance from the edges (Tucker and King, 1984). Additionally, long period body waves incident at shallow angles to a shallow basin structure may become trapped and propagate across the basin as surface waves until reaching the thinning margin when they escape as body waves (Vidale and Helmburger, 1988). In the basin, these locally generated surface waves can give rise to large amplifications and increased durations not predicted by vertically propagating shear waves.

Figure 6-5 shows predicted Fourier spectral amplifications (relative to homogene half-space) for a shallow and wide valley with damping values of 2.5 percent for the alluvium. The valley has a shape ratio of 0.1 and spectral amplifications are shown for sites ranging from valley edge (1) to valley center (8). Frequency is normalized by the 1-D resonant frequency for the valley center ($\beta/4h$). The dark solid line represents 2-D response including a velocity gradient in the sediments, the light solid site represents a constant velocity alluvium, and the dashed line represents a 1-D response for the gradient profile. Figure 6-5 shows, in going from the edge to the valley center, the diminishing effects of surface waves because of material damping and the predominance of vertically propagating shear waves. The fluctuations shown in the amplifications as a function of frequency for the 2-D computations are a result of interference between the incident primary wave and scattered surface wavefields. Interestingly, the 1-D results overpredict at the edge, underpredict just off the edge (sites 2 and 3), and then do a very acceptable job out to the valley center generally showing differences less than a factor of 2 from the 2-D results. From an engineering perspective, 1-D results may be adequate for all sites depicted. Near the valley edge (sites 1-3), depending upon the frequency range of interest, the broad-band amplification resulting from the interference of scattered surface waves and vertically propagating shear-waves can be accommodated by extending some percentage of the 1-D fundamental resonance to higher frequencies. Away from the edge, a 1-D response analysis using a reasonable variation in parameters would likely encompass the differences between 1-D and 2-D amplifications shown at the remaining sites. The edge effects, however, may result in significant differential motions perpendicular to the valley edge.

The effects of body wave trapping and generation of long period surface waves is clearly illustrated in the particle velocity records integrated from strong motion recordings of the 1971 San Fernando earthquake. The earthquake occurred beneath the northern edge of the San Fernando Valley, shown in the upper panel of Figure 6-6 and was recorded along a profile of stations (Figure 6-7, left panel) extending south of the epicenter across the San Fernando Valley, then across the Santa Monica Mountains, and then across the Los Angeles basin. The velocity model used to compute synthetic seismograms is shown in the upper panel of Figure 6-6. A profile of the envelope of transverse velocity finite difference synthetic seismograms for a point source at a depth of 10 km (Vidale, 1987; Vidale and Helmberger, 1988) is shown in the center panel of Figure 6-6. These synthetic seismograms show the development of Love waves in the San Fernando Valley, their disappearance at the Santa Monica Mountains (where they are converted to SH body waves), and their reappearance at the northern edge of the Los Angeles basin because of the interaction of SH waves with the thickening basin margin.

The same features are seen in the profile of velocity seismograms derived from the recorded accelerograms shown in the bottom panel of Figure 6-6. The recorded tangential component velocity seismograms are interspersed with synthetic seismograms in Figure 6-7, center panel. The development of Love waves in the San Fernando Valley, their disappearance in the Santa Monica Mountains, and their reappearance in the Los

Figure 6-5. Smoothed SH transfer functions to homogeneous halfspace outcrop motions computed at eight sites for a wide and shallow alluvial valley with a shape ratio of 0.1. Two-dimensional calculations for a gradient shear-wave velocity profile (heavy solid line) and for a constant velocity alluvium (thin solid line) are shown. Dotted line represents one-dimensional results. Frequency has been normalized by the frequency of the fundamental resonance for the homogeneous layer at site 8 (after Bard and Gariel, 1986).

Figure 6-6. Crustal structure and seismogram profiles along a north-south path across the Los Angeles region from San Fernando (A) to Palos Verdes (A') shown in the left panel of Figure 6-7. The upper panel shows the structure model of Duke and others (1971); the center panel shows synthetic seismograms computed using a finite difference method; and the lower panel shows velocity seismograms derived from recorded accelerograms (after Vidale, 1987; Vidale and Helmberger, 1988).

Figure 6-7. Comparisons in waveform (center panel) and variation of peak velocity with distance (right panel) or recorded and synthetic seismograms along the profile shown in the left panel. In the center panel, recorded seismograms are shown as heavy lines and synthetic ones as light lines. In the right panel, recorded values are shown as dots, and synthetic values for complex and flat layered structures are shown as lines (after Vidale, 1987; Vidale and Helmberger, 1988).

Angeles basin are apparent in both the recorded and synthetic seismograms. The observed variation of peak velocity with distance along the profile is compared with that of the synthetic profile in Figure 6-7, right panel. The synthetic amplitudes for the 1-D layer structure, which cannot trap the waves, are much smaller than the data in the valley sites. A 1-D relative site response analysis of recordings in the Los Angeles region of the 1971 San Fernando earthquake as well as Nevada Test Site nuclear explosions also showed computed amplifications somewhat smaller than observed for periods between about 3-10 sec (Rogers et al., 1985). In this case as well, the departures were attributed to surface waves. These results and observations demonstrate that important aspects of long-period wave propagation across the San Fernando Valley and Los Angeles Basin may not be accurately modeled by 1-D structure but can be explained by the trapping mechanism produced by 2-D structure.

For deep and narrow valleys with large shape ratios (≥ 0.25), a change in response occurs that involves a new set of mode shapes affecting the valley as a whole (Bard and Bouchon, 1985; Bard and Gariel, 1986). This class of mode shapes involves in-phase, large amplitude motions of the whole valley. Predicted results for these high aspect ratio valleys are shown in Figure 6-8, which is analogous to Figure 6-5 except the shape ratio has been increased from 0.1 to 0.4. The differences in response, from those of the shallow valleys (Figure 6-5), are seen as much more complicated resonance phenomena and generally higher amplifications away from the valley edge (site 1). The whole valley in-phase resonance is seen beginning at site 2 as a gradual increase in the peak near the dimensionless frequency 1 as the sites progress toward the valley center. For valleys of this class, deep and narrow, the 1-D theory gives a conservative prediction near the edges (sites 1 and 2 in Figure 6-6) but seriously underpredicts the valley effects at high frequencies (by a factor of 2-4) at sites 3 and 4 and into the valley center.

Perhaps the most important aspect of the resonance phenomenon shown for deep valleys is the oscillating nature of the amplifications showing several maxima where the 1-D theory shows only the fundamental and perhaps the first overtone. Additionally, the 2-D resonances associated with deep and narrow valleys are expected to give rise to significant degrees of differential motions (Bard and Gariel, 1986). From a viewpoint of design ground motions, 2-D computations for a variation in parameters would likely result in a near continuum of resonances and thus a very broad-band amplification of motion. Interestingly, near the valley center at sites 7 and 8, the 2-D fundamental resonance has an amplitude nearly twice that corresponding to vertically propagating shear-waves and at a slightly higher frequency. It should be noted that the details in resonances and amplitudes of peaks and troughs shown in the 2-D modeling may tend to be smoothed out in real situations. This arises because wavefields may be forward- and back-scattered into basin structures because of surface topography, lateral crustal heterogeneity, and three-dimensional effects. Table 6-2 shows an influence matrix of 2-D effects that summarizes the results discussed here for topographic as well as alluvial valley features.

Figure 6-8. Smoothed SH transfer functions to homogeneous halfspace outcrop motions computed at eight sites for a wide and shallow alluvial valley with a shape ratio of 0.4. Two-dimensional calculations for a gradient shear-wave velocity profile (heavy solid line) and for a constant velocity alluvium (thin solid line) are shown. Dotted line represents one-dimensional results. Frequency has been normalized by the frequency of the fundamental resonance for the homogeneous layer at site 8 (after Bard and Gariel, 1986).

Table 6-2
2-D GEOLOGIC STRUCTURAL EFFECTS
INFLUENCE MATRIX

Structure	Conditions	Type	Size	Quantitative* Predictability
Surface Topography	Sensitive to shape ratio, largest for ratio between 0.2-0.6. Most pronounced when wavelength $\approx$ mountain width.	Amplification at top of structure, amplification and deamplification at base, rapid changes in amplitude phase along slopes.	Ranges up to a factor of 30 but generally from about 2-10.	Poor: generally underpredict size. May be due to ridge-ridge interaction and 3-D effects.

Sediment-Filled Valleys

1) Shallow and wide (shape ratio $\lesssim$ 0.25)	Effects most pronounced near edges. Largely vertically propagating shear-waves away from edges.	Broad band amplification near edges due to generation of surface waves.	1-D models may underpredict at higher frequencies about 2 near edges.	Good: away from edges 1-D works well, near edges extend 1-D amplifications to higher frequencies.
2) Deep and narrow (shape ratio $\gtrsim$ 0.25)	Effects throughout valley width.	Broad band amplification across valley due to whole valley modes.	1-D models may underpredict for a wide bandwidth by about 2-4 away from edges. Resonant frequencies shifted from 1-D.	Fair: given detailed description of vertical and lateral changes in material properties.
3) General	Local changes in shallow sediment thickness.	Increased duration.	Duration of significant motions can be doubled.	Fair.
4) General	Generation of long period surface waves from body waves at shallow incidence angles.	Increased amplification and duration due to trapped surface waves.	Duration and amplification of significant motions may be increased over 1-D predictions.	Good at periods exceeding 1 sec.

Good (generally within a factor of 2)
Fair (generally within a factor of 2-4)
Poor (qualitative only, can easily be off by an order of magnitude)

Observed spectral amplifications of alluvial valley sites (Fourier spectra) with respect to outcrop motion generally ranges up to about 10 (King and Tucker, 1984) and are in reasonable accord with predictions. Spectral amplifications as high as 30 have been measured for the lake bed in Mexico City (Lermo et al., 1988). Seed et al. (1988) modeled the amplification effects of the shallow ($\approx$ 60 m) clay layer resulting from the September 19, 1985 M 8.1 earthquake remarkably well using the simple 1-D theory. However, the increased durations compared to outcrop motions at some of the sites is unaccounted for in the simple theory and may be related to lateral changes in thickness in the shallow clay layer and thus local generation of surface waves (Bard et al., 1988) (depicted at site 5 in Figure 6-3).

Variability of Observed 2-D Site Effects

As a result of the careful observations of both topographical and alluvial valley effects in the Garm region of the USSR, the standard error of variation in amplification has been quantified (Tucker and King, 1984). After careful instrument calibration that quantified the variability of system response, repeated measurements of ridge and valley effects has shown that the observed variability in amplifications is approximately 1.5 (Tucker and King, 1984; Tucker et al., 1984; King and Tucker, 1984) and that ridge and valley effects depend weakly upon source azimuth and incidence angle. Observed topographic and alluvial valley effects, ranging from about 2 to 10 are then resolvable on a repeatable basis and are generally significantly greater than the measurement uncertainty.

To summarize, topographic effects resulting from rapid and significant changes in elevation over the dimensions of approximately one wavelength generally range from about 2 to 10 and are most pronounced at the ridge or hill crest and for wavelengths comparable to the width of the structure. The sides of topographic highs undergo patterns of amplification and deamplification with associated rapid changes in phase. Alluvial valley effects that result in departures from the vertical propagating shear-wave model, are largest for sites located in high aspect ratio valleys (large thickness to half-width ratios, ≥ 0.25) and away from valley edges where the simple 1-D theory may underpredict the effects by factor of 2 to 3 (Bard et al., 1988). For shallow and wide valleys (shape ratio ≥ 0.25), such as the lakebed sites in Mexico City have demonstrated, the short period response is dominated by vertically propagating shear-waves, particularly away from the edges. Although the 1-D theory captures many of the essential features of amplification resulting from alluvial valleys, it fails to explain the increased durations observed at some sites. The increased durations of significant motion shown by some of the lakebed sites in Mexico City require the effects of local generation of laterally propagating energy, perhaps because of thickness variations in the shallow clay layer (buried valley or depression within a valley).

In addition, the long period response of large basin structures may be dominated by trapped body waves that propagate across the basin as surface waves with large amplifications and increased durations. Careful observations of topographic as well as

alluvial valley effects have quantified the variability of observed amplifications to a factor of about 1.5. Additionally, the observations have shown a weak dependence of amplifications to source azimuth and incidence angle (Tucker and King, 1984).

1-D STRONG GROUND MOTION MODEL

A convenient mechanism for separating the effects of source size, propagation path, and general 1-D site conditions upon strong ground motion is through a recently developed stochastic ground motion model. The Band-Limited-White-Noise (BLWN) model, in which energy is distributed randomly over the duration of the source, coupled with a single corner frequency-omega square source model (Brune, 1970; 1971) was first developed by Hanks and McGuire (1981). This model presents the simplest physically reasonable representation of the source, propagation path, and site effects while keeping the number of free parameters to a minimum. This relatively new ground motion model has proven remarkably effective in correlating with a wide range of ground motion observations (Hanks and McGuire, 1981; Boore, 1983; Boore and Atkinson, 1987; Silva and Darragh, 1989). In this model, the source, propagation path, and site terms separate naturally. The shape of the acceleration spectral density is given by

$$a(f) = \frac{CM_o\, f^2}{1+\left(\dfrac{f^2}{f_c}\right)} \bullet \frac{e^{-\dfrac{\pi f R}{\beta_o Q(f)}}}{R} \bullet A(f)e^{-\pi \kappa f} \qquad (6\text{-}1)$$

$$= \text{Source} \bullet \text{Path} \bullet \text{Site};$$

where

f_c = source corner frequency

M_o = seismic moment

R = hypocentral distance

β_o = shear wave velocity at the source

$Q(f)$ = frequency dependent quality factor

$A(f)$ = near-surface amplification factors (Boore, 1986; Silva and Darragh, 1989)

κ = high-frequency truncation parameter and

C = $(1/\rho_o\beta_o{}^3) \,^{\circ}\, (2) \,^{\circ}\, (0.63) \,^{\circ}\, (1/\sqrt{2}) \,^{\circ}\, \pi$

C is a constant that contains ρ_o (density) and β_o terms and accounts for the free-surface effect (factor of 2), the source radiation pattern averaged over a sphere (0.63) (Boore, 1983), and the partition of energy into two horizontal components ($1/\sqrt{2}$).

Source Term

Source scaling is provided by specifying two independent parameters, the seismic moment (M_o) and the high-frequency stress parameter ($\Delta\sigma$). The stress parameter $\Delta\sigma$ is taken to be independent of magnitude (Atkinson, 1984; Boore and Atkinson, 1987; Toro and McGuire, 1987) and relates the corner frequency f_c to M_o through the relation

$$f_c = \beta_o(\Delta\sigma/8.44\ M_o)^{1/3} \tag{6-2}$$

The spectral shape of the single-corner-frequency ω-square source model is then described by the two free parameters M_o and $\Delta\sigma$. The corner frequency increases with the shear-wave velocity and with increasing stress parameter, both of which are region dependent. The stress parameter is generally taken to be moment independent with a value of 50 bars in western North America (Boore, 1986) and 100 bars in eastern North America (Toro, 1985; Boore and Atkinson, 1987; Somerville et al., 1987).

It is important to point out the sensitivity of the model to changes in corner frequency. Because of the frequency square term, the spectral density given by Equation 6-1 will be increased (or decreased) by the ratio of the square of the new corner frequency to the old for frequencies higher than the largest corner frequency. For the differences in stress parameters between stable and tectonically active regions, the acceleration amplitude spectrum for 100 bars will exceed that of 50 bars by $2^{2/3} \sim 1.6$ for frequencies greater than that associated with the 100-bar stress parameter. For frequencies less than the corner frequency associated with the 50-bar stress parameter, the spectral densities are equal. Taken in context with the 1-D site terms that amplify as well as attenuate the amplitude spectrum, the source term, resulting from the effect of the stress parameter upon short periods, may be a factor in evaluating the effects of wavelength dependent topographical features.

Path Terms

The path term accounts for both geometrical attenuation and energy absorption appropriate for a body-wave propagating in a homogeneous whole-space. Energy loss resulting from intrinsic absorption as well as scattering along the crustal path is accounted for in the $Q(f)$ term. The combination of the source and path terms represents seismic radiation from a point source and models direct shear waves propagating in a homogeneous half-space.

The $Q(f)$ models are based upon analyses of attenuation in WNA by Nuttli (1986) and in ENA by Shin and Herrmann (1987). These models are shown in Table 6-3. The

Table 6-3
EARTHQUAKE SOURCE AND WAVE PROPAGATION PARAMETERS

Parameters	WNA	ENA
ρ_o (g/cm^3)	2.7	2.5
β_o (km/sec)	3.2	3.5
kappa(sec)	0.020	0.006
Q(f)*	$150(f)^{0.60}$	$500(f)^{0.65}$
$\Delta\sigma$ (bars)	50	100
M_o (dyne-cm)	$\log M_o = 1.5\ M + 16.1$	$\log M_o = 1.5\ M + 16.1$
Amplification Factors	See below	1.0
Geometrical Attenuation	R^{-1}	R^{-1}
Source Duration	f_c^{-1}	f_c^{-1}
$(f_c)^3$	$\beta^3\Delta\sigma/8.44M_o$	$\beta^3\Delta\sigma/8.44M_o$
Filters (5 pole Butterworth)	0.1 - 62.5 Hz	0.1 - 62.5 Hz

* WNA from Nuttli (1986); ENA from Shin and Herrmann (1987).

NEAR SURFACE AMPLIFICATION FACTORS
(From Boore, 1986)

Log Frequency	$\log \dfrac{(\beta_o\rho_o)^{1/2*}}{\beta_R\rho_R}$
-1.0	0.01
-0.5	0.04
0.0	0.13
0.5	0.34
1.0	0.37

* ρ_o and ρ_R are assumed to be equal.

o, R refers to average crustal properties and near-receiver properties, respectively.

Q(f) term is responsible for the distance dependency of spectral shapes. With the Q(f) models adopted here, spectral shapes are largely independent of distance for distances less than 50 km in WNA and 100 km in ENA (Silva and Green, 1989).

Site Term

The site term, represented by the combination of the amplification factor A(f) and the kappa factor, is an attempt to model the effects of near-surface material properties and structural complexity upon the propagated wavefield. The frequency dependent amplification factor accounts for the general increase in amplitude as the wavefield propagates upward through lower velocity near-surface crustal material (Boore, 1986; Silva and Darragh, 1989).

The κ factor is an attempt to model the observation that acceleration spectral density appears to fall off rapidly beyond some site-dependent maximum frequency. This observed phenomenon truncates the high-frequency portion of the spectrum and is responsible for the band-limited nature of the model. This spectral fall-off has been attributed to near-site attenuation (Hanks, 1982; Anderson and Hough, 1984) or to source processes (Papageorgiou and Aki, 1983) or perhaps to both effects. In the Anderson and Hough (1984) attenuation model adopted here, kappa (κ), at zero epicentral distance, is given by

$$\kappa = \frac{H}{\bar{\beta} \ \bar{Q}_s} \tag{6-3}$$

The bar represents an average of the shear-wave velocity and Q_s over a depth H on the order of a few hundred meters to a few kilometers (Anderson and Hough, 1984) beneath the recording site. The value of κ at zero epicentral distance is attributed to attenuation in the very shallow crust directly below the site (Hough et al., 1988). The intrinsic attenuation along this part of the path is thought not to be frequency dependent and is modeled as a frequency independent, but site dependent constant κ (Hough et al., 1988; Rovelli et al., 1988).

For a given seismic moment, the source and path terms are controlled by the region dependent parameters ρ, β, $\Delta\sigma$, and Q(f), which are density and shear-wave velocity appropriate to the source depth, stress parameter, and the path attenuation model. The site terms are controlled by the site-specific near surface amplification and frequency independent energy loss.

FACTORS AFFECTING GROUND MOTIONS AT ROCK SITES

The value of kappa and those of the frequency dependent amplification factors A(f) result from the particular shear-wave velocity and damping (Q_s^{-1}) profiles directly

beneath the site. From Equation 6-3, kappa varies inversely with the average shear-wave velocity and quality factors (Q_s) over a depth H beneath the site.

Kappa Term

The functional form of the kappa operator shown in Equation 6-1 has been fit to Fourier spectral densities computed from observations at a variety of seismic recording sites (e.g., Anderson and Hough, 1984; Hough et al., 1988; Rovelli, 1988; Silva and Darragh, 1989). Kappa values have also been estimated by fitting spectral shapes computed from the BLWN model to shapes computed from motions recorded at rock sites in ENA, WNA, Mexico, Italy (Friuli), USSR (Gazli), and Taiwan (SMART1) (Silva and Darragh, 1989). Results of these analyses indicate that kappa is strongly dependent upon the material properties of the site. Rock sites characterized as soft, such as sedimentary, showed significantly higher kappa values than those characterized as hard, e.g., crystalline basement. Hard and soft rock sites may exist in either WNA or ENA; however, on the average, sites in stable cratonic regions are more likely to be classified as hard while those associated with active tectonic regions are more likely to be soft (Silva and Darragh, 1989).

On average, kappa values associated with hard rock sites are approximately 0.006 sec. while soft rock sites are approximately a factor of 3 greater or approximately 0.02 to 0.03 sec. This difference is large and results in significantly different attenuation rates at short periods for ground motions associated with hard or soft rock sites. To complete the picture, the values of the amplification factors and the conditions under which they are applied must be evaluated.

Amplification Factors

The amplification factors result from an increase in amplitude as a wavefield propagates from higher velocity material at depth to lower velocity material nearer the surface. The physical mechanism responsible for the amplification is energy conservation. If material damping is neglected, the flow of energy per unit time and per unit area (energy flux) is given by $\rho\beta u^2$ (ρ = density, β = shear wave velocity; u = particle velocity), is conserved. Therefore, if β decreases, u must increase in an elastic system. In any rock column, however, material damping is always present and the net amplification (or deamplification) involves an interplay between counteracting effects. This process naturally occurs at soil sites and results in different values of amplification for peak particle velocity and peak acceleration occurring at the surface of soil sites relative to rock because of the different predominant frequency of the two measures of strong ground motions.

Amplification factors for average soft rock sites, typical of WNA, were estimated by Boore (1986) using the method of Joyner and Fumal (1984) from an average WNA shear-wave velocity model based on a number of factors including measured values of near-surface velocities (Fumal, 1978), travel-time data, crack closure experiments (Nur

and Simmons, 1969), and standard WNA crustal velocities. Boore (1986) assumed that the standard upper crustal shear-wave velocity of 3.2 km/sec. was reached at a depth of 1.2 km and that variations in density are relatively minor over this depth and can be ignored. Figure 6-9 (solid line) shows a smoothed velocity model from the surface to 1.5 km derived from Boore's layered model. This shear wave velocity model is for an average strong motion recording rock site in WNA. Amplification factors calculated from Boore's original layered model are reproduced in Table 6-3 from Boore (1986). The factors range from approximately 1.0 at 10 sec. to 2.3 at 10 Hz.

For hard rock sites, typical of ENA, the shear-wave velocity is much greater at the surface than for soft rock sites and the corresponding velocity gradients are generally much smaller (Boore and Atkinson, 1987). This is in agreement with sonic well log data, which generally show small overall velocity gradients in the upper kilometer at hard rock sites (Silva and Darragh, 1989). To illustrate the difference in velocity gradients between average hard and soft rock sites, a smoothed shear-wave velocity profile of the Moodus well in Middlesex County of Connecticut is shown in Figure 6-9 (dotted line) (Silva and Darragh, 1989). Figure 6-9 shows for this hard rock site, surface shear-wave velocities of about 2.7 km/sec. and increasing to near 3.5 km/sec. at a depth of about 1.2 km. Amplification factors for sites such as these will be much smaller than those for soft rock sites and are generally taken to be unity (Boore and Atkinson, 1987; Toro and McGuire, 1987).

Figure 6-10 shows a comparison of the amplification factors computed for the soft-rock and hard-rock profiles shown in Figure 6-9. The plane-wave propagators of Silva (1976) are used to compute the A(f) factors. Also shown in Figure 6-10 is the assumed amplification factor of unity for ENA and Boore's (1986) A(f) based upon the technique of Joyner and Fumal (1984). Apart from the resonances, the amplification factors for the soft-rock shear-wave velocity agree well with Boore's (1986) estimates, as expected. The fundamental resonance of the profile is seen near 1.5 sec. and the overtones are seen at shorter periods. The site amplification of 3.4 near 40 Hz is caused by a resonance in the upper most layers in the model.

The amplification factors for hard rock vary from unity at long periods to an average value of about 1.1 at high frequencies. The assumption of unity for hard-rock amplification is then quite reasonable.

To summarize, 1-D rock site effects result from the shear-wave velocity and damping profiles that exist directly beneath the site to depths on the order of 1 km. These changes in dynamic material properties give rise to amplifications, parameterized with the A(f) factors, as well as attenuation of high frequencies through kappa.

To compute net or inelastic amplification factors, given by A(f) times the kappa term (in Eq. 6-1), Q_s profiles are required for soft- and hard-rock site conditions. To compute the Q_s profiles, the relationship where γ is a parameter with a value of 0.01

SHEAR WAVE VELOCITY PROFILE
AVERAGE ROCK (1.5 km)

LEGEND
—————— GRADIENT MODEL FOR ROCK MODIFIED FROM BOORE (PERSONAL COMM., 1988)
• • • • MOODUS WELL LOG VELOCITY FIT TO QUADRATIC

Figure 6-9. Comparison of average shear-wave velocity profile for WNA (Boore; personal communication, 1988) (solid line) with quadratic fit to ENA well log profile (Moodus) (dotted line).

SOFT ROCK AND HARD ROCK

LEGEND
- — — — AMPLIFICATION FACTORS FOR SOFT ROCK FROM BOORE (1986)
- — · — AMPLIFICATION FACTORS FOR SOFT ROCK SHEAR-WAVE VELOCITY PROFILE
- ——— AMPLIFICATION FACTORS OF UNITY FOR HARD ROCK
- - - - - AMPLIFICATION FACTORS FOR HARD ROCK SHEAR-WAVE VELOCITY PROFILE

Figure 6-10. Soft rock (WNA) amplification factors computed from response analysis without damping (Q=10,000) using WNA shear-wave profile (Figure 6-9) compared to Boore's (1986) amplification factors (top set). Hard rock (ENA) amplification factors computed from response analysis without damping (Q=10,000) using ENA shear-wave profile (Figure 6-9) compared to unity.

$$Q_s(Z) = \gamma \beta \ (Z) \tag{6-4}$$

and 0.02 sec./m for soft- and hard-rock sites, respectively, was adopted. The simple functional form of Equation 6-4 was chosen based on the observation that both Q_s and β generally increase with depth since they both depend on similar rock material properties. The Q_s profiles through γ are constrained by estimates of kappa for hard rock (0.006 sec.) and soft rock (0.02 sec.) and by measurements of Q in boreholes. For the soft-rock site model, Q_s varies from 10 at the surface to 32 at a depth of 1.2 km. A minimum value for Q_s of 10 was selected to be consistent with minimum values estimated in boreholes. The average shear-wave velocity and quality factors are 2.54 km/sec. and 26 at the soft-rock site, respectively. For the hard-rock site model, Q_s varies from 58 at the surface to 72.5 at a depth of 1.2 km. The average shear-wave velocity and quality factors are 3.15 km/sec. and 65 at the hard-rock site, respectively. The densities are taken as 2.7 and 2.5 gm/cm^3 at soft- and hard-rock sites, respectively (Boore, 1983; Boore and Atkinson, 1987). Values of density different from these values have a negligible effect on the predictions by the ground motion model.

Figure 6-11 shows the site amplification (inelastic, $\bar{Q}$ = 26) for a rock site, characterized by 1.2 km of soft rock underlain by a half-space with WNA propagation parameters (Table 6-3). For reference, the frequency-dependent amplification factors (Table 6-3) multiplied by the kappa term is Equation 6-1 with κ = 0.02 sec. is shown as the long dashed line. A kappa value of 0.02 sec. constrains the average Q_s in the upper 1.2 km to be approximately 25. Again, the fundamental resonance of the profile is seen near 1.5 seconds and the harmonics are seen at shorter periods. Between 1 to 10 Hz, the site amplification is approximately 1.5. At higher frequencies ($\gtrsim$10 Hz), the attenuation in the profile decreases the site amplification asymptotically to zero.

Figure 6-11 also shows the site amplification (inelastic, Q = 65) for a rock site characterized by 1.2 km of hard rock underlain by a half-space with ENA propagation parameters (Table 6-2). For reference, the kappa term in Equation 6-1 with kappa value of 0.006 sec. is shown as a solid line (amplification factors of unity). A kappa of 0.006 sec. constrains the average Q_s in the upper 1.2 km to be approximately 65. The site amplification is approximately 1 from 0.1 sec. to longer periods. At higher frequencies, the site amplification smoothly decreases to approximately 0.25 at 100 Hz.

A comparison between the curves for soft and hard rock shows the increased site amplification between approximately 15 Hz and 2.0 sec. for a soft-rock site (typical WNA strong motion recording site). At high frequencies ($\geq$15 Hz), the hard-rock site response is greater than the soft-rock site response.

In order to assess the degree to which the ground motion model correlates with the source and site dependencies of spectral shapes shown in Figure 6-2 for ENA and WNA ground motions, Figures 6-12 through 6-15 show the corresponding model predictions for M 6.4 (ENA, Figure 6-12; WNA, Figure 6-13) and M 4.0 (ENA, Figure 6-14; WNA, Figure 6-15). In the M 6.4 WNA comparison of model prediction with shapes

SOFT ROCK AND HARD ROCK

LEGEND
- - - - AMPLIFICATION FACTORS FOR SOFT ROCK (BOORE (1986)) INCLUDING K=0.02 SEC
— · — AMPLIFICATION FACTORS FOR SOFT ROCK Vs AND Qs PROFILES
——— AMPLIFICATION FACTORS OF UNITY AND K=0.006 SEC IN BLWN MODEL
- - - - - AMPLIFICATION FACTORS FOR HARD ROCK Vs AND Qs PROFILES

Figure 6-11. Comparison of amplification factors computed by response analysis using WNA shear-wave velocity profile (Figure 6-9) and $Q_s=0.01$ β $(Q_s \geq 10)$ with Boore's (1986) amplification factors combined with a kappa operator ($\kappa=0.002$ sec) (upper set). Comparison of amplification factors computed by response analysis using ENA shear-wave velocity profile (Figure 6-9) and $Q_s=0.02$ β with a kappa operator ($\kappa=0.006$ sec) (lower set).

NAHANNI EARTHQUAKES
Magnitude 6.4

LEGEND
- - - - - 5 %, ALL STATIONS: AVERAGE OF 6 HORIZONTAL COMPONENTS
• • • •   5 %, ALL STATIONS: MINIMUM OF 6 HORIZONTAL COMPONENTS
• • • •   5 %, ALL STATIONS: MAXIMUM OF 6 HORIZONTAL COMPONENTS
————   5 %, RVT, R=10 KM, M=6.5, KAPPA=0.008 SEC

Figure 6-12. Plot of average 5% spectral shape for all stations for the magnitude 6.4 Nahanni earthquake. Solid line is the BLWN model shape computed with ENA parameters at 10 km for a moment magnitude 6.5 using a kappa of 0.008 sec.

SAN FERNANDO 02/09/71
Magnitude 6.4

LEGEND
----- 5 %, ALL STATIONS: AVERAGE OF 12 HORIZONTAL COMPONENTS
— · — 5 %, ALL STATIONS: MINIMUM OF 12 HORIZONTAL COMPONENTS
— ▲ — 5 %, ALL STATIONS: MAXIMUM OF 12 HORIZONTAL COMPONENTS
· · · · 5 %, JOYNER & BOORE (1985), R=25 KM, M=6.4
——— 5 %, RVT, R=25 KM, M=6.4, KAPPA=0.030 SEC

Figure 6-13. Plot of average 5% spectral shape for all stations for the magnitude 6.4
San Fernando earthquake. Solid line is the BLWN model shape computed with
WNA parameters at 25 km for a moment magnitude 6.4 using a kappa of 0.030 sec.
Dotted lines is the Joyner-Boore (1985) shape for R=25 km and M=6.4.

6-29

NEW BRUNSWICK 03/31/82
Magnitude 4.0

LEGEND
- - - - - 5 %. STATION MITCHELL ROAD: AVERAGE OF 2 COMPONENTS
· · · · 5 %. STATION MITCHELL ROAD: MINIMUM OF 2 COMPONENTS
· · · · 5 %. STATION MITCHELL ROAD: MAXIMUM OF 2 COMPONENTS
———— 5 %. RVT. R=10 KM. M=4.0. KAPPA=0.008 SEC

Figure 6-14. Plot of average 5% spectral shape for station Mitchell Road for the magnitude 4.0 New Brunswick aftershock. Solid line is the BLWN model shape computed with ENA parameters at 10 km for a moment magnitude 4.0 using a kappa of 0.008 sec.

COALINGA AFTERSHOCKS
Magnitude 3.8-3.9

LEGEND
----- 5 %, ALL STATIONS: AVERAGE OF 10 HORIZONTAL COMPONENTS
..... 5 %, ALL STATIONS: MINIMUM OF 10 HORIZONTAL COMPONENTS
..... 5 %, ALL STATIONS: MAXIMUM OF 10 HORIZONTAL COMPONENTS
——— 5 %, RVT, R=10 KM, M=4.0, KAPPA=0.045 SEC

Figure 6-15. Plot of average 5% spectral shape for all stations over the magnitude range of 3.8-3.9 for the Coalinga aftershocks. Solid line is the BLWN model shape computed with WNA parameters at 10 km for a moment magnitude 4.0 using a kappa of 0.045 sec.

computed from recorded motions (Figure 6-13), the Joyner and Boore (1988) empirical shape is also shown for reference. The kappa values used for each fit are also shown. For both ENA model predictions the value of 0.008 sec. was used while for the rock sites that recorded the 1971 M = 6.4 San Fernando earthquake and the Joyner and Boore (1988) empirical shape, a value of 0.030 sec. appears appropriate. The stations that recorded the suite of Coalinga aftershocks in the magnitude range M 3.8 to 3.9 were fit best with a kappa value of 0.045 sec. These results indicate that the essential elements that control the spectral content at close distances to rock sites are magnitude and upper-crustal rock properties. For a given magnitude, the effects of kappa significantly alter the short-period spectral content resulting in significantly greater energy for low kappa sites.

To isolate the effects of kappa upon spectral content, two rock sites, Gilroy 1 and 6, which recorded the M 5.9 Coyote Lake and M 6.1 Morgan Hill earthquakes are analyzed. Gilroy 1 represents a competent rock site reaching a shear-wave velocity of about 2.0 km/sec. at a depth of 10 m while Gilroy 6 is a fault zone site with sheared rock and low velocities at comparable depths (Fumal et al., 1982). Figures 6-16 and 6-17 show average spectral shapes computed from the recordings compared to model predictions for Gilroy 1 and 6 respectively. For the same two earthquakes, the shapes computed from the recordings show significantly different spectral content at short periods (< 0.2 sec.). Gilroy 1 shows maximum spectral amplification at 0.1 sec., while Gilroy 6 has the peak shifted to about 0.2 sec. The site effect, through kappa, captures the differences in spectral content quite well using values of kappa of 0.025 and 0.055 sec. for the hard- and soft-rock site conditions respectively.

The ground motion model appears to capture well the essential aspects of earthquake source and 1-D rock site effects upon the spectral content of strong ground motions. Of importance to ground motion specification, the parameters used are few, physically simple, and measurable from observations of weak motions. The next step is to evaluate the sensitivities of predicted ground motions to the 1-D site parameters as well as to the stress parameter.

Parameter Sensitivity

As demonstrated in the previous section, site response at rock sites is controlled primarily by the physical characteristics of the rocks beneath the site extending to depths of about 1 km. To the extent that near-surface hard rock conditions are more prevalent within stable or cratonic regions (i.e., ENA), associated earthquake sources are more likely to have higher stress parameters (100 bars; Boore and Atkinson, 1987) than corresponding soft rock conditions typical of active regions (WNA) (50 bars; Boore, 1986). To compare the differences in ground motions at a close distance (10 km) for a range in magnitude, absolute 5 percent damping spectral accelerations are shown in Figure 6-18. For average WNA and ENA conditions (Table 6-3) the spectra were computed by applying Random Vibration Theory (RVT) to the Fourier spectral density (Eq. 6-1) (Boore, 1983). Because of the point source approximation used in the

COYOTE LAKE AND MORGAN HILL
Magnitude 5.9-6.1

LEGEND

-----	5 %, GILROY #1:	AVERAGE OF 4 HORIZONTAL COMPONENTS
••••	5 %, GILROY #1:	MINIMUM OF 4 HORIZONTAL COMPONENTS
••••	5 %, GILROY #1:	MAXIMUM OF 4 HORIZONTAL COMPONENTS
———	5 %, RVT, R=10 KM, M=6.0, KAPPA=0.025 SEC	

Figure 6-16. Plot of average 5% spectral shape for station GA-1 over the magnitude range of 5.9-6.1 for the Gilroy Array. Solid line is the BLWN model shape computed with WNA parameters at 10 km for a moment magnitude 6.0 using a kappa of 0.025 sec.

6-33

COYOTE LAKE AND MORGAN HILL
Magnitude 5.9 - 6.1

LEGEND
- - - - -   5 %, GILROY #6: AVERAGE OF 4 HORIZONTAL COMPONENTS
• • • •   5 %, GILROY #6: MINIMUM OF 4 HORIZONTAL COMPONENTS
• • • •   5 %, GILROY #6: MAXIMUM OF 4 HORIZONTAL COMPONENTS
————   5 %, RVT, R=10 KM, M=6.0, KAPPA=0.055 SEC

Figure 6-17. Plot of average 5% spectral shape for station GA-6 over the magnitude range of 5.9-6.1 for the Gilroy Array. Solid line is the BLWN model shape computed with WNA parameters at 10 km for a moment magnitude 6.0 using a kappa of 0.055 sec.

6-34

WNA ROCK R=10 KM K=0.020 SEC
ENA ROCK R=10 KM K=0.006 SEC

LEGEND

••••	5%, RVT Absolute Acceleration Spectrum Rock M=2.5
— + —	5%, RVT Absolute Acceleration Spectrum Rock M=3.5
— · —	5%, RVT Absolute Acceleration Spectrum Rock M=4.5
— — —	5%, RVT Absolute Acceleration Spectrum Rock M=5.5
- - - -	5%, RVT Absolute Acceleration Spectrum Rock M=6.5
———	5%, RVT Absolute Acceleration Spectrum Rock M=7.5

Figure 6-18. Comparison of 5% absolute acceleration response spectra (Sa) computed for WNA and ENA parameters (Table 6-3).

6-35

ground motion model, absolute values for the larger magnitudes (M > 6.5) may be conservative. However, the interest here is not in examining predictions of absolute levels of motions but to explore the ranges in differences in motions based upon different source and site parameters. Of particular interest in Figure 6-18 is the similarity in absolute level of spectral acceleration at longer periods and the magnitude dependent point of divergence at shorter periods. For M 7.5 and 6.5, ENA motions are somewhat greater than corresponding WNA motions for periods longer than about 0.3 sec. At M 5.5, the motions are nearly the same in this period range. For smaller magnitudes, a crossover emerges and WNA motions are greater than ENA motions for periods longer than the magnitude dependent crossover.

At short periods, ENA motions show much higher spectral levels than corresponding WNA motions because of the differences in kappa values (0.006 sec. and 0.02 sec. for ENA and WNA, respectively). The differences in short-period spectral content and similarities in intermediate-to-long-period spectral content between WNA and ENA are also reflected in the predominant frequencies associated with peak accelerations and peak particle velocities (Table 6-4). The predominant frequencies are estimated using RVT (Boore, 1983) and, for an M 6.5 earthquake are 12 and 25 Hz for peak accelerations corresponding to WNA and ENA motions respectively. The corresponding predominant frequency for peak particle velocities is 2 Hz for both WNA and ENA. At lower magnitudes, there are large differences in predominant frequencies for peak particle velocities with ENA motions up to a factor of 2 greater than corresponding WNA motions (Table 6-4). For earthquakes of M 5.5 to 7.5, the spectral accelerations are similar for periods longer than about 0.3 sec. For shorter periods, to the upper range of general interest, 0.03 sec., ENA motions are predicted to be a factor of three or more greater than corresponding WNA motions. For smaller events, the separation point moves to much shorter periods and the difference in levels of motion between WNA and ENA increases with decreasing magnitude.

In the period range of similar spectral acceleration levels for WNA and ENA motions, the source is primarily controlling the spectra while at shorter periods, the site controls the spectra through kappa. The departures in spectral accelerations at short periods is a result of the magnitude dependent shape (through changing corner frequencies with magnitude) and the effects of kappa. The effect of a change in corner frequency with magnitude, higher corner frequency with decreasing magnitude (Eq. 6-2), results in a narrower band response spectrum. When combined with a high kappa value, the net effect is a shift in the peak acceleration response to shorter periods with decreasing magnitude.

This shift can most easily be seen in the predicted spectral shapes shown in Figure 6-19 (for WNA) and Figure 6-20 (for ENA). For WNA, the maximum spectral amplification occurs at around 0.1 sec. for M 7.5 and has a value of about 2.5. At M 2.5, the peak has shifted to about .025 sec. with a value closer to 2. For larger values of kappa, the period of maximum spectral amplification shifts to longer periods. For a kappa of 0.03 sec., the maximum shifts to about 0.2 sec. for an M = 6.5 earthquake (see

Table 6-4
MOMENT MAGNITUDES, CORNER FREQUENCIES AND PEAK ACCELERATIONS AT R = 100 KM*

M	WNA					ENA				
	f_c (HZ)	A_p (g)	f_p (HZ)	V_p (cm/s)	f_p	f_c (HZ)	A_p (g)	f_p (HZ)	V_p (cm/s)	f_p (HZ)
2.5	14.0	0.007	22	0.071	13	19.2	0.018	39	.1	26
3.5	4.4	0.029	16	0.50	8	6.1	0.059	31	1	14
4.5	1.4	0.079	13	2.2	5	1.9	0.143	27	2	8
5.5	0.44	0.173	12	7.4	3	0.61	0.305	26	9	4
6.5	0.14	0.350	12	23.2	2	0.19	0.613	25	31	2
7.5	0.044	0.685	12	74.7	1	0.061	1.193	25	88	2

* Results are for a point source model and peak values should be viewed as such for large magnitudes. They do not represent predictions but are listed only to show trends in corner frequencies and predominant frequencies.

WNA ROCK R=10 KM
KAPPA=0.02 SEC

LEGEND

••••	5%, RVT Spectral Amplification Rock M=2.5
—•—	5%, RVT Spectral Amplification Rock M=3.5
—•—	5%, RVT Spectral Amplification Rock M=4.5
————	5%, RVT Spectral Amplification Rock M=5.5
-----	5%, RVT Spectral Amplification Rock M=6.5
———	5%, RVT Spectral Amplification Rock M=7.5

Figure 6-19. Comparison of 5% response spectral shapes (Sa/a) computed for WNA parameters (Table 6-3). Note shift in peak response to longer period with increasing magnitude.

ENA ROCK R=10 KM
KAPPA=0.006 SEC

LEGEND

••••	5%, RVT Spectral Amplification Rock M=2.5
—•—	5%, RVT Spectral Amplification Rock M=3.5
—•—	5%, RVT Spectral Amplification Rock M=4.5
————	5%, RVT Spectral Amplification Rock M=5.5
-----	5%, RVT Spectral Amplification Rock M=6.5
————	5%, RVT Spectral Amplification Rock M=7.5

Figure 6-20. Comparison of 5% response spectral shapes (Sa/a) computed for ENA parameters (Table 6-3). Note slight shift in peak response to longer period with increasing magnitude.

Figure 6-13), which is comparable to the empirical shapes for rock motion (Seed et al., 1976; Mohraz, 1976; Joyner and Boore, 1985; Idriss, 1985). The large kappa, 0.03 sec., required to shift the peak indicates a predominance of soft-rock sites in the data sets.

The predicted spectral shapes for ENA are shown in Figure 6-20. In this case, because of the primarily much lower value of kappa (0.006 sec.), the period of maximum spectral amplification has shifted to about 0.03 sec. for M 7.5 and the frequency dependence has decreased as well. The maximum spectral acceleration shows less frequency dependence as well and has a value near 2.5 for M 2.5 to 7.5.

To see if this trend in shifting of the peak with magnitude is shown in the observations, a range in M_L from 2.5 to 5.9 for the Coalinga, California, aftershocks is analyzed (Table 6-5). Figure 6-21 shows average absolute spectral accelerations computed by averaging the spectra for the horizontal components at all rock sites for earthquakes with magnitudes at or near the categories shown (2.5, 3.0, 3.5, 3.9, 4.2, 4.6, 5.2 and 5.9). This was done to separate the spectra so that the shift in peak with magnitude is more clearly presented. Also shown in Figure 6-21 are the spectra computed from the model (dotted lines) with a kappa of 0.045 sec. The magnitudes used in the model predictions range up to a half-unit higher than the corresponding M_L magnitudes, which may be the result of a localized difference in the scales. The corresponding M categories that gave the best fits are 3.0, 3.5, 4.0, 4.25, 4.5, 4.6, 5.3 and 5.5. Because radiation patterns and stress drops are largely unknown for these earthquakes and because the source to site distances are variable, the BLWN spectra have been scaled to the average peak accelerations of the recorded motions. From Figure 6-21 it is apparent that the model captures quite well the shift in peak response to longer periods with increasing magnitude. The effect is a result of the decrease in corner frequency with increasing magnitude and the site attenuation through kappa.

The large differences in spectral content at short periods between corresponding WNA and ENA motions cautions against using WNA recordings for analyses appropriate to ENA conditions. Additionally, the strong dependence of the spectral shape upon magnitude may impact analyses based upon simply scaling recorded motions to higher levels to simulate a larger magnitude event.

As previously mentioned, the effect of changes in the stress parameter alone, all other parameters remaining constant, is directly related to the absolute level of the Fourier amplitude spectrum (Eq. 6-1) through a change in corner frequency. This effect pertains to frequencies above the corner frequency and, in the omega-square source model, is equal to the ratio of the new-to-old stress parameters to the 2/3 power. For example, raising the stress parameter for WNA soft rock conditions from 50 to 100 bars, will raise the amplitude spectrum, and consequently the response spectrum, by the factor (100/50) to the 2/3 power $\approx$ 1.6. For an M 7.5 earthquake, the corner period moves from 23 to 18 sec. and for periods shorter than about 18 sec., the motions associated with the higher stress parameter will be about 60 percent higher than those associated with the 50-bar stress parameter. These effects are shown in a

Table 6-5a

STATIONS AND EARTHQUAKES USED FOR COALINGA AFTERSHOCKS ANALYSES (SMA-1)

Earthquake	Date	Magnitude (M_L)	Source Depth (km)	Epicentral Distance (km)	Station Name	No.	Average Horizontal Peak Acceleration (g)
Coalinga (2)	830509	5.1	12.5	14.0	Baths	46T03	0.007
				3.0	Anticline (Palmer)	46T05	0.233
				6.0	Skunk	46T06	0.315
(4)	830709	5.3	9.5	12.0	Baths	46T03	0.059
(5)	830722	5.9	9.2	12.0	Baths	46T03	0.116
(6)	830722	5.0	9.5	10.0	Baths	46T03	0.035
(7)	830725	5.1	9.5	10.0	Baths	46T03	0.185
(8)	830909	5.3	9.5	13.0	Baths	46T03	0.014
	830911	4.2	8.0	12.0	Baths	46T03	0.053

Table 6-5b
STATIONS AND EARTHQUAKES USED FOR COALINGA AFTERSHOCKS ANALYSES (GEOS)

Coalinga Aftershock	Date	Mangitude[b] (M_L)	Source Depth (km)	Epicentral Distance (km)	Station	Average Horizontal Peak Acceleration (g)
A	83050322	3.8	7.64	8.54	LLN	0.0053
B	83050323	3.5	8.75	8.93	LLN	0.0249
D	83050700	3.9	8.92	8.39	LLN	0.0189
F	83050820	3.6	7.67	4.35	LLN	0.0092
G	83050902	5.3	12.04	5.14	LLN	0.1029
H	83050903	3.6	12.31	4.65	LLN	0.0017
I	83050903	4.6	12.43	4.81	LLN	0.0296
K	83051013	3.9	4.79	12.46	LLN	0.0036
K2	83051213	4.5	10.98	6.22	VEW	0.0242
K3	83051405	3.9	11.18	5.56	VEW	0.0269
L	83051601	3.6	12.03	6.59	LLN	0.0050
M	83051614	3.9	9.15	4.94	LLN	0.0084
N	83050613	2.5	9.80	7.56	LLN[a]	0.0005
O	83050705	3.5	8.92	2.59	LLN	0.0069
P	83050801	3.5	8.42	4.35	LLN	0.0011
Q	83050801	3.1	12.34	3.09	LLN[a]	0.0010
				2.84	VEW	0.0013
R	83050801	3.0	8.09	1.69	LLN[a]	0.0054
				3.87	VEW	0.0015
S	83050815	3.1	3.14	9.3	LLN[a]	0.0021
				4.05	VEW	0.0032
T	83050903	3.0	12.22	3.95	LLN[a]	0.0018
				3.34	VEW	0.0013
U	83050903	2.6	11.77	4.26	LLN[a]	0.0015
				3.73	VEW	0.0017
U2	83050907	2.5	6.95	6.37	VEW	0.0003
V	83050920	3.0	6.73	3.08	LLN[a]	0.0039
W	83051108	3.5	11.85	4.93	LLN[a]	0.0019
X	83051221	2.6	5.38	.91	LLN[a]	0.0047

Table 6-5b
(Continued)

Coalinga Aftershock	Date	Mangitude[b] (M_L)	Source Depth (km)	Epicentral Distance (km)	Station	Average Horizontal Peak Acceleration (g)
Y	83051417	2.6	11.30	3.65	LLN[a]	0.0006
				3.42	VEW	0.0009
Z	83051417	3.5	8.88	3.77	LLN[a]	0.0028
Z2	83051604	2.7	7.48	1.61	VEW	0.0030

[a]Only one horizontal component of this station triggered; value from only one component.
[b]M_L groupings used in Figure 19 are 2.5-2.6, 2.9-3.1, 3.5-3.6, 3.8-3.9, 4.2, 4.6, 5.0-5.3 and 5.9

COALINGA RESPONSE SPECTRA
Magnitude 2.5 - 5.9

LEGEND

———	5 %, ALL STATIONS, ML=2.5: AVERAGE OF 12 HORIZONTAL COMPONENTS
———	5 %, ALL STATIONS, ML=3.0: AVERAGE OF 12 HORIZONTAL COMPONENTS
———	5 %, ALL STATIONS, ML=3.5: AVERAGE OF 14 HORIZONTAL COMPONENTS
———	5 %, ALL STATIONS, ML=3.9: AVERAGE OF 10 HORIZONTAL COMPONENTS
———	5 %, ALL STATIONS, ML=4.2: AVERAGE OF 02 HORIZONTAL COMPONENTS
———	5 %, ALL STATIONS, ML=4.6: AVERAGE OF 04 HORIZONTAL COMPONENTS
———	5 %, ALL STATIONS, ML=5.2: AVERAGE OF 16 HORIZONTAL COMPONENTS
———	5 %, ALL STATIONS, ML=5.9: AVERAGE OF 02 HORIZONTAL COMPONENTS

Figure 6-21. Average 5% absolute acceleration response spectra computed from recordings of the Coalinga aftershocks recorded at rock sites (Table 6-5). Magnitude (M_L) categories are 2.5, 3.0, 3.5, 3.9, 4.2, 4.6, 5.2, and 5.9 (solid line). Dotted line shows WNA model calculations using a kappa of 0.045 sec for the magnitude (M) categories (3.0, 3.5, 4.0, 4.25, 4.5, 4.6, 5.3, and 5.5) and scaled to the average peak accelerations of the recorded motions.

6-44

comparison of absolute acceleration spectra computed with 50 and 100 bar stress parameters for WNA motions (Figure 6-22). Figure 6-22 shows the maximum differences at short periods while covering at longer periods as the corner periods appropriate to each magnitude are approached.

The effects of kappa variations upon absolute accelerations spectra are shown in Figures 6-23 and 6-24 for WNA and ENA motions respectively. The spectra have been computed for an M 6.5 earthquake at a distance of 25 km. For WNA (Figure 6-23) kappa varies from 0.01 to 0.04 sec. and the effects upon the short period (<0.3 sec.) portion of the spectra are dramatic. For these motions, doubling kappa decreases short period spectral ordinates and peak accelerations by over 50 percent.

In Figure 6-24, the corresponding ENA spectral ordinates are shown for kappa values ranging from 0.005 to 0.008 sec. As expected, because of the much lower values, the effects of kappa are shifted to shorter periods and are much less severe.

Results of the parameter sensitivities indicate that for M above approximately 5.5, rock site effects are a minimum for periods longer than about 0.3 sec. For periods shorter than this, ENA motions characterized by lower kappa values and higher stress parameter will have levels of 5 percent damping absolute acceleration exceeding corresponding WNA motions by factors approaching three at 0.03 sec. Changes in the stress parameter affect the spectra through the accompanying changes in the corner frequency. A 100 percent change in stress parameter results in a 60 percent change in absolute levels of motion for frequencies higher than the corner frequency. Predictability of the stress parameter for a given source zone probably is not less than a factor of two and may be larger (Somerville et al., 1987). Ranges in ground motions may be expected to vary at least 50 percent because of the uncertainty of this parameter.

Additionally, short period spectral ordinates are sensitive to kappa values for WNA motions for periods less than about 0.3 sec. For these motions a 100 percent change in kappa can change spectral ordinates by about 50 percent. For ENA or hard-rock motions, the kappa sensitivity is shifted to much shorter periods and the effect or varying kappa is much less. Accurate specification of strong ground motions for soft-rock sites then requires a more precise determination of kappa than in hard-rock sites.

FACTORS AFFECTING GROUND MOTIONS AT SOIL SITES

The effects of a soil column upon strong ground motion have been well documented and studied analytically for many years. Wood (1908) and Reid (1910), using apparent intensity of shaking and distribution of damage in the San Francisco Bay area during the 1906 earthquake, gave evidence that the severity of shaking can be substantially affected by the local geology and soil conditions. Gutenberg (1927, 1957) developed amplification factors representing different site geology by examining recordings of microseisms and earthquakes from instruments located on various types of ground. Since the 1930s, a number of Japanese seismologists have made contributions to the

Figure 6-22. Comparison of 5% absolute acceleration response spectra (Sa) computed for WNA parameters (Table 6-3) for stress parameters of 50 and 100 bars.

Figure 6-23. Comparison of 5% absolute acceleration response spectra (Sa) computed for WNA parameters (Table 6-3) for kappa values varying from 0.01 to 0.04 sec.

Figure 6-24. Comparison of 5% absolute acceleration response spectra (Sa) computed for ENA parameters (Table 6-3) for kappa values varying from 0.005 to 0.008 sec.

theory of site response (e.g., Sezawa and Kanai, 1932; Kanai, 1950; Kanai et al., 1959; Tanaka et al., 1973). These contributions generally included observations of site amplification effects from small earthquakes and theoretical developments for solutions of the wave equation at sites with up to three layers. These investigators generally found reasonable agreement between theory and observations in amplitude and predominant periods of site resonances. More recently, Borcherdt and Gibbs (1976), Seed et al. (1969), Wiggins (1964), Idriss and Seed (1968), Berill (1977), Joyner et al. (1976), Silva (1987), and Duke and Mal (1978) have shown that during small and large earthquakes the surface soil motion can differ in significant and predictable ways from that on adjacent rock outcrops. In addition, other investigators have utilized explosion data either independently or in conjunction with earthquake data to examine site response characteristics (Murphy et al., 1971; Rogers et al., 1984; and Hays et al., 1979). Recent work using horizontal as well as vertical arrays of instruments have demonstrated the general consistency of the site response for seismic events of different sizes, distances, and azimuths (Tucker et al., 1984; Benites et al., 1985).

Results of these and other studies have demonstrated, in a general sense, the adequacy of assuming plane-wave propagation in modeling 1-D site response for engineering purposes. The simple model then represents a useful analytical tool to approximate site effects on strong ground motion.

Observations resulting from very general and broad classifications of soil sites suggest some general features of soil effects to strong ground motions. Most notable are: (1) a crossover in amplification to deamplification above around 5 Hz (shown in Figure 6-25 to occur from about 0.1 to 0.2 sec. in the 5 percent damping Joyner-Boore [1988] empirical pseudorelative velocity response), (2) a relative insensitivity of peak acceleration (except for very shallow soil sites; Campbell, 1981) to rock or soil site conditions for recordings at close distances (≤ 50 km) considering the variance in the measured values, (3) a significant and stable amplification of about 1.5 of peak particle velocity at soil sites relative to corresponding rock sites (Joyner and Boore, 1988), and (4) a range of amplification from about 0.8 to about 2.5 (Aki, 1988; McGuire et al., 1989). Apart from the contributions of resonances that are generally averaged out through the sampling of such broad data bases, these observations (as previously discussed) represent the net effect of amplification resulting from velocity gradients and attenuation resulting from material damping.

It is of interest then to determine the degree to which the simple vertically propagating plane shear-wave technique can predict these effects as well as isolate the factors that exert a controlling influence on 1-D site response.

In order to develop generic site amplification factors appropriate to predominantly ENA sites, response analyses were performed for different site depths based upon the generic profile shown in Figure 6-26 (McGuire et al., 1989). This profile was chosen to be consistent with the generally stiff soils present in the eastern and central United States. The profile was based upon the sand-like and till-like profiles determined by

Figure 6-25. Predicted pseudovelocity response spectra for 5% damping at rock sites (heavy line) and at soil sites (thin line) for d=0 and M=5.5, 6.5, and 7.5. Spectra correspond to the randomly oriented horizontal component. Curves are dashed where not constrained by data (after Joyner and Boore, 1985).

6-50

Figure 6-26. Standard soil profile appropriate for sand-like Central and Eastern United States sites (gradient). Site categories I-V are indicated by their respective soil column depths. Constant shear-wave velocity profiles represent averages (over travel time) of the gradient profiles for each site category.

6-51

Bernreuter et al. (1985), from their review of FSARs and PSARs for nuclear power plant sites. Bedrock shear-wave velocity was taken as 6,000 ft/sec. (Bernreuter, 1985). This value is much higher than hard-bedrock shear-wave velocities appropriate for WNA that would average around 4,000 to 5,000 ft/sec. (Campbell et al., 1979). This is consistent with the general nature of the difference in the near-surface crustal rocks between WNA and ENA tectonic regimes.

Levels of input motion (rock outcrop) of 0.1, 0.3, 0.5, 0.75 and 1 g were used to accommodate effects of material nonlinearity upon site response. Outcrop response spectra were computed from the BLWN model (Equation 1) using ENA parameters (Table 6-3). Distances, magnitudes, peak values, and predominant frequencies associated with the outcrop motions are shown in Table 6-6. The equivalent-linear site response is computed by propagating the power spectral density of the outcrop motion through the soil profile using the propagators of Silva (1976). Arbitrary angles of incidence may be specified but normal incidence is used throughout the present analyses. RVT is used to predict peak time domain values of shear-strain based upon the shear-strain power spectrum. In this sense, the procedure is analogous to the program SHAKE except that peak shear strains in SHAKE are measured in the time domain. The purely frequency domain approach obviates a time domain control motion and, perhaps just as significantly, eliminates the need for a suite of analyses based on different input motions. This arises because each time domain analysis may be viewed as one realization of a random process. In this case, several realizations of the random process must be sampled to have a statistically stable estimate of site response. The realizations are usually performed by employing different control motions with approximately the same level of peak acceleration. In the case of the frequency domain approach, the estimates of peak shear strain as well as oscillator response are, as a result of the RVT, fundamentally probabilistic in nature. Stable estimates of site response can then be computed by forming the ratio of spectral acceleration predicted at the surface of a soil profile to the spectral acceleration predicted for control motion.

The modulus reduction and damping curves used in the analysis are shown in Figure 6-27. The variation of shear modulus with strain is taken as the upper range Seed-Idriss sand curve. The upper range was chosen as recent observations of site response (Silva et al., 1987) indicated that in-situ soil response to earthquake motions showed less shear-strain dependency of shear modulus than that predicted by the mid-range values. The damping curve used departs from the mid-range values at low strains to accommodate observations of shear-wave damping for wave propagation at low levels of motion (Joyner et al., 1976; Joyner et al., 1981; Johnson and Silva, 1981). The lower shear-wave damping used here at the higher shear-strain levels is an attempt to reconcile observations of higher peak acceleration values at deep soil sites from the Imperial Valley 1979 event than would be expected from predictions using the mid-range curve.

Results of the response analysis for spectral amplifications at frequencies of 1, 2, 5, 10, and 20 Hz for an outcrop motion of 0.5 g are shown in Figure 6-28. The 0.5 g level of input motion is midway in the range considered and results in an average strain

Table 6-6
MAGNITUDES (M) AND DISTANCES USED
IN OUTCROP MOTIONS

Ap(g)	$f_p{}^a$(Hz)	$V_p{}^b$(cm/sec)	$f_p{}^a$(Hz)	V/a (cm/sec/g)	M	R (km)
0.1	25	3	4	30	5.7	37.0
0.3	25	8	5	27	5.7	14.5
0.5	25	13	5	26	5.7	9.5
0.75	25	42	2	55	7.2	17.0
1.0	25	58	2	58	7.2	12.0

[a]Predominant frequencies associated with acceleration and particle velocity estimated by RVT.

[b]Peak particle velocity.

Figure 6-27. Plot of shear-strain dependency of shear-wave damping and shear modulus used in the site response analyses (after Seed and Idriss, 1970).

RESPONSE SPECTRAL AMPLIFICATION

Figure 6-28. Plot of computed 5% response spectral amplification factors for five site categories (Figure 6-26) for a 0.5 g level of input (rock outcrop) motion. Curves represent frequencies of 1, 2, 5, 10, and 20 Hz.

compatible damping of about 7 percent for the profiles. Figure 6-28 reveals very clearly the interaction of amplification and the effects of damping. At low frequencies, 1 Hz, the amplification is unity for shallow profiles and increases almost linearly to about 2 at 500 ft. At 2 Hz we see the effects of damping and increased amplification reflected in a more rapid increase with profile thickness, a peak around 250 ft at about 2, and then a decrease and finally a crossover with the 1 Hz curve near 400 ft. The curve for 5 Hz shows the same trend displaced toward shallower depths, peaking near 50 ft. The curves for 10 and 20 Hz apparently peak for profiles shallower than the 20 ft minimum used in the analyses. These latter two curves demonstrate the large amplifications possible at very shallow soil (or fractured rock sites) for high frequency ENA type motions. Recordings of aftershocks of ENA events (Boatwright and Astrue, 1983; Mueller and Cranswick, 1985; Cranswick et al., 1985) have shown rather large amplifications (of Fourier amplitude spectra) at high frequencies for these type of sites.

The values of amplification, near 0.5 for the 20 Hz curve for the profile depth of 500 feet, are thought to be too low. These low values probably result from not accommodating the effects of confining pressure upon damping. This would tend to decrease the level of damping at depth for the deep profiles and result in less deamplification at high frequencies. Since adequate models of the effects of confining pressure upon damping are not currently available, a lower limit of 0.8 was chosen based upon general observations (Aki, 1988; McGuire et al., 1989).

In a general sense, although these analyses are more appropriate to an ENA environment having a stiff profile, high bedrock velocity, and a control motion rich in high frequencies, the trends shown in Figure 6-28 are in accord with observations based upon WNA experience. A crossover from amplification to deamplification occurs, in this case at 10 Hz and at a depth of about 300 feet. At 5 Hz the crossover will occur beyond a soil depth of 500 feet. Also the general range in amplification is about 0.8 to about 2.5.

Figures 6-29 and 6-30 show the computed amplification factors for peak acceleration and peak particle velocity for the range in control motions (0.1 to 1 g). For peak acceleration an amplification of about 1 occurs at a profile depth of around 250 feet for an input in the range of 0.3-0.5g (average damping of about 7 percent) (Figure 6-29). In Figure 6-30, the amplification of peak particle velocity reaches about 1.5 for similar input levels and remains relatively constant to depths of 500 feet.

These trends are in reasonable accord with the observations of relative insensitivity of peak acceleration to site conditions (excluding shallow sites <50 feet) and amplification of peak particle velocities of about 1.5 providing the data base is predominated by sites whose depths exceed about 200 feet. While keeping in mind that the site response analyses were performed for soil, bedrock, and outcrop spectral content appropriate to ENA conditions, there is good general agreement between observed soil amplification effects and those predicted by the simple 1-D model.

Figure 6-29. Plot of computed amplification of peak acceleration for the five site categories (Figure 6-26). Size of symbol indicates level of input (rock outcrop) acceleration (0.1, 0.3, 0.5, 0.75, 1 g).

Figure 6-30. Plot of computed amplification of peak particle velocity for the five site categories (Figure 6-26). Size of symbol indicates level of input (rock outcrop) acceleration (0.1, 0.3, 0.5, 0.75, 1 g).

Parameter Sensitivity

From the general observations of site response, the effects of soil upon rock response is a maximum amplification of about 3 on an average basis. This approximate range is reflected in the computed amplifications shown in Figure 6-28, which range from about 0.8 to about 2.5. From Figures 6-29 and 6-30, the maximum range in amplification, due to different levels of input motion, for a given profile thickness is about 1.5 to 2.0. This range in computed amplification results from nonlinear soil response and is over 50 percent of the total effect. Although the change in shear-wave velocity contributes to the lower amplifications at higher strain levels, and can be a controlling factor under certain conditions such as the lakebed sites in Mexico City (Seed et al., 1988), the main dependence for more generic profiles is upon the strain compatible level of damping in the soil. For example, the average damping for a 120 feet soil profile varies from about 3.5 percent to about 7.0 percent for control motions of 0.1 and 0.5 g, respectively.

To summarize, the controlling factor in predicting the response at soil sites is the appropriate value of material damping for the strain levels of interest as well as accommodating the effects of confining pressure (depth). Different values of damping, each reasonable in the context of current understanding of in-situ material properties, can result in differences in computed values of amplification resulting from surficial soils by amounts that are a significant percentage (over half) of the total computed effect.

Variability of Observed 1-D Site Effects

The expected variability in site response at rock sites, for periods shorter than approximately 0.3 sec., ranges up to about 3 and is due to the conditions of the rock beneath the site. For soil sites, the maximum effect of the soil profile is about a factor of 3 as well, and variations in assumed material damping result in a range in computed amplification of about 1.5 to 2.0. The uncertainty in strong ground motion prediction for peak values and response spectral ordinates generally ranges from about 1.5 to 2.0 (Campbell, 1988; Joyner and Boore, 1988). While not strictly a measure of the variability in rock or soil site response of a given site to different sources, the variance about a fit does represent an estimate of statistical stability in measured values. This estimate of variance, 1.5 to 2.0, is in agreement with the value of approximately 1.5 found in site response studies in the Los Angeles Basin (Rogers et al., 1984). If the variance in observed 1-D site effects is taken as approximately 1.5 to 2.0, then differences in properties at rock sites and damping values in soil profiles are significant parameters in specifying site-dependent ground motions.

SUMMARY AND CONCLUSIONS

The effects of site conditions and geometry upon the spectral content of strong ground motions at close distances (≤ 50 km) to earthquakes has been examined. Topographic effects were found to contribute observed amplifications of approximately 2 to 10 at

ridge crests over observations at sites located at the bases for wavelengths roughly comparable to the width of such structures. Predicted values generally ranged less than this (from about 2 to 4). Factors contributing to this discrepancy are 3-D effects as well as ridge-ridge interactions.

Amplification effects resulting from alluvial valleys can be separated into two types depending upon valley shape. Wide and shallow valleys, with a shape ratio ≥ 0.25, are characterized in response by vertically propagating shear waves away from the edges and a superposition of vertically propagating shear-waves with locally generated surface waves near the edges.

Additionally, long-period body waves entering large basin structures at shallow incidence angles can become trapped and propagate across the structure as surface waves. These surface waves can give rise to large amplifications as well as increased durations over predictions using vertically propagating shear waves above.

Narrow and deep valleys, with a shape ratio ≥ 0.25, are characterized by a different set of mode shapes that involve 2-D resonances resulting in broad-band amplification across the entire valley width. The fundamental resonance is shifted from the 1-D peak and the level of amplification is much greater.

To isolate source, propagation path, and 1-D site effects, a simple ground motion model was presented. For rock sites, comparisons of model predictions with recorded motions showed that the effects of near-surface dynamic material properties exerted a controlling influence upon short-period motions (≤ 0.3 sec.). Hard rock sites, associated with low values of the attenuation parameter kappa (~ 0.006 sec.) showed significantly higher motions (up to a factor of 3) than soft rock sites with kappa values around 0.02 sec.

For soil sites, equivalent-linear site response analyses for generic sand-like profiles of different depths were subjected to varying levels of control motions. Response spectral (5 percent damping) amplification factors at different frequencies as well as amplifications of peak accelerations and peak particle velocity were computed. The results indicated a general range in amplification of about 3 (0.8 to 2.5) for profiles ranging in depth from 20 to 500 feet. The controlling parameter in the amplification factors was the level of strain compatible damping. Ranges in control motion from 0.1 to 1.0 g resulted in a range of about 1.5 to 2.0 in values of the computed amplification factors.

RECOMMENDATIONS

2-D Site Effects

For both topographic and alluvial valley effects, clearly the need is for more good quality data with calibrated instrumentation and careful statistical analyses. Model predictions for topographic effects continue to underestimate observed amplifications by

amounts significantly greater than the variance of the observations. If the departures between theory and observations are related to 3-D effects and ridge-ridge interactions, the use of computations to evaluate these effects on a site-specific basis becomes very costly in terms of geotechnical characterization and numerically cumbersome as well. As a result, if the effects can be shown to be stable and robust with respect to a few, simple to measure parameters, empirical correction factors, analogous to Boore's (1986) amplification factors, may prove useful.

For alluvial valley effects, more data are required to better resolve the conditions under which valley amplification as well as motion duration differs in a significant way from 1-D theory. Because the cost of accurately characterizing a 2-D or 3-D valley feature in terms of geotechnical properties is enormous, empirical correction factors applied to 1-D response evaluations may be useful here as well.

In terms of modeling 2-D and 3-D basin response at short periods (< 1 sec.), material damping likely will be a controlling factor. It is essential then that ground motion modeling accommodate accurate damping models in terms of frequency dependence and vertical as well as lateral changes in damping. In addition, for high levels of motion, accurate 2-D and 3-D nonlinear soil models are needed to model basin response realistically.

1-D Site Effects

For rock sites, the effects of near-surface velocity gradients and material damping on short period motions needs to be further quantified. Correlation of rock properties with measured values of kappa at surface sites as well as analyses of vertical array data would be most useful. Analyses of deep wells in hard and soft rock for shear-wave velocity and damping, coupled with ground motion data recorded at least at the surface would be ideal in quantifying the physics of site effects at rock sites.

For soil sites, in evaluating the amplification effects at high levels of motion, appropriate levels of in-situ damping are a controlling influence. To determine the degree to which laboratory based nonlinear soil models correspond to in-situ conditions, more observations of large-strain soil response using vertical arrays coupled with careful laboratory analyses are required. A significant aspect of the recommended observations and analyses is an evaluation of the effects of confining pressure upon damping. This can be done by analyses of the vertical array data correlated with carefully performed laboratory test results.

For recommendations regarding the need for increased good quality data for 2-D topographical and alluvial valley effects as well as 1-D rock site effects, the results of Tucker and King (1984) should be emphasized. They found that the response characteristics of valleys applies to direct shear-waves as well as to coda waves. These results were also found to apply to 1-D soil site effects by Benites (Benites et al., 1985) and Silva (1987), and to both rock and soil sites by Aki and Phillips (1986). In addition, careful

6-61

application of microtremor experiments may reflect amplification patterns applicable to direct shear-wave and to coda waves (Lermo et al., 1988). As a result, experiments designed to observe topographic, alluvial valley, and 1-D site effects may be able to employ coda waves as well as microtremors as seismic sources. This would reduce monitoring time and allow data to be gathered from areas of relatively low-level local seismicity.

PANEL REPORT

The objectives of this panel are twofold: (1) to assess the importance of incident wave-field complexity, vertical and lateral variability of material properties, and site geometry upon strong ground motions and (2) to recommend research areas aimed at quantifying the effects of such complexities on strong ground motion as well as improving the predictive capability of such effects.

IMPORTANCE

Research guidelines in this area are divided into 1-D effects and 2-D to 3-D effects. Largely through necessity, the geotechnical engineer nearly always assumes that site response can be evaluated as a 1-D problem and typically models a vertically propagating plane shear wave from some basement rock at depth through a soil column to the surface. Oftentimes "basement" is poorly defined and may, in reality, be the depth to which the deepest rock or soil core was taken for geotechnical characterization.

For the seismic design of structures, the procedure followed in practice is to input the seismic load at the foundation level of the structure in the form of acceleration time histories or response spectra. Using appropriate analytical techniques, the response of the structure is then analyzed.

In most cases, seismic records of the motion are not available. In such cases, synthetic time histories or records from other earthquakes with similar site characteristics are used. When site-specific records are available, these are generally obtained from recordings made at the ground surface. The surface motions are then transferred to the foundation level using 1-D programs such as "SHAKE" and are then referred to as the design ground motion. If time histories of motion are obtained at rock outcrops near the sites, the same motion is assumed at the bedrock surface underlying the site, and the recorded motions propagated through the soil column, again assuming vertically propagating shear waves.

The 1-D vertical propagation motion model works adequately for many engineering problems and is widely used in practice because of its simplicity and ease of use. In some cases where 2-D or 3-D effects of the ground motions are suspected, the effects of this perturbation may be enveloped by the design response spectra, and thus absorbed in the design. However, recent evidence suggests that 2-D or 3-D models of the

ground motion characteristics can be significant and should be considered for sites founded upon sediment filled valleys or in areas of considerable topographic relief.

EFFECTS OF SITE GEOMETRY ON STRONG GROUND MOTION

Laterally varying structures such as surface topography, dipping interface, and changes in material properties contribute 2-D and 3-D aspects to ground motion specification. These nonhomogeneous effects, resulting from scattering, focusing, and mode conversions, are present at all sites to some extent. In some cases, these effects can significantly alter the spectral content of the ground motions as well as increase the duration of strong shaking.

Topographic Effects

Topographic effects are caused by a focusing of energy near ridge crests and the interaction of the primary (incident) wavefield with outgoing scattered surface waves (Bard, 1983). The resulting total wavefield shows broad-band amplifications at ridge crests and is most pronounced for wavelengths that correspond roughly to the width of the structure. Along the slopes and at the bases of elevated geologic structures, the interaction of the primary field with the scattered fields results in complicated patterns of amplification and deamplification. This varying pattern is associated with rapidly varying phase and may be expected to give rise to differential motions, which could be of concern to extended structures.

Computed values of amplifications at elevated structures generally underpredict observed crest-to-base ratios by considerable amounts. Observed amplifications range from about 2 to 20 in the spectral domain (Fourier and response) (Bard, 1983) and can be as high as 30 (Davis and West, 1973).

In the time domain these amplifications generally are observed to range up to about 5 (Griffiths and Bollinger, 1979). Predicted values of ridge-to-base amplifications are generally much less than these and range from 3 to 4 in the spectral domain to less than 2 in the time domain (Geli et al., 1988) (Table 6-7). The differences between predicted and observed crest-to-base topographical effects are up to about 10, which is a factor of 3 higher than the predicted total effect. Causes of this significant underestimate are related to the influence of 3-D effects, as well as ridge-ridge interactions (Geli et al., 1988).

The lateral dimensions of geologic structures that may impact strong motion depends upon frequency through wavelength. If the bandwidth of interest to engineered structures is taken as 5 sec to 25 Hz and assuming the shear-wave velocities near the earth's surface range approximately from 1 to 3 km/sec for soft and hard rocks respectively (Silva and Darragh, 1989), the corresponding range in wavelength is 40 m to 5 km and

Table 6-7
2-DIMENSIONAL GEOLOGIC STRUCTURAL EFFECTS
INFLUENCE MATRIX

Structure	Conditions	Type	Size	Quantitative Predictability[a]
Surface Topo-graphy	Sensitive to shape ratio, largest for ratio between 0.2 to 0.6. Most pro-nounced when wavelength mountain width	Amplification at top of structure amplification and deamplifica-tion at base, rapid changes in amplitude phase along slopes	Ranges up to a factor of 30 but generally from about two to 10	Poor: generally underpredict size. May be because of ridge interaction and 3-D effects

Sediment-Filled Valleys

Structure	Conditions	Type	Size	Quantitative Predictability[a]
1) Shallow and wide (shape ratio <0.25)	Effects most pronounced near edges. Largely verti-cally propagat-ing shear waves from edges.	Broad band amplification across valley because of whole valley modes	1-D models may underpredict at higher frequen-cies by about two near edges	Good: away from edges 1-D works well, near edges extend 1-D amplifica-tions to higher frequencies
2) Deep and narrow (shape ratio >0.25)	Effects through-out valley width	Broad band amplification across valley because of whole valley modes	1-D models may underpredict for a wide band-width by about two to four away from edges. Resonant frequencies shifted from 1-D.	Fair: given detailed description of vertical and lateral changes in material properties
3) General	Local changes in shallow sedi-ment thickness	Increased duration	Duration of significant motions can be doubled	Fair
4) General	Generation of long period surface waves from body waves at shallow incidence angles	Increased amplification and duration because of trapped surface waves	Duration and amplification of significant motions may be increased over 1-D predictions	Good at periods exceeding 1 second

[a] Good: generally within a factor of two.
Fair: generally within a factor of two to four.
Poor: qualitative only, can easily be off by an order of magnitude.

6-64

120 m to 15 km, respectively. Topographical irregularities of dimensions near to this range may then exert considerable influence upon corresponding ground motions depending upon the shape ratios of the topographic structures (Geli et al., 1988) (Table 6-7).

Alluvial Valley Effects

Consideration of ground motions in alluvial valleys is fundamentally an assessment of departures in response from the classical vertically propagating plane shear-wave 1-D mode (Seed and Idriss, 1969; Schnabel et al, 1972). The main effect of the curvature of the sediment-basement interface is the generation of surface waves, as well as trapped body waves, which propagate in the alluvium and superpose with the vertically-propagating shear waves. This results in an amplification of motion as well as increased duration over 1-D soil effects alone.

Observations suggest that the simple 1-D model works well at and near the valley center in predicting the effect of the valley response to outcrop motions (King and Tucker, 1984). This observation is also predicted in modeling (Bard and Gariel, 1986) that, as one may expect, is more appropriate for shallow and wide valleys (shape ratio ≥0.25, Table 6-7) than for deep and narrow valleys. Edge effects, associated with rapid changes in soil thickness, may give rise to the local generation of surface waves and trapped body waves that because of material damping do not significantly alter the short period spectral content of motions some distance from the edges (Tucker and King, 1984). Table 6-7 lists the range of effects for shallow valley features.

For deep and narrow valleys with large shape ratios (≥0.25), a change in response occurs that involves a new set of mode shapes affecting the valley as a whole (Bard and Bouchon, 1985; Bard and Gabriel, 1986). This class of mode shapes involves in-phase, large amplitude motions of the whole valley. For valleys of this class, deep and narrow, 1-D theory gives a conservative prediction near valley edges (Bard and Gariel, 1986) but seriously unpredicts the valley effects at high frequencies (by a factor of 2 to 4) into the valley center. Table 6-7 shows an influence matrix of 2-D effects that summarizes the results discussed here for topographic as well as alluvial valley features.

Observed spectral amplifications of alluvial valley sites (Fourier spectra) with respect to outcrop motion generally ranges up to about 10 (King and Tucker, 1984) and are in reasonable accord with predictions. Spectral amplifications as high as 30 have been measured for the lake bed in Mexico City (Lermo et al, 1988). Seed et al. (1988), modeled the amplification effects of the shallow (approximately 60 m) clay layer because of the September 19, 1985, M 8.1 earthquake remarkably well using the simple 1-D theory. However, the increased duration compared to outcrop motions at some of the sites is unaccounted for in the simple theory and may be related to lateral changes in thickness in the shallow clay layer and thus local generation of surface waves (Bard et al, 1988).

Variability of Observed 2-D Site Effects

As a result of the careful observations of both topographical and alluvial valley effects in the Garm region of the USSR, the standard error of variation in amplification has been quantified (Tucker and King, 1984). After careful instrument calibration that quantified the variability of system response, repeated measurements of ridge and valley effects has shown that the observed variability in amplifications is approximately 1.5 (Tucker and King, 1984; Tucker et al, 1984; King and Tucker, 1984) and that ridge and valley effects depend weakly upon source azimuth and incidence angle for distant sources. Observed topographic and alluvial valley effects, ranging from about 2 to 10 are then resolvable on a repeatable basis and are generally significantly greater than the measurement uncertainty.

To summarize, topographic effects because of rapid and significant changes in elevation over the dimensions of approximately one wavelength generally range from about 2 to 10 and are most pronounced at the ridge or hill crest and for wavelengths comparable to the width of the structure. The sides of topographic highs undergo patterns of amplification and deamplification with associated rapid changes in phase. Alluvial valley effects that result in departures from the vertical propagating shear-wave model, are largest for sites located in high aspect ratio valleys (large thickness to half-width ratios, >0.25) and away from valley edges where the simple 1-D theory may under-predict the effects by a factor of 2 to 3 (Bard et al, 1988). For shallow and wide valleys (shape ratio <0.25), such as the lake bed sites in Mexico City have demonstrated, the response is dominated by vertically propagating shear waves, particularly away from the edges. Although the 1-D theory captures many of the essential features of amplification because of shallow alluvial valleys, it fails to explain the increased durations observed at some sites. The increased durations of significant motion shown by some of the lakebed sites in Mexico City require the effects of local generation of laterally propagating energy, perhaps because of thickness variations in the shallow clay layer (buried valley or depression with a valley).

Careful observations of topographic as well as alluvial valley effects have quantified the variability of observed amplifications to a factor of about 1.5. Additionally, the observations have shown a weak dependence of amplifications to source azimuth and incidence angle (Tucker and King, 1984).

RESEARCH NEEDS

Shallow Crustal Effects

The effects of vertical gradients of shear wave velocity and material damping in the upper 1 to 2 km beneath the site have been shown to exert a significant influence on the spectral content of ground motions recorded at rock sites for frequencies exceeding about 1 Hz. Presently, disagreement exists as to the cause of such effects as related to source processes or site effects or perhaps to both. In order to resolve this issue as

well as improve the prediction of short period ground motion properties, observations of ground motions at deep borehole sites are needed. Ideal experiments would include boreholes in both soft and hard rock, drilled to depths of 2 to 3 km (some of which already exist), measurement of *in situ* shear wave velocity and damping values, and placement of several three-component instruments within the borehole and at the surface. Analyses would consist of determining how the spectral content varies with depth, coupled with appropriate 1-D or 2-D modeling of the site effects.

Analyses of New and Existing Data Sets Collected Within Complex Basins and at Rock Sites

When feasible, a basin should be instrumented with hundreds of instruments to collect aftershock data to capture the complex response of the basin. This experiment would provide much needed data to study the effects of basin geometry upon strong ground motion. In lieu of the completion of such an experiment, new low-strain microtremor data should be collected at existing strong motion sites and other sites that may be of interest to the basin geometry problem. The site characteristics of the recording sites should be determined in detail; i.e., shear-wave velocities, boundary depths, damping, and density should be obtained to depths of at least 100 to 200 m. At some sites, uphole/downhole installations should be analyzed. These data would provide the bases for a variety of studies.

Existing and new data that measure the variation in spectral site effects for alluvium/rock pairs using both strong motion and weak motion records should be compared to the predicted site effects based on 1-D models. The responses as a function of basin geometry, source position (i.e., intrabasin versus extra basin), wave type, and predominant period should be quantified, and the range of error and mean error should be estimated. The applicability of the engineering practice of propagating time histories through alluvium sites with predicted records based on "propagation" of other nearby recordings through the 1-D alluvium model should then be tested. The comparison should be quantified as a function of basin geometry, source position, and wave-type. An experimental approach to this is as follows:

1. Use data from the SMART-1 array to study the effects of basin geometry. Test the 1-D models predictive capability; i.e., do these models predict spectral and peak ground motion effects across the array?

2. Set up arrays at closely spaced rock sites to study the variability in rock site effects.

3. Obtain the recording site properties, as above.

4. Attempt to model the relative rock-rock variations using 1-D models of the rock column.

Observations of Wavefield Continuity and Complexity in Dynamic Material Properties Upon Strong Ground Motion

In order to resolve the effects of lateral heterogeneities, seismic wavefield observations at 3-D arrays are needed. Material properties in the spatial volume occupied by the array as well as for some distances beyond should be supplied to a scale less than about one-quarter wavelength corresponding to the higher frequencies of interest. Changes in seismic velocities greater than about 10 percent over this scale length should be resolved. Both short-period (small scale) and long-period (large scale) arrays as well as rock and soil conditions should be considered.

A common engineering practice is to assume that a seismic recording from a rock outcrop nearby to a soil site can be deconvolved to generate the input motion at the base of the soil column. Two problems arise: (1) the spatial incoherence of waves contributes variability in the ground motion, even for relatively homogeneous site conditions and (2) the deconvolution process is often ill-constrained because of insufficient knowledge of the soil properties (seismic velocities) and assumes simple, vertical plane-wave propagation. Special 3-D arrays should be designed to place uncertainties on this approach. At the surface, arrays should be designed to capture both soil and rock motions. At depth, seismometers should be placed at each soil and/or rock horizon in order to directly measure the variability in the input motion at each interface.

Analysis of array data would include phase coherency, quantifying the degree of lateral as well as vertical variation in Fourier amplitude and response spectra, and changes in duration aspects across the array.

Results from such analyses would be an association of heterogeneity scale dimensions with wavefield characteristics. The effects of size and depth of laterally heterogeneous features upon seismic waves in terms of amplitude, spectral content, phase distortion, and durations could be assessed. These results would be directly applicable to establishing guidelines in determining resolution required in site investigations in order to obtain given levels of uncertainty in ground motion estimation.

Amplification of Ground Motions by Topography and Basins

Fundamental to the prediction of short period (>1 Hz) basin response is the question of nonlinear soil response. Linear model calibrations or validations using observations of low levels of ground motions are of questionable use in applications to predictions of higher levels of motion (particularly for shear strains exceeding 10^{-2} percent in saturated sandy soils). In general, the question of the degree of nonlinear response of *in situ* soils to strong ground motion must be resolved before linear 2-D and 3-D analyses are used to predict high levels of strong ground motion. This reality must be kept in mind as a bottom line consideration in any research program designed to increase the predictive capabilities of the effects of soils on strong ground motions.

The following research activities are designed to develop an understanding of how these effects are generated and how they can be predicted, and to develop criteria for recognizing the potential presence of these effects.

1. How predictable are these effects, given our current abilities in modeling wave propagation and characterizing material properties?

    Initially, existing methods of modeling the effects of topography and basins may be tested using existing ground motion data. A useful data set would be a profile of recordings across a topographic feature or a basin, including control motions that are remote from the influence of lateral structure. The modeling methods may include both physical models (e.g., using foam rubber) and computer models (using analytical or numerical methods). The approach is to model the recorded time histories across the profile, or the ratio of the structure-affected motion to the control motion. With a relatively modest level of effort, these studies can provide a direct assessment of our ability to predict the effects of topography and lateral variations in subsurface geology.

    As a second phase of this activity, improvement in the accuracy of the modeling results may be sought by improving the characterization of the material properties (wave velocities and damping at the sites). This can be done by acquiring more detailed measurements of the material properties at these sites by geophysical studies. The degree of improvement in predictive ability that results can be evaluated, and used to guide the design of more detailed studies.

    Examples of data sets that are available for the study of topographic effects include aftershock recordings of the San Fernando, Nahanni, Valparaiso (Chile), Superstition Hills, and Loma Prieta earthquakes. For studies of basin effects, examples of available data are the recordings of the San Fernando earthquake in the San Fernando Valley and Los Angeles Basin, the recordings of the Michoacan earthquake in Mexico City, the recordings in the Garm region of the USSR, and recordings at the SMART1 array in Taiwan.

2. What is the cause of the large amplification effects associated with topography and basins?

    Current computational models tend to underpredict the large amplifications that are associated with topography. Fundamental studies of the wave propagation phenomena associated with topographic amplification are required in order to understand the large amplification effects that are observed. It is anticipated that these studies may require the collection of data on topographic effects at sites under conditions in which the seismic source and material properties are well known. It may be possible to adapt existing array sites having good control on material properties, such as those in Parkfield and Taiwan, for these experiments. The detailed design of these experiments can be based on the

knowledge gained about wave interactions with topography in Task 1. It is expected that analysis of the data from these experiments will lead to the development of more accurate methods for modeling wave interactions with topography.

Although body waves entering a horizontally layered structure from below cannot become trapped in that structure, small departures from horizontal layering can result in the trapping of waves within the structure. We need to identify the kinds of lateral variations in structure that can lead to significant amplifications through the trapping of waves. This requires the acquisition of data in basins and valleys where the seismic source and material properties are well known, and the analysis of the wave propagation phenomena that given rise to the observed amplification effects.

It is expected that analysis of the data from these experiments will lead to the development of more accurate methods for modeling the trapping of waves in laterally varying media. Refined computer models that include realistic representations of damping should also be developed.

3.   What are the ranges of these effects on strong ground motions?

> Careful analysis of the strong motion data base using information about the topographic conditions and basin structure can provide an empirical estimate of the ranges of these effects on strong motions. However, we will not always be able to isolate the effects of topography and subsurface geometry from other effects in the empirical data base and the data base may not represent the full range of possible effects. Using modeling methods that have been carefully validated against recorded data, it is possible to explore the ranges of effects that topography and lateral structure may have on ground motions, and thereby extend our understanding of these phenomena beyond the limits of the empirical data base. This can be done by performing sensitivity studies using 2-D models having arbitrary levels of complexity in both surface topography and subsurface velocity structure. Modern computers can readily perform these computations throughout the frequency range of interest to earthquake engineering. With further increases in the speed of computers, it will become feasible to also analyze 3-D linear models. The graphical display of these calculated wave fields in movies or color monitors can play an important role in developing an intuitive understanding of the interaction of wave fields with geological structure and may lead to the formulation of simplified approaches to the calculation of these wave fields.

4. How can the uncertainty in the predicted effects be reduced?

One aspect of prediction uncertainty relates to the adequacy of the model as a presentation of the wave propagation phenomena. This modeling uncertainty can be quantified by measuring the goodness of fit between recorded and calculated ground motions in situations where the material properties of the medium are known. Modeling uncertainty can be reduced by improving the physical basis of the model. A second kind of prediction uncertainty can be estimated by varying the values of the material property parameters within their uncertainties and measuring the effect on the ground motions. It can be reduced by more detailed measurement of the material properties. A third kind of uncertainty is that caused by randomness, such as wave scattering by features of the medium that are not resolved in the structure model. If a model for this scattering process can be developed using in-situ measurements, it may be possible to include it as part of the wave propagation model and thereby reduce the random uncertainty.

5. How can we recognize the potential occurrence of significant amplification effects at a site?

The investigations of the previous tasks are designed to provide us with a physical understanding of the wave propagation phenomena that are responsible for producing amplification of ground motions on ridges and basins, and the ability to predict these effects. Given this basic understanding, it is then possible to describe the conditions under which potentially significant amplifications may occur. If this information is disseminated among practicing engineers, they will be able to recognize potentially hazardous conditions and know how to proceed to evaluate those hazards.

The information to be disseminated can take several forms. Simplified correlations between shape factors and dimensions of ridges or basins and changes in amplitude, frequency content, and duration of ground motion can be developed based on recorded data and modeling results. Catalogs of case histories can be prepared that the engineer could search for analogs to specific sites. The graphical display of recorded or calculated wave fields can play an important role in developing an intuitive understanding of the interaction of wave fields with geological structure, both for the wave propagation specialist and the geotechnical engineer. These information displays should lead to the development of simple criteria for establishing whether potentially hazardous conditions exist that require further evaluation.

Physical Scale Modeling

Physical modeling is a tool that can be used to examine several of the problems that are the topics of this workshop, including the effect of sloping sites, the effects of

spatial variability of the near-surface geology, site geometry. The simplest physical models are made from a homogeneous medium, such as foam rubber, and are excited from below, so that the dominant wave types are body waves. However, it is also not difficult to build physical models with layers of differing properties, and cut the topography into these, or to make physical models with dipping layers. These can be used, for example to study the effects of a hard capstone rock layer overlying softer materials. The layered models will support surface waves, they are as effective for modeling pile foundations or structures with complex foundation shapes as they are for simple foundations.

Compared with numerical models, physical models have some disadvantages and some advantages. Disadvantages of the physical model are that there is little flexibility in modifying the model after it is built, that only a limited frequency band can be studied (but frequencies of interest can always be handled), and attenuation of the model material may be difficult to match to attenuation in the earth. Advantages are ability to easily handle arbitrary 3-D complexity in the geological model, potential lower cost than finite element analysis, ability to handle very large model size, and ease in generation of different types of waves or arbitrary angles of incidence.

Scale models may be used for several applications. First, they may be used to examine what types of 2-D topographies are likely to cause ground motion problems. A critical variable seems to be the shape of the structure and ratio of height to base. Second, they are appropriate to determine what types of subsurface structure are likely to cause critical failures of 1-D analysis. Finally, they should be used to examine when 2-D calculations fail and full 3-D calculations are in order. Our goal is to provide simple guidelines on when a site needs to be flagged for possible problems.

REFERENCES

J.G. Anderson, and S.E. Hough. "A Model for the Shape of the Fourier Amplitude Spectrum of Acceleration at High Frequencies." Bulletin of the Seismological Society of America, Vol. 74, No. 5, October 1984, pp. 1969-1993.

G.M. Atkinson, "Attenuation of Strong Ground Motion in Canada." Bulletin of the Seismological Society of America, Vol. 74, No. 6, December 1984, pp. 2629-2953.

P.Y. Bard "Les Effets de Site D'origine Structurale en Sismologie, Modelisation et Interpretation, Application au Risque Sismique." These d'Etat, Universite Scientifique et Medicale de Grenoble, France, 1983.

P.Y. Bard and M. Bouchon. "The Two-dimensional Resonance of Sediment-filled Valleys." Bulletin of the Seismological Society of America, No. 75, 1985, pp. 519-541.

P.Y. Bard and J.C. Gariel. "The Seismic Response of Two-dimensional Sedimentary Deposits with Large Vertical Velocity Gradients." Bulletin of the Seismological Society of America, No. 76, 1986, pp. 343-346.

P.Y. Bard, M. Campillo, F. Nicollin and F.J. Sanchez-Sesma. "A Theoretical Investigation of Large- and Small-scale Amplification Effects in the Mexico City Valley, the Mexico Earthquake of September 15, 1985." Earthquake Spectra, Vol. 4, No. 4, 1988.

D.L. Bernreuter, J.B. Savy, R.W. Mensing and D.H. Chung. Seismic Hazard Characterization of the Eastern United States: Methodology and Interim Results for Ten Sites. USNRC Report NUREG/CR-3756, 1984.

J.B. Berrill, "Site Effects During the San Fernando, California, Earthquake." In Proceedings 6th World Conference on Earthquake Engineering, India, 1977, pp. 432-438.

R. Benites, W. Silva and B. Tucker. "Measurements of Ground Response to Weak Motion in La Molina Valley, Lima, Peru. Correlation with Strong Ground Motion." Earthquake Notes, Eastern Section, Seismological Society of America, Vol. 55, No. 1, January-March 1985.

J. Boatwright, and M. Astrue. "Analysis of the Aftershocks of the New Brunswick Earthquake." In a workshop on Site-Specific Effects of Soil and Rock on Ground Motion and the Implications for Earthquake-Resistant Design, U.S. Geological Survey, Open-File Report 83-245, 1983.

D.M. Boore, "Stochastic Simulation of High-Frequency Ground Motions Based on Seismological Models of the Radiated Spectra." Bulletin of the Seismological Society of America, Vol. 73, No. 6, Part A, December 1983, pp. 1865-1984.

D.M. Boore, "Short-Period P- and S-Wave Radiation from Large Earthquakes: Implications for Spectral Scaling Relations." Bulletin of the Seismological Society of America, Vol. 76, No. 1, February 1986, pp. 43-64.

D.M. Boore, and G.M. Atkinson. "Prediction of Ground Motion and Spectral Response Parameters at Hard-Rock Sites in Eastern North America." Bulletin of the Seismological Society of America, Vol. 77, No. 2, April 1987, pp. 440-467.

R.D. Borcherdt, and J.F. Gibbs. "Effects of Local Geologic Conditions in the San Francisco Bay Region on Ground Motions and the Intensities of the 1906 Earthquake." Bulletin of the Seismological Society of America, Vol. 66, 1976, pp. 467-500.

J.N. Brune, "Tectonic Stress and the Spectra of Seismic Shear Waves from Earthquakes." Journal of Geophysical Research, Vol. 75, September 1970, pp. 4997-5009.

J.N. Brune, "Correction." Journal of Geophysical Research, Vol. 76, July 1971. p. 5002.

K.W. Campbell, R. Chieruzzi, C.M. Duke, and M. Lew. Correlations of Seismic Velocity with Depth in Southern California. School of Engineering and Applied Science Report No. UCLA-ENG-7965, University of California, Los Angeles, 1979.

K.W. Campbell, "Near-Source Attenuation of Peak Horizontal Acceleration." Bulletin of the Seismological Society of America, Vol. 71, No. 6, December 1981, pp. 2039-2070.

K.W. Campbell, "Near-Source Estimation of Strong Ground Motion for the Eastern United States: Second Quarter Progress Report - FY 1985." Submitted to Nuclear Regulatory Commission, 1985, 14 pages.

G.L. Choy and J. Boatwright. "Teleseismic and near-field analysis of the Nahanni earthquakes in the Northwest Territories, Canada." Bulletin of the Seismological Society of America, Vol. 78. No. 5, 1988, pp. 1627-1652.

E. Cranswick, R. Wetmiller and J. Boatwright. "High-Frequency Observations and Source Parameters of Microearthquakes Recorded at Hard-Rock Sites." Bulletin of the Seismological Society of America, Vol. 75, No. 6, December 1985, pp. 1535-1567.

L.L. Davis and L.R. West. "Observed Effects of Topography on Ground Motion." Bulletin of the Seismological Society of America, No. 63, 1973, pp. 283-298.

C.M. Duke and A.K. Mal. "Site and Source Effects on Earthquake Ground Motion." UCLA - ENG - 7890, November 1978.

T.E. Fumal. Correlations Between Seismic Wave Velocities and Physical Properties of Near-Surface Geologic Materials in the Southern San Francisco Bay Region, California. U.S. Geological Survey Open-File Report 78-1067, 1978, 114 pages.

L. Geli, P.Y. Bard, and B. Jullien. "The Effect of Topography on Earthquake Ground Motion: A Review and New Results." Bulletin of the Seismological Society of America, Vol. 78, No. 1, 1988, pp. 42-63.

D.W. Griffith and G.A. Bollinger. "The Effect of Appalachian Mountain Topography on Seismic Waves." Bulletin of the Seismological Society of America, No. 69, 1979, pp. 1081-1105.

Gutenberg, B. Grundlagen der Erdlebenkunde, Berlin, 1927.

B. Gutenberg, "Effects of Ground on Earthquake Motion." Bulletin of the Seismological Society of America, Vol. 47, 1975, pp. 221-250.

T.C. Hanks, "fmax." Bulletin of the Seismological Society of America, Vol. 72, No. 6. December 1982, pp. 1867-1879.

T.C. Hanks and R.K. McGuire. "The Character of High-Frequency Strong Ground Motion." Bulletin of the Seismological Society of America, Vol. 71, No. 6, 1981, pp. 2017-2095.

S. Hayashi, H. Tsuchida and E. Kurata. "Average Response Spectra for Various Sub-soil Conditions." Third Joint Meeting, US-Japan Panel on Wind and Seismic Effects, UJNR, Tokyo, May 10-12, 1971.

W.W. Hays, A.M. Rogers, and K.W. King. "Empirical Data About Local Ground Response." In Proceeding, 2nd U.S. Nat. Conf. on Earthq. Engrg., Earthq. Engrg. Res. Inst., Stanford University, August 1979, pp. 223-232.

S.E. Hough, J.G. Anderson, J. Brune, F. Vernon III, J. Berger, J. Fletcher, L. Haar, T. Hanks and L. Baker. "Attenuation near Anza, California." Bulletin of the Seismological Society of America, Vol. 78, No. 2, 1988, pp. 672-691.

I.M. Idriss and H.B. Seed. "Seismic Response of Horizontal Soil Layers." J. Soil Mechs. Founds. Div., ASCE, Vol. 94, SM4, July 1968, p. 1003.

I.M. Idriss, "Evaluating Seismic Risk in Engineering Practice." In Proceedings of Eleventh International Conference on Soil Mechanics and Foundation Engineering, August 12-16, 1985, San Francisco, California, Vol. 1, A. A. Balkema, Rotterdam, 1985, pp. 255-320.

L.R. Johnson and W. Silva. "The Effects of Unconsolidated Sediments Upon the Ground Motion During Local Earthquakes." Bulletin of the Seismological Society of America, No. 71, pp. 127-142.

A.M. Joyner, J.C. Tinsley, and R.D. Borchardt. 1985. Predictive Mapping of Ground Motion, in Evaluating Earthquake Hazards in the Los Angeles Region, U.S., Geological Survey Profess. Paper 1360, pp. 203-220.

W.B. Joyner, and D.M. Boore. Prediction of Earthquake Response Spectra. U.S. Geological Survey, Open-File Report 82-977.

W.B. Joyner, R.E. Warrick and A.A. Oliver. "Analysis of Seismograms from a Down-hole Array in Sediments Near San Francisco Bay." Bulletin of the Seismological Society of America, Vol. 66, 1976, pp. 937-958.

W.B. Joyner, and T.E. Fumal. "Use of Measured Shear-Wave Velocity for Predicting Geologic Site Effects on Strong Ground Motion." In Proceedings of the 8th World Conference on Earthquake Engineering, San Francisco, California, Vol. II, 1984, pp. 777-783.

W.B. Joyner, W.B., R.E. Warrick and A.A. Oliver. "Analysis of Seismograms from a Downhole Array in Sediments Near San Francisco Bay." Bulletin of the Seismological Society of America, No. 66, pp. 937-958.

W.B. Joyner, W.B., R.E. Warrick and T.E. Fumal. "The Effect of Quaternary Alluvium on Strong Ground Motion in the Coyote Lake, California, earthquake of 1979." Bulletin of the Seismological Society of America, No. 71, 1981, pp. 1333-1350.

W. B. Joyner and D.M. Boore. "Measurement, Characterization, and Prediction of Strong Ground Motion." In Proceedings of Earthquake Engineering & Soil Dynamics II, GT Div/ASCE, Park City, Utah, 1988.

Kanai. "Effect of Solid Viscosity of Surface Layer on Earthquake Motions and the Nature of Surface Layer." Bulletin of the Earthquake Res. Institute, Vol. 20, 1950, p. 31.

Kanai, Suzuki and Yoshizawa. "Comparative Studies of Earthquake Motions on the Ground and Underground (Multiple Reflection Problem)." Bulletin of the Earthquake Res. Institute, Vol. 34, 1959, pp. 53-88.

J.L. King, and B.E. Tucker. "Observed Variations of Earthquake Motion Across a Sediment-Filled Valley." Bulletin of the Seismological Society of America, Vol. 74, 1984, pp. 137-151.

J. Lermo, M. Rodriguez and S.K. Singh. "Natural Period of Sites in the Valley of Mexico from Microtremor Measurements and Strong Motion Data, the Mexico Earthquake of September 19, 1985." Earthquake Spectra, Vol. 4, No. 4, 1988.

R.K. McGuire, G.R. Toro, J.P. Jacobson, T.F. O'Hara and W.J. Silva. "Probabilistic Seismic Hazard Evaluations at Nuclear Plant Sites in the Central and Eastern United States: Resolution in the Charleston Earthquake Issue." EPRI Research Project P110-53, 1989.

B.J. Mohraz, "A Study of Earthquake Response Spectra for Different Geologic Conditions." Bulletin of the Seismological Society of America, Vol. 66, No. 3, 1976, pp. 915-935.

C.S. Mueller, and E. Cranswick. "Source parameters from locally recorded aftershocks of the 9 January 1982 Miramichi, New Brunswick, earthquake." Bulletin of the Seismological Society of America, Vol. 75, No. 2, 1985, p. 337.

J.R. Murphy, J.R., A.H. Davis and N.L. Weaver. "Amplification of Seismic Body Waves by Low-Velocity Surface Layers." Bulletin of the Seismological Society of America, Vol. 61, 1971, pp. 109-145.

A. Nur and G. Simmons. "The Effects of Saturation on Velocity in Low Porosity Rocks." Earth and Planetary Science Letters, Vol. 7, 1969, pp. 183-193.

O.W. Nuttli, "Yield Estimates of Nevada Test Site Explosions Obtained from Seismic Lg Wave." Journal of Geophysical Research, Vol. 91, 1986, pp. 2137-2151.

A.S. Papageorgiou, and K. Aki. "A Specific Barrier Model for the Quantitative Description of Inhomogeneous Faulting and the Prediction of Strong Ground Motion, Part II, Applications of the Model." Bulletin of the Seismological Society of America, Vol. 73, No. 4, August 1983, pp. 953-978.

H.F. Reid. The California Earthquake of April 18, 1906. The Mechanics of the Earthquake (1910) Carnegie Inst. of Washington, Publ. 87, Vol. 21.

A.M. Rogers, J.C. Tinsley, and R.D. Borcherdt. Predictive Mapping of Ground Motion, in "Evaluating Earthquake Hazards in the Los Angeles Region," U.S. Geological Survey Profess. Paper 1360, 1985, pp. 203-220.

A.M. Rogers, J.C. Tinsley and W.W. Hays. The Issues Surrounding the Effects of Geologic Conditions on the Intensity of Ground Shaking. U.S. Geological Survey, Open File Report 83-845.

A. Rovelli, O. Bonamassa, M. Cocco, M. Di Bona and S. Mazza. "Scaling Laws and Spectral Parameters of the Ground Motion in Active Extensional Areas in Italy." Bulletin of the Seismological Society of America, Vol. 78, No. 2, April 1988, pp. 530-560.

P.B. Schnabel, J. Lysmer and H.B. Seed. SHAKE: A Computer Program for Earthquake Response Analysis of Horizontally Layered Sites. Report No. EERC 72-12, University of California, Berkeley, December 1972.

H.B. Seed, I.M. Idriss and F. W. Kiefer. "Characteristics of Rock Motions During Earthquakes." J. Soil Mech. Found. Eng. Div., ASCE, Vol. 95, No. SM5, September 1969.

H.B. Seed and I.M. Idriss. Soil Moduli and Damping Factors for Dynamic Response Analysis. Report No. EERC 70-10, Earthquake Engineering Research Center, University of California, Berkeley, California, December 1970.

H.B. Seed and I.M. Idriss. "The Influence of Soil Conditions on Ground Motions During Earthquake." J. Soil Mech. Found. Eng. Div., ASCE, No. 94, 1969, pp. 93-137.

H.B. Seed, C. Ugas and J. Lysmer. "Site-dependent Spectra for Earthquake-resistant Design." Bulletin of the Seismological Society of America, No. 66, 1976, pp. 221-243.

H.B. Seed, M.P. Romo, J.I. Sun, A. Jaime and J. Lysmer. "The Mexico Earthquake of September 19, 1985--Relationships Between Soil Conditions and Earthquake Ground Motions." Earthquake Spectra, Vol. 4, No. 4, 1988.

Sezawa and Kanai. "Possibility of Free Oscillations of Strata Excited by Seismic Waves." Bulletin of the Earthquake Res. Institute, Vol. 10, 1932, p. 273.

T-C. Shin and R. B. Herrmann. "Lg Attenuation and Source Studies Using 1982 Miramichi Data." Bulletin of the Seismological Society of America, Vol. 77, No. 2, April 1987, pp. 384-397.

W.J. Silva. "Body Waves in a Layered Anelastic Solid." Bulletin of the Seismological Society of America, Vol. 66, No. 5, 1976, pp. 1539-1554.

W.J. Silva. Soil Response to Earthquake Ground Motion. Report prepared for Electric Power Research Institute, EPRI Research Project RP2556-07, 1986.

W.J. Silva. Estimated Ground Motions for a New Madrid Event. Report prepared for U.S. Army Engineer Waterways Experiment Station by Woodward-Clyde Consultants, 1988.

W.J. Silva, and R.B. Darragh. Engineering Characterization of Strong Ground Motion Recorded at Rock Sites. Report RP2556-48 prepared for the Electric Power Research Institute by Woodward-Clyde Consultants, 1989.

W.J. Silva and R.K. Green. "Magnitude and Distance Scaling of Response Spectral Shapes for Rock Sites with Applications to North American Tectonic Environment." Earthquake Spectra, Vol. 5, No. 3, 1989.

P.G. Somerville, J.P. McLaren, L.V. LeFevre, R.W. Burger and D.V. Helmberger. "Comparison of Source Scaling Relations of Eastern and Western North American Earthquakes." Bulletin of the Seismological Society of America, No. 77, pp. 322-346.

T. Tanaka, S. Yoshizawa, T. Morishita, K. Osaka and Y. Osawa. "Observation and Analysis of Underground Earthquake Motions." In Proceedings of the 5th World Conference on Earthquake Engineering, Rome, Italy, Vol. 1, 1973, pp. 658-667.

G.R. Toro. "Stochastic Model Estimates of Strong Ground Motion." In Seismic Hazard Methodology for Nuclear Facilities in the Eastern United States, Appendix B, McGuire, R.K., ed., Electric Power Research Institute, Project P101-29, April 1985.

G.R. Toro and R.K. McGuire. "An Investigation into Earthquake Ground Motion Characteristics in Eastern North America." Bulletin of the Seismological Society of America, Vol. 77, No. 2, April 1987, pp. 468-489.

B.E. Tucker, J.L. King, D. Hatzfield and I.L. Nersesov. "Observations of Hard-rock Site effects." Bulletin of the Seismological Society of America, Vol. 74, 1984, pp. 121-136.

B.E. Tucker and J.L. King. "Dependence of Sediment-filled Valley Response on the Input Amplitude and the Valley Properties." Bulletin of the Seismological Society of America, No. 74, 1984, pp. 153-165.

J.E. Vidale. 1987. "Application of Two-dimensional Finite-difference Wave Simulation to Earthquakes, Earth Structure and Seismic Hazard." Ph.D. thesis, California Institute of Technology, Pasadena, CA, 150 pages.

J.E. Vidale and D. V. Helmberger. "Elastic Finite Difference of the 1971 San Fernando, California Earthquake," Bulletin of the Seismological Society of America, No. 78, 1988, pp. 122-141.

J.H. Wiggins. "Effects of Site Conditions on Earthquake Intensity." J. of the Structural Division, Proc., ASCE, Vol. 90, st. 2, Part I, 1964.

H.O. Wood. <u>Distribution of Apparent Intensity in San Francisco, in the California Earthquake of April 18, 1906.</u> Report of the State Earthquake Investigation Commission, Washington, D.C.: Carnegie Institute, Vol. 1, pp. 220-245.

State-of-the-Art Speaker — Dr. Brian Tucker

Workshop Panel

Chapter 7   SEISMIC ARRAYS

Chapter 7
SEISMIC ARRAYS

Seismic arrays are being used in a number of countries to collect information about ground response during seismic events. These arrays typically involve accelerometers or seismometers that are located either on or below the ground surface in a seismically active area. Acceleration data collected from these arrays during seismic events have been used to provide valuable information about earthquake source mechanisms, earthquake energy propagation, and topography effects. More recently, data from arrays have provided information about the nonlinear behavior of soil during seismic loading. The current state of the art of seismic arrays relative to dynamic soil property and site characterization was reviewed and summarized by Dr. Brian E. Tucker, Principal Geologist with the California Division of Mines and Geology. Following Dr. Tucker's presentation, a panel consisting of Brian Tucker (panel leader), C.B. Crouse (panel recorder), Norm Abrahamson, G. Bongiovanni. C.Y. Chang, Herman Graves, Tom Holzer, Tsuneo Katayama, Mario Ordaz, and C.K. Shen met, reviewed the state of the art, and then prepared a panel report. The panel report includes a summary of research needs relative to the installation and interpretation of data from arrays.

SOA REPORT

This state of the art report presents, as objectively as possible, the thoughts of researchers who were contacted through the mail regarding the state of the art for networks and arrays. In the present context, networks refer to instruments that are typically installed in structures and cover a large area, whereas the arrays involve multiple instruments installed on or below the ground surface in a local area. Following the state of the art discussions, a summary of the author's views regarding importance, uncertainties/limitations, and research needs is given. Generalizations were made when expressing these views. Whereas others may not share these same views, they will meet the wish of the workshop organizers by "stimulating a spirited discussion during the workshop session."

STATE OF THE ART

In order to answer the questions posed by the workshop organizers, as many operators of strong-motion arrays as possible were contacted in the time available to ask for their opinion of the state of the art. In doing so, the familiar issue of the distinction between arrays and networks had to be faced. Although this workshop is concerned with arrays and, in particular, their use in understanding dynamic soil characteristics, the experience of operators of networks is clearly valuable in answering many of the questions asked about the state of the art. For this reason, questionnaires were sent to operators of arrays and networks alike. The list of network operators that were contacted appears in Appendix C, and the list of array operators appears in Appendix D. Individuals who

responded to the questionnaire are indicated in both lists in bold; their responses to the questionnaire are reproduced in the appendices.

Network

Because the responses from the network operators were so numerous and of less direct bearing on this workshop than the responses of array operators, a summary of the response was prepared. This summary of necessity generalizes the individual responses. For details, the reader is referred to the questionnaires themselves in Appendix C.

What instrumentation is used? Predominantly analog instruments have been installed, but several operators are now beginning to switch to digital. Typically, the accelerometers are installed in small structures and in the basements of buildings, not in specially designed, light-weight structures.

What data have been obtained? One develops the impression from the questionnaire responses that most operators feel they have just begun receiving a return for their investments of time and money. One is struck by the contrast between the large effort expended in designing, installing, and maintaining these networks and the rather small data set that has been obtained thus far. (The network in Guerrero, Mexico, comes to mind as one exception to this statement.).

How were the sites characterized? Typically, network sites were characterized only by visual inspection and the use of a geologic map. Often only simple descriptive terms, such as "hard rock" and "soft soil," are used. In some cases, seismic techniques are used but only rarely down-hole methods. In spite of the rather rudimentary nature of these methods, most network operators seem to feel that they have been adequate, given current budgets.

What simple lessons have been learned regarding the operation of the network? There is a need for a high level of commitment by the operating agency to provide well-trained, well-equipped technicians, to perform instrument calibrations, field maintenance, data processing, and data dissemination. There was a consensus that regular maintenance was as essential to have as difficult to provide. Good, frequent calibration of instrument clocks was important but difficult to obtain. Analog instruments seem adequate for most purposes, but most people feel that soon digital instruments will be the instrument of choice, requiring less maintenance and providing better records. Surface accelerometers are much more reliable than down-hole accelerometers; even the humidity in underground vaults often damages circuitry.

The consensus also indicates that networks need a clearly defined scientific objective. Data acquisition over phone lines is used in several networks and has been found to be reliable and extremely useful. There is a need for well-planned data reports. The concept of a parked, mobile array has its advocates. Although documenting site characteristics is recognized as important, it is expensive and typically the product is not

publishable; thus, archiving and organizing site characteristics is a challenge for isolated researchers and probably needs a long-term commitment by management.

What simple lessons have been learned regarding ground response to earthquakes? One telling response was that there are no simple lessons yet; each new observation has been a surprise. Several operators cited as the most important lesson that soil sites can experience ground motion in some frequency bands, one order of magnitude greater than nearby rock sites experience. Near surface (0-200m) layers, even at so-called "rock" sites, significantly magnify incoming wave fields.

Ground response varies significantly across even a relatively small, flat, and seemingly simple site. One operator reported that response varies with magnitude and epicentral distance of the earthquake. Incoherence increases with frequency and station separation. Topographical effects are sometimes ignored when they should not be. One operator mentioned a new problem connected with site characterization, namely that it is difficult to get consistent field measurements from different survey teams who have made measurements in the same borehole. (Note that this problem is different from--in some ways, more fundamental and troubling--than the two problems identified by the Electric Power Research Institute (EPRI), namely (1) how to combine accurately the results of field and laboratory tests into a reliable prediction of *in situ* characteristics and (2) how to account for the spatial variation of these dynamic properties within the site characterization process.)

Array

Copies of the completed questionnaires from the array operators appear in Appendix D, along with the names and addresses of the respondents. Because these responses are not easily summarized and are so important in assessing the state of the art, they have been reproduced to allow the reader to study them.

In general, the instrumentation is digital, a common time-base is used, and the site conditions have been characterized using several different geophysical, seismological, and laboratory methods. Several general lessons have been learned. Large differences between amplitudes on nearby rock and soil sites have been observed. Variations of motion across a site are larger than was expected and are similar within rock and soil sites. Again, one is left with the impression that the profession has only begun to reap the return for the substantial investments made.

WHEN ARE ARRAYS IMPORTANT?

Arrays, as opposed to networks, are important when the effects of geologic site conditions are of more interest than those of propagation-path, radiation pattern, magnitude, and fault rupture. The time has passed when significant contributions to the understanding of dynamic soil properties can be made with observations from isolated strong-motion stations. Arrays comprised of well-maintained instruments with

matched, known responses, located on sites with well-documented soil properties are necessary for progress in predicting dynamic soil behavior.

WHAT ARE THE UNCERTAINTIES AND LIMITATIONS?

The most fundamental limitation of strong-motion arrays becomes apparent when one compares the proceedings of conferences on soil properties in recent years with the proceedings of conferences on, say, plate tectonics of the 1960s. In the latter case, researchers were continually forced to change their theories and biases in the face of wave after wave of new, compelling data. (Undoubtedly, the process looks simpler 20 years later than it did in its midst.) It appears now that the experiments that were conducted to prove or disprove various plate-tectonic ideas were "tight" enough and well-focused enough to compel changes in the prevailing theories.

This is in contrast, it seems, to the situation today in research on dynamic soil properties. There does not appear to be significant convergence in the development of new models. The experimental observations that are being made do not appear to be forcing theories to evolve, die, or be born. The questions being asked and answered by soil dynamic experiments do not seem to be the right ones to change and improve theories.

Certainly part of the problem is because of the inherent difficulty of collecting unambiguous strong-motion data. As documented above, this takes considerable time and money and a continuity of interest of dedicated, trained technical and scientific staffs. Even more time, money, and dedication are required to collect, before the occurrence of a large earthquake, the data on soil characteristics that are required to narrow the interpretation of the strong-motion observations. When records are obtained, at last, there is a tendency to place more weight on the results of "your" experiment than those less familiar and understood. When records are finally in hand, one wants to publish them without, perhaps, taking additional time to document the soil characteristics. These tendencies are understandable, but they have limited the progress made in distinguishing among existing models of dynamic response.

Another part of the problem--addressed in other sections of this workshop--is because of the inherent difficulty of collecting good soil property data. As mentioned above, it is not clear how to combine field and laboratory data nor how to account for spatial variations. A more fundamental difficulty is that it is not even clear how to combine field data from the same site. In the Turkey Flat experiment, supposedly redundant measurements of geotechnical properties were made in the same borehole. In some cases, different methods were used to measure the same property; in other cases, similar methods but different operators or slightly different procedures were employed. In several cases, the differences in the inferred properties (e.g., velocity, density, and damping) were larger than the previously believed experimental errors would have allowed; professional judgment was used to select the preferred properties.

In summary, the primary limitation of arrays is that they are not collecting data good enough and fast enough to influence significantly the development of theory. Increasingly sophisticated theories are appearing, but the observations of soil dynamics are not providing definitive tests and comparisons of these theories.

WHAT ARE THE PRIORITIES FOR IMPROVEMENT AND RESEARCH?

1. Design experiments using arrays to answer specific questions. Ensure that the instrumentation and soil data are adequate to answer those questions before earthquakes are recorded.

2. Compare and test existing models. Compare them with each other and test them against unambiguous strong-motion observations. Do so in a manner that is conclusive, clearly indicating why some models succeed and others fail.

3. (Somewhat beyond the topic of arrays, per se.) Measure the uncertainty of the models. It may well be that we do not know how inadequate our models are. Are researchers able to make realistic estimates of their errors? Other fields have experienced a consistent and substantial underestimation of errors. It is clearly important that we start gaining an appreciation for the source of our errors. One way to do this is to have all predictions of ground motion response include confidence intervals. If the predictions of different theories vary but the error bars associated with the predictions overlap each other and with the observation of ground response, then our "art" is healthy. If, however, the error bars neither overlap each other nor include the observation, then we have only begun to understand dynamic soil characteristics. This may be the case. In any case, until we make several tests and comparisons of existing theories at several well-instrumented sites where topography and soil properties are well documented, we will not know the state of our art.

PANEL REPORT

IMPORTANCE OF ARRAYS

Arrays can play a very important role in site characterization and in determining dynamic soil properties for earthquake resistant design and analysis. However, for arrays to play an important role in site characterization, they must be carefully designed with clearly stated purposes.

Carefully designed arrays are those with adequate instrumentation and spatial coverage that can provide detailed physical and geometrical characterization of a site. Data from these arrays can provide the ultimate tests of laboratory and theoretical models of soil behavior during seismic loading. Specifically, they can provide measures or estimates of:

- Linear and nonlinear soil behavior
- Soil strains
- Ground motion input to models of soil structure interaction (SSI)
- Full 3-D wavefield
- Angles of incidence of the waves comprising the wavefield
- Coherence of wavefield propagation
- Stochastic characteristics of ground motion
- Earthquake source characteristics

This list includes topics of interest to engineers, seismologists, geophysicists. Moreover, array data can improve the fundamental understanding of the governing physical processes. As a result, the development of new or improved 3-D mathematical models of the soil, wave propagation, and soil-structure interaction can be foreseen.

CURRENT STATE OF PRACTICE

A number of strong-motion arrays are presently operating in several countries including the United States, Japan, Taiwan, Mexico, and PRC. They differ in size (i.e., number of instruments), density, and geometric configuration. In addition, present arrays were motivated by different purposes. Some are oriented toward seismological research and others to more practical engineering issues.

Since ground-motion observations from arrays is a relatively new research field, the problems and issues to be addressed by an array were not always clearly stated, and the physical structure of the array was often determined by intuition rather than in-depth analysis.

At present, there are no existing means to establish a database or publish catalogs that document existing strong-motion arrays or strong-motion data obtained from arrays. In addition to the lack of documentation on arrays, there is no existing method to share or disseminate strong-motion data, such as could be accomplished by a central repository or world data bank.

Generally, the instruments currently used in arrays are appropriate. Surface instrumentation performs well and can be easily maintained. Borehole seismometers can now be made to remain operational for 10 years or more. On the other hand, pore pressure devices undergo much faster deterioration because of their contact with water. The general belief is that available technology probably exceeds our capacity to analyze the measurements commonly made. However, the possibility of developing instruments to measure new parameters, more directly related with the physics of the phenomena, should be explored. Furthermore, consideration should be given to the design and operation of "active" arrays capable of measuring soil properties during strong shaking in order to obtain high-strain properties.

The solar power technology is becoming more conventional in existing networks and arrays. This is because of the recent progress concerning solar cells and related devices. This technology is now considered the best alternative to power digital accelerographs.

While the existing arrays consist of both digital and analog instruments, the general tendency is to shift towards digital devices, which are easier to operate in terms of data retrieval and processing. Digital instruments also permit remote access to the data via phone lines. This technique has proved to be an extremely efficient way to retrieve data. For this reason, it is now frequently used.

Many accelerometers currently being developed for strong-motion instruments employ the strong electronic feedback (e.g., force-balanced or closed loop) sensor design. The cross-axis sensitivity is difficult to measure or control in the motion detection sensors. Self noise has been reduced significantly and most new closed-loop, hard feedback sensors are approaching an operational dynamic range of 140 db to 150 db.

Most of these closed-loop accelerometers are limited to frequencies under 150 Hz; some are limited to frequencies less than 50 Hz. At the very low frequency band (f <0.1 Hz), "1/f-noise" in the electronic circuitry limits the lower ranges of useful information. This "1/f-noise" introduces errors into the system, especially when the acceleration time-histories are integrated (twice) to obtain displacement time-histories. These errors that are introduced by this "1/f-noise" rarely impact dynamic response (or dynamic response spectral estimates); but the contribution of this "1/f-noise" will invalidate long-term displacement estimates of settlement of soil that may occur over days, weeks, or years.

Modern design and manufacturing techniques produce high quality feedback acceleration sensors that are presently adequate for applications in array studies. However, proper installation and coupling of accelerometers to the soil media (both surface inspection and borehole installation) is still open to considerable debate and disagreement.

With respect to the processing of digital data, some of the newer, high-resolution digitizers are now claiming a capability of converting analog electrical signals into digital samples to an accuracy of 24 bits and at rates of 80 or 100 samples per second per data channel. The dynamic range of these 24-bit ADCs are compatible or consistent with the newer electronic feedback accelerometers.

TOPICS ADDRESSED BY ARRAY DATA

Arrays have contributed to varying degrees toward a resolution of several topics of interest in geotechnical engineering, engineering seismology, or earthquake engineering. Several of these topics are listed below followed in parentheses by the type of array data that has offered the insights (i.e., downhole (D); 1-dimensional (1-D); 2-dimensional (2-D); 3-dimensional (3-D) arrays).

- Differential motion at base of structures (2-D)

- Relation between pore pressure buildup and ground motion (D)

- Gross understanding of size of geological and topographic site effects (2-D)

- Adequacy of 1-D models (D)

- Coherency of wave motion versus frequency and distance (1-D and 2-D)

- Liquefaction (D and 3-D)

- Nonlinear behavior at special sites (D, 1-D, and 2-D)

- Angles of incidence of the waves (2-D and 3-D)

Because of their expense, true 3-D arrays do not exist. Arrays that attempt to cover three dimensions are undersampled with respect to the third dimension (depth); i.e., downhole instrumentation is not installed at every station comprising the 2-D surface array.

LIMITATIONS/UNCERTAINTIES WITHIN STATE OF THE ART/STATE OF PRACTICE

Certain limitations and uncertainties currently exist within the state of the art and state of practice as they pertain to the information that can be obtained from array data. These limitations are summarized below.

1. As the size of the array (number and type of instruments) increases, the data recording, processing, storage, and retrieval requirements increase, which at some point will exhaust the capabilities of the system used to perform these tasks.

2. Current strong-motion data processing algorithms were developed for analog systems. They have not been modified for digital system development that is used in the design of new arrays.

3. Relatively little funding is available for data analysis. Consequently, available data may not be thoroughly or systematically analyzed. Furthermore, high costs are associated with array design, installation, maintenance, and site characterization. Long-term continuing funding is essential for maintenance of arrays, data collection, and analysis. This commitment is needed partly because it is uncertain when an earthquake of sufficient magnitude will occur to trigger the instruments.

4. Orientation of downhole instruments is commonly a problem, but techniques are available to estimate their in situ orientation. Also special encasement and installation procedures are generally needed to ensure proper coupling of instruments with soil media. Once in or on the ground, the instrument is limited to measure a few parameters directly. For example, the strong-motion instrument measures the three translational components of motion instead of all six components. Long-term reliability of instrument performance has been a problem in certain instances.

5. Using ground-motion data from downhole arrays to estimate dynamic soil properties is an indirect way of determining these properties. Assumptions and idealization are needed in data analyses that introduce uncertainties.

6. Spatial variability of subsurface conditions results in spatial variability of, for example, pore pressures and ground motions, which are measured at several locations within an array. Analysis and interpretation of the data for site characterization need to account for spatial variability.

NEEDS AND PRIORITIES FOR RESEARCH

The panel agreed that the establishment of strong-motion arrays should be an integral part of earthquake research. The needs and priorities for research involving arrays are listed below.

Considerable funding and effort have gone into establishing and operating arrays; however, in many cases, the data are not readily available. Data should be compiled and documented in a systematic, orderly, and continuous manner. A mechanism or organization responsible for the data dissemination should be developed. A prototype model for such an operation is contained in the 1989 report "Research Report on Development of a Database for Strong-Motion Array Records" published by the Japan Society of Civil Engineers. The overall database management effort should be coordinated with the operations underway in Japan (and other countries) and the United States designated test sites for geotechnical research (NSF, 1988).

Additional strong-motion arrays should be established. Joint industry or university/industry experiments should be supported to leverage manpower and funding.

Proposals for future arrays should include: (1) clear statements of the purpose of the array, (2) commitments for long-term maintenance and operation, (3) plans to characterize the site soil properties, and (4) plans for conducting post-earthquake investigation, data processing, and analysis.

Different soils should be instrumented to provide a database covering a range of site conditions. The highest priority should be given to sites with soft deposits, such as those in the San Francisco Bay area, which suffered heavy damage during the October 17, 1989, Loma Prieta earthquake.

To address the problem of dynamic soil response and site characterization, the minimum array configuration should consist of a layered 2-D array (horizontal array on the surface and at depth) combined with several vertical arrays with multiple receivers.

Because large earthquakes are rare events, surface arrays that can be quickly redeployed to record aftershocks are attractive. In conjunction with these parking arrays, a set of downhole instruments including pore-water pressure transducers should be kept in reserve to be deployed rapidly after an earthquake to record site effects during the aftershock sequence.

The following research areas are suggested to further our understanding:

1. Correlation of spatial variation of ground motion with spatial variation of the physical properties of the soil. This would lead to a physical model of spatial coherency that can be applied to new sites.

2. Develop (consider) instrumentation that can provide more direct measurements of soil properties, for example, strain meters, velocity meters (geophones), and 6-component accelerometers. Develop improved digital processing techniques including methods to compute permanent ground displacement from accelerograms.

3. Develop and improve techniques to calculate/estimate soil properties from array data.

4. Use blind predictions to test existing analytical and empirical methods for determining soil response under seismic loading, including acceleration time histories, pore pressures, strain, and settlement.

5. Use blind prediction of SSI methods to validate and improve current analytical methods for high-rise buildings, bridges, lifelines, and embankments. This would include prototypes of a soil structure or embankment.

Because of the nature of array operation and the relatively long time intervals between large earthquakes, the funding of arrays needs to be a long-term commitment. Because

of the diverse, multidisciplinary interests in array data, more consideration should be given to multidisciplinary teams to conduct research involving these data.

ACKNOWLEDGMENTS

REFERENCES

NSF. "Designated Sites for Geotechnical Experimentation in the United States." Proceedings of the Workshop at the University of New Hampshire, J. Benoit and T. do Alba, eds., September 1988, 165 pages.

State-of-the-Art Speaker — Dr. Gonzalo Castro

Workshop Panel

Chapter 8   SLOPING GROUND SITE

Chapter 8
SLOPING GROUND SITES

The final topic related to dynamic soil property and site characterization involves sloping ground sites. In contrast to previous discussions that are focused more towards wave propagation issues, the discussion of sloping ground sites considers the loss of stability at a site due to seismic loading. This loss in stability can result in downslope ground movement that varies from a few inches to many tens or hundreds of feet. Various studies have shown that the potential for such downslope movement is controlled more by the manner in which soil strength varies with shearing strain than the stiffness and energy dissipative properties of the soil (although stiffness and damping still have strong influence in that they will determine the level of shearing strain). Instability at a site can be disastrous; therefore, a discussion of this topic was considered critical. Dr. Gonzalo Castro, a principal with GEI Consultants, Inc., led the discussion with a state-of-the-art (SOA) presentation. Following the presentation, a panel comprised of Gonzalo Castro (panel leader), Les Youd (panel recorder), K. Arulanandan, Pedro de Alba, Jean-Lou Chameau, Liam Finn, Geoff Martin, Peter Robertson, and Ron Scott developed a series of recommendations and priorities for research.

SOA PRESENTATION

The SOA comments presented herein are not intended to be a summary of the state of the art but, rather, a listing of the most significant uncertainties and research priorities. These comments are based on the panel leader's views presented in the accompanying SOA paper (Appendix E) and are presented assuming that the reader is familiar with the paper.

GENERAL PROBLEM

The subject of sloping ground sites includes consideration for earth embankments and their foundations. The most significant feature at sloping ground sites is the presence of driving (static) shear stresses (τ_d) in the soil mass, i.e., the shear stresses that are required for equilibrium. There are two types of problems that can arise when sloping ground is shaken by an earthquake; namely:

- Loss of static stability, when there is an earthquake-induced reduction in the strength of the soil below the value of τ_d

- Earthquake-induced limited deformations without a loss in stability

Both problems are important and need to be addressed in an engineering evaluation of a slope or embankment. The following comments relate to undrained behavior of saturated soils.

LOSS OF STABILITY

The loss of stability requires two conditions: (a) that the driving shear stresses exceed the undrained steady-state strength of the soil (S_{us}) in a sufficiently large zone of the soil mass and (b) that the earthquake shaking be sufficiently severe so that the induced strains are large enough to exceed the strain at peak strength and thus the failure is triggered (see Figure 9b of Appendix E).

Determination of S_{us}. Methods currently used to determine steady-state strength in the laboratory are as follows:

Test/Soil	Sands	Silts	Clays
Triaxial	•	•[1]	
Vane		•[2]	•
Rotational Shear		•[3]	•[3]

Notes:

[1]Triaxial tests may not provide sufficient strain capability to reach steady state. Thus, one needs to perform tests with different stress paths (drained, undrained, compression, extension, cyclic, monotonic, etc.) and different initial structures. If all tests end on the same steady-state line, then it is reasonable to assume that steady state was actually reached.

[2]The vane test may need to be performed much faster than conventional vane tests to ensure undrained behavior.

[3]These tests are drained. Determination of void ratio at end of test is difficult because specimen is built thin (a couple of mm) to promote shear throughout the full thickness and thus obtain a reasonably uniform void ratio.

The test procedures listed above relate to homogeneous specimens. In reality, soils are not homogeneous, but stratified. For very large deformations, there is apparently some mixing of layers, as indicated by observations of the failure zone in the Lower San Fernando Dam. However, the deformations required for mixing are much larger than can be achieved at present in the laboratory in undrained tests.

Test data for stratified specimens indicate a steady-state line (SSL) higher than the line for mixed homogeneous specimens. These data are consistent with the fact that more widely graded sands have a lower SSL than soils with more uniform gradations. However, more systematic research is required. The research should involve tests on stratified specimens, both for layers of different sand gradations and for the same soil but with different densities. Water redistribution can occur for these cases.

Research is also required to investigate the effect of rate of strain and of intermediate principal stress on S_{us}.

Actual failures should be analyzed to estimate the strengths of the soils during the failure. The analysis should consider inertial effects. Such evaluations involve many uncertainties but provide invaluable data for understanding the mechanism of stability failures.

Triggering of Instability. In sands, very small strains (about 1 percent) are sufficient to overcome the peak and trigger the failure. In clays, the strains required to trigger are typically very large, and thus earthquake shaking will seldom trigger slope failures in clays (except, of course, sensitive clays that have a low strain at peak).

Research needs on triggering include the effect of creep, pore pressure increase, value of τ_d relative to S_{us}, effective stress ratio, and other factors on the earthquake-induced strain needed to trigger.

Limited Deformations

In this case, the soil mass is inherently stable with sufficiently high values of S_{us}; however, damaging deformations can occur. Evaluation of these deformations is a difficult task.

The Newmark type of analysis assumes that one can define a yield strength of the soil; i.e., one assumes the soil to have a rigid-plastic type of stress strain behavior. A reasonable value of yield strength is S_{us} for contractive granular soils, while for plastic clays with large strains at peak, the peak undrained strength can be used as a yield strength. However, for dilative sands or silts, S_{us} is not a good value for yield strength since significant deformations can occur, even if the static plus earthquake shear stresses do not exceed S_{us}.

For dilative soils, one can obtain a reasonable value of yield strength from the results of cyclic tests on anistotropically consolidated specimens. The yield strength is defined as the shear stress above which there is a significant accumulation of strain. (Note that the relevant result is the accumulation of strain rather than the cyclic strain or the pore pressure increase.)

Computation models have been developed by several authors to estimate seismically induced deformations. The soil model will necessarily be a simplified representation of actual behavior, and, thus, it is important to identify the key aspects of soil behavior that one must represent; i.e., (a) the soil has a finite strength, even if **momentarily** the effective stresses become zero, (b) inertia effects are considered for cyclic as well as accumulated movements, (c) the result of interest is accumulated, not cyclic, strain, and (d) the soil has nonlinear behavior or at least strain-dependent moduli.

MODEL TESTS

Model tests, particularly in the centrifuge, can be powerful tools to fill the research needs discussed above. One of the main difficulties encountered to date is the control of the void ratio of granular materials, particularly in relatively large models. For example, it has been difficult to reproduce flow slides in sands because of the difficulty in preparing models with sufficiently loose sands.

PANEL REPORT

The members of Panel 6 prepared the following summary of their views regarding the state of the art as well as needs and priorities for research. Sloping ground sites are addressed from the standpoint of seismically induced instability and deformations. The question of the influence of sloping ground on ground response (amplification or attenuation) is discussed in Chapter 6.

INTRODUCTION

With respect to the earthquake behavior of sloping rock sites, two aspects of soil behavior are important:

a.   Earthquake-induced strength loss leading to static instability

  •   Loss in strength of loose, saturated granular soil
  •   Loss in strength of sensitive clays
  •   Brittle failures of other soils and rock on steep slopes

b.   Earthquake-induced deformation of soil masses without development of instability

  •   Accumulation of deformation of granular soils by shaking
  •   Accumulated deformation of cohesive slopes
  •   Accumulated deformation of jointed rock slopes

The following discussion comments on problems related to geometric site characterization and the determination of soil properties for site characterization of saturated sandy soils, cohesive soils, and rock in relation to sloping ground. Comments are also made on the value of physical modeling prior to summarizing the needs and priorities for research.

GEOMETRIC SITE CHARACTERIZATION

Tools and techniques are available to define adequately subsurface stratigraphy at most soil sites, including the thickness, depth, slope, and areal extent of soil layers. An

exception is gravel sites where standard techniques such as conventional boring and penetration procedures may not work and where even specialized techniques such as Becker penetration soundings and geophysical techniques may not give adequate definition of sediment stratigraphy.

Limitations of current practice are a lack of application of available techniques and sparse application of the techniques that are used. For example, use of geophysical procedures such as ground-penetrating radar and tomography is seldom applied to sloping ground sites, and because of budgetary and other constraints, standard boring and penetration procedures generally have not been applied with sufficient coverage to adequately define three-dimensional sections of pertinent sites.

Applied research is needed to further develop and apply geophysical techniques to geotechnical sites, including sloping ground sites, for delineation of subsurface stratigraphy for engineering purposes.

Site investigations at some important sites of past ground displacement need to be reevaluated and perhaps augmented to further quantify the amount and quality of subsurface stratigraphic data required to adequately characterize a site for assessment of ground deformation during ground shaking.

SOIL PROPERTY CHARACTERIZATION

The soil properties needed to characterize a sloping ground site will be described below for determination of stability and for estimating deformations. The discussion focuses on saturated sands and nonplastic silts because these are the soil types that most often (but not exclusively) are involved in seismically induced instability or large deformations. However, some comments relative to clays and rock are made later in this section.

Saturated Sands and Nonplastic Silts

Several issues related to the behavior of saturated sands and nonplastic silts were identified. Those included the determination of steady-state strength, effects of pore pressure redistribution, the triggering of stability failure, and estimating limited deformations. Research topics in these areas are summarized below.

Steady-State Strength. For conditions of potential instability, the steady-state strength, S_{us} (called the "residual" strength by some authors), is of primary importance for any study concerning the behavior of sloping ground under earthquake loading. Castro's state-of-the-art paper (Appendix E) presents a summary of the state of knowledge regarding the steady-state concept. Although the framework of steady state is quite well understood, there is a need for further research.

8-5

There is still some uncertainty related to the definition of steady state and how it should be determined. There is a need for continued research to clarify the soil variables and the testing method. At present, S_{us} for a given soil is assumed to be only a function of void ratio. However, questions have been raised as to whether S_{us} is a function of other variables such as stress path, initial soil fabric, rate of strain, and intermediate principal stress. Since the determination of S_{us} is of primary importance to any evaluation of stability, further research is required to clarify whether these variables affect S_{us}. There is also a clear need to define a standard testing procedure to determine S_{us}.

Current practice in laboratory steady-state research and engineering applications is to prepare laboratory samples with a high degree of homogeneity. However, in nature, deposits are often highly nonhomogeneous, and further research is required to study the influence of nonhomogeneous sample site conditions on the determination of S_{us}.

Within the framework of the steady-state concept, the precise and reliable definition of void ratio is a critical issue. Inadequate knowledge of void ratio has negative implications with regard to both interpretation of laboratory experiments and application of the steady-state concept to field problems. This question raises the issue of the physical scale of the determination. At which scale are spatial variations in void ratio and other nonhomogeneities significant? Image analysis studies show large variations of void ratio within laboratory specimens that would be classified as uniform from a macroscopic standpoint. Such variations can also be illustrated from simulation studies. Their physical and statistical significance is not known, and the scale at which they should be determined is also unknown. Obviously, variations in void ratio relate to variations in fabric (e.g., clusters of grains, number of contacts, orientation of contact forces).

The above remarks made for laboratory specimens raise other important interrelated questions for both laboratory and field investigations:

a. Do *in situ* materials exhibit spatial variations in void ratio and fabric that are similar to or different from laboratory specimens?

b. Are efforts made in specimen preparation techniques to maximize the level of uniformity warranted when compared to *in situ* materials?

c. Are "microscopic" effects more important for cohesionless materials with significant amounts of fines?

d. How much refinement should be given to assessing these variations (both *in situ* and in the laboratory); i.e., at which "microscopic" scale do the variations become insignificant with respect to overall behavior?

e.   Is void ratio a sufficient descriptor for defining steady-state conditions, or should some descriptors of fabric (possibly on a statistical basis) be considered?

At a more fundamental level, these questions relate to a better understanding of the process of shearing from a micromechanistic standpoint.

In the absence of standardized and economical laboratory testing procedures for determining steady-state strength, correlations with field test values have been proposed as an alternative technique for estimating this important parameter. Research by Seed and others has developed preliminary relationships between residual strength or steady-state strength and corrected standard penetration resistance $(N_1)_{60}$. Research should continue to develop these correlations further. Such results will augment laboratory research by providing economical methods to define stratigraphy and material properties of soil layers and to extrapolate results from tests on a few laboratory specimens to soil layers in the field.

Avenues of research that will address these questions include:

a.   Better physical and statistical characterization of void ratio and fabric of laboratory specimens before, during, and after shearing. Image analysis techniques could play a role.

b.   Continued development of techniques to evaluate the void ratio, and, in general, the state of a soil *in situ*. Electrical resistivity techniques are one example; however, other approaches could be developed.

c.   Evaluation of the fabric and subsequent laboratory testing of undisturbed soil specimens. This raises the need to develop improved procedures to obtain undisturbed samples reliably and efficiently. Freezing is one possibility; however, more cost-efficient and simpler technologies can be considered, such as impregnation with different chemical products.

d.   Theoretical and numerical modeling of the micromechanisms of shearing, i.e., providing a better understanding at the particulate level of the processes that lead to phenomena of engineering interest, such as steady-state deformation. This could also support research in the area of progressive failure phenomena.

Current practice to evaluate *in situ* values of S_{us} is either to obtain samples and perform laboratory tests (as described above), which require some correction to the *in situ* void ratio, or to empirically correlate S_{us} with a field measurement such as penetration resistance. Major areas of uncertainty relate to the difficulty in obtaining undisturbed samples and monitoring their changes in void ratio and in the uniqueness of the existing empirical correlations between penetration resistance and S_{us} for all soil types. Hence,

a major priority should be to develop improved methods for the determination of S_{us}. This is closely related to the *in situ* determination of *in situ* state.

Pore Pressure Redistribution/Dissipation. For most practical situations, particularly for those involving fine sands and silts, it is often assumed that there is relatively little pore pressure redistribution or dissipation during earthquake loading and reconsolidation will be a post-earthquake process. However, it has been suggested that, for coarser sands or stratified cohesionless soils, significant redistribution or dissipation may occur both during and following earthquake loading. It has been observed in past earthquakes that, in some instances, large slope displacements have been initiated sometime after the earthquake ground shaking ceased. This suggests that pore pressure redistribution may be affecting the overall shearing resistance of the soil mass.

For the case of a layer of sand located beneath an impervious clay boundary, it has been suggested that pore pressure redistribution effects under conditions of constant volume may tend to increase void ratios in the upper half of the layer and decrease those in the lower half. It has been postulated that, in the extreme, a thin zone of water may accumulate at the upper sand-clay interface. Clearly, the above phenomena could greatly influence the available strengths that can be mobilized.

The key parameter controlling the redistribution of earthquake-induced excess pore pressures, both before and after the earthquake, is the coefficient of consolidation, C_v ($= k/m_v\gamma$, where k = coefficient of permeability and m_v = coefficient of volume decrease). During the initial stages of pore pressure buildup during an earthquake, it is reasonable to assume constant values of k and m_v to evaluate redistribution or dissipation effects. However, when effective stresses become very low, values of m_v will increase significantly and, hence, c_v values will decrease. Large cyclic shear strains, say in excess of 1 percent, which may accompany low effective stresses, may also influence m_v and k as a result of changes in soil structure.

Clearly, the pore pressure redistribution/dissipation process is very complex; nevertheless, it may play an important role in the assessment of the earthquake stability or deformations of saturated cohesionless soil slopes or strata. Research on the changes in m_v and k would provide an essential database on values of C_v to use in analytical studies addressing the role of redistribution/dissipation of pore pressures on stability analyses. Laboratory studies should address gravel, sands, and silts to cover the full range of k and m_v values.

Triggering of Stability Failure. If a soil mass is deemed to be potentially unstable, if the strength of the soils were to decrease to S_{us}, one needs to determine whether the expected earthquake shaking will be sufficient to trigger the failure. In sands, very small strains (about 1 percent) are sufficient to overcome the peak and trigger the failure. In clays, the strains required to trigger are typically very large; thus, earthquake shaking will seldom trigger slope failures in clays (except, of course, sensitive clays that have a low strain at peak). Triggering criteria based on mobilized effective

stress ratio have been proposed for sand. The triggering of the failure will be a progressive phenomenon. Initially, a limited zone of the soil mass may reach S_{us}, and then the failure will propagate until the soil mass reaches overall instability.

Research is required in two main areas: (1) stresses and strains that are required to cause a soil element to decrease in strength towards S_{us} and (2) consideration of the progressive nature of the failure in numerical analyses. In the first area, one needs to consider the potential effects of creep (rate of loading) and whether triggering correlates better with an accumulation of strain, an increase in pore pressure, or the development of particular value of effective stress ratio.

Limited Deformations. In this case, the soil mass is inherently stable with sufficiently high values of S_{us}. However, damaging deformations can occur. Evaluation of these deformations is a difficult task.

The Newmark type of analysis assumes that one can define a yield strength for the soil; i.e., one assumes the soil to have a plastic type of stress-strain behavior. A reasonable value of yield strength is S_{us} for contractive granular soils, while for plastic clays with large strains at peak, the peak undrained strength can be used as a yield strength. However, for dilative sands or silts, S_{us} is not a good value for yield strength since significant deformations can occur even if the static plus earthquake shear stresses do not exceed S_{us}.

For dilative soils, one can obtain a reasonable value of yield strength from the results of cyclic tests on anisotropically consolidated specimens. The yield strength is defined as the shear stress above which there is a significant accumulation of strain. (Note that the relevant result is the accumulation of strain rather than the cyclic strain or the pore pressure increase.)

Computational models have been developed by several authors to estimate seismically induced deformations. The soil model will necessarily be a simplified representation of actual behavior; thus, it is important that it properly represents the key aspects of soil behavior.

Two important factors that control the deformations of sloping ground to earthquake shaking are the evolution of the soil properties during shaking and the role of dilation in limiting deformations for both dry and saturated granular materials. The example of saturated sands may be useful in clarifying the issues involved. In these sands, continued shaking and seismically induced pore water pressures reduce the effective stresses that lead to softening of the moduli and a possible reduction in strength. These effects are usually attributed solely to changes in effective stresses. It is important to determine whether this is the case. One way of achieving this is by measuring the initial shear moduli of saturated samples after various degrees of shaking under undrained conditions. The entire stress-strain curves for such materials should also be developed.

In some cases, when the strains become large, dilation reduces the pore water pressures and leads to increased resistance to unidirectional deformation. Dilation is a complicated function of void ratio (or density), confining pressure, and strain. Most data on dilation currently available have been derived from monotonic compression tests. Data are needed to increase our understanding of dilation under cyclic loading conditions.

CLAY SOILS

Most of the considerations discussed in the previous section for slopes in sandy soils are also applicable to slopes in clay soils. In this section, only those considerations that are peculiar to the clay soils are discussed. (Note that this discussion deals with clay soils of moderate sensitivity, as opposed to highly sensitive quick clays.)

Undrained strength and stiffness reduction of soft sensitive clay soils under cyclic earthquake loading require much larger strains than for contractive sands; therefore, lesser deformation could generally be expected for similar earthquake and slope conditions. Historically, however, there have been large movements of slopes which some authors have attributed to clay soils; e.g., the Fourth Avenue slide triggered in downtown Anchorage, Alaska, by the 1964 Prince William Sound earthquake translated nearly 20 feet during shaking. Evaluation of that slide indicated that important factors to developing such movement were progressive softening of the soil (strength and stiffness) because of excess pore pressure accumulation under cyclic loading and achievement of a low, undrained steady-state strength within the failure zone of the clay.

Progressive softening of sensitive clays under cyclic earthquake loading is related to the effective stress changes associated with excess pore water pressure accumulation and/or remolding by cyclic straining. Little data are available on the relationship between effective stress, strength, and stiffness changes, including the rate of excess pore pressure accumulation and the extent to which pore pressure will accumulate. Thus, there is a need for laboratory cyclic load testing of sensitive clay soils of various characteristics (plasticity, sensitivity, etc.). It is anticipated that soil behavior patterns developed during these laboratory programs would provide a basis for defining sensitive clay soil characteristics and for using analytical effective stress constitutive models for deformation evaluation in clays.

The undrained steady-state strength of sensitive clay soils has been determined by large rotation vane shear tests and/or CPT sleeve friction values. Direct measurement of undrained steady-state strength for clay soils cannot be performed in the triaxial apparatus because the strains required greatly exceed those possible in the test.

ROCK SITES

Few analytical techniques are available to estimate the deformation of rock masses under dynamic conditions. The simplest is a soil-mechanics-like stability analysis based

on possible failure mechanisms intimately related to the patterns of the rock jointing and fracture systems, with occasional reference to the strength properties of the solid rock.

Such a failure analysis requires field investigation and description (stereometric plot) of the orientations of fractures and joints in the material and laboratory determination of the normal stress versus shearing strength properties of the joints, which may contain infilling material. The field investigation requires observation of joints at the surface and on open rock surfaces as well as study of oriented cores from boreholes performed vertically or at angles to the vertical. In many cases the relationship and continuity of joint and fracture systems are not easy to determine in the field. Depending on the scale of the problem, difficulties will also be encountered in the assessment of the shearing strength properties of the joints and fractures. The strength depends on the scale length of rock roughness so that small-scale laboratory tests do not give shear strength results applicable to joints in the field, which may be meters to possibly hundreds of meters in length. In some instances (Kurobe IV in Japan), very large blocks of rock have been isolated in tunnels, stressed by jacks, and sheared to give strength values at a scale roughly comparable to the joint dimensions in the rock mass.

The other type of analytical technique that has been employed is the discrete or distinct element method (DEM), in which the equilibrium of the block masses isolated by the joint end fracture systems is examined under the applied loads. The contacts between rock masses are simulated by springs, friction elements, and dashpots. Analysis is performed by finite difference techniques. Such an evaluation gives both deformation and failure mechanisms and numerical values, but, to our knowledge, no validation has been performed by comparison of analyses with field case studies. The same input information in shear strength of joints and joint and fracture geometry is required as for the simple analysis. More complicated constitutive relationships for jointed and fractured rock masses at all scales appear to be unapproachable at this time.

CASE HISTORIES AND INSTRUMENTED SITES

The mechanisms controlling the development of either flow slides or limited deformation under earthquake load remain poorly understood. Further, there are significant differences of opinion on how representative are soil strength values determined in the laboratory or from empirical correlations, and how they should be applied to a potential sliding mass in the field, especially in view of the heterogeneity of natural deposits and hydraulic fills. Finally, we have very little information on the distribution of strains in the sliding mass.

Case Histories

Field studies of slopes that did (or did not) slide during earthquakes and for which the pre- and post-slide geometry can be defined are invaluable for better understanding the mechanisms of failure and for back-calculating values of steady-state strength and

verifying numerical techniques. Although at this time we have available a number of case histories of slope deformation, it is fair to say that the large majority are of limited value because of poor site characterization and/or insufficient knowledge of the characteristics of the earthquake motions at the site.

There is consequently a need to develop carefully documented case histories for which an extensive site characterization program is carried out using simple penetrometer tests (SPT, CPT) supplemented by tomographic methods to establish the spatial variability of the problem materials. While there is disagreement over whether penetrometer tests can be directly related to steady-state strength, they will provide information on the geometry and homogeneity of the problem deposits. On the basis of these studies, decisions can be made on more elaborate testing at selected locations, i.e., attempts to characterize the soil site (void ratio, fabric, and in situ stresses). We should emphasize that currently available techniques for obtaining the in situ soil state are highly important and further research on this topic is imperative.

Instrumented Sites

Since opportunistic studies such as those described above will often have to be done on the basis of limited data on site response to the earthquake, there is also a great need for more instrumented sites that are potentially susceptible to large deformations.

In areas that are otherwise heavily instrumented for strong motion measurements, additional instrumentation should be installed to determine the deformation of the mass, with a deep benchmark outside the potential sliding area, surface monuments, and inclinometer casings in the problem soil. Important information on deformation could thus be obtained at a relatively low cost.

Some sites will be deemed important enough to be fully instrumented; in these cases, deformation measurements should be supplemented with downhole accelerometer and piezometer arrays, both in the potentially liquefiable soil and in stable materials. The use of velocity transducers, from which time histories of displacement may be inferred, is strongly encouraged.

Thorough site characterization by means mentioned above is obviously essential at instrumented sites.

PHYSICAL MODELING

Historically, many soil research investigations have been performed using small model tests in the laboratory. Considerations in the design of retaining walls, footings, and piles and the stability of the slopes have been obtained from model tests at linear scales in the range of 1/5 to 1/100 of the dimensions of prototypes. Usually, but not always, the physical property limitations of such tests have been recognized, and they have been performed to evaluate mechanisms of deformation and failure in a

qualitative way. It was recognized that the response of soil in a prototype situation, at stresses 5 to 100 times those in the model, was different, at least numerically, from that of the model material, even if it were the same soil. It was not so clearly understood that the qualitative behavior would also be different.

One-G Models

Scaling relations for soil began to be examined seriously in the 1930s in connection with early centrifuge experiments and were placed on a firm basis by the work of Rocha and Roscoe in the 1960s. The consequences of these analyses led to centrifuge testing, which has proliferated in recent years. This has developed, in consequence, a widespread impression that centrifuges are the **only** means of performing reduced-scale model tests rigorously. In the particular case of the undrained shear of saturated cohesive soils, this is not the case. It is simply necessary in such circumstances to maintain the dimensionless strength, $c/\gamma h$ (where c is shear strength, γ is the unit weight, and h is a characteristic length), to have a constant value in both model and prototype and for the model to represent correctly a number of features of the prototype behavior quantitatively as well as qualitatively, including, for example, failure loads. The failure loads in the model are $1/n^3$ times those of the prototype (of the same unit weight), where n is the ratio of a characteristic prototype length to that in the model. For example, for normally consolidated clay in both model and prototype, the load displacement relations are similar in model and prototype; thus, field conditions can also be scaled correctly.

It was generally considered that this scaling requirement could not be emulated for sands, but recent work in the critical/steady state for soils in general led to the conclusion that sand tests can also be scaled properly. For the clay material, the constant dimensionless variable requirements lead to a model clay with a shear strength S_u, smaller by $1/n$ that of the prototype. For the same clay, this is achieved by mixing the model clay to a higher water content in the model than in the prototype. This means that the model clay state (water content and stress) bears the same relation to the critical/steady-state line as the prototype state. The model clay has a higher water content, corresponding to $1/n$ lower stresses than in the prototype. The unit weight is not changed much by the relatively small changes in water content required.

The same result can be used for sands. If the model sand is prepared at a higher void ratio than the (same) prototype sand in such a way that both states lie on a line parallel to the critical/steady-state line, with the model soil stresses being a factor of n smaller than the prototype, then the stress-strain relations, including dilatancy, of the two materials will be similar, and this can be used to construct scaling relationships for models. Most model tests on sands in the past have been conducted on soil with the same void ratio, or relative density, as the prototype. However, the above requirement means that the model sand must be less dense. Because of the range of void ratios available for one material, there are limitations to this physical modeling approach, depending on the properties of the medium and length scaling adopted.

Centrifuge Testing

Centrifuge test methods and associated scaling relationships are well known and need no description here. The study of mechanisms and mode of deformations with well-defined boundary conditions and known soil properties can be performed using centrifuge models. Continued research into the use of centrifuge studies in the verification of numerical procedures is needed.

For cyclic or dynamic simulations, difficulties occur when pore pressures and diffusion develop in model and prototype because of the different scales for time required by dynamic and diffusion (consolidation) processes. This has been avoided in some cases by using a more viscous fluid than water in the model, but more study is needed of the effects of this substitution.

Proper centrifuge modeling requires that the determination of model properties be representative of field conditions. In this context, research is needed in the development of nondestructive techniques that can measure model properties without soil disturbance.

NEEDS AND PRIORITIES FOR RESEARCH

A.   Site Characterization To Delineate Stratigraphy

1.   Applied research is needed to develop and use better tools and technologies to improve the state of practice in site investigations. This research should include development and utilization of tools and technologies from other disciplines, such as newly developed geophysical methods.

2.   Applied research is needed to evaluate the degree of detail required for various applications, such as calculating ground response, stability, and ground displacements on sloping ground.

B.   Soil Constitutive Models

The development and testing of mathematical constitutive models to represent soil behavior more realistically is encouraged. Present studies of field events, especially including large deformations, are based very strongly on antiquated models that have their foundation in small-strain linearly viscoelastic behavior, with empirical modifications, not justified by mechanical principles, to moduli and damping factors to account for nonlinear soil response. Accompanying the development of new models in which nonlinearity and finite strains are properly accounted for will be the laboratory tests required to determine the necessary material constants. The values of these may be obtained from existing test equipment (consolidation, triaxial, simple shear) or may require the modification

8-14

of this apparatus or development of new tests to account properly, for example, for large strain effects.

C.   Characterization of Sandy Soils

1. Development of improved testing methods is needed for determination of S_{us} in the laboratory, including attaining sufficient levels of strain to reach the steady-state condition, retaining homogeneity of the specimen and retaining well-defined and measurable values of stresses and void ratio at large strains.

2. Clarification is required on the degree of influence of stress path, initial fabric, intermediate principal stress, and strain rate on S_{us}.

3. Given the sensitivity of S_{us} to void ratio, it is important to develop improved methods for obtaining undisturbed samples and measuring *in situ* void ratios. Consideration should be given to the use of electrical, nuclear, and other *in situ* methods to measure void ratio.

4. Research should be carried out to determine the coefficient of consolidation, C_v, to be used in analytical studies addressing the role of redistribution/dissipation of pore pressures in stability. Laboratory studies should address both gravel, sands, and silts to cover the full range of possible C_v values.

5. Clarification is required on the relationships between triggering of instability and strains, pore pressures, mobilized stress ratios, accumulated and cyclic soil type, initial state, and creep.

6. Research should continue to collect data and possibly to develop empirical correlations between field measurements, such as standard penetration resistance, and steady-state or residual strength. These correlations would provide economical estimates of residual strength for engineering analyses and for extrapolation of results on laboratory test specimens to soil layers in the field.

7. Development of general effective stress models of the behavior of dry and saturated soils, applicable to dynamic loading conditions, should be continued and encouraged.

8. Development is needed for constitutive models that account for variations in soil behavior during cyclic loading, including dilative response. Tests in modes other than triaxial compression may be required.

9.   In the development of new laboratory or field testing methods and equipment, attention needs to be given to the tests' ability to measure parameters needed in constitutive models.

10.   Applicable case history data should be used as they become available to test constitutive models. In particular, new computer codes should be tested to verify the proposed constitutive models.

D.   Characterization of Clay Soils

1.   Cyclic laboratory testing programs should be performed for a variety of natural sensitive clay soils. These testing programs should consider and examine the relationship between excess pore water pressure accumulation (rate and total extent), peak undrained shear strength, and stress-strain characteristics and changes.

2.   Laboratory and *in situ* testing techniques should be evaluated for the purposes of characterizing the undrained steady-state strength of sensitive clay soils and for defining the levels of shear strain (deformation) at which that strength may be achieved.

E.   Characterization of Rock Slopes

1.   Simple failure analysis

a.   Better methods are needed to identify fracture and joint patterns and orientation in a rock mass.

b.   Laboratory and *in situ* tests are required to solve the problem of shear strength across joints and its variation with scale.

c.   Mathematical modeling of shear strength and studies of its dependence on rock material properties and their variation with scale are needed.

d.   Quantitative understanding of the influence of water in rock joints in relation to slip and failure is needed.

2.   Discrete, distinct element modeling (DEM)

a.   The importance of the selection of the interblock springs and dashpots to the displacement/failure process needs to be assessed.

b.   The importance of the selection of the global damping needed for numerical stability needs to be studied.

c. Verification of the DEM by reference to field case histories is needed.

d. More study of the input of seismic vibrations to the DEM is required.

F. Case Histories and Instrumented Sites

1. The documentation and collection of case history data should continue and be augmented to provide detailed three-dimensional delineation of sediment stratigraphy, measured soil properties, topography, and distribution of ground displacements.

2. Further analysis of case history data is needed to develop a better understanding of ground failure processes and mechanisms to assure that the correct phenomena are being considered and modeled.

3. Case history information is needed to provide data for empirical correlations.

4. Case history data also are needed for verification of analytical models.

5. Well-characterized and -instrumented sites, which are potentially susceptible to major deformations, are needed to provide ground-motion and pore-pressure records, not generally available at case history sites. A special effort should be made to measure displacements within the failed materials.

G. Physical Modeling

1. More tests are needed with 1g models with reference to prototype measurements to verify the applicability of the technique in dynamic conditions.

2. Tests are needed on saturated sands and silts to examine the generation and dissipation of pore pressures at the model scale.

3. Tests should be conducted to determine whether a 1g model can simulate instability and flow sliding.

4. Mechanisms and modes of deformations with well-defined boundary conditions and known soil properties should be studied using centrifuge models to understand the mechanisms of instability and deformation. Continued centrifuge testing can also assist in the verification of numerical procedures.

H.   Research is needed on mitigation measures for sloping ground where instability or large deformations are predicted.

Appendix A   AGENDA

Appendix A

NSF/EPRI WORKSHOP AGENDA
DYNAMIC SOIL PROPERTIES
AND SITE CHARACTERIZATION
FOR EARTHQUAKE RESISTANT
DESIGN AND ANALYSIS

Wednesday, November 8, 1989

Hospitality Room at the Hyatt   Wednesday Evening

Thursday, November 9, 1989

7:30 -	8:00 a.m.	Continental Breakfast and Registration in Camino A
8:00 -	8:30	Introductions
8:30 -	10:00	SOA Presentations
10:00 -	10:30	Break
10:30 -	12:00 p.m.	SOA Presentations
12:00 -	12:10	Announcements
12:15 -	1:15	Lunch in Camino B
1:15 -	4:30	Concurrent Panel Meetings*
4:30 -	6:00	Plenary Session** in Camino A
7:00 -	9:00	Dinner with Professor Mike Agbabian, invited speaker, in Camino B

Friday, November 10, 1989

7:30 -	8:00 a.m.	Continental Breakfast in Panel Meeting Rooms
8:00 -	12:00	Concurrent Panel Meetings
12:00 -	1:30 p.m.	Lunch in Camino B***
1:30 -	3:15	Plenary Session in Camino A
3:15 -	3:30	Closing Remarks
3:30 -	??	Panel Report Preparation

Saturday, November 11, 1989

Organizing committee plus SOA speakers/recorders stay and finalize draft of workshop report.

---

*   Each panel consisted of approximately 10 people. The panels met in separate rooms. Discussions were led by the SOA speaker and assisted by the recorder. Each panel discussed the research needs that fell within its topic area.

**   Plenary sessions involved short panel reports by the panel SOA speaker. This was followed by open discussions.

*** Brief presentations by Holzer, Tucker and Seed on Loma Prieta (San Francisco) earthquake.

Appendix B   ATTENDEES

Appendix B
ATTENDEES
NSF/EPRI WORKSHOP
NOVEMBER 9-11, 1989

Norm Abrahamson	Woodward-Clyde Consultants	818-449-7650
M. S. Agbabian	University of Southern California	213-743-4658
John Anderson	University of Nevada--Reno	702-784-4265 x3628
Don Anderson	CH2M HILL	206-453-5000
Kandiah Anulanandan	University of California, Davis	916-752-0895
C. J. Astill	NSF	202-357-9500
Terry Barker	S-Cubed	614-587-7208
Shebha Bhatia	Syracuse University	315-443-2311
Giovanni Bongiovanni	ENEA--Italy	1-39-6-3048-4705
Roger Borcherdt	USGS	415-329-5619
Gonzalo Castro	GEI Consultants, Inc.	612-721-4000
J. Chameau	Purdue	317-494-5030
C. Y. Chang	Geomatrix Consultants	415-957-9557
John Christian	Stone & Webster	617-589-2060
Wayne Clough	VPI	703-231-6635
C. B. Crouse	Dames & Moore	206-728-0744
Pedro de Alba	University of New Hampshire	603-862-1428
Ricardo Dobry	Rensselaer	518-276-6934
John A. Egan	Geomatrix Consultants	415-957-9557
Liam Finn	UBC--Canada	604-228-4938
Fred Followil	Lawrence Livermore Labs	415-422-3920
Herman Graves	U. S. NRC	301-492-3813
Bob Henke	Dynamic Testing	301-252-4474
C. J. Higgins	Applied Research Associates	703-329-0200
Tom Holzer	USGS	415-329-5613
Hiroshi Ito	CRIEPI--Japan/EPRI	415-855-2504
Michele Jamiolkowski	Technical University of Torino, Italy	39-11-5567840
W. B. Joyner	USGS	415-329-5640
T. Katayama	University of Tokyo	Japan-3-402-6231
Ann Kiremidjian	Stanford	415-723-4164
Hon-Yim Ko	University of Colorado	303-492-6716
Richard S. Ladd	Woodward-Clyde Consultants	201-785-0700
John Lysmer	University of California--Berkeley	415-642-1262
Geoff Martin	Earth Technology	213-495-4449
Farrokh Nadim	NGI--Norway	472-23-03-88
Jerry Nelson	Consultant	415-382-9210
Gary Olhoeft	USGS	303-236-1302
Mario Ordaz	UNAM--Mexico	5505215
Jacob Philip	U.S. Nuclear Regulatory Commission	301-492-6231
S. Prakash	UM Rolla (MO)	314-341-4489
Robert Pyke	Consultant	415-283-6765
G. Z. Qi	University of Maryland	301-454-7696
Bruce Redpath	Consultant	209-728-3705
Peter Robertson	University of Alberta	403-492-5106
Jose M. Roesset	University of Texas--Austin	512-471-4927

Appendix B
ATTENDEES
NSF/EPRI WORKSHOP
NOVEMBER 9-11, 1989
(Continued)

Al Rogers	USGS	303-236-6978
Tony Saada	Case Western University	216-368-2427
Woody Savage	Pacific Gas and Electric	415-972-3116
John Schneider	EPRI	415-855-7921
Ron Scott	Caltech	818-356-4233
Ray Seed	University of California--Berkeley	415-642-1262
C. K. Shen	U. C. Davis	415-752-1753
Walt Silva	Pacific Engineering and Analysis	415-893-3600
Phil Sirles	U. S. Bureau of Reclamation	303-236-4196
Paul Somerville	Woodward-Clyde Consultants	818-449-7650
Carl Stepp	EPRI	415-855-2103
Ken Stokoe	University of Texas--Austin	512-471-4929
M. Sugito	Kyoto University/Stanford	415-725-0361
H. T. Tang	EPRI	415-855-2012
Y. K. Tang	EPRI	415-855-2473
B. E. Tucker	California Division Mines/Geology	916-445-1923
Erik Vanmarcke	Princeton University	609-921-3028
Andy Veletsos	Rice University	713-527-8101
Richard Woods	University of Michigan	313-764-4303
Jackson Yang	University of Maryland	301-454-7694
T. Leslie Youd	Brigham Young University	801-378-6327
T. Zimmie	NSF	202-357-9542

NSF/EPRI WORKSHOP
PANEL ASSIGNMENTS

Panel 1 (Camino A)
Low- and High-Strain Properties

Ricardo Dobry/Rensselaer--S
S. Bhatia/Syracuse--R
Bob Henke/Dyn. Testing
C. J. Higgins/Applied Research
M. Jamiolkowski/Torino--Italy
H-Y Ko/Colorado
Dick Ladd/Woodward-Clyde
S. Prakash/Missouri
Tony Saada/Case Western
Phil Sirles/B of Rec

Panel 3 (Marsten Room)
Spatial Variability

Gary Olhoeft/USGS--S
John Christian/Stone & Webster--R
Wayne Clough/VPI
Fred Followil/Lawrence Livermore
H. Ito/CRIEPI--Japan
Farrokh Nadim/NGI--Norway
Jerry Nelson/Consultant
Erik Vanmarcke/Princeton

Panel 5 (Holtum Room)
Arrays

Brian Tucker/CDMG--S
C. B. Crouse/Dames & Moore
Norm Abrahamson/Woodward-Clyde
G. Bongiovanni/ENEA--Italy
C-Y Chang/Geomatrix
Herman Graves/NRC
Tom Holzer/USGS
T. Katayama/Tokyo--Japan
Mario Ordaz/UNAM--Mexico
C.K. Shen/UC Davis

Pannel 2 (Edwards Room)
Energy Dissipation

Jose Roesset/Texas--S
Dick Woods/Michigan--R
Bill Joyner/USGS
John Lysmer/UC Berkeley
Bob Pyke/Consultant
Bruce Redpath/Consultant
Ken Stokoe/Texas
Andy Veletsos/Rice
Jackson Yang/Maryland

Panel 4 (Foster Room)
Site Geometry

Walt Silva/Pacific Engineering-S
John Schneider/EPRI--R
John Anderson/Nevada
Terry Barker/S Cubed
A. Papageorgiou/Rensselaer
Jacob Philip/NRC
Al Rogers/USGS
Woody Savage/PGE
Ray Seed/UC Berkeley
Paul Somerville/Woodward-Clyde

Panel 6 (Wilshire Suite)
Sloping Ground Sites

Gonzalo Castro/GEI--S
Les Youd/BYU--R
K. Arulanandan/UC Davis
Jean Chameau/Purdue
Pedro de Alba/New Hampshire
John Egan/Geomatrix
Liam Finn/UBC--Canada
Geoff Martin/Earth Technology
Peter Robertson/Alberta, Canada
Ron Scott/Caltech

Note: S = Speaker
         R = Recorder

EPRI
Electric Power
Research Institute

Proceedings: NSF/EPRI Workshop on Dynamic Soil Properties and Site Characterization

Volume 2

Proceedings: NSF/EPRI Workshop on Dynamic Soil Properties and Site Characterization
Volumes 1 and 2

Experts in geophysical sciences and earthquake engineering convened to evaluate state-of-the-art technology in geotechnical property characterization for earthquake-resistant design and analysis. Workshop areas discussed in this report will help focus and prioritize research on seismic hazard mitigation and seismic design improvement.

INTEREST CATEGORIES

EPRI R&D planning
Nuclear seismic risk,
   design, and qualification

KEYWORDS

Soils
Site characterization
Geotechnical engineering
Seismic effects

BACKGROUND   Earthquake experience shows that site geology and local soil properties exercise a decisive influence on seismic ground motions and structural damage potential. Progress has been made in measuring dynamic soil properties and understanding site characteristics. However, technologic limitations and resultant uncertainties have restricted the overall ability to confidently characterize a site for seismic design and analysis.

OBJECTIVES

• To discuss the current state of dynamic soil property measurement and site characterization for earthquake-resistant design and analysis.

• To explore ways to achieve necessary advances and identify research priorities.

APPROACH   Sixty-seven engineers, geologists, geophysicists, and seismologists from the United States and abroad participated in a two-day workshop November 9–10, 1989, in Palo Alto. State-of-the-art presentations focused on six previously selected technical topics, designed to help the National Science Foundation (NSF) and EPRI plan future research programs aimed at characterizing the dynamic material properties of sites for seismic design. Following these presentations, participants formed six panel groups to discuss the state of the art and to suggest research needs and priorities for each topic. The organizing committee met after the workshop to synthesize results and recommendations.

KEY POINTS   The workshop addressed six key technical topics, including low- and high-strain cyclic soil material properties, mechanisms for energy dissipation, spatial variability of soil properties, effect of site geometry and global characteristics, seismic arrays, and sloping ground sites. Experts determined that

• The highest priority research need industrywide is development and operation of field test sites for site soil characterization and method validation in seismically active areas.

• Other research needs exist in the following areas: technology enhancement of soil in situ and laboratory testing; investigation of physical-chemical processes affecting property changes; sensitivity evaluation of dynamic soil property variations; and improvements in data processing methods, field data interpretation techniques, and ground-response modeling procedures.

Proceedings: NSF/EPRI Workshop on Dynamic Soil Properties and Site Characterization

Volume 2

Proceedings: NSF/EPRI Workshop on Dynamic Soil Properties and Site Characterization

Volume 2

NOTICE

DISCLAIMER OF WARRANTIES AND LIMITATION OF LIABILITIES

ORDERING INFORMATION

Requests for copies of this report should be directed to Research Reports Center (RRC), Box 50490, Palo Alto, CA 94303, (415) 965-4081. There is no charge for reports requested by EPRI member utilities and affiliates, U.S. utility associations, U.S. government agencies (federal, state, and local), media, and foreign organizations with which EPRI has an information exchange agreement. On request, RRC will send a catalog of EPRI reports.

CONTENTS

Appendix C RESPONSE FROM NETWORK OPERATOR

STRONG-MOTION ARRAYS/NETWORKS
AND THEIR OPERATORS
RESPONSES TO QUESTIONNAIRES

CANADA   Deiter Weichert
                                    Pacific Geoscience Center
                                    P.O. Box 6000
                                    Sidney, British Columbia V8L 4BZ
                                    CANADA

                                    Philip S. Munro
                                    Canadian Geophysical Survey
                                    1 Observatory Crescent
                                    Ottawa, Ontario K1A 0Y3
                                    CANADA

COSTA RICA   Guillermo Santana
                                    Apartado Postal 592
                                    2150 Moravia, COSTA RICA

GREECE   Panayotis Carydis
                                    National Technical University
                                    42 Patision Street
                                    Athens (147), GREECE

INDIA   A. R. Chandrasekaran
                                    Department of Earthquake Engineering
                                    University of Roorkee
                                    Roorkee 247 667, INDIA

IRAN   A. A. Moinfar
                                    No. D2 6th St. Farmaz St.
                                    Mohseni Square Mirdamad
                                    Tehran, IRAN

ITALY

Duilio Benedetti
Polytecnico di Milano
Piaz, Leonardo da Vinci 32
20133 Milano, ITALY

Franco Paparelli
ENEL - DCO
92, Via Ostiense
I-00154 Roma, ITALY

MEXICO

John Anderson/James Brune
Seismology Laboratory
MacKay School of Mines
University of Nevada, Reno
Reno, NV 89557

NEW ZEALAND

Graeme H. McVerry
D.S.I.R.
Engineering Seismology
Private Bag
Lower Hutt, NEW ZEALAND

USA

Doug Johnson
Lamont-Doherty Geological Observatory
  of Columbia University
Palisades, NY 10964

Andy Viksne
U.S. Bureau of Reclamation
P.O. Box 25007
MC D-1631
Denver, CO 80225

Roger Borcherdt
U.S. Geological Survey, MS 977
345 Middlefield Road
Menlo Park, CA 94025

STRONG-MOTION ARRAY QUESTIONNAIRE

network, (not interconnected)

1. Where is your ~~array~~ located and how long has it been operating?

1. Eastern Canada, mid '60's;   EARLY 60!
2. WESTERN CANADA - VANCOUVER ISLAND - MAINLD
3. QUEEN CHARLOTTE ~~AT~~ ISLANDS AREA. 6
4. TEMPORARY ~~IT~~ INSTALLATIONS - POST

2. Please describe your array, in terms of the type and number
of instruments, their spacing, their triggering, their
recording means (film, tape, or disc; analog or digital),
and their foundation and housing.

1. ALL SMA-1's;   20-25; SPACING 10's TO 100 km
2.) "   "   NOW; 30-40 (CURRENTLY 36) FILM, VERTIC.
3.)   SPACING CLOSER THAN 1   1½ g   7i
              A FEW km to 10's km
4. 4-10, VARIABLE, SMA-1's

1-3 BUILDING BASEMENTS, LOW RISE IF POSSIBLE; SOME FOR ENGINEER
     PURPOSES, E.G, IN 2 DAMS. NOW CHANGED.
     FOUNDATION FROM ENGINEERING REPORT; EXTRAPOLATION OF
4. SOME GEOLOGIC MAPS. NO SPECIAL INVESTIGATION EXCEPT INFE
   (MOUNTAINTOPS, ROCK SITES IF POSSIBLE. SOME LATER IDENTED AS
                                                            BEC-VER

3. Describe the nature of the data you have obtained, in terms
of the number of events recorded, their range of magnitudes,
and their distances from the array.

1. 1 EVENT IN 1978-80; M5 @ 50 km.

2.) FROM 1961-89: ABOUT 4 EVENTS FROM M 4.? TO 7.0 AT
3.)   DISTANCES OF 10's TO 200 km.

4. AFTERSHOCK SURVEYS M3.+ - 5.+, TEN's OF km
   IN NEW BRUNSWICK
   & NAHANNI 3.+ to 6.9, 5 km to 30 km DISTANCE,
                          HYPOCENTRAL

4. What means were used to characterize the site conditions?

ENGINEERING REPORT, GEOLOGIC MAPS, VISUAL INSPECTION

WEICHERT

5. If you were to establish a new array, what means would you
    now use to characterize site conditions?
    SAME, BUT MORE CAREFULLY.
    WOULD BE DIFFICULT IN SOME AFTERSHOCK SCENARIOS.

6. What lessons have been learned

    o regarding the operation of the array?
    — SMA1 RELIABLE. GOOD ENOUGH FOR OUR LOW DATA CRITICAL
                                             EXPECTATION.
    — FOR AFTERSHOCK DEPLOYMENT WOULD PREFER DIGITAL. INSUFFICIENT
    ABS. EXPERIENCE TO COMMENT ON RELIABILITY.
    — TIME DATA CONTINUES TO BE A PROBLEM IN OUR OPERATION.

    o regarding ground response to earthquakes?
    WE HAVE NOT YET LEARNT OUR LESSON. ALWAYS NEW SURPRISES.

7. Can you comment on the relevance of ambient vibration
    measurements and forced vibration testing?
    NOT AUTHORITATIVELY

8. ADDITIONAL COMMENTS AND ADVICE (please use additional pages
    if desired)

Thank you!

DIETER WEICHERT
Name

Canadian strong motion seismograph networks*

D.H.Weichert
Pacific Geoscience Centre, Geological Survey of Canada, Sidney, British Columbia

P.S.Munro
Geophysics Division, Geological Survey of Canada, Ottawa, Ontario

ABSTRACT: The Canadian strong motion seismograph network was started in 1963 and some 70 accelerographs are now in operation. Site selection is governed primarily by seismological rather than engineering priorities. The federal government networks are supplemented by privately-owned instruments in special engineered structures, mainly dams. In western Canada, 36 accelerographs are installed in the Vancouver-Victoria, Central Vancouver Island, and Queen Charlotte areas. The Vancouver-Victoria region is a high-density population centre, just inland from the Juan de Fuca subduction zone, which may be capable of large subduction earthquakes, while the latter two regions have a proven potential for large earthquakes (M8.1 and M7.3). Four earthquakes have yielded records of up to 0.06 g horizontal acceleration. In eastern Canada, 17 of the 19 accelerographs are now centered on the Charlevoix seismic zone, which has a long history of strong earthquakes. In 1982, an earthquake series in New Brunswick yielded the first significant near-source ground motions in eastern Canada of up to almost 0.6 g. Only one accelerograph was located in northern Canada until a series of strong earthquakes occurred in 1985 in the Northwest Territories. Instruments installed in the Nahanni aftershock zone recorded horizontal accelerations over 1 g and a vertical acceleration peak of over 2 g.

1 Introduction

Parts of Canada are strongly seismic. On the west coast, part of the circum-Pacific seismic belt, one M8.1 and several M7 earthquakes are known to have occurred in historical times. In eastern Canada, populated regions are known to have experienced magnitude 6 to 7 earthquakes as early as 1663, with three M6 or greater events since 1925.

This activity motivated the initiation of a modest strong motion program in western Canada by the Dominion Observatory, then a branch of the Department of Energy, Mines and Resources (EMR) and, almost concurrently, the National Research Council of Canada (NRCC) began to install a strong motion network in eastern Canada. Subsequent to some reorganization within the Canadian government, both networks are now under the direction of the Geological Survey of Canada (GSC) of the Department of Energy, Mines and Resources. This paper reviews the development, current status and proposed expansion of these networks, and tabulates the most notable strong motion records.

2 History

The first two instruments of the Canadian strong motion program were installed in early 1963 in Victoria and Vancouver. The early history of the network was described by Rogers, Milne and Bone (1970), and was reviewed by Rogers (1976). Most of the early instruments were located on the densely populated Lower Mainland and southern Vancouver Island. The locations were chosen to sample the response of the different soils and alluvial thicknesses of the Fraser valley deposits, and instruments were placed mostly in basements or ground floors of low-rise buildings.

The National Research Council of Canada (NRCC), through its Division of

* Geological Survey of Canada Contribution Number 48786.

Building Research, installed the early strong motion network in eastern Canada, starting in 1966 (Rainer and Luctkar 1983). About a dozen accelerographs were placed in the large cities of Montreal and Quebec, and in the villages near the historical Charlevoix seismic zone, downriver from Quebec City.

In the late 70s there was a demand for seismic hazard estimation for a projected northern pipeline, and a few accelerographs were installed by EMR to capture ground motion on permafrost. Only one of these now remains in the Yukon Territory at Haines Junction.

Both EMR and NRCC also encouraged builders of large-scale engineered structures (mainly dams) to install their own accelerographs, and, in fact, the government agencies serviced these instruments for several years, until the industries took over this responsibility. Currently, four hydroelectric dams in British Columbia and three in Quebec

are privately instrumented.

High on the list of Canadian concerns was the lack of good "free-field" groun motion relations for eastern Canada, where typical source parameters and attenuation are different from western North American earthquakes. This has been addressed in a network expansion i: 1984. In western Canada, concerns are with the attenuation from earthquakes o: about 50 km depth, and also with ground motion from very large earthquakes with spatially extended sources.

In 1982, a M5.7 earthquake in Miramichi, New Brunswick, provided a strong impetus for expansion of the eastern network, and, in cooperation with the U.S. Nuclear Regulatory Commission (USNRC), 8 accelerographs were deployed in the Miramichi after- shock area for 2 years. Some of these instruments captured the first signifi- cant near-source ground motions on bedrock in eastern Canada (Weichert et

MAGNITUDE

* 7 ≤ M
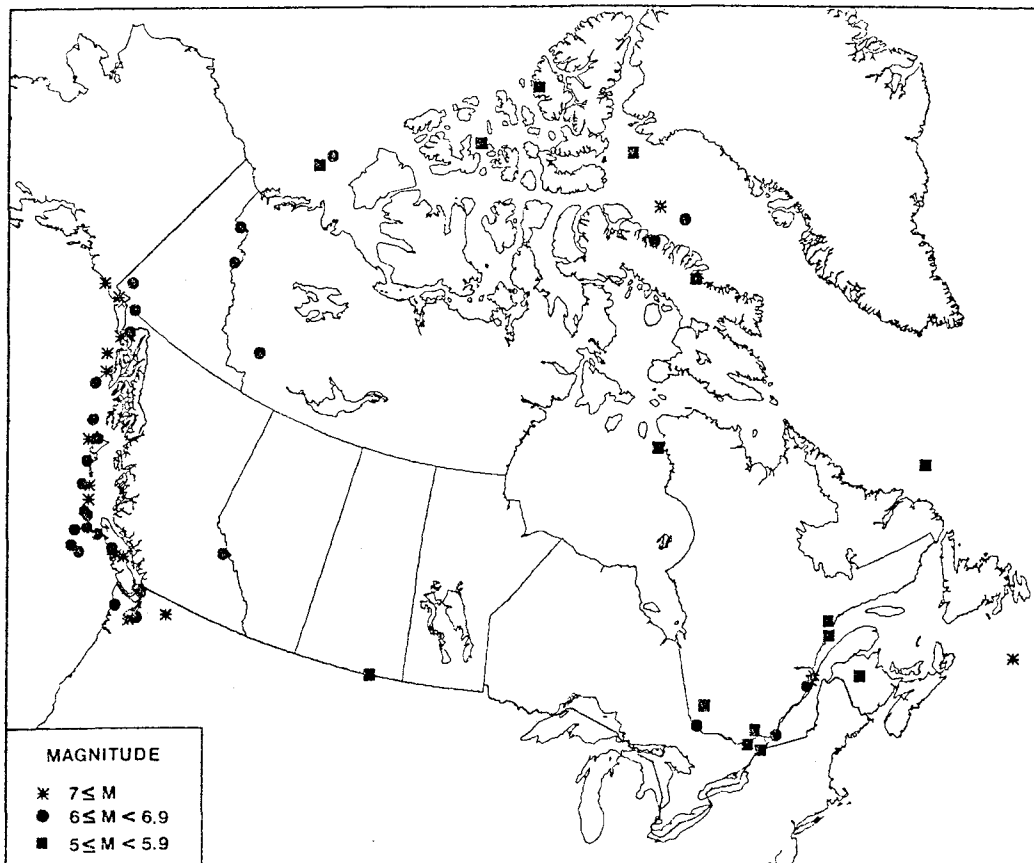● 6 ≤ M < 6.9
■ 5 ≤ M < 5.9

Figure 1: Some earthquakes of significance to Canada; 1663 to 1985.

al. 1982; also, see Table 1).

The eastern NRCC network was transferred to EMR in 1984 and was retrofitted and reconfigured using the decommissioned New Brunswick equipment and some new instruments. The number of instruments centered on the Charlevoix seismic zone more than doubled. Particular attention was paid to establishing "free-field" sites.

In 1985, a magnitude 6.6 earthquake occurred in the Mackenzie Mountains of the Northwest Territories. Three strong motion accelerographs were deployed during aftershock surveys and recorded very significant ground motion during a second large earthquake (M6.9). These and the 1982 Miramichi records will be described later (see Section 6 and Table 1).

A considerable number of seismoscopes had been installed in the earlier phases of the program (see Rogers 1976), but have now been removed because of servicing and cost/benefit considerations.

3 Instrumentation

The existing network of analog film recording accelerographs is still considered to be the best compromise of cost, reliability and data quality for the level of seismicity found in Canada, although a digitally recording accelerograph has been acquired. At present, most accelerographs in western Canada are 1 g Kinemetrics SMA-1 units, with six 1 g RFT- 250 units. In the east, most instruments are Kinemetrics SMA-1 1 g units with time code generators. The exceptions are three 1/2 g Kinemetrics SMA-1 units whose resonant frequencies are near 18 Hz, as compared to 25 Hz for the 1 g units; they are not considered to be appropriate for eastern Canada where higher than average ground acceleration frequencies and higher than 1/2 g amplitudes have been observed. Retrofit to 1 g is planned during 1987.

Detailed instrument and site data are given in the annual publication 'Canadian Seismograph Operations' of the Geological Survey of Canada. Through cooperation with the private operators, data on their stations are included in this publication.

Responsibility for the western strong motion stations, including the Yukon, lies with the Cordilleran and Pacific Margin Division of the GSC (Pacific Geoscience Centre, Sidney) and for the eastern stations with the Geophysics Division of the GSC (Ottawa). Maintenance is mainly by contract, with one scheduled visit every six months for all but the most remote sites, where visits are annual. Some of these stations have a simple monitor unit attached externally (see Rogers and Bennetts 1975). The curators of these instruments are contacted by mail a few times a year, and asked to record and send in the monitor readings. Abnormal readings may result in an early or unscheduled service trip.

Both offices of the GSC now have some spare instruments, which serve to maintain the networks and are readily available for deployment in aftershock zones of significant earthquakes.

4 Western Earthquake Potential and Networks

Canada's southwestern coast is part of the circum-Pacific seismic belt, comprised here of short ridge segments and transform faults separating the Pacific plate and the Juan de Fuca and Explorer platelets a few hundred kilometres offshore (Figure 2). These plate remnants are believed to subduct under Vancouver Island and the Lower Mainland of British Columbia where they give rise to earthquakes in the overlying crust and within the subducting plate (cf e.g. Keen and Hyndman 1979). Several earthquakes near and above M7 have occurred within a few hundred kilometres of the metropolitan centres of Vancouver and Victoria (Figure 1). Moreover, the potential of large thrust earthquakes on the Juan de Fuca subduction interface must be considered. Although not observed during historical times, evidence is mounting that such earthquakes may have occurred with average recurrence times of 400 to 500 years and magnitudes between 8 and 9 (Heaton and Kanamori 1984; Weichert and Rogers 1985).

Further north, the Pacific-North American plate boundary consists of the Queen Charlotte fault, a right-lateral strike-slip fault with a probable small subduction component near the south end of the Queen Charlotte Islands. A magnitude 8.1 earthquake occurred in 1949 along this section of plate boundary.

All M5 and some M6 western earthquakes have been excluded from Figure 1 to avoid overcrowding the diagram.

4.1 The Vancouver-Vancouver Island Network

Figure 3 shows the current network and planned additions in the southwestern corner of British Columbia. The historical earthquake zone (Milne et al. 1978) extends from Seattle-Tacoma at the south end of the Puget Sound in the State of Washington, to about the 49th parallel, halfway between the two metropolitan areas of Vancouver and Victoria. The larger earthquakes here occur within the subducting plate. There is a relatively quiet zone just to the north of 49°N, followed by a zone of moderate earthquakes northwest of the Vancouver-Lower Mainland area. Large events with an epicentre in the Gulf

Figure 3: Accelerographs in the Vancouver-Victoria area - 1986.

Figure 2: Accelerographs in western Canada - 1986 PP=Pacific Plate;AP=North American Plate; JFP=Juan de Fuca Plate; EP=Explorer Plate; QCF= Queen Charlotte Fault. Double bars at lower left represent transform faults; single-headed arrows show relative plate motion.

Islands are considered to be the closest likely threat to the metropolitan areas. For this hypthetical epicentre the Vancouver-Lower Mainland network has one approximately north-south profile and a second profile approximately following the Fraser River with about 10 km spacing. Most accelerographs are on basement concrete slabs. Three of the sites along the northern profile are founded on bedrock while the east-west profile is founded mainly on alluvium, silt, sand or clay.

On the south side of the hypothetical epicenter, the accelerograph spacing is somewhat wider, a few tens of kilometers. All sites but one are on bedrock. The siting of a few stations was influenced by engineering interests and instruments were located in structures of local importance and uniqueness. The southernmost example is an instrument at the coal shipping terminal on silt fill (Roberts Bank); another one is at the bottom of a tunnel under the Fraser River with a second "free-field" instrument a few hundred metres away. A third instrument is placed in the basement of a 22-storey concrete building in downtown Vancouver (B.C. Hydro) and a fourth is on the bedrock abutment of the Capilano concrete dam structure. One privately-owned instrument is located at Lake Cowichan (Teleglobe Canada) and another is at the Allouette dam on the

Fraser River.

Further to the northwest, central Vancouver Island has a high potential for a magnitude 7 event. Earthquakes occurred near the west coast of the island in 1918 (M7.0) and 1957 (M6.0), and in 1946 (M7.3) near the east coast. The currently existing and proposed accelerographs will cover the potential epicentral area well (see Figure 2), and completion of this network is expected by 1988. Remoteness and sparse population place restrictions on site selection; some instruments are not deployed in "free-field" conditions. The three proposed accelerographs for central Vancouver Island will be co-located with telemetred digital seismographs. This has potential advantages for data interpretation.

One instrument of the two in Port Alberni is located on a concrete floor built on a stiff cellular substructure of wood piles. This is a typical structure in forest product oriented west coast towns; a comparison with a nearby rock site would be highly relevant to engineering design.

4.2 The Queen Charlotte Network

Figure 2 shows the Queen Charlotte area network and Figure 1 indicates the high seismicity near the Queen Charlotte Islands. Instrument location is governed by the paucity of permanent settlements.

Instruments along the mainland coast are at a greater distance from the active principal Queen Charlotte fault zone, but seismic activity has been established to the east of the main fault between the Queen Charlotte Islands and the mainland. Accelerographs are located at the important seaport of Prince Rupert (GSC) and at the Kemano hydroelectric site (privately owned by ALCAN). Another accelerograph at the economically important location of Kitimat would be desirable.

4.3 B.C. Hydro Accelerographs

Cooperation between EMR and B.C. Hydro resulted in accelerograph installations in several dams in the early years of the EMR program. Ladore dam on Vancouver Island was instrumented by EMR in 1965, and the Mica Creek dam in the Rocky Mountain trench followed in 1972 (3 units, see Figure 2). More recently,

B.C. Hydro has set up its own monitoring program and is expanding. Currently the utility company operates accelerographs at the Bennett dam in the Peace River area, Mica Creek dam, Revelstoke dam in the interior (5 units) and Allouette dam in the Lower Mainland. Other installations are planned (private communication, Tim Little, B.C. Hydro 1986).

5 Eastern Earthquake Potential and Networks

Seismicity in eastern Canada is well documented although not as well understood within the framework of modern plate tectonics (Basham et al. 1979). The Charlevoix seismic zone is historically the most active, with at least five earthquakes of magnitude 6 or greater (1663, 1791, 1860, 1870 and 1925). The 1925 event is the only earthquake with magnitude near 7 on land in eastern North America in the twentieth century. This source zone is considered to have the highest potential for strong ground motion and has had the highest priority for instrumentation.

Several other clusters of seismicity exist throughout eastern Canada, in which the activity is significantly higher than the general background. One of the most important is the western Quebec zone that contains the major population centers of Montreal and Ottawa. Past experience suggests that maximum magnitude earthquakes of at least M7 must be assumed here, but the
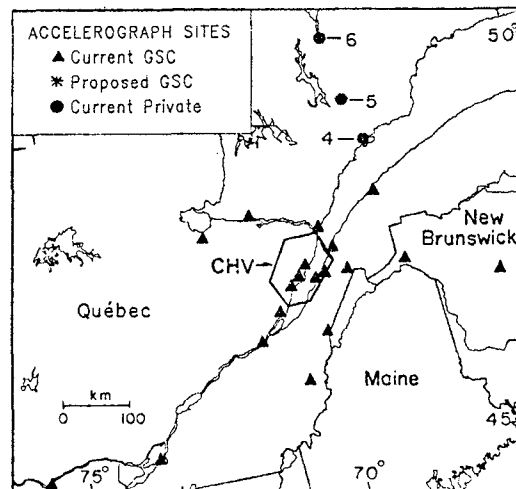

Figure 4: Accelerographs in eastern Canada - 1986. CHV=Charlevoix Seismic Zone.

probability for strong ground motion for these cities is smaller than for the Charlevoix zone.

Another source zone that includes one major historical event of M7.2 is a small area at the edge of the continental slope, at the mouth of the Laurentian Channel.

5.1 The Eastern Canadian Network

Figure 4 shows the eastern network, which comprises 19 sites and significantly improves the coverage of the Charlevoix seismic zone. The station layout approximates profiles both into the paleozoic terrain of the Northern Appalachians and into the Canadian Shield. Siting is constrained in the Shield region northwest of Charlevoix by a lack of villages. This configuration has two Northern Appalachian station profiles within Canada: one to the east ending at Miramichi, New Brunswick; and one to the south near the Quebec-Maine border.

The Charlevoix seismic zone shows activity over an epicentral region about 70 km by 30 km, centered along the river. A significant earthquake anywhere within this zone could trigger 5 strong motion seismographs within 50 km and 10 within about 100 km.

The single accelerographs in Montreal and Ottawa extend coverage into these densely populated and seismic areas.

5.2 Private Accelerographs in the East

Cooperation between NRCC and Hydro-Quebec resulted in accelerograph installations in three hydroelectric dams, starting in 1974 (Rainer and Luctkar 1983). Fifteen SMA-1 accelerographs are currently deployed, of which 11 are 1/2 g units.

6 Canadian Records and Data Processing

The first strong motion records were captured in Victoria from the 1965 Seattle earthquake (M6.5) at a distance of 140 km. A few more low level records were collected in the latter 60s and early 70s in the Victoria and the Queen Charlotte areas. The first significant set of records resulted from a M5.4 event in 1976 between the cities of Vancouver and Victoria (Weichert and Milne 1980). Eight accelerographs triggered, with maximum peak horizontal

accelerations between 0.04 and 0.06 g a distances of about 30 to 60 km on various soil types.

In eastern Canada, the first accelerogram with maximum peak acceleration of about 0.01 g was obtained in 1979 from a shallow M5.1 event in the Charlevoix zone at a distance of 55 km. When the 1982 Miramichi, New Brunswick earthquake series started there were no nearby strong motion seismographs, until a temporary network was installed as mentioned earlier. A set of 19 records was captured from shallow earthquakes o M3.4 to M4.8 at distances from 4 to 30 km. Their significance lay in the high dominant frequencies (averaging 24 Hz) and high peak ground accelerations, up to almost 0.6 g (Weichert et al. 1982).

In northern Canada, the first set of records was captured after the M6.6 event of 5 October 1985. To the end of September, 1986, accelerograms had been recorded from over 80 smaller aftershocks and from a second large earthquake of M6.9 (23 December, 1985), at distances of approximately 8 to 30 km. The significance of these records are three-fold: they are the first strong motion records from a very large Canadian earthquake; the peak accelerations recorded are very high (1.32 g horizontal and greater than 2 g vertical), and the ground motions of th large December event are expected to be widely used for engineering design studies (Wetmiller et al. 1987).

Available Canadian records have been published in Open File Reports (Weicher and Milne 1980; Weichert et al. 1982; Weichert et al. 1986). Table 1 gives a selection of relevant ground motion parameters for the most important Canadian strong ground motion records captured to date. Shown are peak horizontal accelerations and velocities as well as the approximate 5% damped spectral levels of acceleration and velocity, together with earthquake magnitude and epicentral distance.

The earliest records were processed in-house. We now use commercial digitization facilities, and, in the last five years, the facilities and the programs of the U.S. National Strong Motion Data Centre of the USGS in Menlo Park (AGRAM Program Package, Converse, 1984) have been used. The processed data have been included in the USGS archive.

The digitized data from processed records are available on tape, at the

Table 1. Peak horizontal ground motion parameters of the most notable Canadian strong motion records.

Earthquake - site & condition	Nominal Dist. (km)	Acceler. (g)	Velocity (m/s)	5% damped response spectrum	
				Acceler. (g)	Velocity (m/s)
Miramichi M4.8 **31 March 1982**					
- Holmes Lake, 5 m alluvium	6	0.34	0.014	0.6	0.05
- Mitchell Lake, bedrock	4	0.23	0.019	0.7	0.06
- Loggie Lodge, 5 m alluvium	6	0.56	0.041	0.8	0.06
- Indian Brook, gravel	3	0.42	0.031	0.8	0.06
Nahanni M6.9 **23 December 1985**					
- Site 1, bedrock	8	1.32	0.46	3.0	1.0
- Site 2, bedrock	8	0.53	0.33	1.5	0.6
- Site 3, bedrock	25	0.19	0.06	0.7	0.1

user's expense. Requests should be made to the Head, Canadian Seismograph Network, Geophysics Division, Geological Survey of Canada, 1 Observatory Crescent, Ottawa, Ontario, Canada, K1A 0Y3.

7 Summary

The Canadian strong motion network started almost 25 years ago. The program is now the responsibility of the Geological Survey of Canada. Over 70 accelerographs are now in place, and large events in the Queen Charlotte, Central Vancouver Island, Vancouver-Victoria and Charlevoix areas should be adequately recorded. The GSC will continue to supplement permanent network data by deploying portable instrumentation in the aftershock zones of large events in these and other areas. In western Canada, the network should continue to grow to the outlined configuration before 1990. There are no expansion plans for the eastern network. Critical facilities should be instrumented by their owners; for example, the Canadian Standards Association provides guidelines on the installation of strong motion accelerographs in nuclear power plants (CSA-N289.5).

Recently captured strong ground motion records have a been received with great interest by the engineering community, emphasizing the socio-economic importance of maintaining a viable strong motion program in Canada.

8 Acknowledgements

9 References

Basham, P.W., D.H. Weichert & M.J. Berry 1979. Regional assessment of seismic risk in eastern Canada. Bull. Seis. Soc. Am. 69:1567-1602.

Canadian Standards Association. Seismic instrumentation requirements for CANDU nuclear power plants, CSA Standard N289.5, (in preparation). Canadian Standards Association, Rexdale, Ontario, M9W 1R3.

Heaton, T.H. & H. Kanamori 1984. Seismic potential associated with subduction in the northwestern United States. Bull. Seis. Soc. Am. 74:933-941.

Keen, C.E. & R.D. Hyndman 1979. Geophysical review of the continental margins of eastern and western Canada. Can. Jour. of Earth Sciences. 16:715-747.

Milne, W.G., G.C. Rogers, R.P. Riddihough, G.A. McMechan & R.D. Hyndman 1978. Seismicity of western Canada. Can. Jour. of Earth Sciences. 15:1170-1193.

Rainer, J.H. & E.C. Luctkar 1983. The eastern Canadian strong motion seismograph network. Proc. Fourth Cdn. Conf. on Earthquake Eng., Vancouver, 1983: 519-528.

Rogers, G.C. 1976. A survey of the Canadian strong motion seismograph

network. Can. Geotechnical Jour. 13:78-85.

Rogers, G.C., W.G. Milne & M.N. Bone 1970. The strong motion seismograph network in western Canada. Pub. Earth Physics Branch. 41:15-29.

Rogers, G.C. & H.J. Bennetts 1975. A simple monitoring device for strong motion seismographs. Bull. Seis. Soc. Am. 65:1502-1503.

Weichert, D.H. & W.G. Milne 1980. Canadian strong motion records. Earth Physics Branch Open File Report 80-1, Ottawa.

Weichert, D.H., P.W. Pomeroy, P.S. Munro & P.N. Mork 1982. Strong motion records from the Miramichi, New Brunswick, 1982 aftershocks. Earth Physics Branch Open File Report 82-31, Ottawa.

Weichert, D.H. & G.C. Rogers 1985. Seismic risk in western Canada. Proc. 3rd inter. symp. on analysis of seismicity and seismic risk, Liblice, Czechoslovakia.

Weichert, D.H., R.J. Wetmiller, R.B. Horner, P.S. Munro & P.N. Mork 1986. Strong motion records from the 23 December 1985, Ms6.9 Nahanni, N.W.T., and some associated earthquakes. Geological Survey of Canada Open File Report 1330, Ottawa.

Wetmiller, R.J., P.W. Basham, D.H. Weichert and S.G. Evans 1987. The 1985 Nahanni earthquakes: problems for seismic hazard estimates in the northeast Canadian Cordillera. Proc. Fifth Cdn. Conf. on Earthquake Eng. (this volume).

STRONG-MOTION ARRAY QUESTIONNAIRE

1. Where is your array located and how long has it been operating?

   See enclosures

2. Please describe your array, in terms of the type and number of instruments, their spacing, their triggering, their recording means (film, tape, or disc; analog or digital), and their foundation and housing.

   See enclosures

3. Describe the nature of the data you have obtained, in terms of the number of events recorded, their range of magnitudes, and their distances from the array.

   Only records of significance are the suite captured for the Saguenay Earthquake of 25 November, 1988.

4. What means were used to characterize the site conditions?

   "Free-field" sites were chosen as much as possible.

5. If you were to establish a new array, what means would you
   now use to characterize site conditions?

   Continue to choose "free-field" sites.

6. What lessons have been learned

   ● regarding the operation of the array?

     - twice annual maintenance of photographic
       SMA's is essential.

   ● regarding ground response to earthquakes?

     - very useful data set to work on ground motion
       attenuation in Eastern North America (ENA)

7. Can you comment on the relevance of ambient vibration
   measurements and forced vibration testing?

8. ADDITIONAL COMMENTS AND ADVICE (please use additional pages
   if desired)

Thank you!

_____
Name *Philip L. Munro*

(613) 995-4669

STRONG-MOTION ARRAY QUESTIONNAIRE

1. Where is your array located and how long has it been operating?

   Location: Entire Republic of Costa Rica

   Time of operation: Since oct. 1984.

2. Please describe your array, in terms of the type and number of instruments, their spacing, their triggering, their recording means (film, tape, or disc; analog or digital), and their foundation and housing.

   Type of Instrument: SMA-1 & SSA-1 Kinemetrics (23 and 2 respectively)

   Triggering: 1% g.

   Recording means: 70 mm film for the SMA-1 and micro chip for SSA-1.

   Housing: Fiber glass Refuges (19)
             Sunken concrete box (1)
             Concrete pedestal with metalic cover (1)
             In buildings (2)

3. Describe the nature of the data you have obtained, in terms of the number of events recorded, their range of magnitudes, and their distances from the array.

   Number of events recorded: 17

   Range of magnitude: from 3.7 to 6.3

   Distance from arrang: min 9 km.
                           max 240 km.

4. What means were used to characterize the site conditions?

   Seismic retraction test for depth of about 30 meters near the station sites.

5. If you were to establish a new array, what means would you now use to characterize site conditions?

Seismic refraction device of more range and increased number of test location

6. What lessons have been learned

● regarding the operation of the array?

The maintenance of instruments becomes critical for tree held stations in the subduction zone of Central America. Adverse climate conditions.

● regarding ground response to earthquakes?

In the first years of operation several stations were relocated because of lack of proper information on the local soil conditions.

7. Can you comment on the relevance of ambient vibration measurements and forced vibration testing?
Convenient in order to have an upper limit on stiffness carachteristics for instrumented buildings.

8. ADDITIONAL COMMENTS AND ADVICE (please use additional pages if desired)

Thank you!

Dr. Guillermo Santana B.
Name

STRONG-MOTION ARRAY QUESTIONNAIRE

1. Where is your array located and how long has it been
   operating?
   a) One array on the monument of Parthenon in Athens,
      Greece. Is operating since 1986
   b) Six arrays on Dams* around Greece. They are installed
      since the construction (10-15 years ago) of the
      respective dam but they are operating only relatively
      lately, due to various difficulties (moisture, cabling etc.
      etc.)
   c) One array on the telecommunications tower in major
      Athens. It is operating since 1985.

2. Please describe your array, in terms of the type and
   number of instruments, their spacing, their triggering, their
   recording means (film, tape, or disc; analog or digital),
   and their foundation and housing
   a) CRA-1 Central Recording Accelerograph, with 12 FBA-11
      Uniaxial Force Balance Accelerometers, full scale ± 1g, the
      pick-ups are mounted on various parts of the monument and on
      the foundation ground. TS-3 triaxial seismic trigger at
      level 0.005g. Recording on photographic film. The CRA-1 is
      housed under the staircase of the monument.
   b) ● Mornos dam; two SMA-1, trigger level 0.005 g
      ● Assomaton dam; six SMA-1, trigger level 0.01g; One
        FBA-13DH; four PAR-400 peak accelerometers
      ● Sfikias dam; six SSA-302, trigger level 0.01g; four
        PAR-103 peak accelerometers
      ● Polyfytou dam; two SMA-1, trigger level 0.01g
      ● Kremasta dam; two SMA-1, trigger level 0.01g
      ● Pournariou dam; four SA-302, trigger level 0.05g;
        one SMA-1, trigger level 0.01g; four PAR-103 peak
        accelerometers

---

* They are operating under the Greek Public Power
  Corporation jurisdiction

c) Three SMA-1, full scale ±1g, vertical trigger on
   the basement of the building

3. Describe the nature of the data you have obtained, in
   terms of the number of events recorded, their range of
   magnitudes, and their distances from the array.
   Very few and poor data (almost none!). The reasons are:
   distant events and bad condition of the instruments.

4. What means were used to characterize the site conditions?
   a) It is a sound rock
   b) There are available ample bore hole data and geolgoical
      investigation reports
   c) There are available bore hole data

5. If you were to establish a new array, what means would
   you now use to characterize site conditions?
   Microtremor measurements and bore hole data. Also,
   general topographic and geological conditions of the major
   area

6. What lessons have been learned
   ● regarding the operation of the array?
     Needs much maintenance
     The array under (a) above, was, two times up to now,
        severely damaged due to lightnings; the sensors are exposed
        bare, without any other protection. Almost, all of the IC
        were damaged both of the 12 sensors and of the central unit.
     We are facing difficulties in the connecting cables and in
        the triggers.
     There are cases in which connecting cables among the
        various parts of the array and with the mains were brocken
        or disconnected due to ignorance or negligence
   ○ regarding ground response to earthquakes?
     All our arrays are on buildings and structures

7. Can you comment on the relevance of ambient vibration
   measurements and forced vibration testing?
   We have carried out more than one hundred ambient
   vibration measurements* and very few forced vibration
   testing, and therefore we can not comment. But, ambient
   vibrations present always a "stiffer" situation than it is
   in the reality.

8. ADDITIONAL COMMENTS AND ADVICE (please use additional
   pages if desired)
   Need more data about ground conditions, or the structure,
   if the array is on structure.
   You have to use well trained personnel and to take into
   account many parameters, as for example, where you will put
   the trigger, sensitivities, etc.

                        Name

                  Panayotis Gr. Carydis
              Professor of Earthquake Engineering

---

* please, refer to the enclosed paper

1.

Small Amplitude Vibration Measurements of Buildings Undamaged, Damaged, and Repaired After Earthquakes

Panayotis Carydis, M.EERI, and Harris P. Mouzakis

Ambient vibrations provided the means to measure dynamic properties of reinforced concrete undamaged buildings, damaged and repaired after the destructive earthquakes of February 24,1981,in the major area of Athens and in Central Greece. Each fundamental period is given as function of the number of stories, the height of the building, the dimensions of its plan and the percentage of shear walls. The shape of the deformation of the vertical centerline and the associated percentage of critical damping resulted also from the measurements, which in addition proved that for the damaged buildings the vertical centerline presents a discontinuity at the level where the damages are concentrated.For the repaired buildings this line becomes smooth.

INTRODUCTION

Ambient vibrations having a small amplitude,arise from many disturbances of the environment, such as wind, distant waves of the sea, influence of the sun, distant storms, various microtremors of the Earth crust, traffic and the various vibrations caused by the activities of man.

These disturbances have a wide range of frequencies, thus many normal modes of structures can be excited by them. Exploiting these inherent small amplitude vibrations of buildings, their fundamental period and the deformation of their vertical centerline can be determined. The method applied for the determination of damping differs either at the stage of data reduction or at the stage of measurements – particularly at the excitation of the structure for the production of free vibrations. In the present measurements the latter excitation is carried out by specially trained, one or two, men.

Modern earthquake resistant regulations take into account the fundamental period of the structure to determine earthquake loads. The deformation of the vertical centerline in the fundamental mode is important for the determination of the distribution of lateral earthquake loads with height. Damping is also important to determine the structure's earthquake response.

The degree of deterioration or damage of a structure may,to a certain extent, be determined by field measurements of its vibrations. Changes in the predominant periods of vibration as well as discontinuity along the

height in the deformation of the vertical centerline arise from discontinuity of stiffness, which in most cases is due to damage of either the structural system, secondary elements (mainly partitions) or both.

The dynamic characteristics (fundamental periods, modal shapes and corresponding damping values) of a building depend on many factors, the most important of which are:

(1)   The particular structural system, that is the vertical (columns, shear walls), the horizontal (beams, slabs) elements and the way they are connected.

(2)   The material of the structural system, that is concrete, steel, brick, stone etc. and/or a combination of these.

(3)   The mass of the building and how it is distributed in height and plan.

(4)   The geometry of the building (height, dimensions of the plan) and the various irregularities, if any, in height and plan of the various stories.

(5)   The infill panels and non structural elements of the building, their construction and attachment to the structural system.

(6)   The particular kind of soil as well as the type of foundation (isolated footings, shallow foundation, stiff or deep foundation).

(7)   The age of the building, the quality of maintenance and the level and duration of its vibrations due to its use and its environment.

(8)   The extent, location, and severity of damage along the height and plan of the building and the damaged elements (slabs, beams, columns, shear walls, infill panels) importance.

(9)   In case of repair, alteration, or strengthening, the kind, the extent and material of repair in relation to the kind, the position and the percentage of existing failures.

(10) The amplitude of the vibration of the building during measurements in relation to previously experienced amplitudes.

The last factor is particularly important, since the amplitude of the vibration relates directly to the prior stress level and the degree of yielding which in turn directly influences the response of the structure, through intensely nonlinear behavior. For the same reasons the results of field measurements only have meaning for corresponding amplitudes of vibration. For the buildings discussed below the materials are in their linear range, strains being too small to develop nonlinear properties.

During the earthquake response of a building its dynamic characteristics change abruptly enough and its model for the analysis should be changed accordingly, as shown schematically in Figure 1. For small amplitude

translations where there are only compressional stresses at the level of foundation, one may consider the frame fixed at its base, Figure 1b,which coincides with the typical way of analysis; for translations of a greater amplitude, however, where tensional stresses are created at the level of foundation, the frame must not be considered as fixed at its base and the model for the determination of the member forces, displacements etc. becomes complicated, Figure 1c,1d.

FIGURE 1. The amplitude of the translations of the stories affect not only the behavior of the members (linear-non linear) but also the model of the structure: (a) elevation of a typical frame; (b) for small amplitudes the frame may be considered as fixed at its base - the typical model for analysis; (c),(d) a magnified and exaggerated response of the frame during a strong earthquake which produces tensional vertical stresses at the foundation level.

If the analysis includes soil structure interaction, particularly with a non linear soil response, the stresses and strains computed will certainly be closer to reality, however the computational difficulty is substantially increased. Clough and Huckelbridge (1977) found that the stress in structures not fixed at their base during strong earthquakes is smaller than that calculated with the hypothesis of fixed base.

The dynamic characteristics of the structures to which the various earthquake resistant regulations refer should differ depending on the particular method of analysis that will be applied; for example, for the method of equivalent static load the fundamental period should most probably correspond to some mean value of those that the structure will exhibit during its earthquake response. Notwithstanding this fact the relations used by most regulations for the calculation of the fundamental period are to a great extent based on small amplitude vibrations similar to those that are reported herein.

The shape of the deformation of the vertical centerline due to horizontal translations of the floor diaphragms is influeced by the above mentioned factors, mainly, in order of importance: (8),(9),(4),(5),(1), (6),(3),(2),(7) and (10). Damping is influenced by the following factors, again mentioned in order of importance: (10),(2),(8),(9),(5),(7),(1),(6), (3) and (4).

With all these comments and with several reservations as far as the mean values are concerned (due to the small population of each case) the

results of the measurements follow.

NOTATION

In the text the various symbols used have the following meaning,unless otherwise noted each time the symbol is used.

A: cross-section of cantilever (m^2)

B: width of building perpendicular to the considered direction of vibration (m)

β_i: regression coefficient

D: length of building along the considered direction of vibration (m)

E: modulus of elasticity of the material (MPa)

E(f): expected value of f

ζ: damping ratio

G: modulus of elasticity in shear (MPa)

H_o: height of building from its foundation level (m)

H: height of building above ground level (m)

I: moment of inertia of cross section (m^4)

K: mean value of story indices (KNm^{-1}) (story index=sum of stiffness of the columns of the story under the shear building hypothesis)

k: cross section form factor

m: mass distributed along the height of the structure (kgm^{-1})

M_k: lumped mass at the k-th level (kg)

N: number of stories above ground level (not necessarily the foundation level)

ν: Poisson's ratio

ρ: ratio between the cross section of the shear walls and the sum of the cross sections of shear walls and columns, mean value of the different stories

ρ': ratio between the cross section of the shear walls whose lenght is along a particular direction and the area of the plan of the building, mean value of the different stories

r: correlation coefficient

σ: standard deviation

T_f: fundamental period of structure for deformation in flexure (sec)

T_i: i fundamental period of structure (sec)

T_s: fundamental period of structure for deformation in shear (sec)

ω_n: circular frequency of the n mode (sec^{-1})

INSTRUMENTS USED FOR THE MEASUREMENTS,
METHOD OF MEASUREMENT AND METHOD OF DATA REDUCTION

Two systems were used to measure and record the vibrations of buildings depending on the particular needs and the availability of transportation.

The first system, Figure 2, is a one-channel VM-1 (Vibration Monitor-1) by Kinemetrics;it has an integrated amplifier system, a thermal pen recorder and low pass filters. The electromagnetic accelerometer EM-4, from the same manufacturer, with a maximum sensitivity of $10^{-2}g$ is used as pickup. The second system, Figure 3, is a four-channel VSS-1(Vibration Survey System) by Kinemetrics with SS-1 (Ranger Seismometer) electromagnetic velocity transducers, and a separate signal amplifier which has integration and differentiation circuits as well as a series of low pass filters all

INSTRUMENTS USED FOR THE MEASUREMENTS,
METHOD OF MEASUREMENT, AND METHOD OF DATA REDUCTION

Two systems were used to measure and record the vibrations of buildings,
depending on the particular needs and the availability of transportation.

FIGURE 2. The one-channel "Vibration Monitor VM-1" by Kinemetrics

FIGURE 3. The four-channel "Vibration Survey System VSS-1" by Kinemetrics

Photos courtesy of Kinemetrics/Systems

integrated in the instrument SC-1 (Signal Conditioner). The signals are
recorded on analog magnetic tape (FM) recorder and light beam oscillograph.

     The selection of positions and directions for the tranducers in the
building along the height and in the plan depends on the direction of the
vibrations to be measured and on the discontinuities of stiffness and
distribution of mass, in height and plan, as well as the extent and kind
of damage and/or the repair and strengthening.

     Torsional vibration around a vertical axis is likely for each building
in addition to translation along its two main axes. For the determination

of these vibrations, measurements were taken at various levels of the building and along its two main axes. For example, for a building of N stories without discontinuities, vibration measurements were taken at the following levels:

    (1)   At the top story; measurements of ambient vibrations and free vibrations after excitation with the "man power" technique, in order to find damping.

    (2)   At intermediate stories, the choise of which depended on the total number of stories N. This measurement was to determine whether the period of vibration was constant along the height of the building and for determining the deformation of the vertical centerline of the building along the height, and

    (3)   On the ground and along the three directions – length, width and vertical – inside and outside, but near the building plan, in order to determine the degree of soil structure interaction.

For building with an open first story (termed "Pilotis") measurements were also taken on the first story level to determine the deformation of the vertical centerline of the building.

The instruments used are very sensitive: they can clearly record accelerations of the order of $10^{-5}g$ (receiver 10^{-2} g and amplifier 10^{-3}). This sensitivity is necessary since the vibrations measured were mainly of very small amplitude.

For measurement of translational vibrations of the buildings, the transducers were placed at each level in such a position as to avoid the influence of torsional vibrations. The center of rotation was chosen as such a position. This is the best selection that can be made even though it is not free of torsional motions a multi – story building. This is due to: a) the difficulty in locating a purely translational point and b) the influence of the other stories. The measurements were taken along the two main axes of the building. It must be noted that the "vertical centerline" of multi-story buildings is not always a straight, vertical line, although its deformation from equilibrium is presented as if the centers of gravity were on a vertical line.

The measurements were taken at times specially chosen so that the movement of people in the buildings, the traffic and the wind were minimized. Care was taken in all the measurements so that there would be control of the variability of the vibrations. The vibrations recorded were only those that were permanent and not due to temporary causes. This is of particular importance in cases where only one recording channel was used and two consecutive measurements were separed by a time interval. The use of the low pass filters was very important in facilitating measurements and distinction of the fundamental period from other periods.

When the buildings were cracked, the number of points where measurements were taken was incereased in the vicinity of the cracks. A difficulty was encountered here, since the center of rotation (known from

the data of the design and from the drawings) was considerably moved and not easy to calculate.

The "zero crossing" method of K.Kanai (1961) was used for data reduction, according to which the sample of the measurements must be 120 sec. The analysis was done by hand and by a small, portable programmable calculator. The histogram of the time intervals between two consecutive zero crossing points of the vibration curve was calculated for the 120 seconds of the record. The reader is refered to Mouzakis (1980) for the determination of the second fundamental period, as well as for the computational procedure. The mean period and its standard deviation were found next. For the calculation of the damping the "man power" method was used, that is the excitation of the building by means of the inertial force exerted by one or two persons pushing against the building trying to follow the needle of the recorder. The damping ratio was calculated from the following free vibration of the building according to the relation:

$$\zeta = \frac{1}{2\pi n} \ \ell n \ \frac{x_n}{x_o} \tag{1}$$

The damping determined by the above method is of a rather small importance since it generally refers to small amplitudes of vibration and the friction damping (Coulomb damping) that is certainly developing during the earthquake response of structures is not observed and therefore not considered in this calculation.

The procedure results in the reduction of the field data to the following items, that are of particular interest:

● Basic information about the use of building in plan and along the height,its age,exposure to previous disturbances, etc.

● Data about the geometry of the building (number of stories,plans and sections with the positions and the dimensions of the parts of the structural system as well as of the infill panels), the materials and the degree of completion of the building when the measurements took place.

● Data about the soil.

● The lowest periods of the building along the two main directions the plan with the corresponding maximum amplitudes.

● The maximum simultaneous amplitudes of deformation of building and along the two horizontal directions of the plan as well as the maximum vertical amplitudes of ground and building in selected points of building and ground.

● The damping in each direction, with the corresponding amplitude.

● Data about the climatic conditions, the traffic and generally the conditions of the environment and the use of the building during measurements.

CLARIFICATION OF SOME OF THE TERMS AND SYMBOLS USED

The number N corresponds to the number of levels of the building and is equal to the number of degrees of freedom of motion in each direction. When there is a mezzanine with peripheral beams it is also considered as a story.

Depending on the dynamic deformation curve, vertical cantilevers with distributed mass and constant stiffness (cross section that does not change along the height) are either shear (s) or bending (f) cantilever beams.

SHEAR CANTILEVER BEAM

The circular frequencies, $\omega_{s,n}$ of the various normal modes n, are given by the following formula:

$$\omega_{s,n} = (2n-1) \; \frac{\pi}{2H} \; \sqrt{\frac{kG}{\rho_1}} \quad (\text{sec}^{-1}) \; , \; n=1,2,3,\ldots \tag{2}$$

where H: the height of the cantilever beam, in meters, from its base
       to its free end
   k: cross section form factor according to Blevins (1979); it is
       equal to
       $k=6(1+\nu)/(7+6\nu)$ for circular cross section
       $k=10(1+\nu)/(12+11\nu)$ for rectangular cross section
         where ν is Poisson's ratio
   ρ_1: the mass density of the material (kg m^{-3})

The period of free vibration of the normal modes of shear cantilever beam is independent of the area and the moment of inertia of the cross section of the cantilever.

The following relations are also valid for shear cantilever beam:
$\omega_{s,2}=3 \; \omega_{s,1}$, $\omega_{s,3}=5 \; \omega_{s,1}$.

BENDING CANTILEVER BEAM

The circular frequencies of the various normal modes are given by the following formulae:

$$\omega_{f,n} = \frac{a_n}{H} \; \sqrt{\frac{EI}{m}} \; = \frac{a_n}{H} \; \sqrt{\frac{EI}{\rho_1 A}} \quad (\text{sec}^{-1}), \tag{3}$$

$$a_1=3.516, \; a_2=22.034, \; a_3=61.696$$

where H: the height of the cantilever beam, in meters, from its base
       to its free end
   ρ_1: the mass density of the material (kg m^{-3})

The period of vibration of the normal modes for the case of bending cantilever depends on the cross section of the cantilever (area and moment of inertia).

The following relations are also valid in the case of bending cantilever beam:

$$\omega_{f,2}=6.28\ \omega_{f,1}, \quad \omega_{f,3}=17.6\ \omega_{f,1}$$

OTHER CLARIFICATIONS

The terms length (D) and width (B) used are not related to the stiffness of the buildings but refer to the longer and the smaller dimension of their plan respectively; therefore, when the longer dimension of a building is mentioned, this does not necessarily mean that along this direction the building has its maximum stiffness. In the case of a square plan, these terms lose their meaning. The separation of measurements into measurements along the length and measurements along the width proved to be of rather small importance in this analysis. It has only been observed to be important when the greater the dimension along one direction the more the building tends to have shear behavior along this particular direction, in relation to the other direction where the dimension of the building is smaller.

All the buildings measured had reinforced concrete load bearing systems. The vertical elements of these load bearing systems were columns or shear walls or combinations of both.

In the present investigation as shear walls are considered those vertical structural elements which are strained and stressed in their plane mainly in shear, having a cross section of minimum dimensions 1.00×0.20 (m^2). The shear walls taken into consideration were only those having their own foundation; deep horizontal beams and walls supported by columns were therefore excluded.

BUILDING CLASSIFICATION AND DESCRIPTION

A total of 110 buildings were measured. A file is maintained in the Laboratory for Earthquake Engineering of the N.T.U. of Athens for most of these buildings, with the basic structural drawings, photographs, and information about damage and repair. All these buildings are free standing, have a rectangular plan and are of reinforced concrete. About 90 of these buildings are located in the central area of Athens. The dynamic properties of these buildings were measured before the destructive earthquakes of February-March 1981 which struck Central Greece. For more information about these earthquakes, as well as about the damages to engineering structures, building code and practice, see the relevant reconnaissance EERI/NRC report by Carydis et al (1982). After these earthquakes , measurements were made for about 25 damaged buildings (a few in central Athens area, coinciding with the previously measured buildings, and the most in the epicentral region, not measured before). Only 20 of these buildings could be measured after their repair.

The measured buildings were classified in nine categories according to their use as it is briefly presented in Table 1.

Files are maintained for each of these buildings: the location, the code number according to use, the number of stories above and below ground surface, the height above ground, the depth of foundation, the floor area, the dimensions of the plan, a destription of the structural system, the material of partitions and the ratio ρ (see notation) for both of the main

T A B L E 1. CLASSIFICATION OF BUILDINGS ACCORDING TO THEIR USE		
Code	Use of Building	No of measured buildings
A	Apartments with an open and free of use first story (on "pilotis")	34
B	Apartments on "pilotis" and a mezzanine	4
C	Apartments with brickwall partit.all over the height	40
D	Offices all over the height	17
E	Offices with a mezzanine	8
F	Apartments with shops at the first story	2
G	Offices with shops at the first story	1
H	Hotels	2
I	Hospitals	2
	T o t a l	110

directions of the plan. For damaged buildings brief data is kept about the
kind and extent of damages, based on a damage classification presented in
Table 2; for repaired buildings, a brief description of the repair and the
extent of its complition when measured, it is also given,Laios (1982).

T A B L E 2. DAMAGE CLASSIFICATION				
	DAMAGES:	SIMPLE CRACKING (a)	EXTENDED CRACKING (b)	SEPARATION (c)
1	Infill walls	1a	1b	1c
	DAMAGES:	SIMPLE CRACKING (a)	LOCAL DISORGANIZATION (b)	DISCONTINUATION (c)
2 Horizontal elements	1 Beams	21a	21b	21c
	2 Slabs	22a	22b	22c
3 Vertical elements	1 Columns	31a	31b	31c
	2 Short Columns	32a	32b	32c
	3 Walls	33a	33b	33c

All buildings were classified in three major groups with respect to
the continuity of their stiffness and mass along the height, after the
measurements were completed:

(1) Buildings with continuity of stiffness and mass and a bare
     structural system (no columns "planted" on beams, small or no
     variation of the height of the stories and the dimensions of the
     vertical and horizontal elements of the structural system from
     story to story, small or no variation of the plan of the stories).
     These are office buildings or buildings for multi-story shops and

parking. There are very few or no partitions that may add
stiffness and/or mass to the structural system. In this category
the buildings of codes D,E and G are included.
This group is named "office buildings".

(2) Buildings with apparent continuity of their stiffness and mass
with many infill walls (brickwalls in all stories as for example
in apartment buildings). Any discontinuity of both stiffness and
mass of the structural system should be small, compared to that
of brickwalls, or other relevant partitions. In this category
the buildings of codes C and I are included.

This group is named "apartment buildings with constant stiffness".

(3) Buildings with stiffer and heavier upper stories compared to the
first story. This discontinuity of their stiffness and/or mass
may be due either to the structural system (columns or walls
planted on beams of the first story, walls supported on columns
of the first story, higher first story compared to upper stories,
smaller cross sections of columns and beams of the first story
compared to those of the upper stories, reduction of the plan of
the first story) and/or to the infill walls (considerable reduction
of infill walls in the first story, as for example in the case of
apartment buildings whose the first story is an open space or
shops). The coexistence of both these reasons of discontinuity is
very common. In this category the buildings of codes A,B,F, and
H are included.
This group is named "apartment builidngs on pilotis".

With the discontinuity of stiffness obvious for cracked buildings, in
order to facilitate comparison, such damaged buildings were classified in
the same groups as they would have been if the building was without damage.

PRESENTATION OF RESULTS OF MEASUREMENTS OF UNDAMAGED
AND DAMAGED BUILDINGS

Following the method of data reduction described earlier, the mean
period and its standard deviation, the deformation shape for each one of
the lowest modes of vibration, as well as the mean value of the damping
for each building were subject to further processing. The latter one was
carried out only to those measurements which presented very small errors.
The criterion set was the standard deviation of the corresponding period
(first and second mode) of each building to be less than 0.02 to 0.03 sec.

The method of processing and the results obtained are given in this
section.

UNDAMAGED BUILDINGS

Relation Between Period and Number of Stories or Height of Building.
A linear relationship between the mean fundamental period T as
calculated previously and the number of stories N, or the height H of the
building, was computed, for the case of measurements before the earthquakes

(undamaged buildings). This has the following form:

$$T=a_1N+b_1 \quad \text{or} \quad T=a_2H+b_2 \tag{4,5}$$

For all buildings that were measured and for the buildings included in each of the above defined three groups, the values of a_1,b_1 and a_2,b_2 of Eqs. 4 and 5 were found by use of a least squares regression analysis. The resulted relationships between mean period and number of stories, the corresponding Figure number (4 to 7) for the respective regression lines and their correlation coefficients r are given in Talbe 3.

T A B L E 3. RELATIONSHIP BETWEEN MEAN FUNDAMENTAL PERIOD AND NUMBER OF STORIES N (undamaged buildings)

Building Group	Relationship	r	Corresp. Figure No
All Buildings	T=0.043N+0.107	0.782	4
Office Buildings	T=0.045N+0.207	0.786	5
Apartments with constant stiffness	T=0.032N+0.145	0.750	6
Apartments on pilotis	T=0.049N+0.028	0.923	7

The relationship between mean period and building height are given in Table 4.

T A B L E 4. RELATIONSHIP BETWEEN MEAN FUNDAMENTAL PERIOD AND BUILDING HEIGHT (undamaged buildings)

Building Group	Relationship	r
All Buildings	T=0.012H+0.131	0.785
Office buildings	T=0.013H+0.216	0.783
Apartments with constant stiffness	T=0.011H+0.144	0.570
Apartments on pilotis	T=0.013H+0.107	0.732

It follows from the comparison of relationships shown in Figures 6 and 7 that the constant term of the first relation (Fig.6) is considerably larger than the one of the second relation (Fig.7). This constant term must represent the influence of the soil. This means that the influence of the soil is far larger in an apartment building with constant stiffness (and more stiff building) than in a pilotis building, which has a more flexible first story. This conclusion was expected, since the period of vibration of a completely stiff building is approximately the same with the period of vibration of the ground, Carydis (1972).

Results on Modal Shapes and Damping

The ratio of the period of the first normal mode to the period of the second normal mode was estimated to be approximately equal to three. This means that apartment buildings without pilotis can - with a good approximation - be considered as shear cantilever beams with distributed mass and stiffness. However, for office buildings the ratio of the period of the first normal mode to the period of the second one is considerably higher than three and quite often is approximately equal to 6.3 for

FIGURE 4. Relationship between
fundamental period and number of
stories for all undamaged buildings.

FIGURE 5. Relationship between
fundamental period and number of
stories for undamaged office
buildings.

FIGURE 6. Relationship between
fundamental period and number of
stories for undamaged apartment
buildings with constat stiffness.

FIGURE 7. Relationship between
fundamental period and number of
stories for undamaged apartment
buildings on pilotis.

oscillation along the small direction of the building, which means that
some slender office buildings behave clearly like bending cantilever
beams.

For each of the mentioned three groups of buildings, the mean value
of the first and second normal shapes were calculated. Each one of these
shapes was normalized (with a unit displacement at the top), and the
respective comparison among the three groups is given in Figure 8.

It was measured that the acceleration and displacement in the second
normal mode of some apartments on pilotis were larger at the second story
than at the top one. The behavior, however, of this group of buildings
resembles, due to the stiffness discontinuity in the first story,   that
of another building with damages in its first story, Matsushima and
Carydis (1969).

FIGURE 8.   Comparision of the first and second modal
shapes among the three groups of buildings:
————— Office buildings
—·—·— Apartment buildings on pilotis
————— Apartment buildings with constant stiffness

The measurements of the ambient vibrations were performed also on the
ground, around and near the plan of each building,the pickups were placed
at the vertical and horizontal direction. From the measurements on the
ground it was verified that building and foundation soil constitute an
integrated system of vibration and therefore of response to the earthquake.
It has been observed that the vertical vibration of the ground near the
"long" and the "short" side of the building, almost coincided (in phase
and frequencies) with its horizontal vibration along the "short" and

"long" axis respectively. This concidence was more accurate in the case of soft ground and buildings with almost constant stiffness. In some cases in which the ground water table was quite high, the horizontal vibrations on the ground were very much reduced, instead, the vertical ones were more pronounced.

The vertical vibrations of structures are of great interest, particularly in cases of measurements taken near the columns having their own foundation. It appeared that from a certain height upwards, the vertical vibrations of the buildings were not directly related to the vertical vibrations of the soil, this however can be explained by the transmissibility of vibrations of each buildings.

Finally, as far as the damping is concerned it was observed that the younger the building the higher the damping ratio, which may be due to the fact that the materials and the member connections are still young and have suffered no fatigue due to the use of the building (e.g. separation of infill walls from load bearing system, small fissures and cracks due to the previous deformational history of the building). This means that with larger amplitudes, than the ones that the structure has already experienced, new damping mechanisms will be activated and the observed damping will be higher. The value of damping found here by the application of the "man - power technique" was less than 3% in all cases.

Relation Between Period, Heigh of the Building, Dimension B and Shear Walls Ratio ρ for All Apartment Buildings.

The following statistical models were used for this correlation:

$$T_i = \beta_0 H_i^{\beta_1} B_i^{\beta_2} (H_i + \rho_i B_i)^{\beta_3} 10^{e_i} \qquad i=1,2,\ldots,n \tag{6}$$

$$T_i = \beta_0 (H_i/B_i)^{\beta_1} (1+\rho_i)^{\beta_2} 10^{e_i} \qquad i=1,2,\ldots,n \tag{7}$$

$$T_i = \beta_0 (H_i/\sqrt{B_i})^{\beta_1} (1+\rho_i)^{\beta_2} 10^{e_i} \qquad i=1,2,\ldots,n \tag{8}$$

$$T_i = \beta_0 H_i^{\beta_1} B_i^{\beta_2} 10^{e_i} \qquad i=1,2,\ldots,n \tag{9}$$

where n is the number of the sample, $E(e_i)=0$ and $E(e_i e_j)=\delta_{ij} \sigma^2$. From the above relations (6) up to (9) it follows that:

$$\log T_i = \log \beta_0 + \beta_1 \log H_i + \beta_2 \log B_i + \beta_3 \log(H_i + \rho_i B_i) + e_i \qquad i=1,2,\ldots,n \tag{10}$$

$$\log T_i = \log \beta_0 + \beta_1 \log(H_i/B_i) + \beta_2 \log(1+\rho_i) + e_i \qquad i=1,2,\ldots,n \tag{11}$$

$$\log T_i = \log \beta_0 + \beta_1 \log(H_i/\sqrt{B_i}) + \beta_2 \log(1+\rho_i) + e_i \qquad i=1,2,\ldots,n \tag{12}$$

$$\log T_i = \log \beta_0 + \beta_1 \log H_i + \beta_2 \log B_i \qquad i=1,2,\ldots,n \tag{13}$$

Using the regression method, the following regression lines were determined:

$$T_i = b_0 H_i^{b_1} B_i^{b_2} (H_i + \rho_i B_i)^{b_3} \qquad i=1,2,\ldots,n \tag{14}$$

$$T_i = b_0 (H_i/B_i)^{b_1} (1+\rho_i)^{b_2} \qquad i=1,2,\ldots,n \tag{15}$$

$$T_i = b_0 (H_i/\sqrt{B_i})^{b_1} (1+\rho_i)^{b_2} \qquad i=1,2,\ldots,n \tag{16}$$

$$T_i = b_0 H_i^{b_1} B_i^{b_2} \qquad i=1,2,\ldots,n \tag{17}$$

where b_0, b_1, b_2, b_3 are unbiased estimators of $\beta_0, \beta_1, \beta_2, \beta_3$ respectively.

Particularly for a sample n=66 it follows, from relation (14) that:
$\log b_0 = -1.3452 \rightarrow b_0 = 0.045$, $b_1 = 0.8827$, $b_2 = -0.1096$, $b_3 = -0.1083$

From relation (15) it follows that:
$\log b_0 = -0.58614 \rightarrow b_0 = 0.259$, $b_1 = 0.4856$, $b_2 = 0.1429$

From relation (16) it follows that:
$\log b_0 = -0.99741 \rightarrow b_0 = 0.101$, $b_1 = 0.745$, $b_2 = -0.185$

From relation (17) it follows that:
$\log b_0 = -1.33384 \rightarrow b_0 = 0.046$, $b_1 = 0.7727$, $b_2 = -0.1242$

Then, the regression lines are defined by the following relations:

$$T = 0.045 \, H^{0.883} \, B^{-0.110} \, (H+\rho\beta)^{-0.108} \tag{18}$$

$$T = 0.259 (H/B)^{0.486} \, (1+\rho)^{0.143} \tag{19}$$

$$T = 0.101 (H/\sqrt{B})^{0.745} \, (1+\rho)^{-0.185} \tag{20}$$

$$T = 0.046 \, H^{0.773} \, B^{-0.124} \tag{21}$$

Several methods for selecting the best regression relationship have been used. All of them, however, do not necessarily lead to the same conclusions. The residual mean square estimates the variance σ^2, and an objective method consists in choosing the relation with the lowest residual mean square. As such, relations (6) and (9) were found. Relation (9) is finally chosen instead of (6) because it is simpler, although relation (6) has a slightly lower residual mean square. The proposal for all apartment buildings is relation (21).

DAMAGED BUILDINGS
     First, second and higher modes of vibration (period and shape) as well as the percentage of damping were measured for each of the 25 buildings studied after the earthquakes and are kept in NTU files. There are also sketches and description of damages according to the classification in Table 2. Each of these buildings is identified with a number 1 to 25. For example, a front view of the damages along one direction of buildings No 1 and 11 are shown in Figures 9b and 10b respectively, Laios (1982). In Figures 9 and 10 appear also the first and second modes along the "Long" and "Short" direction of the building.

     It must be noticed here that some modes of higher order appeared in some damaged regions of the buildings, parts of buildings showed a rigid body response. Torsional vibrations also appeared and the measurements became cumbersome and time consuming besides the risks involved, since the buildings were evacuated due to their damages.

Fundamental Periods

The damaged buildings had high values (double, as an average) of their fundamental periods compared to similar undamaged buildings measured earlier by the same instrument in the area of Athens. The regression analyses for the relation between mean fundamental periods and number of stories showed low correlation coefficients. The extent of damages in the buildings considered in this regression analysis are of class (b) (see Talbe 2). It was found for apartment buildings with constant stiffness:

$$T=0.077N+0.109$$
$$r=0.489 \tag{22}$$

And for apartment buildings on pilotis:

$$T=0.038N+0.399$$
$$r=0.496 \tag{23}$$

The fundamental periods of the damaged buildings are certainly related to their stiffness before the earthquake, however, they are even more related to the damage of their load bearing system, as well as of their infill panels.

For apartment buildings on pilotis the percent increase of the fundamental period of the damaged buildings is calculated, by means of a regression analysis to be:

$$T\%=-6.97N+153.16$$
$$r=-0.329$$

This implies that maximum damage for this series of earthquakes (near field effect, high frequency content of ground motion) appears in low rise buildings, while for buildings of $N \approx 153/7 \approx 22$ stories there should be little damage.

It was found that buildings with damage to several stories (in beams, columns, walls, slabs and infill masonry) have higher fundamental periods than buildings with damage of higher degree (deterioration etc.) but concentrated in a few particular points. The second fundamental period is not considerably increased, and therefore it is reasonable to assume that lowrise buildings of 4-6 stories were not excited at the second normal mode by these earthquakes, hense the participation of that normal mode, in the earthquake stresses considered, was small.

Modal Shapes

It was found that the shear cantilever beam model does not represent very well buildings with damage over the height and many cracks in slabs and beams. The same is valid for buildings with considerable damage to the infill walls extending to a great height. Buildings with damage to only a few vertical elements satisfactorily follow the shear cantilever beam model. These conclusions follow from the ratios of the fundamental periods of the first normal mode to those of the second normal mode and from the shape of deformation of the vertical centerline resulting from measurements at various levels, Laios (1982).

The zero crossing point as well, as the maximum of the horizontal

deformation of the vertical centerline which corresponds to the second modal shape, are always found at lower positions than those of buildings without damage. The maximum appears near the area of damages. The ratio of this maximum amplitude divided by the amplitude of the top may be even larger than 2:1. It was observed that this ratio is usually larger in the direction of the longer of the two sides of the building. Some examples are presented in Figures (9a,c) and (10a,c), while the damages along the two directions of each building are almost equal.

Damping
The damping of these buildings does not seem to have changed very much from that of undamaged buildings. This is reasonable since the amplitude of the present measurements is small. Therefore, the results of the measurements of damping are of a rather limited value. The present values of damping (up to 3%) are valid for a future earthquake only if the amplitudes caused by that earthquake are smaller than those which caused the cracking of the building in a previous loading stage. Finally, there seems to be an intense nonlinearity in the values of the damping of cracked buildings.

In cases where many brickwalls have collapsed, the amount of energy absorbed by the remaining brickwalls was small, which explains the very small percentage of damping found - obviously for these small amplitudes of vibration.

MEASUREMENTS IN REPAIRED BUILDINGS

DESCRIPTION AND CLASSIFICATION OF REPAIRS
The various techniques that may be applied for the repair of a structure may or may not cause an increase of the stiffness of the repaired elements or of the total stiffness of the structure. There are techniques which do not cause an increase of the stiffness of the elements:

- Epoxy glues
- Replacement by elements of equal stiffness
- Addition of strengthening elements without virtual increase of the initial stiffness (e.g. flexible strengthening elements of metal)

As well as techniques that do increase stiffness:
- Concrete mantle or increase of dimensions
- Addition of new stiffening elements

The repairs may cause a change of the deformation of the vertical centerline of the structure (due to an increase of the stiffness of only some stories) or creat eccentricities if more stiff elements are eccentrically placed in the plan.

RESULTS
The various measurements taken after repair to find their influence on the stiffness gave rather consistent results. It was found, generally, that the fundamental period decreased considerably, for all the measured buildings. Where strengthening was also performed, the fundamental period was lower than for the respective undamaged building as is expected.

FIGURE 9. First and second normal modes of the damaged building no 1

FIGURE 10. First and second normal modes of the damaged building no 11

The vertical centerline was shaped like that of the undamaged case, as it is schematically shown in Figure 11, when the repairs were simple, that is without adding stiffening elements at isolated stories.

FIGURE 11. Second modal shape
— — — Damages in the lower story
———— After repair

It was observed that in some buildings on pilotis, and after the repair done with considerable strengthening of the two only lower stories, the deformation line along the height shows a singularity point at the third story. This means an increase of stresses at that particular point. There is a high possibility of damage at this point in a potential future earthquake.

CONCLUSIONS

Undamaged broad apartment buildings behave like shear cantilever beams, while slender office buildings behave like bending cantilever beams. The best expression for the fundamental period of apartment buildings is given by $T = 0.046 \ H^{0.773} \ B^{-0.124}$. The fundamental periods of damaged buildings are considerably increased, the large increase coinciding with low lise buildings for the case of the earthquakes considered. Higher rigid body modes appear in some parts of the buildings above the damaged level. The deformation of the vertical centerline of the damaged buildings shows a singularity in the level where the damages are concentrated. The repairs restored the periods and the modal shapes to the undamaged case. When buildings were strengthened with stiffening elements placed at some stories only, the deformation of the vertical centerline shows a discontinuity at the levels where these stiffening elements stop (top and bottom side of the element).

REFERENCES

Blevins D.R.(1979).Formulas for natural frequency and Mode Shape. Van Nostrand Reinhold Company, pp.492.

Carydis P.G.(1972). Ground Effect on Dynamical Characteristics of Structures. *Proceedings of the International Conference of Microzonation for Safer Construction Research and Application*. Seattle, Vol.II, pp. 771-787.

Carydis P.G.,N.R.Tilford,G.E.Brandov, and J.O.Jirsa (1982). The Central Greece Earthquakes of February-March 1981, A Reconnaissance and Engineering Report. *EERI/NCR, National Academy Press*, Washington, D.C.

Clough, R.W. and A.A.Huckelbridge (1977). Preliminary Experimental Study of Seismic Uplift of a Steel Frame, *U.C.Berkeley, EERC Report 77/22*.

Kanai K. and T.Tanaka (1961). On Microtremors VIII. *Bulletin of Earthquake Research Institute*, University of Tokyo, Vol.39.

Laios J.(1982). Vibration measurements of buildings with seismic damages and after repair. *Diploma thesis*, in Greek, Earthquake Engineering Laborary, N.T.University of Athens.

Matsushima Y. and P.G.Carydis (1969). Contribution to Aseismic design of Shear Structures. *Bulletin of the International Institute of Seismology and Earthquake Engineering*, Vol.6(1969), pp.103-142.

Mouzakis H.(1980). Vibration measurements of buildings without damages in the major area of Athens. *Diploma thesis*, in Greek,Earthquake Engineering Laboratory, N.T.University of Athens.

Pollard J.H.(1977). A Handbook of Numerical and Statistical Techniques, with Examples Mainly from the Life Sciences, *Cambridge University Press, Cambridge*.

National Technical University of Athens
Earthquake Engineering Laboratory
42 Patission Street
106 82 Athens,Greece

Department of Earthquake Engineering

धर्मं विना न किमपि साध्यम्

Our Ref. No. EQD/ARC/ 2657

दिनांक Date

Dr. A.R. Chandrasekaran
Professor

Sept. 19, 1989

Dear Brian,

   Your letter dated Aug. 25, 1989 reached Roorkee while I was on tour. Please find herewith the answers to the questionnaire.

   With best wishes,

Yours sincerely,

A.R. Chandrasekaran

Dr. B.E. Tucker,
Acting State Geologist,
Department of Conservation
Division of Mines and Geology
Division Headquarters
1416 Ninth Street, Room 1341,
SACRAMENTO, CA 95814
U.S.A.

Q.5. If you were to establish a new array, what means would you now use to characterize site condtions?

Ans. If funds and manpower are available, we would carry out Geo-Technical Investigations and atleast obtain one bore-log data.

Q.6. What lessons have been learned

(i) regarding the operation of the array?

Ans. Attenuation of peak values of response and shape of spectra.

(ii) regarding ground response to earthquakes?

Ans. August 1988 earthquake has given valuable information and detailed studies would throw interesting conclusions. The records have shown larger values of spectral response in short period range and a more rapid attenuation in longer period range as compared to shape of USNRC Spectra.

Q.7. Can you comment on the relevance of ambient vibration measurements and forced vibration testing?

Ans. May be useful to establish foundation characteristics. Not very relevent in Himalayan region.

Q.8. ADDITIONAL COMMENTS AND ADVICE (Please use additional pages if desired)

Ans. None

STRONG-MOTION ARRAY QUESTIONNAIRE

Q.1. **Where is your array located and how long has it been operating?**

Ans. There are Two arrays in operation in the Himalayan region of India. The third one is under installation. The first array in North West region in the State of Himachal Pradesh is in operation since 1983 and the second in the North East region is in the States of Assam and Meghalaya and is in operation since 1985. The third is planned in the Central Himalayas in the State of Uttar Pradesh.

Q.2. **Please describe your array, in terms of the type and number of instruments, their spacing, their triggering, their recording means (film, tape, or disc; analog or digital), and their foundation and housing.**

Ans. The arrays are mainly instrumented by SMA-1 analog accelerographs of M/S Kinemetrics U.S.A. The two arrays have TCG's for absolute time recording. The third array would have Omega time receivers. In addtion there are 5 digital accelerographs A-700 of M/S Teledyne. There are 50 SMA's in NW and 45 in NE and 40 are planned for Central Himalayas. The distance between accelerograph stations generally vary between 10 to 20 km and records are obtained on 70 mm film.

The instruments are located in the Ground Floor of Single storeyed Government Houses on base plates anchored to the floor by four bolts.

Q.3. **Describe the nature of the data you have obtained, in terms of the number of events recorded, their range of magnitudes, and their distances from the array.**

Ans. The NW region recorded only one 5.7 Magnitude event on April 26, 1986. Nine SMA's were triggered. The maximum acceleration recorded was 0.24 g.

The NE region recorded 4 events :

(i) Sept. 10, 1986 (ii) May 18, 1987, (iii) Feb.6, 1988 and (iv) Aug 6, 1988. The Sept. 1986 event was by 12 instrumets, May 1987 by 14 instruments, Feb 1988 by 18 instruments, Aug. 1988 by 33 instruments. The maximum acceleration was in Aug. 1988 and had a value of 0.34 g with a record duration of about 120 sec.

Q.4. **What means were uded to characerize the site conditons?**

Ans. The site conditions one characterised by visual inspection and data from construction agencies.

A. A. Moinfar
D2,Nowavar,
Farnaz,Mohseni SQ.
Mirdamad,Tehran
September 13, 1989

Dr. Brian E Tucker
Department of conservation
Division of mines and geology
1416 Ninth street, Room 1341
Sacramento, Ca 95814

Dear Dr. Tucker

Today I received your letter of August 25, 1989. As I have
no FAX facility, I will answer your questions by this hasty
note, I hope you will received it in due time.

1 - Establishment of Iranian Strong Motion Acclerograph
Network started in 1973 with some six instruments. the
number of instruments gradually increased. The instruments
are located allover the country.

2 - There are more than 275 operational strong motion
accelerogaphs (type SMA-1) and about 300 seismoscopes
(Wilmot type and Iranian manufactured twin pendulums
seismoscopes) . Recording means of SMA-1 is 70 mm film and
triggering is about 10 gals.

3- The number of events which recorded by the network are
some several hundreds, these records obtained from small
earthquakes up to big one,such as great Tabas Earthquake of
September 16, 1978 and its after-shocks . The magnitude of
earthquake was Ms=7.4 and the main shock was recorded in 8
stations from 5 km.to 250 km. far from the fault break. The
maximum acceleration which recorded from 1978 earthquake in
the vicinity of the fault break was .90g.

4-There were no consideration for the site conditions.

5-Selecting new instruments for new network, depends to the
budgets. The price of SMA-1 instrument is reasonable , but
there are a lot of problems in reading the films especially
when the amplitude of records are big and the trace of one
component is mixed with other,we had this problem in reading
the record of the earthquake of September 16, 1978. However
if the budget allow the digital instrument is preferable.

6-I have no comments for other items. Sorry for this hasty
and insufficient answer.

Sincerely yours

A. A. Moinfar

Milan 09/15/89

POLITECNICO DI MILANO
DIPARTIMENTO DI
INGEGNERIA STRUTTURALE

Piazza Leonardo da Vinci, 32
20133 Milano (Italy)

Dr. Brian E. Tucker
Division of Mines and Geology
Department of Conservation
1416 Ninth Street
Sacramento, Ca 95814 U.S.A.

Dear Dr. Tucker:

I enclose the responses to your questionnaire.
I am not sure they will be of interest to you since our
arrays relate to structural monitoring, aimed to the
identification of structural properties. The arrays are
located on two systems of masonry buildings. It is not of
our present interest to investigate the influence of site
conditions on the recorded ground motions.

With best wishes for your work I remain.

Sincerely,

Duilio Benedetti

RESPONSES:

1- Two towns in Umbria (Central Italy): Gubbio and Citta' di Castello. Buildings instrumented since 1985.

2- Instruments: A-700 Teledyne Steady State accelerocorders. Number of instruments: 6 on a array in Gubbio (one on the ground); 4 on a historical building in Citta' di Castello (one on the ground).
    Triggering: varying from 0.04g (ground) to 0.09g (top).

3- Since the installations two events have been recorded (a_m = 0.05g, a_m = 0.07g)

4- Void

5- Void

6- Need of high reliability of instruments.

7- The aim of the two arrays is just concerned with this topic.

8- For structural monitoring, when cable connections for syncronised triggering is not possible due buildings characteristics and usage, it would be highly welcome a radio system able to activate recording of all the instruments when one is triggered.

Rome Sept 11th 1986

Dear MR TUCKER

I am answering to your letter August 25th, hoping my answers will be useful to your expectations.
As you suggested I am writing long hand, because I am leaving for holydays next monday.

ANSWER 1

Please read page 7 of my "APPENDIX A" attached - At the moment the number of accelerometers is about 270 but in the next future this number will reach 300 units.

ANSWER 2

As you can see from fig 1, the instruments on spread all over our country - They are all analogic ones, that: 34 Teledyne RFT-250 and the remainings ones kinemetrics SMA-1. The acceleration threshold is .01g for all and as you know the recording means is 70mm film.
Up to now we never used digital instruments for many reasons, but now we are moving towards this new field
We are ordering solid state accelerometers from kinemetric and from CONTRAVES (an italian firm)

ANSWER 3
Starting from August 1974 to now, we recorded almost 800 events. The maximum acceleration is .35g (Friuli

and Irpinia earthquakes). The quality of the records are very good.

ANSWER 4

The choice of the sites has been realized following the earth quakes historical information (E. IACCARINO - C. ZAFFIRO, 1972. No work to characterized the sites has been performed. We are doing now this job at the sites that recorded the IRPIA earthquakes. This is our way to operate: do everything is necessary to better know the site when a strong earthquake has been recorded.

ANSWER 5
) think we will do what we are doing now (ANSWER 4)

ANSWER 6
a 1st Sub answer

The operation of an array is a very complicated and hard tasks. My brief personal opinion is the following:
- The most important thing is to make people TRUST on the job they are doing. To work on this field is very strange compared with other ones. It looks you are working for years to get nothing. Some time you could feel frustrated. But the moment you fail a strong earthquake could strike!!
- You need a very well equipped lab with a suitable shake table and electronic instruments to check and maintain the accelerometers in all their parts.
- The lab personnel has to have a very good electronic

and mechanic backgrounds.
- As far as it is possible to create a number of centers around
the country to prevent people to travel too much and to
stay away too long from home
- No sites must be f left without an instrument even for hour
- Every one, from the chief manager to the last worker, needs
to be tenacious; ready to move. You have to feel like an
earthquake is happening any moment now. It is an hard
life but at the end it will pay off!

    o 2nd SUB ANSWER

) cannot tell you too much in this field because I am
particularly involved in seismic instrumentation.

ANSWER 7

My organization never did ambient vibration and
forced vibrating tests - So I am not be able to give you
any comment.

ADDITIONAL INFORMATION

To give you more information about our network, I a
sending you some fotoes regarding installations of a
instruments:
Foto 1 e 2 : standard installations. The accelerometer is pow
red from the mains (220 v ca) through the battery charge
and the battery. Foto 2 is related to an installation in fu
field near a nuclear power station. We installed two ins
ments (1 g and 1/4 g) connected in the master - slave

configuration to better cover the amplitude and frequency ranges.

FOTO 3 : Shows an installation with a RFT-250 TELEDYNE accelerometer.

FOTO 4 : shows an installation with a 20 watts peak solar panel to supply an accelerometer trough a special battery charger and a battery, as we did when the mains is not available. We will use solar panels, & in parallel with the supply by mains, to charge a battery for supplying the digital instruments.

FOTO 5 : shows part of our lab with an electrodynamic shaking table, used to perform dynamic calibrations of the sensors in the 2.5 ÷ 40 Hz range

SHEET A Results of an inspection of the all parts of an accelerometer are reported. As you can see we have a TCG (ISMES) designed by ourselves and that we are installing in all our instruments. The % of critical damping and the full scale deflection values are missing because they need to be read on the films, after the "tilt" calibration. At the moment we ordered an accurate instruments to perform this task (PROFILE READER) but we did not get it yet.

SHEET B The threshold values obtained by a "FIELD CALIBRATOR" and a small shaking table are reported in the 2÷10 Hz range. On the "Note" the kind of work performed and the single parts raplaced on the starter are reported.

The other diagrams you will find enclosed are referred to the dynamic calibration of a SMA-1 sensor. We will perform this check on all the sensors. We already controlled 300 sensors (only SMA - sensors)

Dear Mr. Tucker I believe we need much more time to explain our jobs in full details. I hope my notes are useful and clear to you. I never attended a workshop like yours and I think it would be very interesting to participate.

Looking forward meeting you in the future, feel free to contact me again whenever you realize it could be useful for you.

Sincerely yours

Francis Zapelli

Here in) will give you a brief description of this calibration. Referring to the following drawing, we set the SMA-1 and

the SUNDSTRAND servo accelerometer on the shaking table, which is excited by a random signal. We take the signals out from the damping coil and the servoaccelerometer and send both of them to the GEN-RAD analyzer. After 200 average we get:

__A__. Linear transfer function (we cut the frequency analysis to 40 Hz)

$$TF = \frac{\frac{d\ddot{a}}{dt} \ (output \ from \ SMA-1 \ coil)}{a \ (output \ from \ reference \ acel.)}$$

__B__ - linear coherence function

__C__ - as in A but amplified

__D__ - After divided $\frac{d\ddot{a}}{dt}$ per $j\omega$, we get the real acceleration magnitude transfer function as it is normaly known.

__E__ - linearization transfer function of the sensor (Amplitude)

__F__ - Phase transfer function

__G__ - linearization phase transfer function

__H__ - Magnitude T.F and coherence T.F (The same as in A and B together.

ENEL STRONG MOTION NETWORK
- ORIGINAL CONFIGURATION

FIG 1

ENEL STRONG MOTION NETWORK

● STATIONS TRIGGERED
BY SEISMIC EVENTS

FIG. 2

STRONG-MOTION ARRAY QUESTIONNAIRE

1. Where is your array located and how long has it been operating?

    MEXICO — Guerrero & adjacent states
    Operating since 1985.

2. Please describe your array, in terms of the type and number of instruments, their spacing, their triggering, their recording means (film, tape, or disc; analog or digital), and their foundation and housing.

    30 instruments : mix of DSA-1, PDR-1, DCA-333
    All digital, recording on tape

    All are free field. Small piers anchored to rock, steel housing, adjacent tower for solar panel.

    Most sites are on igneous, plutonic rock. Some are on metamorphic or igneous extrusive outcrops
    One site on alluvium.

3. Describe the nature of the data you have obtained, in terms of the number of events recorded, their range of magnitudes, and their distances from the array.

    Start of array — Dec 1988: About 190 separate earthquakes. Average 2 to 3 stations trigger per earthquake. Magnitudes 2.2 to 8.1.
    Distances depend on magnitudes, to 350 km.
    Peak accelerations "as" small as 0.2 cm/sec² on PDR-1 instruments.

4. What means were used to characterize the site conditions?

    All sites : geological descriptions
    Some sites : short baseline refraction surveys
                 (about 12)

    Some sites : we have spectral amplification
                 of S-waves relative to the array
                 average. (18 sites)
    Several sites : density & shear velocity from drill cores
                 (cores were taken when rock was drilled to anchor pier)

(over)

limitations to site characterizations

- short baseline refraction ⌐ · both are limited
& core studies   ⌐ by lateral
                              variability of rock
                              at the site

core - also limited because it necessarily
       samples the more intact parts of
       the outcrop.

5. If you were to establish a new array, what means would you
    now use to characterize site conditions?

    A. All of above answers to question 4 (very low cost techniques)
    But note limitations.

6. What lessons have been learned

    ● regarding the operation of the array?
       1. A highly qualified team to run the array is invaluable
       2. Taking the time for training & organization of the team —
          general management skills
       3. Well planned data reports help everyone use the data.

    ● regarding ground response to earthquakes?
       1. Impressed by 1985 Sept 19 & other earthquakes by the
          importance of site effects.
       2. A big range of events sizes can be properly recorded — on
          scale — by digital instruments. 3. Spectra scale roughly as in
          seismology scaling laws.

7. Can you comment on the relevance of ambient vibration
    measurements and forced vibration testing?

    Not yet — we will have comparisons with other
    techniques eventually.

8. ADDITIONAL COMMENTS AND ADVICE (please use additional pages
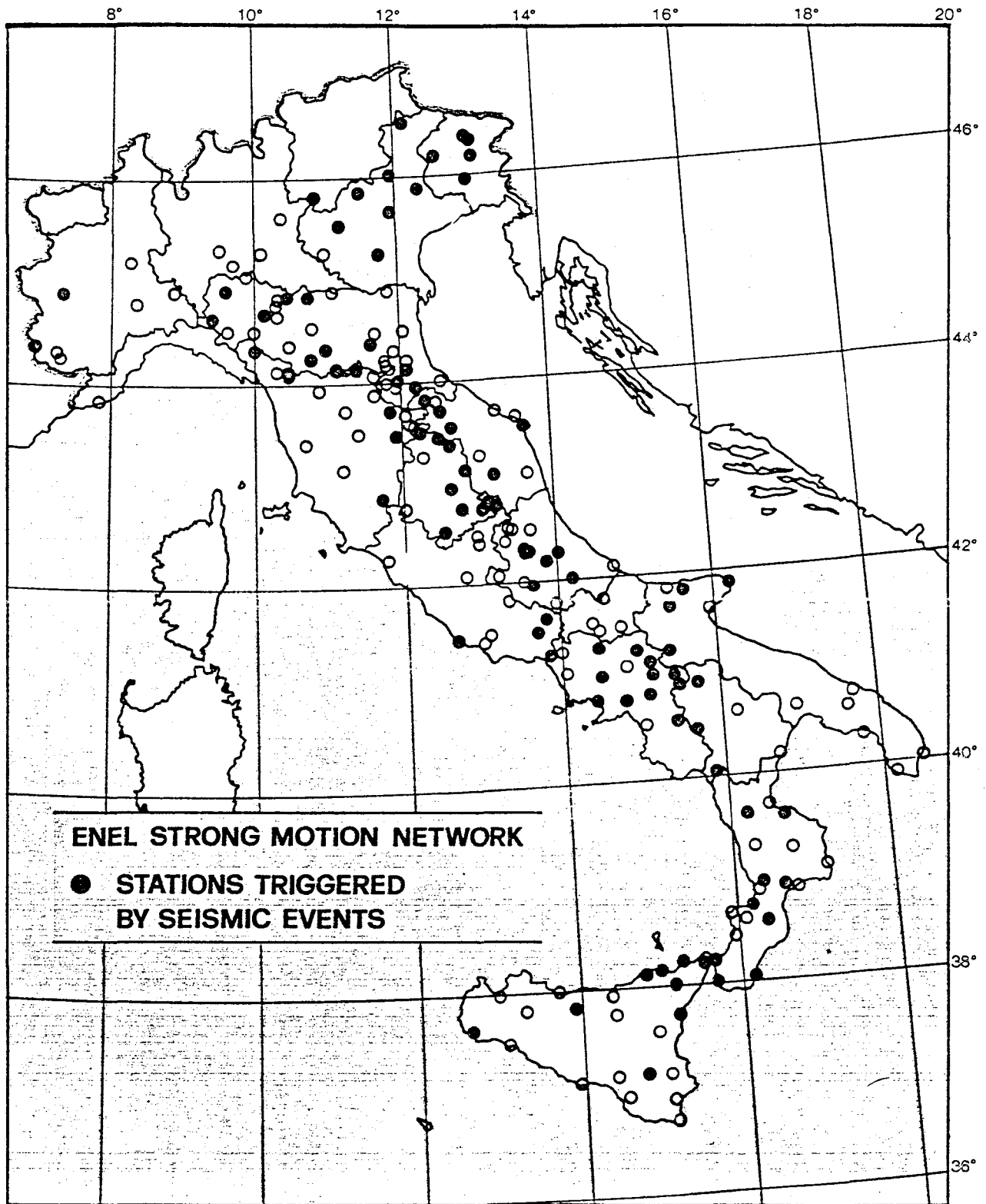   if desired)

    See you at the workshop!

Thank you!

JOHN G. ANDERSON
Name

STRONG-MOTION ARRAY QUESTIONNAIRE

1. Where is your array located and how long has it been operating?

   ARRAY LOCATED THROUGHOUT NEW ZEALAND (SEE ENCLOSED FIGURE). MODEST BEGINNINGS IN 1968, PRESENT STYLE OF NETWORK ESTABLISHED 1965 AND HAS BEEN BUILT UP GRADUALLY SINCE.

2. Please describe your array, in terms of the type and number of instruments, their spacing, their triggering, their recording means (film, tape, or disc; analog or digital), and their foundation and housing.

   171 FILM RECORDING MO ACCELEROGRAPHS OF VARIOUS MODELS,

   10 DIGITAL SOLID STATE MEMORY ACCELEROGRAPHS (TERRA TECHNOLOGY DCA 333R) RECEIVED FEBRUARY 1989

   61 SCRATCH PLATE ACCELEROSCOPES

   SEE ENCLOSED PAPERS FOR FURTHER INFORMATION

3. Describe the nature of the data you have obtained, in terms of the number of events recorded, their range of magnitudes, and their distances from the array.

   INFORMATION FOR GROUND ACCELEROGRAMS GREATER THAN 0.1g IN TABLE 1 OF VOLUME 3 PUBLICATION ENCLOSED.

   ALSO BRIEF SUMMARY IN SWCEE PAPER

4. What means were used to characterize the site conditions?

   GENERALLY ONLY BRIEF DESCRIPTIONS FROM GEOLOGICAL MAPS.

   BOREHOLE INFORMATION AT SOME SITES.

   A PROJECT IS UNDERWAY IN CURRENT 1989-90 YEAR TO COMPILE ALL READILY AVAILABLE INFORMATION FOR SITES.

5. If you were to establish a new array, what means would you now use to characterize site conditions?

STILL BROAD BRUSH DESCRIPTIONS BECAUSE OF LACK OF STAFFING & FUNDING FOR ANYTHING BETTER. DETAILED STUDIES OR SITES PRODUCING IMPORTANT RECORDS.

WE NOW ATTEMPT TO GATHER TOGETHER EXISTING INFORMATION ON SITES MORE THAN WE DID IN THE PAST.

6. What lessons have been learned

    o regarding the operation of the array?

    A LARGE ARRAY ALLOWS INSTRUMENT FAULTS TO BE DISCOVERED RAPIDLY BECAUSE THERE ARE SEVERAL DOZEN TRIGGERINGS EVERY YEAR. INDIVIDUAL SITES OR CITIES MAY EXPERIENCE MANY YEARS WITHOUT TRIGGERINGS, MAKING PROBLEMS DIFFICULT TO DISCOVER. GOOD DOCUMENTATION FOR RECOVERED RECORDS ESSENTIAL.

    o regarding ground response to earthquakes?

    NATURE OF N.Z. GROUND MOTIONS SOMEWHAT DIFFERENT IN DETAIL FROM BOTH USA & JAPAN.

    SOME AREAS OF LIKELY SITE RESONANCES SHOWN UP IN RECENT SMALL AMPLITUDE RECORDS.

    ANALYSIS OF MATAHINA EARTH DAM RECORDS UNDER WAY AT PRESENT PRODUCING VERY VALUABLE INFORMATION ON YIELDING RESPONSE OF THE DAM.

7. Can you comment on the relevance of ambient vibration measurements and forced vibration testing?

    IMPORTANT TO AID INTERPRETATION OF STRUCTURAL RESPONSE RECORDS AND TO DETECT CHANGES. HOWEVER, ONLY A HANDFUL OF N.Z. INSTRUMENTED BUILDINGS HAVE BEEN MEASURED.

8. ADDITIONAL COMMENTS AND ADVICE (please use additional pages if desired)

Thank you!

_____

Name

Figure 1: The New Zealand strong-motion network as at November 1987. The bracketed numbers show how many instruments there are at locations having more than one, and names given in capitals indicate that records were obtained during the Edgecumbe earthquakes.

1 BACKGROUND INFORMATION ON THE NETWORK

Acceleration history records of design level New Zealand ground shaking,
such as in the epicentral region of a shallow magnitude 7 earthquake like
Inangahua, have not yet been obtained. The New Zealand records obtained to
date show quite different frequency content to the Californian records,
such as the 1940 El Centro accelerogram, that are used as the basis of most
design spectra. The spectral shapes of New Zealand records resemble
Japanese records, but the strength of shaking seems to decay much more
rapidly with distance from the source than in Japan. The selection of
appropriate design spectra for New Zealand is a contentions issue at
present with the review of the Loadings Code NZS:4203. A number of
New Zealand records show indications of soil layer resonances, similar to
sites in Mexico City, which require confirmation with further records.

Worldwide, there have been even fewer records of design-level structural
responses than records of strong ground shaking. For example, in the
September 1985 Mexico earthquake there were excellent ground acceleration
records on a variety of soil types but not a single structural response
record from a building because maintenance of structural instrumentation
had ceased due to lack of funding. Among buildings designed to current
New Zealand codes, there is a preponderance of reinforced concrete
structures. Detailing requirements of the New Zealand concrete code are
generally much more severe than required overseas, making it important to
obtain records of the performance of New Zealand structures under severe
earthquakes to confirm that New Zealand design loads and detailing
requirements are appropriate.

INDIVIDUAL INSTRUMENTS

Location	Number of Instruments MO2 & MO2A	MO1	Owner
Zone 1			
Hamilton Post Office		1	PEL
Thames Telephone Exchange	1		PEL
Zone 2			
Hutt Valley Microzoning			
Belmont El Substation	1		PEL
Elizabeth St Pumping Station	1		PEL
Institute Nuclear Sciences	1		PEL
Naenae Reservoir	1		PEL
PEL		1	PEL
Woollen Mills El Substation	1		PEL
Petone Municipal Building	1		PEL
Wellington Microzoning			
Airport	1		DSIR Head Office
ANZ Bank	1		DSIR Head Office
Church Street Sub Station	1		DSIR Head Office
Vivian Street Gray & Elliot	1		DSIR Head Office
Library, Central	1		DSIR Head Office
Otaki	1		Roads Board
New Plymouth	1		PEL
Atiamuri (Temporary)	1		PEL
Iwitahi	1		Roads Board
Ohakea	1		Roads Board
Palmerston North		1	PEL
	18	3	

Location	Number of Instruments MO2 & MO2A	MO1	Owner
b/f	18	3	
Zone 3			
Masterton Telephone Exchange	1		PEL
Napier Telephone Exchange		1	PEL
Rotorua Police Station	1		Roads Board
Te Araroa High School		1	PEL
Turangi		1	PEL
Maraenui School	1		Roads Board
Woodville Post Office	1		Roads Board
Waipawa Post Office	1		PEL
Martinborough Post Office	1		PEL
Wairoa Telephone Exchange		1	PEL
Dannevirke Telephone Exchange		1	PEL
Zone 4			
Cheviot Post Office		1	PEL
Blenheim Post Office		1	PEL
Haast Post Office	1		PEL
Hokitika Post Office		1	PEL
Springs Junction Ranger Station	1		PEL
Nelson Telephone Exchange			PEL
Reefton, Forest Fire Station	1		PEL
Westport Telephone Exchange		1	PEL
Takaka	1		Roads Board
Fox Glacier	1		Roads Board
Murchison MWD Depot		1	PEL
Zone 5			
Dunedin Post Office	1		PEL
Invercargill Telephone Exchange		1	PEL
Te Anau	1		PEL
Wanaka	1		PEL
Flock Hill	1		PEL
Mt Cook	1		Roads Board
Mt Mary (NZED financed)	1		MOWD NZED Power Division
	35	15	

Installed three component accelerographs (as at January 1987)

Location	Number of Instruments MO2 & MO2A MO1	Owner
DAMS, POWER STATIONS & SUB STATIONS		
Arapuni Dam	2	NZ Electricity Dept
Benmore Dam (only 3 financed by NZED)	7	NZ Electricity Dept
Haywards Sub Station	1	NZ Electricity Dept
Inangahua Sub Station (PEL financed)	1	NZ Electricity Dept
Kikiwa Sub Station (PEL financed)	1	NZ Electricity Dept
Manapouri Hydro Power Station	1	NZ Electricity Dept
Matahina Dam	5	NZ Electricity Dept
Marsden B Thermal Power Station	1	NZ Electricity Dept
Moawhango Dam (1 installed at present)	3	NZ Electricity Dept
Patea Dam	1	NZ Electricity Dept
Pukaki Dam	3	NZ Electricity Dept
Ruataniwha Dam	4	NZ Electricity Dept
Te Marua Water Storage	3	Wellington Reg Council
Tuai Hydro Power Station	1	NZ Electricity Dept
	34	
SITE INVESTIGATIONS		
Atene Hydro Station	3	Ministry of Works & Dev
Clyde Dam (under construction)	1	Ministry of Works & Dev
Kaipara Harbour Power Station	2	Ministry of Works & Dev
Mohaka River Hydro Station	2	Ministry of Works & Dev
Seddonville	1	Ministry of Works & Dev
Te Kuha	1	Ministry of Works & Dev
	10	
MANUFACTURING & NATURAL GAS		
Kariot Pulp Mill	1	Winstone Samsung Ind Ltd
Maui Gas Prod Platform	2	Shell BP & Todd Ltd
Oaonui Gas Processing Plant	1	Shell BP & Todd Ltd
	4	

Location	Number of Instruments MO2 & MO2A MO1	Owner
BUILDINGS		
Auckland		
Civic Centre	3	Auckland City Council
Customhouse	3	State Services Commission
Savings Bank	3	Auckland Savings Bank
Union House	2	PEL
Hamilton		
Police Station	4	Ministry of Works & Dev
Wellington		
Challenge House	4	Challenge Corp Ltd
Dalmuir House	3	Presbyterian Church of NZ
Postal Centre	4	Ministry of Works & Dev
Reserve Bank	3	Reserve Bank of NZ
Rutherford House	4	Ministry of Works & Dev
Vogel Building	4	Ministry of Works & Dev
William Clayton	5	Ministry of Works & Dev
Hospital	3	Hospital Board
Beehive	2	Ministry of Works & Dev
Massey		
University	4	Ministry of Works & Dev
Gisborne		
Post Office	4	Ministry of Works & Dev
Christchurch		
Police Station	4	Ministry of Works & Dev
University Library	4	Ministry of Works & Dev
Savings Bank	3	Christchurch Savings Bank
	66	
BRIDGES		
Bowen Street (Wellington)	2 + Digital	Roads Board
Shell Gully (Wellington)	3	Roads Board
South Rangitikei Bridge	3	New Zealand Railways
Cromwell	3	Roads Board
	11 + Digital	

Explanation of instrument types:

Digital

3 component direct digital recording accelerograph recently
developed.

3 component film recording accelerographs

MO1 – first model of mechanical-optical accelerograph, recording
      acceleration history on film, no environmental sealing, no
      time-marks.

      Introduced 1966.

MO2 – rugged construction, fully sealed, timemarks at 0.02 second
      intervals, can be interconnected for simultaneous triggering of
      several instruments.

      Introduced 1968.

MO2A improved electronics, ~~infrared~~ *improved* clock, event time recorded.

      Introduced 1981.

2 horizontal component acceleroscope

SP – scratches trace of horizontal acceleration on microscope slide.
     Essentially a peak-recording device, much cheaper than MO
     accelerographs.

     Introduced 1963.

Scratch-Plate Sites (61)

Whangarei	Te Kuiti	Masterton	Picton	Harewood (Chch)
Workworth	Taumaranui	Castlepoint	Havelock	Ashburton
Birkenhead	Awakino	Pahiatua	Motueka	Timaru
Te Atatu	New Plymouth	Dannevirke	Reefton	Oamaru
Manurewa	Maui platform	Marewa (Napier)	Westport	Dunedin
Te Kauwhata	Hawera	Tuai	Greymouth	St Clair (Dunedin
Thames	Wanganui	Gisborne	Hokitika	Lauder
Waihi	Ohakune	Toluga Bay	Haast	Roxburgh
Tauranga	Taihape	Opotiki	Cheviot	Balclutha
Hamilton	Palmerston North	Taupo	Hanmer Springs	Gore
	Levin		Kaikoura	Invercargill
	Paraparaumu			Te Anau
	Haywards			Mossburn
	PEL			Queenstown
				Omarama
				Lake Coleridge

10 TERRA TECH DCA 333A solid state accelerograph installed 1989.

6 sites in Hutt valley Wellington (mainly to give ready access for
Wanganui, Hastings, Gisborne, Masterton) evaluation, also for microtremor
studies

THE NEW ZEALAND STRONG MOTION
EARTHQUAKE RECORDER NETWORK

R.T. Hefford, P.M. Randal, R.I. Skinner, J.L. Beck and R.C. Tyler*

SYNOPSIS

The network of strong-motion earthquake recorders, maintained throughout New Zealand by the Engineering Seismology Section of the Department of Scientific and Industrial Research, is described. The instruments are either deployed as ground instruments to measure potential earthquake attack on structures, or in structures, e.g. buildings, dams and industrial installations, to record structural response. Details are given of installation of instruments, maintenance, laboratory work, record retrieval and digitisation, costs and staffing for the network. Future developments mooted include an improved digitising system, the introduction of an improved version of the existing mechanical-optical instrument in 1979, and, in the long term, the introduction of an entirely new digital recorder, having an electrical output from its accelerometers, which will make possible the transmission of data by telephone or radio link.

1. INTRODUCTION

The Physics and Engineering Laboratory first became interested in earthquake recording in the 1950s as the result of requests from designers about the effect of earthquakes in New Zealand on engineering structures. Instruments were designed and developed and a network of strong motion recorders has been gradually built up throughout the country. The network was first described in the Bulletin of the New Zealand Society for Earthquake Engineering in 1970[1] when there were 77 three component records and 74 two component (non time-base) recorders. By the end of 1978 the number of three component recorders had risen to 125 while the number of two component records remained the same, the increase in the number of three component recorders resulting mainly from requests for installations in important structures such as power stations, bridges and buildings.

With an increasing number of records accumulating at the Laboratory, emphasis is now being placed on their digitisation and routine analysis, so that they can be used in research and in the computerised design of structures, thereby enabling improvements to be made in earthquake-resistant design.

2.0 THE INSTRUMENTS

2.1 MO2 Accelerograph (Fig. 1)

The primary instrument of the New Zealand network is type MO2 (mechanical-optical) accelerograph, which records accelerations at its location in three orthogonal directions, from the motions of damped pendulums. It records high definition traces on unperforated 35 mm film. Time marks are provided which are controlled either by a tuning fork clock, or more recently by a crystal oscillator, imprinted along the edge of the film at 0.02 second intervals. Starting is initiated by a vertical sensing geophone. For inter-

connected accelerographs, any one instrument started by an earthquake acceleration will also start all the others in that system. The film cassette holds sufficient film for nine records, each of 47 seconds duration.

The accelerograph is fully sealed and operates off a 12 volt dry cell power supply. More detailed information on the accelerograph is outlined in the instrument manual[2].

2.2 MO1 Accelerograph

The MO2 was developed from the type MO1 three component accelerograph and 24 of the type MO1 are still in operation in the network. They are gradually being replaced by the type MO2 recorder, as they do not have the facility for inter-connection or time marking, and are not sealed.

These instruments are mainly situated in telephone exchanges as this gives the best environment for successful operation.

2.3 SP2 Accelerograph

The two component SP (scratch plate) accelerographs (Fig. 2), recording accelerations in the horizontal plane only, were the first instruments to be used in the network. Although limited in accuracy and lacking a time base, they have given records at many points where otherwise none would have been available, notably during the Inangahua earthquake. When installed beside a MO2 accelerograph they have provided a valuable back-up.

The accelerograph is based on an inverted pendulum with an undamped period of 0.06 seconds, and a damping factor of about 60% of critical, the damping being provided by silicone oil. The relative displacement of the pendulum weight, with respect to the base, is a measure of the amplitude and direction of the horizontal acceleration of the instrument[2]. The movement of the pendulum weight is amplified by the lightweight extension arm into which is plugged a smoked

---

* Physics and Engineering Laboratory, Department of Scientific and Industrial Research.

glass disc. A fine line, (about 0.01 mm wide) is inscribed on the smoked surface of the moving disc by a specially sharpened steel needle, this giving the acceleration record. The instrument has proved to be very reliable and the only cause of inoperation has been vandalism.

3. THE NETWORK

3.1 Instrument Distribution

The distribution of MO1 and MO2 recorders throughout the country is illustrated in Figure 3, and the breakdown in terms of buildings, dams and bridges and individual instruments is given in Table 1. The distribution of SP recorders is shown in Figure 4. The build-up of MO instruments since 1965 is shown in Figure 5, the most rapid increase in numbers occurring in the two years following the Inangahua earthquake in 1968. Of the total of 125 three component recorders distributed throughout the country only 15 MO2s and 19 MO1s were purchased by the Laboratory, the remainder either being purchased by government departments or by private building owners on the advice of consulting engineers. Agreement has been obtained for the installation of a further 29 instruments in buildings, bridges and power stations (Table 2).

From Table 1 it is seen that all of the instruments purchased by other authorities have been required for particular structures, while those purchased by PEL have been for ground installation, either to fill gaps in the network (22 instruments) or for micro-zone installations in the Wellington and Hutt Valley areas (12 instruments). All the projected installations listed in Table 2 are for structures, over half of which, 18 instruments, are for the Wellington area.

The instruments in the network have been deployed to gather data of two kinds to promote the design of more efficient and economical earthquake resistant structures. Firstly, ground accelerations are recorded so that designers have a wider data base from which to select the most appropriate earthquake loadings for use in structural design. Secondly, accelerations are recorded at several locations throughout major structures to monitor their performance during strong-motion earthquakes (Fig. 6).

Most ground based instruments are located in areas of highest seismicity, which are indicated by the map prepared by the Seismological Observatory showing the occurrence and distribution of earthquakes in New Zealand since 1840 (Fig. 7). This shows that the major earthquakes occur in a zone which is along a band running roughly between Milford in the south-west to Cape Runaway in the north-east. Although the Laboratory does not intend to increase the total number of instruments in the network, a comparison between this map and the distribution of MO2 instruments (Fig. 3) indicates that more instruments of this type should be added to fill in gaps along this band, particularly in the area north of the Wairarapa through to Napier. Some redistribution is possible, however, e.g. no records have been obtained from Auckland from the time the network was first started and it is less likely that performance data into the

ductile range will be obtained from the instrumented tall buildings there. Perhaps therefore the number of instruments in these buildings should be reduced in favour of ground-based instruments only in Auckland. Also, improvements are being carried out by selectively replacing SP instruments by MO2 instruments in preferred locations, the service time for the two instruments being about the same.

3.2 Local Microzone Networks

Two local networks in the Hutt Valley and in the Te Aro district of Wellington City have been set up to study the influence of local geological features and of soil properties on ground motion.

3.3 Networks at Dam Sites

Instrument arrays have been installed at dam sites, either to study local seismicity and microzone effects during a site investigation (e.g. Atene) or to study structural response, as at the earth dams of Matahina and Benmore. One particular use of an array of instruments on a dam is in recording the effect of any local earthquakes which may be caused by filling the lake behind the dam. Improved knowledge of the seismic behaviour of dams is of great importance from the safety aspect.

3.4 Instruments in Industrial Installations

The safety aspect is also of considerable importance in industrial installations. Two MO2 recorders have recently been installed at the Maui A offshore gas rig which will enable the loading on the structure in the event of an earthquake to be assessed. Similar safety aspects apply to the installation of a recorder at the Karioi wood-pulp mill where it will be possible to assess loadings on the machinery and pipework and its fixings. In addition, a request has recently been received for an installation in a thermal power station, together with an earthquake trigger which will give a warning to engineers in noisy areas that an earthquake is taking place, thereby allowing emergency measures to be taken. Such a trigger has already been manufactured for an industrial installation from standard MO parts, and a commercial device should soon be available.

3.5 Instrument Installation

The instruments are normally bolted firmly down to a concrete plinth which can be set conveniently above the normal concrete floor level. In the field the plinth needs to be keyed thoroughly to the surface for which motion is to be recorded. Occasionally instruments may be bolted to a vertical concrete wall in bridge or building applications. They are protected by a padlocked steel case.

3.6 Instrument Siting

Because of the risk of vandalism of field instruments, instruments of the main ground network are normally located in the basements of smaller public buildings such as post offices, telephone exchanges and fire stations. Within multi-storey buildings instruments are located in storerooms or

FIG. 1 MO2 Accelerograph - checking circuits

Removable Cap

Lugs to Hold Cap
(3 at 120°)

Suspension Wires
(2 pairs at 90°)

Stylus Holder

Smoked Glass Disc

Extension Arm

Fixed Barrel

Diaphragm
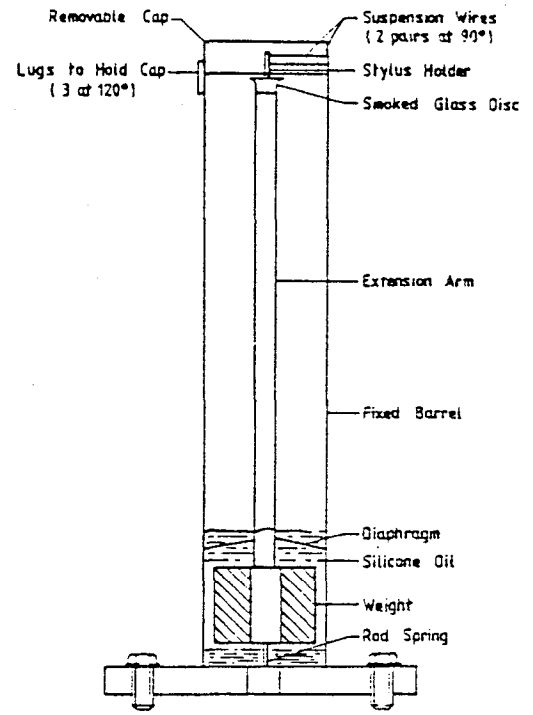
Silicone Oil

Weight

Rod Spring

FIG. 2 Scratch plate instrument

FIG. 3 Distribution of MO2 Accelerographs throughout New Zealand
(February 1979)

FIG. 4 Distribution of scratch plate instruments throughout New Zealand
(February 1979)

closets which are often to be found adjacent to lift shafts and stairs in the core of the building. A check is made with the building designer to ensure that the instruments are located at the most desirable points within the structure. Damp sites can cause sticking in the cassettes and, at such locations, a drying agent is kept in the instruments to absorb moisture.

3.7 Maintenance of Network

From the point of view of servicing the instruments, New Zealand is divided into 6 zones (Figure 8, with zone 6 being Wellington and the Hutt Valley), all having approximately equal service time. In early 1969 a strict service schedule was adopted in which each of the instruments was visited at intervals of close to 6 months. Where possible a shorter interval between visits was adopted during the year or so following installation. This system improved the reliability of the instruments, while the personal contacts established during the regular visits, and the frequent explanations of the working of the instruments, prevented them being broken into for examination by inquisitive local people, which had previously occurred from time to time.

As the reliability of the MO2 recorders increased it became less necessary to carry out servicing every 6 months and in 1975 the service interval was extended to 8 months, and remains at this interval, to reduce the servicing load brought about by the increased number of instruments.

3.8 Laboratory Work on Instruments

Although the MO2 accelerograph is manufactured commercially under licence, the calibration of each sensing unit is still carried out by the Laboratory using a static calibration method, as already outlined[1], and the calibration constants are stored in a computer file which can be accessed during record processing. Performance checks are also carried out on the unit before installation in the field.

Depending on the availability of spare instruments, one or two MO2 recorders are replaced on each zone visit with fully overhauled instruments, upgraded to the latest design specifications. At the present time this includes the fitting of crystal oscillators, for time marking from the start of the trace, replacing the obsolescent tuning fork circuit previously fitted. Interconnection facilities are now standard for all instruments. With a total of 125 instruments to be serviced the replacement programme will take about 10 years with the staff available.

3.9 Record Processing

The work of the processing and storing film records is carried out entirely by the Engineering Seismology Section of the Laboratory in order to ensure that earthquake records are not lost. Any events recorded are identified and copied using a direct print method. All further record processing, such as digitising, is carried out using film copies to avoid damage or loss to the original film record, which is archived.

Sections of the test film from each

instrument brought back from the service visits are filmed and checked against samples obtained previously from the same instrument. In this way any faults in film transport or trace definition can be noted and corrected on the next visit.

Scratch plate slides returned from sites are examined for the pattern indicating a recorded earthquake. A photograph is then made of the pattern which is filed; plate slides showing exceptional patterns are also filed, while those showing no record are discarded. New slides are placed in each instrument on every service trip.

3.10 Record Publication and Digitisation

All records of earthquakes obtained from MO accelerographs in the years 1965 to 1972 have been published in the form of a copy of the film trace. The records from 1973 onwards have not been published because of plans for a more effective presentation of data, as was done for the 1976 Milford earthquake[4]. Staff shortages and the priority given to instrument operation and maintenance have delayed the introduction of the new method of publication but substantial progress is now being made. The practice of publishing copies of the traces is to be discontinued in favour of a system for publishing copies of records in digital form. About one dozen selected records have so far been digitised, including those from earthquakes which occurred at Milford in 1976, Atene 1973, Inangahua (aftershocks) 1968, and Wellington (Vogel Building) 1977. It is hoped that modern digitising equipment will be purchased shortly which will increase the numbers of records available in this form. A summary of those records with peak accelerations greater than 10%g is given in Table 3. Altogether, 246 records have been obtained which have shown accelerations greater than 1%g.

3.11 Costs

3.11.1 Capital Cost

The cost of a single MO instrument is approximately $2,000. Thus the investment in the MO network alone is $250,000.

3.11.2 Servicing Costs

The cost of servicing the existing network of 125 MOs and 74 SPs is as follows per annum:

	$
Spare parts purchased and miscellaneous laboratory equipment	1,000
Batteries (No. 6 cells at present)	2,000
Mileage - 90,000 km at $0.1345/km	12,000
Travelling expenses for 2 NO. staff for 5 x 10 day trips	4,000
Salaries and overheads for two technicians (approximately)	40,000
	$59,000

It is apparent that if it is desired to increase the size of the network then the servicing costs do not increase linearly with the number of instruments as the mileage of 90,000 km already covers visits to most parts of New Zealand.
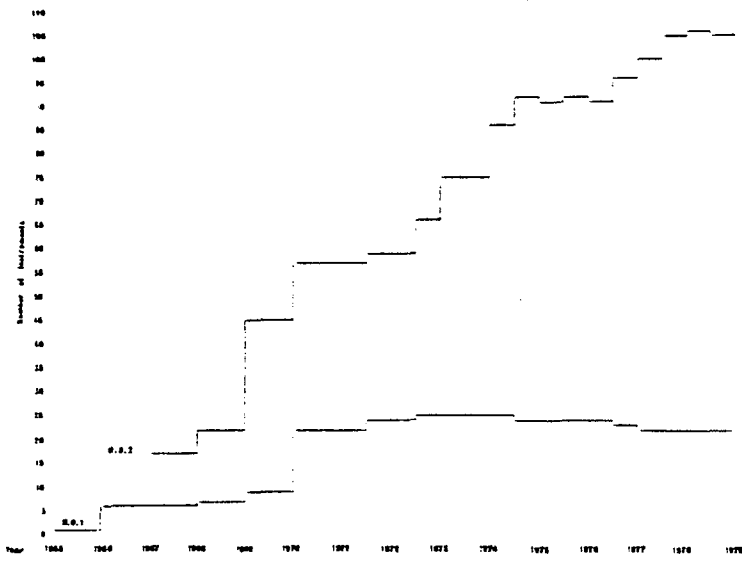
FIG. 5 Numbers of strong-motion recorders in
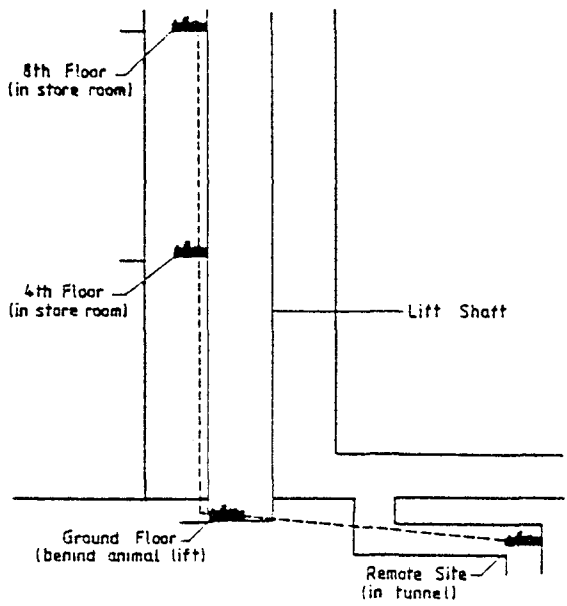New Zealand since 1965

FIG. 6 Interconnected system of accelerographs
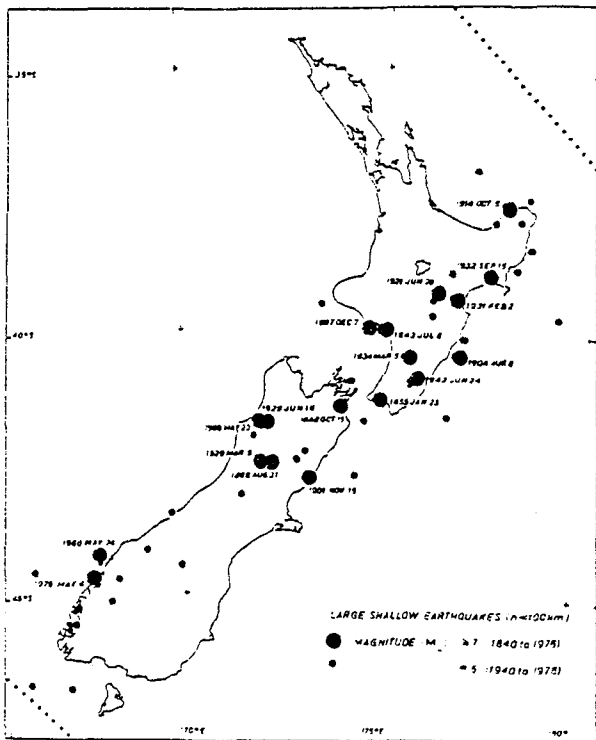for building (Massey University)

FIG. 7 Occurrence and distribution of earthquakes
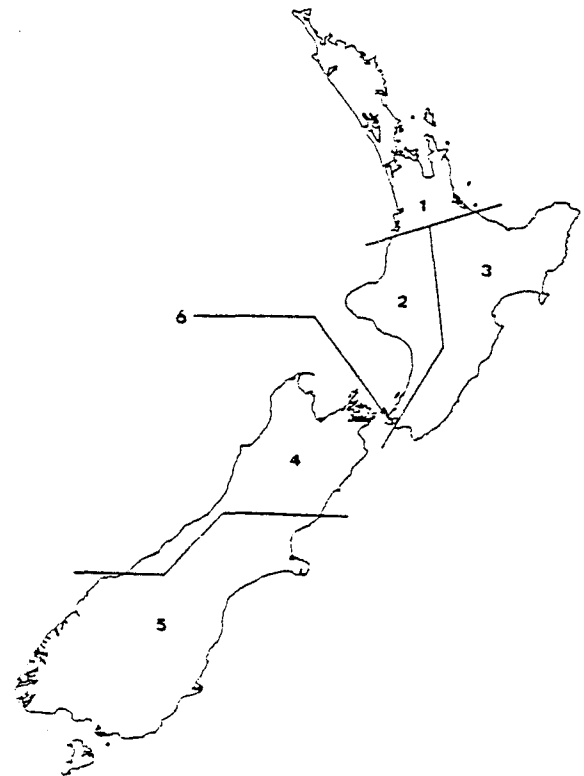throughout New Zealand (from Seismological Observatory)

FIG. 8 Service Zones for instruments

3.12 Staffing

Two technicians are employed full time in maintaining the network of 125 MO recorders and 74 SP recorders and in upgrading them to new specifications. Each of the six zones requires 32 working days of each technician's time and a further 32 days per year are spent in preparing reports and exhibitions and in general office administration. This gives times allocated as follows:

Description of Work	Time Spent per zone (days)		Total days for 2 technicians per annum for 6 zones
	Technician No.1	Technician No.2	
Site visits	8	2	60
Servicing & upgrading returned instruments	6	-	36
Instrument development	4	-	24
Processing film & SP slides	3	4	42
Record work including digitising & posting on worldwide network	4	12	96
Preparing films, batteries, SP slides and other stores for next trip	3	10	78
Administration for visits, including booking vehicles and correspondence with authorities and site representatives	4	4	48
Sub-total per zone	32	32	
Preparing reports and exhibitions and office administration			64
TOTAL DAYS FOR 2 TECHNICIANS			448

In addition, further assistance is co-opted as required to generally assist in the work in a non-specialist way, e.g. to assist in carrying equipment, running leads, or acting as a station reporter when checking interconnected systems. The amount of time involved is about 6 man days per zone, i.e. 36 man days per year, but this time is not included in the table, as recruitment is as required for each trip, made either from the Laboratory or through local DSIR establishments, e.g. at Christchurch or Auckland.

The table shows that only 60 working days are spent in the field in servicing instruments. This represents only about 1/8th of the total time, the remainder being spent in providing a back-up for the service. Thus while offers have been made from time to time by local authorities to service instruments, if adopted this would only represent an increase of about 1/8th in the number of instruments which could be serviced, which would largely be nullified by the communications problems which would exist between the Laboratory and the zones. It is felt therefore that the present arrangement of servicing the network from a central source is the best one.

4. FUTURE DEVELOPMENTS

In 1979 it is proposed to introduce a major upgrading of the MO2 instrument, to be called the MO2A. A new lightweight geared motor will be fitted together with an electronic clutch which will replace the mechanical clutch, which has occasionally given trouble. A press-button film release will also be introduced to make film rewinding easier and hence minimise scratches and static electricity on the film. Also under development is a facility to record the elapsed time from the last visit to the event recorded. This will ensure the correlation of records with other instruments in the network recording the same event and facilitate identifying a record with a particular earthquake. The latter will enable epicentral distances to be estimated from the epicentre determinations of the Seismological Observatory.

In a few years it may also be possible to supplement and eventually replace the film recording system with an electronic bubble memory on which the record is made in digital form, the sensing unit being three orthogonal accelerometers with electrical output. In this way occasionally troublesome film or magnetic tape transport will be avoided in the instruments. It will also eliminate the need for film processing and record digitising. Such a device could also be used as a trigger with little modification. In addition, a record could be transmitted by a radio link or integrated into the telephone system to allow the data to be obtained by dialling the instrument. These facilities are important where information on the condition of important installations, e.g. unmanned dams, is required immediately following an earthquake.

5. REFERENCES

1. Skinner, R. I., Stephenson, W. R. and Hefford, R. T., "Strong-Motion Earthquake Recording in New Zealand". Bull. of the N.Z. Nat. Soc. for Earthq. Eng., Vol. 1, No. 4, p.31 (1970).
2. Physics and Engineering Laboratory DSIR. "Type MO2 Accelerographs (Skinner-Duflou) Installation and Operating Manual". (Available through manufacturers: Victoria Engineering, Lower Hutt.)
3. Skinner, R. I. and Duflou, P. C. J. (1965) "New Strong-Motion Accelerographs". Proc. Third World Conference on Earthquake Engineering.
4. Hodder, S. B., Skinner, R. I., Hefford, R. T. and Randal, P. M., "Strong Motion Records of the Milford Sound Earthquake 1976, May 4", Bull. of the N.Z. National Soc. for Earthq. Eng., Vol. 11, No. 3, September 1978.

TABLE 1

INSTALLED THREE COMPONENT ACCELEROGRAPHS
(as at December 1978)

Location	No. of Instruments MO2	MO1	Owner
DAM SITES			
Arapuni	2		
Atene	3		
Benmore	7		
Matahina	5		MWD
Moawhango	3		
Mokihinui	1		
Te Kuha	1		
BUILDINGS			
Auckland			
Civic Centre	6		Auckland City Council
Customhouse	3		State Services Commission
Savings Bank	3		Auckland Savings Bank
University Science Bldg	5		MWD
Hamilton			
Police Station	4		MWD
Wellington			
Charles Ferguson	4		MWD
Challenge House	4		Challenge Corpn. Ltd
Dalmuir House	3		Presbyterian Church of NZ
Postal Centre	4		MWD
Reserve Bank	3		Reserve Bank of NZ
Rutherford House	4		MWD
Vogel Building	4		MWD
Massey			
University	4		MWD
Christchurch			
Police Station	4		MWD
University Library	4		MWD
BRIDGES			
Shell Gully (Wellington)	3		MWD
South Rangitikei Bridge	1		NZR
FACTORIES, POWER STATIONS, ETC.			
Tuai Hydro Station		1	PEL
Karioi Pulp Mill	1		Winstone Samsung Ind Ltd
Maui A	2		Shell, BP, Todd
Kaipara Harbour			
Investigation	2		MWD
Haywards Sub Station	1		NZED
Inangahua	1		PEL
c/f	92	1	
b/f	92	1	
INDIVIDUAL INSTRUMENTS			
Zone 1			
Hamilton P.O.		1	
Thames P.O.	1		PEL
Whangarei Tel. Ex.		1	
Zone 2			
Hutt Valley Microzoning			
Belmont El. Substation	1		
Elizabeth St. Pumping Stn.	1		
Gear Meat Pumping Stn.	1		
Institute Nuclear Science	1		
Naenae Reservoir	1		PEL
PEL			
Woollen Mills	1		
El. Substation	1		
Wellington Microzoning			
Airport		1	
ANZ Bank	1		
Church Street Sub Station	1		
Vivian Street Gray & Elliot	1		
Library, Central	1		PEL
Zone 3			
Masterton Tel. Ex.		1	
Napier Tel. Ex.		1	
Te Araroa High School		1	PEL
Turangi		1	
Zone 4			
Cheviot P.O.		1	
Blenheim Tel. Ex.		1	
Haast P.O.		1	
Hokitika P.O.		1	PEL
Muruia Springs Hotel		1	
Nelson Tel. Ex.		1	
Reefton, Forest HQ	1		
Westport Tel. Ex.		1	
Zone 5			
Dunedin P.O.		1	
Invercargill Tel. Ex.		1	PEL
Milford Hotel	1		
Te Anau		1	
Wanaka		1	
TOTAL	106	19	

TABLE 2

AGREED FUTURE INSTALLATIONS OF MO2 ACCELEROGRAPHS

Location	No. of Instruments	Owner
BUILDINGS		
Wellington		
Hospital	3	Wellington Hospital Board
Freyburg	1	MWD
Beehive	5	MWD
BNZ	3	BNZ
William Clayton	3	MWD
Christchurch		
Postal Centre	3	MWD
Law Courts	3	MWD
BRIDGES		
South Rangitikei	3 (more)	NZR
Bowen Street Wellington	3	MWD
FACTORIES, POWER STATIONS, ETC.		
Marsden Point	1	NZED
Huntly	1	NZED
TOTAL	29	

SUGGESTED EXTENSIONS OF THE NEW ZEALAND
STRONG MOTION ACCELEROGRAPH NETWORK

J.B. Berrill*

ABSTRACT

The principal aim of the present network of strong motion accelerographs
is to record the response of structures to earthquakes, and instruments are
concentrated in the larger cities where modern, tall buildings are found.
However, the behaviour of structures during earthquakes is now comparatively
well understood. At the present time, estimating design ground motions is the
weakest part in the process of designing structures to resist earthquakes.
There is a strong need for more recordings of ground shaking, particularly
sets of several accelerograms from single earthquakes. It is not certain that
the present accelerograph network would capture any significant record of
strong motion during a major earthquake in New Zealand; and the chance of a set
of three or more strong accelerograms being recorded is quite small. It is
recommended that 25 additional instruments be installed promptly, to fill the
main gaps in the present network, and to extend the capacity of the existing
local network in the Wellington area.

1. INTRODUCTION

The existing network of strong motion
accelerographs which at present covers New
Zealand is orientated mainly to the measure-
ment of structural response during
earthquakes. Nearly half of the 125 presently-
deployed accelerographs are sited in the
upper floors of tall buildings, most of which
are clustered together in the two or three
larger cities. However, work in the last
few years has resulted in a good understanding
of the behaviour of structures during earth-
quakes. The greatest difficulty now, in the
earthquake-resistant design of a structure
is in estimating the ground motions likely to
occur during the life of the structure. Our
knowledge of strong ground shaking is very
meagre. We have a fundamental understanding
only of its gross properties; and even on a
worldwide basis we lack sufficient data to
formulate satisfactory empirical models.
The difficulty this poses is particularly
acute in New Zealand, where we have recorded
no significant strong motion accelerograms.

It follows that the main purpose of the
national accelerograph network should be to
gather data about ground motion. However,
the capacity of the present network to do so
is quite low. The distribution of instruments
is sparse, and there are some large gaps in
the network.

The simple analysis undertaken in this
paper shows that with the installation of
about 25 additional instruments the major
gaps in the network could be closed, and it
would become a much more effective means of
capturing records of strong ground shaking.

2. THE PRESENT NETWORK

The present strong motion accelerograph
network comprises 125 MO1 or MO2 accelerographs
installed in 64 separate structures in about
40 different geographical localities[1]. In
addition to these sites, there are firm
plans to install a further 29 accelerographs
in 10 additional sites[1]. Except for one,
these new sites are all in presently
instrumented localities. The 74 existing
and planned sites are shown in Figure 1.
A more detailed description of the network
and instruments, together with some of its
history, is given by Hefford et al[1].

As well as the network of time-base
MO1 and MO2 accelerographs, there are 74
scratch plate instruments, similar to the
seismoscope, installed about the country[1].
Since these do not yield a time-history
record they are not considered further in
this discussion. Their value is in providing,
essentially, one response spectrum ordinate,
reliably and cheaply.

It is interesting to study the ownership
of accelerographs in the network. Of the
154 present and proposed instruments, only
34 are owned by the Department of Scientific
and Industrial Research (DSIR) which has the
responsibility for maintaining the network.
These are mostly single-instrument stations
in rural areas. Of the remainder, which for
the most part are installed in the larger
cities, 82 are owned by the Ministry of
Works and Development, 3 by the New Zealand
Electricity Department, 10 by other govern-
ment departments, 6 by local bodies, and 19
by private owners (presumably installed on
the advice of consulting engineers). Thus
the present network has been shaped largely
by the earthquake engineering community as
a whole: the DSIR has followed the
apparently-uncoordinated wishes of a number
of different groups. Clearly, a coherent
plan is needed for future extensions to the
network. The proposals made in section 4
are offered as a basis for detailed planning
and assignment of priorities.

3. COVERAGE OF PRESENT NETWORK

To obtain a useful record of strong
ground shaking from a large earthquake, it

---

* University of Canterbury, Christchurch.

Lamont-Doherty Geological Observatory
of Columbia University
Seismology, Geology and Tectonophysics

Palisades, NY 10964

October 2, 1989

Brian E. Tucker
Calfornia Division of Mines and Geology
1416 Ninth St. Room 1341
Sacremento, Ca. 95814

Fax No. 916-445-5718

Re. Strong-Motion Array Questionnaire.

Dear Brian,

My apologies for being so late (but just at the last date you specified!).

LDGO operates two arrays: one in the Shumagin Islands in Alaska, and one primarily in the Eastern U.S. as part of the National Center for Earthquake Engineering(NCEER) effort. We are currently between P.I.s on the Shumagin program, so if you need further info contact me. For the NCEER info, contact me or Klaus Jacob or Bob Busby.

The questionnaires are attached. We don't expect much change in the Shumagin array in the next year, although we have been trying to replace the SMA-1's with SSA-1's for the last two years: no $$. The NCEER array will get 5 more units within the next 6 months. In addition two of the units have just been returned from Australia (Tennent Creek area), and will be deployed in the U.S. in the near future.

Some comments re the workshop objectives:
Characterizing site response is a very complex problem, and the data collected to date is limited by the fact that much of the instrumentation has been installed as code compliance effort and is usually confused by the specific"site" response. While the problem of soil/structure response will have to be solved eventually, our effort has been to first see if we can get enough data in relatively simple "free field" sites. Hopefully this will help someone to generate a resonably accurate method for predicting "input" ground motion at a site of interest. But even this is a relatively complex problem if one tries to take into account non-hard rock sites. Moreover what is a "site response" vs a propagation effect vs instrument

installation distortion?

It looks as though we will have to continue to employ a mix of techniques (artificial source, ambient noise response, actual acceleration measurement, etc). If actual acceleration measurements are to be of general value, specific data regarding the site are essential, including both geologic data and site response data.

Much of the code compliance type installations would be more useful if we had a free field measurement in the area.

Regards

Douglas H. Johnson
Technical Manager, Seismology
FAX No. 914-359-5215

STRONG-MOTION ARRAY QUESTIONNAIRE

1. Where is your array located and how long has it been operating?

SHUMAGIN ISLANDS, ALASKA. EVOLVED OVER A NUMBER OF YEARS; TOOK PRESENT FORM ≈ 1982.

2. Please describe your array, in terms of the type and number of instruments, their spacing, their triggering, their recording means (film, tape, or disc; analog or digital), and their foundation and housing.

(1) KINEMETRICS SSA-1 @ SAND POINT: ACCESSIBLE VIA TELEPHONE

(8) SMA-1'S COLOCATED @ SP NETWORK STATIONS. TIME CORRECTION TRANSMITTED DAILY TO CENTRAL STATION. TRACE DATA (FILM) RECOVERED DURING ANNUAL FIELD SERVICE (IN SUMMER). SMA'S MOUNTED ON 1" ALUMINUM PLATES SET IN 1-4" CONCRETE, ON ROCK OR LESS THAN 1 METER OF WEATHERED-

3. Describe the nature of the data you have obtained, in terms of the number of events recorded, their range of magnitudes, and their distances from the array.

GENERATING SUMMARY - DATA TO FOLLOW ASAP.

4. What means were used to characterize the site conditions?

VISUAL / REVIEW OF SP NETWORK DATA. CONTRAINT WAS COLOCATION WITH EXISTING SP NETWORK STATIONS.

↳ ROCK / SOIL (VERY LITTLE ORGANIC MATERIAL), COVERED WITH PLASTIC "TUB".

5. If you were to establish a new array, what means would you now use to characterize site conditions?

- GEOLOGIC SURVEY
- NOISE SURVEY (GEOPHONES OR FBA'S WITH PORTABLE DIGITAL RECORDERS)

6. What lessons have been learned

o regarding the operation of the array?

POOR ECONOMY TO USE INADEQUATE INSTRUMENTATION (ie: SMA-1's).

o regarding ground response to earthquakes?

7. Can you comment on the relevance of <u>ambient vibration measurements</u> and <u>forced vibration testing?</u>

(A) — GOOD IF POSSIBLE TO REFERENCE TO STD. REF STATION @ SAME TIME

(B) — LOGISTICS PRECLUDES USE IN THIS APPLICATION.

8. ADDITIONAL COMMENTS AND ADVICE (please use additional pages if desired)

SEE NCEER QUESTIONNAIRE

Thank you!

Doug Johnson
_____
Name

STRONG-MOTION ARRAY QUESTIONNAIRE

1. Where is your array located and how long has it been operating?

EASTER U.S. & CANADA + 1 @ DUTCH HARBOR, ALASKA & 1 IN AUSTRALIA (TENNENT CREEK). SINCE FALL, 1987.

2. Please describe your array, in terms of the type and number of instruments, their spacing, their triggering, their recording means (film, tape, or disc; analog or digital), and their foundation and housing.

ALL KINEMETRICS SSA-1's ON DIAL-UP TELEPHONES. INDIVIDUAL TRIGGERING: 1-5 mg. 4 IN NEW MADRID AREA, 2 IN E. TENN., 4 IN NORTHERN N.Y., 3 IN CANADA (CHICOUTIMI), 4 IN MAINE, 1 IN ALASKA, 1 @ LDGO, 1 IN AUSTRALIA. MOSTLY "FREE-FIELD" (IE: NOT IN STRUCTURE, OR (HOPEFULLY) IN NON-RESONANT STRUCTURE). BOLTED DOWN ON ROCK OR IN LARGE STAINLESS STEEL —

(20) No of 10/1/89

3. Describe the nature of the data you have obtained, in terms of the number of events recorded, their range of magnitudes, and their distances from the array.

$1.9 \leq M \leq 6.8$, $10Km \geq D \geq 800 Km$

CHICOUTIMI EVENT (M≈6) RECORDED ON 9 INSTROMENTS. TENNENT CREEK AFTER SHOCKS ON 3 UNITS. OTHERWISE, TYPICALLY ONE RECORDING / EVENT (BUT 3 UNITS/1 EVENT IN N. MAD RD)

4. What means were used to characterize the site conditions?

GEOLOGIC OBSERVATION.

— NEMA BOX, BURIED ≈ 6" & SET ON 2-4" CONCRETE (FOR SOIL INSTALLATIONS).

5. If you were to establish a new array, what means would you now use to characterize site conditions?

SITE AMPLIFICATION : NOISE & NATURAL EVENTS (THE LATTER TAKES TIME, SO YOU MIGHT AS WELL INSTALL THE STATION).

6. What lessons have been learned

- regarding the operation of the array?

SSA-1'S WORK WELL.
TELEPHONE CONTROL & DATA RETRIEVAL WORKS VERY WELL — PERMITS LOW THRESHOLD TRIGGER WITHOUT WORRYING ABOUT DATA CAPACITY.

- regarding ground response to earthquakes?

RESEARCH STILL IN PROGRESS — CONTACT DR SUE HOUGH FOR CHICOUTIMI

7. Can you comment on the relevance of ambient vibration measurements and forced vibration testing?

FORMER GOOD — BUT NEEDS REF. TO "STD" RESPONSE STATION : OR AREA SURVEY TO DISTINGUISH AREA' RESPONSE FROM 'SITE' RESPONSE.

8. ADDITIONAL COMMENTS AND ADVICE (please use additional pages if desired)

WE HAVE TIME CORRECTION TECHNIQUE VIA TELEPHONE WHICH PROVIDES TIMING ACCURACY TO ± .01 SEC.

Thank you!

Doug Johnson
Name

October 2, 1989

Brian E. Tucker
Calfornia Division of Mines and Geology
1416 Ninth St. Room 1341
Sacremento, Ca. 95814

Fax No. 916-445-5718

Re. Strong-Motion Array Questionnaire.

Dear Brian,

Shumagin array has recorded 25 events between 1970 and 1987, ranging in
magnitude from 3.4 to 6.5. Distances within +/- 250 km. Number of stations
recording per event from 1(most common) to 5(1 event).

Regards

Douglas H. Johnson
Technical Manager, Seismology
LDGO
FAX No. 914-359-5215

STRONG-MOTION ARRAY QUESTIONNAIRE

1. Where is your array located and how long has it been operating?

    see   attachment

2. Please describe your array, in terms of the type and number of instruments, their spacing, their triggering, their recording means (film, tape, or disc; analog or digital), and their foundation and housing.

    see   attachment

3. Describe the nature of the data you have obtained, in terms of the number of events recorded, their range of magnitudes, and their distances from the array.

    See   attachment

4. What means were used to characterize the site conditions?

    See   attachment

STRONG MOTION ARRAY QUESTIONNAIRE

1. The Bureau of Reclamation has been involved in Strong Motion Instrumentation programs since April 1937 when the first array was installed in Hoover Dam (Arizona/Nevada). At present there are 41 arrays in the program, located throughout the western United States, namely in Washington, Oregon, California, Arizona, Utah, Idaho, Montana, Wyoming, and Colorado, primarily associated with Seismic Zones 3 and 4.

2. All instruments deployed to date are analog, primarily model SMA-1's and several CRA-1/FBA-3,13DH systems; 1 to 6 instruments per site and/or structure. All arrays are associated with water resources related lifeline structures or sites, such as dams (earthfill and concrete) and power/pumping plants. All triggers are set to start the systems at 0.01g. Generally the instruments are located on 5ftx5ftx0.5ft concrete pads attached to the structure or site of interest and protected by lightweight fiberglass housing units. When the arrays are associated with concrete dams the instruments are located inside the dam galleries. Several downhole systems are located in boreholes in earthfill dams.

3. Numerous events have been recorded since the deployment of the first array in 1937. Most of the accelerations recorded have been in the <0.05g peak range. However, in May 1983 a series of significant strong motion acceleration time histories were recorded by the array located in and adjacent to the Pleasant Valley Pumping Plant, California. The magnitude 6.5 earthquake which did extensive damage to the town of Coalinga caused a 0.54g peak acceleration at the switchyard of the Pleasant Valley Pumping Plant, located approximately 9 km from the epicenter.

4. Generally, no special program is performed for the acquisition of the data for characterization of the strong motion instrumentation sites. However, frequently the information needed to accomplish this is available as a result of to previous efforts performed for site and materials evaluation required for the design, construction, and maintenance of water resources related lifeline structures. For example, parameters such as shear wave velocity and density distribution with depth in a large number of earthfill dams and foundations were obtained in situ as a result of the Bureau of Reclamation geotechnical investigations for its Safety Evaluation of Existing Dams Program. Should a significant acceleration time history be recorded at a structure where some aspects of site condition information is lacking, this would be supplemented by a subsequent geotechnical exploration program as was the case at Pleasant Valley Pumping Plant.

Bureau of Reclamation - MC D-3611
P.O. Box 25007
Denver, CO 80225

5. If you were to establish a new array, what means would you now use to characterize site conditions?

Same as # 4.

6. What lessons have been learned

- regarding the operation of the array?

Too many to discuss at this point

- regarding ground response to earthquakes?

Same

7. Can you comment on the relevance of ambient vibration measurements and forced vibration testing?

8. ADDITIONAL COMMENTS AND ADVICE (please use additional pages if desired)

Thank you!

Andy Viksne
—————————————
Name

STRONG-MOTION ARRAY QUESTIONNAIRE

1. Where is your array located and how long has it been operating?

   Parkfield, CA

   1 ½ years

2. Please describe your array, in terms of the type and number of instruments, their spacing, their triggering, their recording means (film, tape, or disc; analog or digital), and their foundation and housing.

   14 sites recorded on GEOS : 200 sps, 16 bit digital, 6 channels

   5 of the sites : 3 component FBA, vol. strain & gains, 3 vel.

   1 site : 3 comp FBA, 3 vol. strain (@ High gain > accouple
   low gain

   mod gain > decouple
   8 sites : 3 comp. FBA, 3 comp vel. trans.

3. Describe the nature of the data you have obtained, in terms of the number of events recorded, their range of magnitudes, and their distances from the array.

   ~ 45 events most less than M ~ 2.5

   1 event M 4.0 on all stations

   distances 4 – 45 km .

4. What means were used to characterize the site conditions?

   Bore hole logs at some (shear & P wave)

   geologic logs at others.

5. If you were to establish a new array, what means would you now use to characterize site conditions?

Bore hole logs

6. What lessons have been learned

● regarding the operation of the array?

Well qualified conscientious field personnel expedite installation and improve reliability

● regarding ground response to earthquakes?

Near surface layers (0-200m) even at so called rock sites significantly modify incoming wave fields.

7. Can you comment on the relevance of ambient vibration measurements and forced vibration testing?

In certain situations they have been useful in identification of resonant phenomena.

8. ADDITIONAL COMMENTS AND ADVICE (please use additional pages if desired)

Brian,
Hope these brief comments are helpful.
A copy of our 9th WCEE paper is enclosed.

Thank you!

Roger D. Borcherdt
Name

A BROAD-BAND, WIDE-DYNAMIC RANGE, STRONG-MOTION ARRAY NEAR PARKFIELD, CALIFORNIA, USA FOR MEASUREMENT OF ACCELERATION AND VOLUMETRIC STRAIN

Roger D. BORCHERDT[1], Malcolm J.S. JOHNSTON[1], Thomas C. NOCE[1],
Gary M. GLASSMOYER[1], and Douglas MYREN[1]

[1]United States Geological Survey, Menlo Park, California, USA

SUMMARY

Installation of a 14-station array was completed July, 1987, to provide on-scale, broad-band, high resolution measurements of earthquakes occurring near the segment of the San Andreas fault zone that is expected to rupture before 1993 with a moderate earthquake similar to the 1966 Parkfield, California event. The array is designed to provide on-scale measurement of volumetric strain, ground acceleration, and ground velocity to permit the observation of co-seismic strain offsets, seismic strain radiation, and strong ground motions of engineering interest. Data sets are presented to illustrate array bandwidth (0-100 Hz), dynamic range (145 dB), and detection levels for strain (10^{-11} at 1 Hz) and acceleration (6×10^{-6}g). Use of volumetric strain meters as strong-motion sensors allows the bandwidth for observation of near-source motions to be extended to periods longer than that of conventional accelerometers and permits the inference of seismic wave field characteristics not permitted by either sensor alone.

INTRODUCTION

Scientific evidence suggests an occurrence probability of 0.95 for a moderate earthquake (M~6) before 1993 along the Parkfield segment of the San Andreas fault (Refs. 1, 2, 3). This event has afforded the scientific and engineering communities the opportunity to establish experiments to study earthquake related phenomena (Ref. 4). This report is concerned with an experiment designed to obtain high-fidelity measurements near the rupture zone.

The experiment includes an array of fourteen stations equipped with accelerometers, velocity transducers, and volumetric strain sensors (Fig. 1). Eight stations are equipped with accelerometers and velocity transducers (see Fig. 1) to provide on-scale recordings of ground motions ranging in amplitude from near seismic background noise to 2g in acceleration. Six sites are equipped with volumetric strain sensors and accelerometers to provide on-scale recordings for events larger than magnitude 2.5.

The use of dilatational strain sensors (Sacks-Evertson dilatometers, Ref. 5) extends the bandwidth for observation of near-source motions to periods longer than those detectable by conventional accelerometers. The bandwidth allows observation of pre- and post-seismic strain changes and co-seismic strain offsets. Dynamic range of the dilatometers allows the sensors to be used as both near-source strong-motion sensors as well as sensors to detect strain variations including changes in DC level at levels of seismic background noise near 10^{-11}. In addition, because the dilatometers respond to dilatational strain but not shear strain, they respond to P and Rayleigh energy but not shear or Love wave energy. As a result when dilatometers are colocated with conventional three-component seismometers and accelerometers, they can be used to resolve superimposed wavefields and infer characteristics of seismic wavefields not permitted by either sensor alone (Refs. 6, 7).
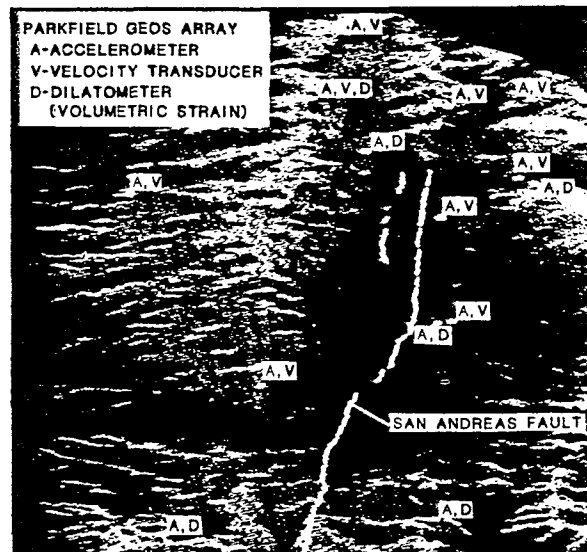
Fig. 1. Location map for GEOS array near Parkfield, California.

This report describes instrumentation, expected data sets, and theoretical results pertinent to interpretation of seismic radiation fields recorded on colocated sensors.

INSTRUMENTATION

Signals from the two types of sensors at each station location are recorded on-site in event-detect mode with broad-band, 16-bit (96dB) digital, six-channel recorders (General Earthquake Observation System, GEOS, Ref. 9) at sampling rates of 200 sps per channel. A detailed account of the recording system characteristics is provided by Borcherdt et al. (Ref. 9). Signals from the dilatometers at six of the sites are recorded in both AC and DC coupled modes at high and low gain levels. In addition, the dilatometer signals are recorded continuously in Menlo Park, California via 16 bit satellite telemetry at a low sampling rate (1 sample per 10 minutes) for purposes of earthquake prediction (Ref. 8).

For those sites equipped with accelerometers, velocity transducers, and GEOS recorders, the effective dynamic range exceeds 130 dB over a bandwidth for signal resolution of about 15 to 0.01 seconds. For those sites equipped with accelerometers and dilatometers, the lower limit for resolution of acceleration is $6x10^{-6}$g. The period band for detection of volumetric strain at earth-strain noise levels is greater than 10^8 to 0.05 secs. (Ref. 8).

An average estimate of earth strain noise is shown in Fig. 2. The spectrum, obtained for a site in the eastern Mojave desert, California, reveals peaks due to microseisms near 4 and 8 seconds, peaks due to earth tides near 12 and 24 hours, and a decrease in noise with period of about 10 dB per decade. The spectrum shows a detection bandwidth of more than 8 orders of magnitude at earth noise levels. Maximum strain detection limits of 10^{-6} strain for the dilatometers located at depths of 150-200 m suggests a dynamic range for strain detection of 145-150 dB.

In the time interval 7/87 through 12/87, 36 of the earthquakes in the Parkfield region had been recorded on one or more stations in the array (Ref. 10). These events ranged in magnitude from less than 1 to 2.5. As no event larger than 2.5 for which the array was designed has occurred since completion of the array, examples of data sets from similar installations in other locations of California are used for illustration purposes.
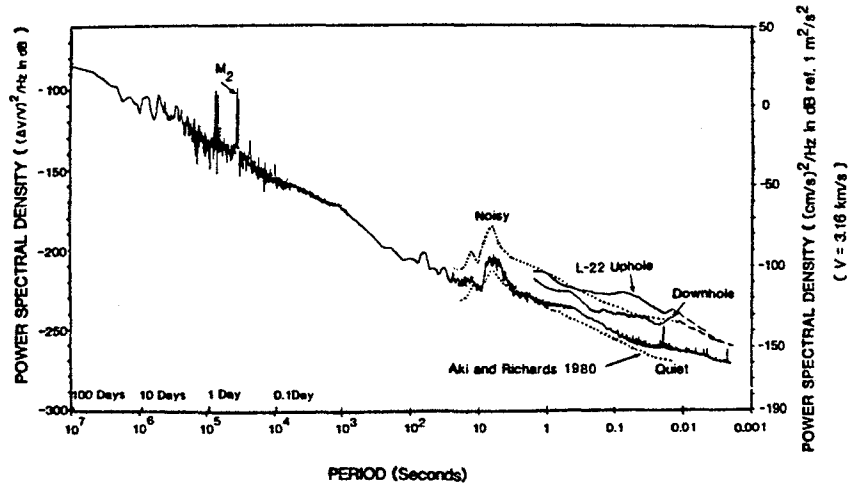
Fig. 2. Earth strain noise observed with dilatometer and seismometers illustrates array detection levels for periods ranging over more than 8 orders of magnitude.

ANTICIPATED NEAR-SOURCE MEASUREMENTS

Recordings of a moderate earthquake near North Palm Springs, California, obtained at a distance of 130 km illustrate the types of signals expected on the array (Fig. 3). The first trace shows the continuous volumetric strain time history as recorded at 1 sample per 10 minutes for a 48-hour time interval. This trace shows strain variations due to earth tides, atmospheric pressure changes, and the strain offset of 17 nanostrain associated with the earthquake. This offset, when interpreted with respect to a dislocation model, yields an estimate of moment magnitude for the event of 6.0 (Ref. 11).

Traces 2 through 5 of Fig. 3 show the corresponding volumetric strain and three-component seismometer signals recorded at the site at 200 samples per second in the intervening ten minute time interval between samples recorded continuously *via* satellite telemetry (see trace 1, Fig. 3). The traces recorded at high sampling rates illustrate the capability of the array to observe seismic radiation fields from both types of sensors in an overlapping period band of engineering interest, while at the same time suggesting the capability to observe characteristics of the seismic radiation field at periods longer than those permitted by conventional accelerometers. Analysis of the colocated signals has been shown by Borcherdt *et al.* (Ref. 10) to yield estimates at the site of local material velocity (2.9 km/s), attenuation ($Q_{MS}^{-1} = 0.1$), and the vertical free surface reflection coefficient for SP (0.8).
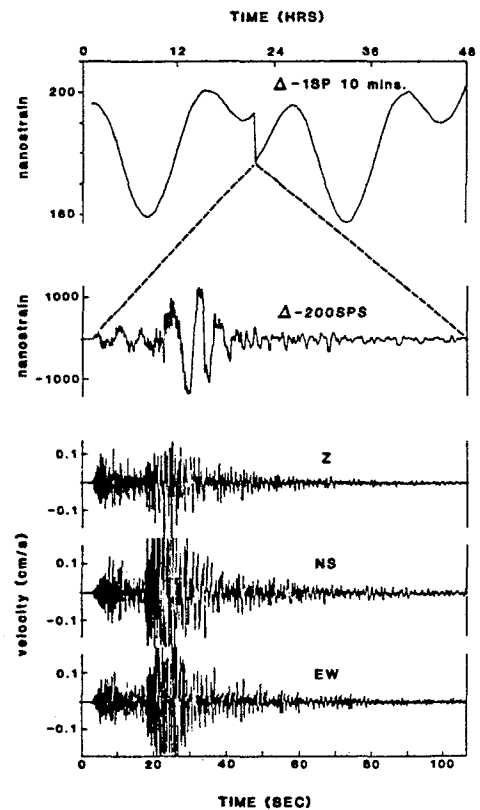

Fig. 3. Volumetric strain (Δ) and ground velocity for North Palm Springs earthquake (M6.0) shows tidal variations and co-seismic strain offset observed at 10 minute intervals (trace 1), seismic strain radiation at 200 sps (trace 2), and absence of long period energy detected by 1 Hz seismometers (traces 4, 5, 6).

Recordings of small events (M<2.0) near the source (<8 km) serve to illustrate the capability of the volumetric strain meter to respond to dilatational energy but not shear energy (Fig. 4). For comparison purposes, the volumetric strain signal (bold) recorded for this event is superimposed on that of the vertical seismometer. The traces have been filtered in a pass band (2 to 6 Hz) common to the two sensor types. Comparison of the straingram and vertical seismogram shows a small phase shift due to vertical spatial separation of the sensors and considerable similarity in wave form during arrival of the initial P-wave energy. Comparison of the signals during the arrival of the S energy, evident on the radial and transverse components of the horizontal seismometers, suggests the dilatometer is showing a relatively small response to the incident S energy.
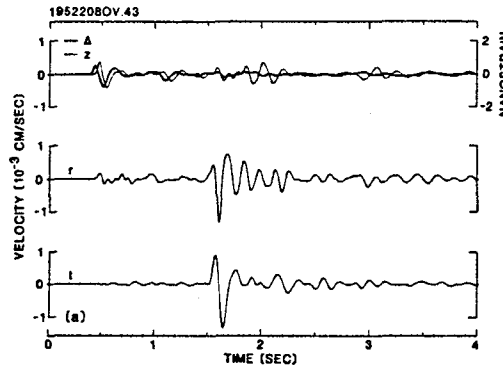

Fig. 4. Volumetric strain (A) and ground velocity (z, r t) recorded near (<8km) small earthquake (M<2.0) suggests that dilatometer responds to P energy but not incident S energy.

Theoretical descriptions of the response of a volumetric strain meter to incident P-, S-, and Rayleigh-type waves on a viscoelastic half-space are provided by Borcherdt (Ref. 7). They show that the effect of the free surface must be considered in order to account for the response of a dilatometer to incident S energy. The free surface, volumetric-strain reflection coefficient for a homogeneous S wave incident on the free surface of a viscoelastic half-space is shown (Fig. 5) for Pierre Shale (Ref. 8). The computed reflection coefficient suggests that the response of the volumetric strain sensor near the time of incident S energy vanishes for angles of incidence near vertical and 45 degrees and reaches a maximum for angles (28°) beyond the elastic critical angle (22°). For angles of incidence corresponding to maximum response, velocity Q^{-1} and particle motion ellipticity for the reflected dilatational disturbance are 25 percent less, 300 percent greater, and 60 percent greater respectively than those for corresponding homogeneous P wave (Figs. 5b-5d).
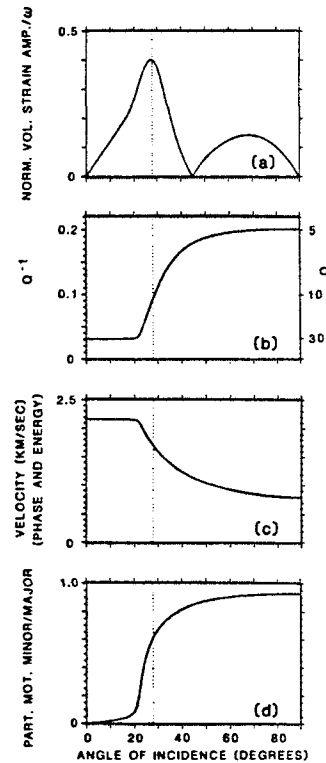

Fig. 5. Volumetric strain reflection coefficient (a) for S wave incident on free surface and Q^{-1} (b) velocity (c), and particle motion axis ratio (d) for reflected P wave.

Although no near-source recordings of a moderate earthquake have yet been obtained on a comparable array using colocated volumetric strain meters and accelerometers, the records from the 1966 Parkfield array with maximum acceleration near 0.5 g serve as a basis to determine gain settings for the corresponding sensors. Guidance regarding estimates of maximum strain levels as observed in boreholes located in sandstone and granite at depths of sensor emplacement (~150-200 m) is provided by model estimates (Fig. 6, Ref. 12). Estimates of coseismic strain offset at each of the stations is not expected to exceed 10^{-6} (Fig. 6). The estimates suggest that the maximum offsets are likely to be measured for sites near rupture initiation and termination.
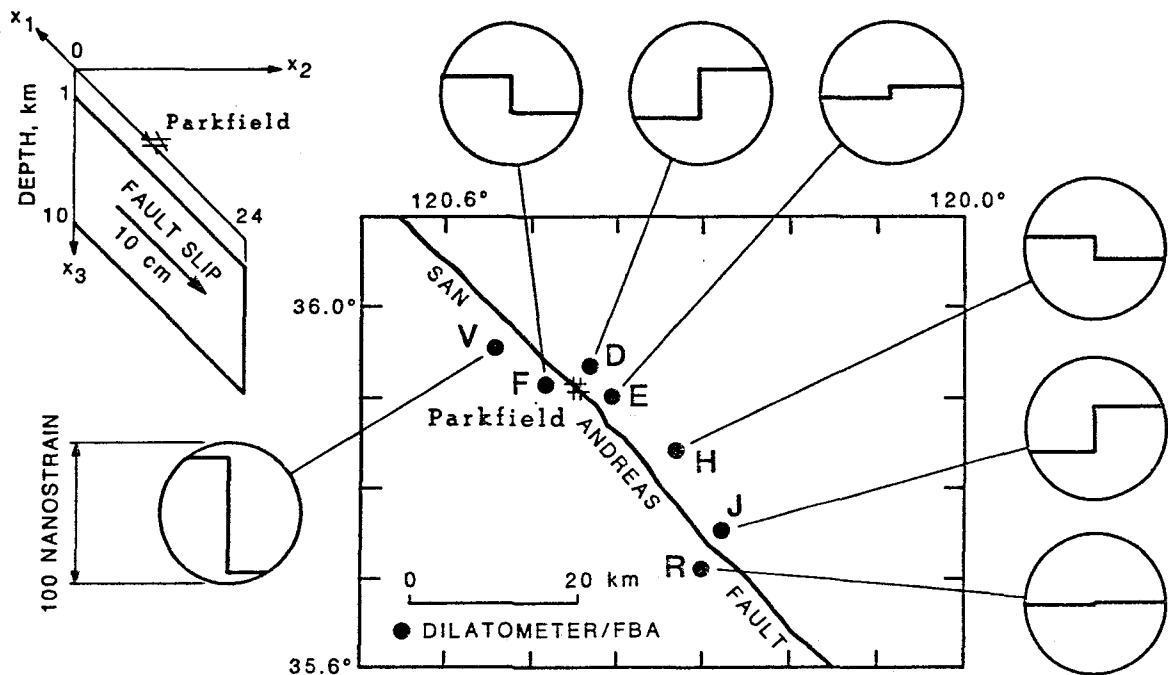

Fig. 6. Estimates of co-seismic dilatational strain offset, using the indicated dislocation model for the anticipated Parkfield earthquake.

ACKNOWLEDGMENTS

REFERENCES

1.   Bakun, W.H. and T.V. McEvilly, "Recurrence models and the Parkfield, California earthquakes," J. Geophys. Res., 89, 3051-3058, 1984.

2.   Agnew, D.C., et al., "Probabilities of large earthquakes occurring in California on the San Andreas fault," U.S. Geol. Surv. O.F. Rept. 88-398, 62 pp, 1988.

3.   Bakun, W.H., and A.G. Lindh, "The Parkfield, California earthquake prediction experiment," Science, 229, 619-624, 1985.

4.   Tucker, B., et al., "Strong-motion seismology experiments in the near field of the predicted Parkfield, California, earthquake," Proc. 9th WCEE, 1988.

5. Sacks, I.S., S. Suyehiro, D.W. Evertson, and Y. Yamagishi, "Sacks-Evertson strain meter, its installation in Japan and some preliminary results concerning strain steps," Pap. Meterol. Geophys., **22,**, 195-207, 1971.

6. Benioff, H. and B. Gutenberg, "The response of strain and pendulum seismographs to surface waves," Bull. Seismol. Soc. Am., **43**, 229-237, 1952.

7. Borcherdt, R.D., "Volumetric strain in relation to particle displacement for body and surface waves in a general viscoelastic half-space," Geophys. J. Roy. Astro. Soc., **93**, 215-228, 1988.

8. Johnston, M.J.S., A.T. Linde, M.T. Gladwin, and R.D. Borcherdt, "Fault failure with moderate earthquakes," Tectonophysics, **144**, 189-206, 1987.

9. Borcherdt, R.D., J.B. Fletcher, E.G. Jensen, G.L. Maxwell, J.R. Van Schaack, R.E. Warrick, E. Cranswick, M.J.S. Johnston, and R. McClearn, "A general earthquake observation system (GEOS)," Bull. Seismol. Soc. Am., **75**, 1783-1826, 1985.

10. Borcherdt, R.D., M.J.S. Johnston, G. Glassmoyer, and D. Myren, "Observations of anelastic free-surface reflection coefficients using borehole volumetric strain meters," Seismol. Res. Letters, **59,**, 27, 1988.

11. Johnston, M.J.S., R.D. Borcherdt, M.T. Gladwin, and G. Glassmoyer, "Static and dynamic strain during the M_L 5.9, Banning, California, earthquake on July 8, 1986," Trans. Am. Geophys. Un., **68**, 1244, 1987.

12. Press, F., "Displacements, strains and tilts at teleseismic distances," J. Geophys. Res., **84**, 5423-5435, 1965.

13. Aki, K. and P. Richards, Quantitative Seismology, Theory and Methods, W.H. Freeman, San Francisco, CA, 932 pp, 1980.

Appendix D ARRAY OPERATORS

OPERATORS OF ARRAYS
RESPONSES TO QUESTIONNAIRES

CHINA

Dr. Li-Li Xie, Vice Director/W. D. Iwan
Institute of Engineering Mechanics
State Seismological Bureau
Harbin, CHINA

Lotung

George Lui/K. Wen
Institute of Earth Sciences
Academia Sinica
Taipei, Taiwan, Republic of China

Lotung

Yi-Ben Tsai
Geosciences Department
Pacific Gas and Electric
One California Street, Room F-200
San Francisco, CA 94106

ITALY

Mauro Basili/G. Bongiovanni
ENEA
Via Anguillarese Km 1,300
Roma, ITALY

JAPAN
    Ashigara Valley

Kazuyoshi Kudo
Strong-Motion Observation Center
Earthquake Research Institute
University of Tokyo
1-1-1 Yayoi, Bunkyo-ku
Tokyo, JAPAN

Tsuneo Katayama
Institute for Industrial Science
University of Tokyo
1-1-1 Yayoi, Bunkyo-ku
Tokyo, JAPAN

USA

Parkfield, Imperial Valley

Thomas Holzer
U.S. Geological Survey, MS 977
345 Middlefield Road
Menlo Park, CA 94025

Turkey Flat

Charles R. Real/Anthony Shakal
Division of Mines and Geology
630 Bercut Drive
Sacramento, CA 95814

Parkfield

Carl Stepp/John Schneider
Electric Power Research Institute
3412 Hillview Avenue
P.O. Box 10412
Palo Alto, CA 94303

Diablo Canyon

Yi-Ben Tsai
Geosciences Department
Pacific Gas & Electric
One California Street, Room F-200
San Francisco, CA 94106

STRONG-MOTION ARRAY QUESTIONNAIRE

1. Where is your array located and how long has it been operating?

   Beijing Parking Array   1983— present.   Beijing

   Tangshen Experimental Array   1982.7 — 1989.12   Tangshan, Hebei Province.

   Three Dimensional Array   1984 — 1987   Waste coal mine, Tangshan

   kangding Network   1984 — present   Kangding, Sichun province

   Yunnan (West) Array   1984 — present   West Yunnan.

2. Please describe your array, in terms of the type and number of instruments, their spacing, their triggering, their recording means (film, tape, or disc; analog or digital), and their foundation and housing.

   See attached papers

3. Describe the nature of the data you have obtained, in terms of the number of events recorded, their range of magnitudes, and their distances from the array.

   See attached papers

4. What means were used to characterize the site conditions?

   "rock, firm soil, general soil and soft soil." — a very simple descriptive categories have been used for chara

5. If you were to establish a new array, what means would you now use to characterize site conditions?

Geometrical + Geotechnical parameters (such as depths of layer, number of layers, dimensions of valley, Velocity structures (Vp, Vs, etc) density, modulus-strain relation, damping-strain relations etc.)

6. What lessons have been learned

- regarding the operation of the array?
  - much attention should be paid to power supply, trigger system (prevention from mis triggering caused by environmental disturbances)
  - Select suitable sensitivity of instruments, if no of auto-gain rangers are available to your system.   • Correct your timing system in time.
- regarding ground response to earthquakes?
  - make sure to keep the transducers fixed on the pier.
  - Keep certain distance of your instrument from other structures
  - Considering the topographical effects of the site on obtained ground motions.

7. Can you comment on the relevance of ambient vibration measurements and forced vibration testing?
It is valuable to use your structural array to measure the ambient vibration (such as tremor, response of structures subjected to the wind load) and forced vibration excited by sychronizing eccentric mass exciter. The array should be so designed as to be able to measure the translational and torsional components.

8. ADDITIONAL COMMENTS AND ADVICE (please use additional pages if desired)
   - An important measure of rapidly increasing the valuable strong motion data base is to develope the regional movable strong motion array.
   - Structural array should be developed as equally as would ground motion array.
   - much effort should be done to develop the method for application of the

Thank you! strong motion records (both ground and structures) in various field.

_____

Name

Li-Li XIE

Remember to send me a copy of your Workshop Proceedings. Thank you.

BP — Beijing Parking Array
TS — Tangshan Experimental Array
TDSA — Three Dimensional (space) Array
KD — Kangding Array
DX — Yunnan (West) Array or Dianxi Array

Peng, Kezhong — TABLE 1

Array Code	Array Types	Observ. Objects	Period	No. of Stations	No. of Deploying	No. of Maintenance (BSMOC/Local)	No. of Events	No. of Records	Fig. of Arrays
BP	TE, SR DA, PA	2,3,5, 6,7,8	82.7– now	28	28	462/0	0	0	Fig. 1 Fig. 2
TS	SE, SM DA	2,3,4, 5,7	82.7– 87.12	24	65	491/0	707	1622	Fig. 3
TDSA*	TD, SM	2,3,4, 5	83.3– 87.12	(8)	(33)	(60)/0	(36)	(236)	Fig. 4
KD	SE	1,2,3, 4	82.12– now	5	5	29/220	0	0	Fig. 5
DX	SE, LS SM	1,2,3, 4,5,7	83.5– now	20	29	192/627	15	24	Fig. 6
HR	MO	1	82.12	3	3	12/0	1	2	
LQ	MO	1	85.4	1	1	10/0	1	1	
Total				81	131	1196/847	724	1649	

NOTES:

Array Types:
TE – Topography Effect
SR – Structure Response
TD – Three Dimension Space
LS – Local Site Effect
SM – Source Mechanism and Wave Propagation
PA – Parking Array
DA – Dense Array
SE – Simple Extended
MO – Mobile Observation

Observ. Objects
1. For catching large earthquakes.
2. For measuring the source parameters and studying source mechanism.
3. For studying the nature of the rupture propagation.
4. For deriving the law of wave propagation and attenuation.
5. For the study of site effects.
6. For the study of soil-structure interaction.
7. For the study of variations of strong ground motions in a small area.
8. Parking array.

No. of deploying – No. of station-times deployed.
No. of maintenance – No. of station-times maintained.

* All the data with bracket of TDSA is included in TS.

Fig. 1

Section A-A

Parking array site on western outskirts of Beijing

Dense Array

Fig. 2

OCTOBER 1ST SCHOOL

N

DISTRIBUTION OF INSTRUMENTS ON DENSE ARRAY

Fig. 3

STRONG GROUND MOTION ACCELEROGRAPH ARRAY IN TANGSHAN, CHINA

Tangshan Experimental Array

Fig. 4 Plane of TDSA Array

Fig. 5

The Active Tectonic System and Strong Motion Accelerograph Stations in Kangding Area , China

Fig. 6

The Active Tectonic System and Strong Ground Motion Instrumental Array in western Yunnan , China

Fig. 7

SAO52-154,155,156   82046/TS12   IEM 017

TIME: 292 2046 01.738

c922045T=.012 COMP:1(UP),2(H=0),3(H=90)

STRONG-MOTION ARRAY QUESTIONNAIRE

1.   Where is your array located and how long has it been
      operating?

      a.   SMART-1 array (Strong Motion Array in Taiwan, phase 1)
            locatein the Lanyang plain, northeastern Taiwan. It was
            installed at Sep. 1980.

      b.   LSST array (Large Scale Seismic Test Program) located
            within the SMART-1 array, and operated from Nov. 1985.

2.   Please describe your array, in terms of the type and number
      of instruments, their spacing, triggering, their recording
      means (film, tape, or disc; anolog or digital), and their
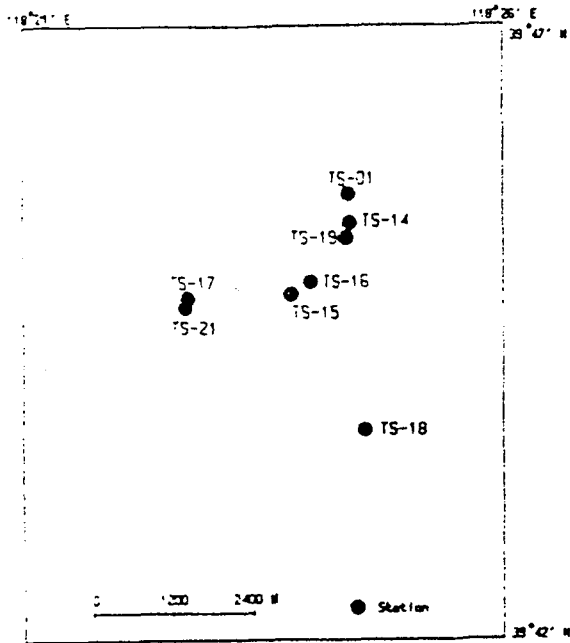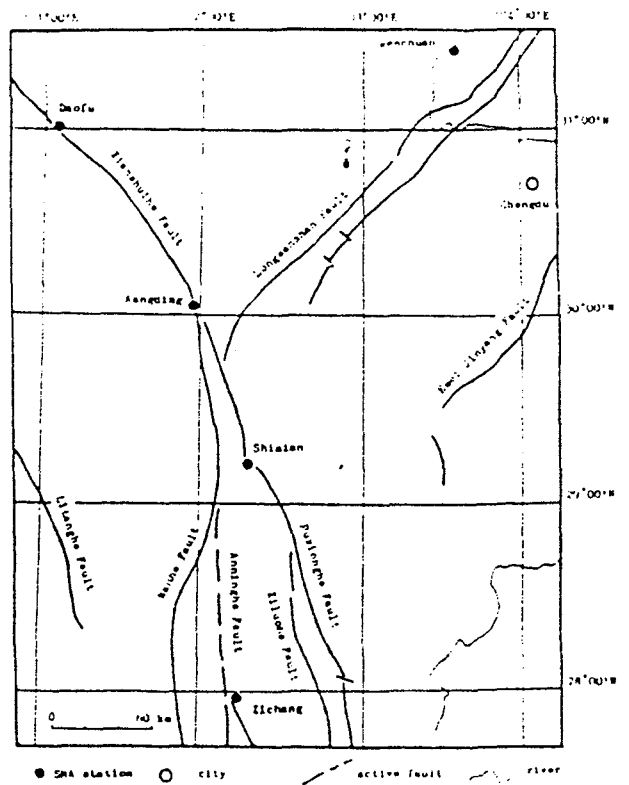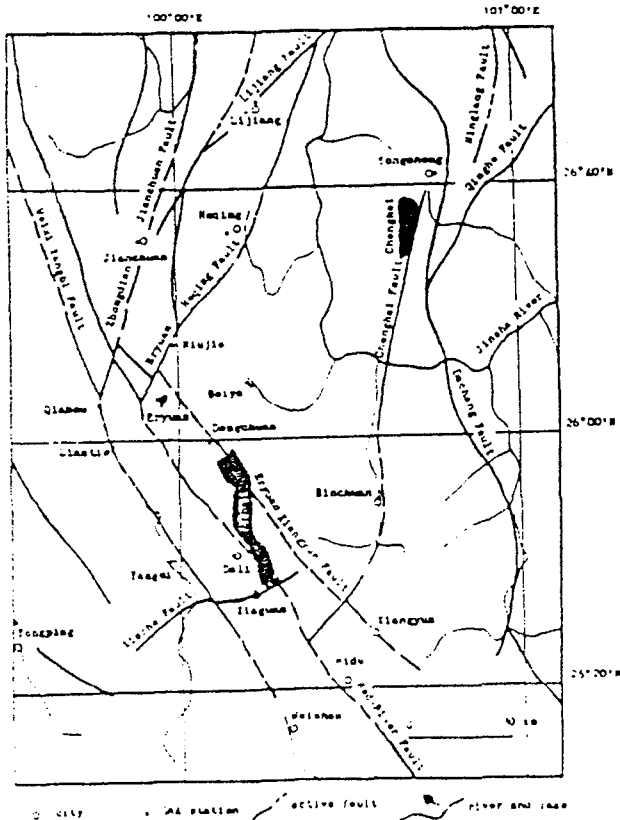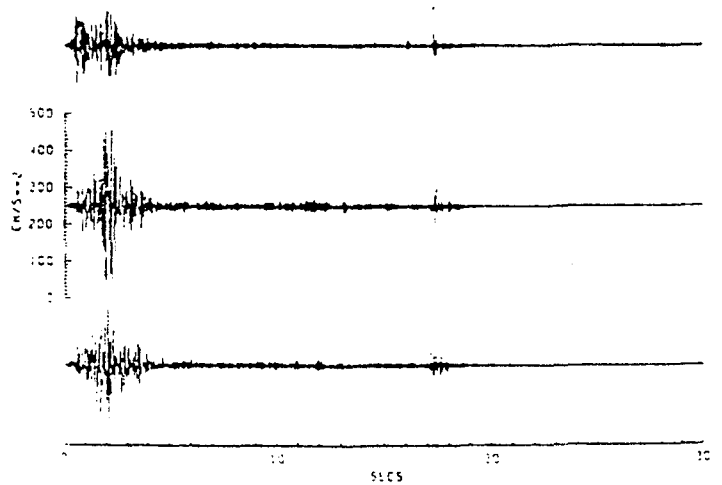   foundation and housing.

      a.   The SMART-1 array consists of a center site, 6 extension
            sites and three concentric circles, each with twelve
            evenly spaced sites and radii of 200m, 1km and 2km,
            respectively. Each of 43 accelerographs consists of a
            SA-3000 force-balance accelerometer, capable of
            recording ±2G, and a DR-100 digital event recorder that
            uses a magnetic tape cassette. Signals are digitized
            with 12-bit resolution at 100 samples per second.

      b.   The LSST array consists of 12 structural accelerometers,
            15 surface accelerometers (which are radially spaced at
            120 degree and extend outward from a 1/4 scale
            containment model), 8 downhole accelerometers (2 sets,
            each set placed down to 4 holes of about 6m, 11m, 17m,
            and, 47m in depth respectively), and 20 pressure gauges.
            All accelerometers are ±2G FBA-13 triaxial force balance
            accelerometer, and data are collected by a 144-channel
            digital central recording system. signals are digitized
            with 12-bit resolution at 200 samples per second, and
            recorded on 48 digital cassette recorders.

      c.   All surface accelerometers af SMART-1 and LSST array,
            are bolted to low concrete pedestals. To assure close
            coupling with its fonndation, the pad have short piers
            extening into the ground. For each stand-alone unit, or
            each surface accelerometer of LSST array, a lightweiht
            fiber glass enclosure is used to provide protection
            against weather and minor vandalism.

3.   Describe the nature of the data you have obtained, in terms
      of the number of events recorded, their range of magnitudes,
      and their distances from the array.

      a.   Through Sep. 1989, 55 earthquakes were recorder by the
            SMART-1 array, with local magnitude from 3.6 to 6.9, and
            epicentral distances (from the array to center) are range
            from 2km to 194km.

b. LSST array had recorded 27 earthquakes. The range of magnitudes are 4.5 to 6.8, and the epicentral distances are range from 5km to 96km.

4. What means were used to characterize the site conditions?

   Geological survey and geophysical survey (include seismic reflection and refraction survey, cross-hole and up-hole shooting methode). LSST array also has 100 meters geological log of drill hole.

5. If you were to establish a new array, what means would you now use to characterize site conditions?

   Geological survey, geophysical survey, and geotechnical survey.

6. What lessions have been learned

   ● regarding the operation of the array ?

   1. In comparing surface instruments with downhole instruments, surface instruments have greater reliability.
   2. It's need a lot of manpower To keep the time accuracy and maintain a station without commercial AC power in SMART-1 array.
   3. Should use solid state accelerographs in the future to reduce mechanical failures and related problems which caused by moving parts of recorders.

   ● regardin ground response to earthquakes?

   1. Spatial variation of ground motions.
   2. Seismic wave intensity of strong ground motion.
   3. Statistical properties of PGA and response spectral values.
   4. Comparison of soil and rock sites.
   5. Identification of wave types.

Date: Sep. 25 , 1989

By :   *Kuo-Liang Wen*

       Chun-Chi Liu
       _____
       Kuo-Liang, Wen
       Associate Research Fellow
       Chun-Chi, Liu
       Chief Engineer

       Institute of Earth Sciences
       Academia Sinica
       P.O. Box 23-59
       Taipei, Taiwan, ROC

STRONG-MOTION ARRAY QUESTIONAIRE

1. Where is your array located and how long has it operating?

   The SMART1 array (an abbreviated name for the Strong-Motion Array in Taiwan, Phase 1) is located in Lanyang Plain area in northeastern Taiwan, near the town of Lotung. The array has been in operation since October 1980.

2. Please describe your array, in terms of the type and number of instruments, their spacing, their triggering, their recording means (film, tape, or disc; analog or digital), and their foundation and housing.

   Type of instruments: DR-100 recorders by Sprengnether, accelerometers by Columbia.
   Number of instruments: 39
   Array layout: 12 instruments are evenly spaced on each of the three concentric rings with radii 0.2, 1.0, and 2.0 km, respectively. With an instrument at the array center, the 37 instruments form 12 radial arms with an equal azimuthal spacing of 30 degrees. One of the arms extends outward with two additional instruments, with the outer one being placed on the rock outcrop at the edge of the alluvial plain.
   Timing and triggering: Each instrument has an internal clock. The array is synchronized twice a week with a master clock. The instruments are triggered individually on preset acceleration thresholds.
   Recording means: digital cassette tapes.
   Instrument foundation: 20-cm thick concrete pad poured in place over steel wire mesh.
   Instrument housing: Prefabricated fiber glass housing.

3. Describe the nature of the data you have obtained, in terms of the number of events recorded, their range of magnitudes, and their distances from the array.

   Number of events: over 50.
   Magnitude range: 3.6-6.8 M_L.
   Distance range: very close to 200 km.
   Focal depth range: very shallow to 100 km.

4. What means were used to characterize the site conditions?

   a. Surface geology.
   b. Several seismic refraction prifiles through and within the array area.

5. If you were to establish a new array, what means would you now use to characterize site conditions?

a. Surface geology.
b. Borings.
c. Borehole seismic velocity measurements.

6. What lessons have been learned

   o regarding the operation of the array?

   Regular check-up of the instruments in the field by
   dedicated technicians is a must.
   Competent electronic engineers to perform instrument trouble
   shootings can improve drastically the integrity and the data
   recoverage rate of the array.

   o regarding ground response to earthquakes?

   Ground response to earthquakes varies significantly even in
   a relatively small, flat and seemingly simple site area.
   Ground response characteristics vary with magnitude and
   distance of earthquakes.
   Incoherence in ground motions clearly increases with station
   separation as well as with frequency.
   Ground responses are different on soil and rock sites.

7. Can you comment on the relevance of ambient vibration
   measurements and forced vibration testing?

   One main advantage of ambient vibration measurements is that
   they are inexpensive and convenient, in particular, with the
   new solid-state recorders with adjustable full-scale settings.
   These measurements can provide predominant frequencies in the
   ground response of soil sites at low strain levels.
   Unfortunately, the relation between these frequencies of
   ambient vibrations and those of strong motions is not yet well
   established.
   I am not informed enough to comment on the relevance of forced
   vibration testing.

8. Additional comments and advice.

   Except for arrays that are tied to specific project sites or
   facilities, selection of the array location is very crucial
   to the success of an array project. Basically, one would go to
   a location where the earthquakes are frequent, and
   preferrably, varied in their hypocentral locations and
   source characteristics. Operating an array for long time
   without getting some useful records could wear out the array
   operators logistically, and even emotionally. In addition,
   easy access to adequate technical support is also an important
   factor to consider.

Strong-Motion Array Questionnaire

1 To date, we are operating two special purposes strong-motion arrays, that will be called A and B.

A) Southern Lazio (100 Km south of Rome), designed to study the boundaries between two areas, one of which does not show any seismicity. Full operating July 1984.

B) Cerreto di Spoleto (Umbria, Central Appennine), designed to study topographical effects, mainly for the seismic behavior of historical hilltown. Full operating end of the current year.

2 A) 10 triaxial digital strong-motion accelerometers. Threshold triggering (0.005 g vertical). Tape recording system. Pre-event 3 seconds. They are aligned over a length of 20 Km. The instruments are anchored to a concrete pile (40X40X70) anchored on the soil. The housing is light cabinet anchored to a R.C. basemat (thick 15 cm).

B) 4 triaxial digital strong-motion accelerometers. Solid state memory. Pre-event 3 sec. Threshold triggering (0.005 g vertical). One instrument is on the top, another is at midheight and a third one is at the base of a ridge. The ridge is 200 m height and the instruments are about 300 m far each from the other. All of them are on rock, the fourth instrument is about 500 m on the bed of a river. Since the ridge is made of calcareous rock up to the last few centimetres of soil the foundations are very light, though strongly anchored to the rock. For the instrument on the bed of the river a stiffer pile has been provided. Housing is similar to the other array.

3 A) A 4.7 Ml earthquake with epicentral distance about 30 Km from the array happened, with some aftershoks, in May 1984 while the array was being deployed so that only few instruments were operating. The six records obtained are not considered useful to match the array purpose.

B) No significant events.

4 A) No specific characterization of the sites. They have been selected on geological and geomorphological basis. Geophysical and geotechnical surveys are foreseen.

B) Same as A

5   Supposedly, when you decide to establish an array in a certain area you know what you are looking for. So you should know the global geological characteristics of that area. Based on this knowledge you should determine a detailed map of the soil and subsoil through geophysical survey. Finally geothecnical surveys and laboratory tests are to be performed.
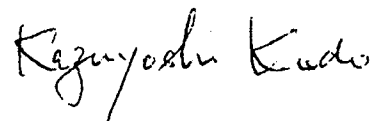
6   ,,,,,,,,,,,,,,,,,,,

7   If the geometry of the subsoil is simple enough it is interesting to use forced vibration (esp. esposions) to test propagation and specific computer codes.

8   ,,,,,,,,,,,,,,,,,,,,

The answer to the strong-motion array questionnaire

1. *Ashigara valley, 70km south-west of Tokyo, Japan.*
   It has been operating since December of 1987.

2. Combination of simple extended array consists of 7 rock site, 8 sediments and three bore holes at -10,-30 and -100m depths.
   Spacing: 1-5km.
   Triggering: Threshold of acceleration(1-4gal). Record-starting for the whole instruments of array is controlled by judging the plural site satisfy the presetted triggering conditions. The control is carried out using low cost(50 BAUD) dedicated telephone lines.
   Recording means: Cassette tape and IC-memory (2 Mbytes), Digital(14bits+AGC).
   Foundation: Base(50cmx50cm)-isolated,
   Housing: Reinforced-concrete (2mx2mx2m).

3. Approximately 20 events have been recovered.
   Range of Magnitude: 4-6.7
   Distance: 10km(M4) - 120km(M6.7)
   Maximum acceleration at sediment site: 0.1g (M6.7)

4. Surface geological map and bore hole geological data were used.
   The data of seismic prospectings were also referred, they were limited though.

5. Seismic prospecting would be most important data for characterizing the site condition for a newly designed array.

6. a) On the operation of the array
   i) Common triggering system for the whole instruments is very useful for recovering the moderate ground motion. It is very rare that the miss-triggering is caused by man-made noise, which we have been troubled at a single observation site in downtown area.
   ii) Data acquisition using public telephone line is skillful. However, we have faced to the long elapse time for acquiring full data in case of earthquake swarm.
   b) On ground response to earthquakes
   Precise analyses have not been done yet. Through the qualitative consideration from the observed data, the amplification due to soft sediments is significant as that the particular band of spectra at sediment site exceed 10 times those at rock site. The nature of spectral ratio of sediment site to rock one is slightly depend on the incidence of seismic motion to the valley.

7. The review by Prof. Aki(1988,Earthquake Engineering and Soil Dynamics II-, ASCE) is essential. However, microtremor measurements might be applicable to understand the relative shakeability at sediment site in a narrow area. In a strict sense, a simultaneous observation more than 2 sites should be required.

Kazuyoshi KUDO

USE OF DENSE ARRAY DATA IN THE DETERMINATION OF ENGINEERING PROPERTIES OF STRONG MOTIONS

by

Tsuneo KATAYAMA
Institute of Industrial Science
University of Tokyo

SUMMARY

A dense seismometer array in Chiba Experiment Station of the Institute of Industrial Science, University of Tokyo, was introduced including its complementary observation system for measuring soil and buried pipe strains. By using the dense array data, the variation of peak accelerations within a small area was examined. It was conclusiv.,y found that the axial pipe strain is almost equal to the surrounding soil strain in the pipe direction. The soil strains evaluated from dense array data were generally in good agreement with the directly measured soil strains and pipe strains even for a small finite element if the original accelerograms are processed through proper filters. For an incident wave of dominantly shear type, the pipe strain was found to be small, namely the pipe strain measured in 10^{-6} being only 0.15-0.30 times the peak acceleration measured in cm/s/s.

CHIBA DENSE ARRAY

A dense seismometer array network located in Chiba Experiment Station of the Institute of Industrial Science, University of Tokyo, has been operating since April, 1982. In this network a total of 155 components of ground motions, comprising 123 components of ground acceleration on and in the ground and 32 components of strains in ground and in buried pipes, are

simultaneously recorded.

THE SITE: The observation site is located in the Chiba Experiment Station of the Institute of Industrial Science, University of Tokyo. The topographical and geological conditions of the site are generally simple with the ground surface being almost flat. Figure 1 shows the typical soil profiles obtained from the three of the boreholes in which seismometers were installed. The top 4-5 m of the site is covered with loam with the standard penetration N value being less than 10. The loam layer is underlain by the clayey layer with a thickness of 3-4 m whose N values are also less than 10. The sand layer underlying the clayey layer generally has N values greater than 20-30. This sand layer, although its stiffness generally increases with depth, is interspersed with clay which shows relatively smaller values of N. In spite of the slight differences in the locations of the boundaries between different layers from one borehole to another, the overall agreement is good and indicates a relatively simple soil structure. By assuming the thickness and the S wave velocity of the topmost layer to be $H=5m$ and $Vs=140$ m/s respectively, the dominant period is estimated as 0.14 s.

THE DENSE ARRAY: Figure 2 shows the layout of the on-ground (-1 m from the ground surface) seismometers. There is a large triangular network P0-P8-P5 with each of the three sides being approximately 300 m in length. Around point C0 are located eight on-ground seismometers, four of which are only 5 m from C0, and the remaining are 15 m from C0. The former are denoted by C1, C2, C3 and C4, and the latter by P1, P2, P3 and P4. The number and locations of in-ground seismometers differ for different groups of points as shown in Table 1. At 11 out of the total 15 boreholes, seismometers were installed at a depth of 10 m from the ground surface. The larger, triangular network was laid to obtain the macroscopic propagation properties of seismic waves, while the very densely located array was established to investigate the local soil strain characteristics during an earthquake.

THE BOREHOLE SEISMOMETER: The piezo-electric type

acceleration transducer, which recently became
commercially available for earthquake ground motion
measurement, was used for the array observation. Three
transducers (two horizontal and one vertical) and their
amplifiers are installed in a cylindrical steel casing
with an external diameter of 65 mm and a length of 335
mm. Table 2 summarizes some of the important
characteristics of the seismometer. The seismometer is
supposed to have a practically flat sensitivity in the
frequency range between 0.1 Hz and 30 Hz. The results of
the shaking table test performed on one of the prototype
seismometers are shown in Fig.3. Judging from the
characteristics of the three reference transducers used
for the test, it was confirmed that the amplitude
sensitivity is flat with $\pm$ 3 percent variation within
the frequency range between 0.1 Hz and 50 Hz. The output
sensitivity of the transducer and amplifier system is 5
V per 1000 cm/s/s and the output impedance is 10 ohms.
Because of the aforementioned properties, the signal can
be recorded without any additional amplification and may
be easily transmitted over a distance of 200 m by a
cable. Some of the advantages of the piezo-electric type
accelerometers are 1) Since the mass and spring are
inherently an almost single structure, there is
practically no movable mechanical part, and hence,
troubles associated with wear and fatigue are minimal,
and 2) Because of the same aforementioned reason, the
transducer has strong resistance against shock, and
hence, it is reliable during handling and installation.
On the other hand, since the amplifiers are housed
within the casing, electricity should be supplied to the
casing. Therefore, if an abnormally high-voltage current
is accidentally supplied, the pickup-amplifier system
may be damaged. Hence, sufficient care should be taken
to prevent such an accident since the casing, once
installed in a borehole, is practically unrecoverable.

Seismometers were installed in boreholes with
diameters of 116 mm. This diameter was determined by
considering that a maximum of five seismometers were to
be installed in a borehole at different depths. Each
seismometer was fixed at a predetermined depth by using
cement mortar. Even though the casing is manufactured to
be waterproof up to a pressure of 10 kg/cm^2, its
exterior was coated by epoxy resin for further

protection.

THE RECORDING UNIT: The signals from the seismometers are recorded by three 64-channel digital recorders at every 0.005 s. The system is always kept in full operational status except for the driving unit of tape. The signals are continuosly fed into the storages which are capable of keeping the most recent 1.5 s signals. The recording devices are activated when a trigger experiences motion above a preset threshold level. At present the system is set so that the recording devices are activated when any one of the three component motions at P5 (-40 m) exceeds 1.0 cm/s/s. The system continues in operation for 30 s after the motion falls below the trigger threshold level. The recorder has a digital magnetic tape with a recording capacity of 30 minutes. Timing information is internally generated, and in addition, the absolute time is corrected hourly by utilizing the signal from N.H.K. (the Japan Broadcasting Corporation). Since the magnetic tape and its driving unit are operated in standby mode, the tape is fed once every day by a fractional amount so that strain and dust do not cause any harmful effect. Some of the important characteristics of the recording unit are summarized in Table 3.

THE COMPLEMENTARY MEASUREMENTS: The relative displacements of ground are directly measured by means of three displacement transducers, oriented in G1, G2 and G3 directions as shown in Fig.4. The system, installed at the depth of 1.3 m, is shown in Fig.5(a). It consists of two 9 mm-thick discs with a diameter of 80 cm, fixed at a distance of 3 m, external and internal pipes, and displacement transducer hosted inside the pipes (see Fig.5(b)). Two pipes, one welded steel and the other ductile-cast-iron, were also installed at the depth of 1.3 m (Fig. 4). A total number of 29 strain gauges were attached to the pipes, which measure either the strain in the steel pipe or the relative displacement over the joint in the ductile-cast-iron pipe.

STRONG-MOTION RECORDS

Observation of earthquake ground motions began in April, 1982, by using 36 accelerometers in and on the ground. In December, 1982, the system was expanded with a complementary system to measure relative displacements in ground, strains of the buried steel pipe and relative displacements at the joints of the ductile-iron-pipe. In January, 1985, several accelerometers were added to further expand the array network.

As of March, 1988, a total of 144 earthquakes had been recorded since the expansion of the system in December, 1982. The strongest event, so far recorded by the network, was the Chibaken-Toho-Oki Earthquake of December 17, 1987 with the peak acceleration of about 400 cm/s/s and the maximum buried pipe strain of 64×10^{-6}. Out of these recorded earthquakes 45 had either acceleration exceeding 10 cm/s/s or pipe strain exceeding 5×10^{-6}. Table 4 is the list of 10 earthquakes which generated pipe strain exceeding 10×10^{-6}.

ACCELEROGRAMS: The Chibaken-Toho-Oki earthquake, which means an earthquake that occurred off (=Oki) the east coast (=Toi o) of Chiba Prefecture (=Chibaken), shook Chiba Prefecture and the eastern portion of the Metropolitan Tokyo at 11:08 AM on December 17, 1987. This magnitude 6.7 earthquake had its epicenter at 140° 29'E and 35° 21'N with a focal depth of 58 Km. Figure 6 shows the location of the epicenter and the distribution of ground motion severity as expressed by the Japan Meteorological Agency's intensity scale.

Figure 7 shows the horizontal motions at different depths in borehole CO. The peak accelerations are 326 cm/s/s and 216 cm/s/s in the North-South and the East-West direction, respectively. The record C001NS, for example, indicates that it is recorded by the North-South component (=NS) of the seismometer at depth 1 m from the ground surface (=01) in Borehole CO.

Eleven horizontal accelerograms recorded at 1 m depth are shown in Fig.8 for the North-South direction and in Fig.9 for the East-West direction. Figures 10 and 11 are similar paste-ups for the accelerograms at 10 m from the ground surface.

SOIL AND PIPE STRAINS: Figure 12 shows the directly

measured soil strain (G1), the axial strain of welded pipe (SS3A) and the relative displacement over joint in the ductile-cast-iron pipe (DJ3). As it can be seen from Fig.4, the horizontal soil strain is measured in the direction parallel to the buried pipes. The waveforms are similar, indicating that pipe strains are directly governed by the strains of the surrounding soil. Although the magnitudes of strains are of the same order, the soil strain is the largest and the strain calculated from the joint relative displacement is the smallest. Welded pipe strain is slightly smaller than soil strain because a certain amount of soil strain is carried by the stiffness of the pipe. The strain calculated from the joint relative displacement becomes the smallest because the total pipe strain cannot be released at the joint.

SCATTER OF PEAK ACCELERATIONS

As illustrated in Figs. 8 through 11, the waveforms at the same depth in different boreholes show apparent similarities. However, if one examines these waveforms in detail, it is easily seen that they often differ substantially from one place to the other. Especially, the scatter of peak accelerations is found to be rather large although all the boreholes are within a distance of about 150 m. The implication of this fact seems to be important because the peak acceleration is commonly used as a decisive design factor to represent the severity of ground motion.

THE CHIBAKEN-TOHO-OKI EARTHQUAKE: Peak accelerations of the three components of the ground motion recorded by all seismometers are summarized in Table 5. The spectrum intensities computed from the records obtained at depths of 1 m and 10 m are summarized in Table 6. The spectrum intensity (=SI) here is defined as the average spectral amplitude of the 20%-damped velocity spectrum over the period range between 0.1 s and 2.5 s. Note that this is different from the original definition proposed by G.W. Housner.

The means, standard deviations, and the coefficients of variation are summarized in Table 7 for

the peak acceleration and the spectrum intensity. Eleven sample values are available for both the parameters at the depths of 1 m and 10 m from the ground surface. The mean peak acceleration near (i.e. 1 m from) the ground surface is 337 cm/s/s in the North-South direction and 250 cm/s/s in the East-West direction. The general difference in the peak acceleration in these two directions may be easily observed by comparing the accelerograms in Figures 8 and 9. The coefficient of variation of the peak accelerations within an area of about 100 m radius may be seen to be approximately 10%.

Although the difference of the peak accelerations in the two perpendicular directions is significant near the ground surface, it almost disappears at the depth of 10 m. It may be too simple to say that this difference is due to the directivity of the surface layer characteristics, and further analysis is needed.

It is interesting to note that the SI values do not show such directional difference even near the ground surface (i.e. -1 m). This implies that the damageabilities of the North-South and the East-West ground motions are almost the same in spite of the large apparent difference ⌐ the peak accelerations. The spectrum intensity may be a more stable and reliable parameter to describe the effect of seismic ground motion on structures in general.

From the results of the analyses on a number of strong motion records and their associated damage, it has been conclusively found that damage is more strongly related to the spectrum intensity than to the peak acceleration (Fig. 13). Based on this finding, the author tentatively proposed SI=30 cm/s as the threshold to estimate whether or not damage in an area concerned becomes substantial. Although the peak acceleration was definitely in the range of 300 to 400 cn/s/s in the area surrounding the Chiba Experiment Station, damage in that area was negligible because the level of SI was far smaller than the aforementioned threshold. The reasons for SI being small may be attributed to high dominant frequencies and short duration of strong motion phase.

OCTOBER 4 AND NOVEMBER 6, 1985, EARTHQUAKES: These earthquakes correspond to Event 4 and 5 in Table 4. For these events, the scatter of peak accelerations in

boreholes (-1 m and -20 m from the ground surface), which are 100-150 m apart from each other, was examined.

The maximum acceleration amplitudes of the ground surface were in the ranges of 60-110 cm/s/s and 50-80 cm/s/s for Events 4 and 5, respectively (Table 8). In terms of the coefficient of variation, the values ranging from 10% to 20% were obtained. However, the coefficients of variation of maximum acceleration amplitudes displayed smaller variation at deeper layers, the values ranging from 5-10% at the depth of 20 m.

OTHER WEAKER GROUND MOTIONS: Table 9 shows the means and covariances of the peak accelerations observed during weaker ground motions. The data in nine boreholes C0-C4 and P1-P4 within 15 m from borehole C0 (see Fig. 2) were utilized. Ground motions were vectorially converted into the radial (R) and tangential (T) directions. It is seen that the covariance of observed peak accelerations within a radius of 30 m often shows values of 10-20%. Scatter of peak accelerations at points deeper in the ground generally becomes smaller.

STRAIN DETERMINATION FROM DENSE ARRAY DATA

It is well recognized that the seismic-induced ground strain is one of the important contributing factors in seismic behavior of the buried linear structures such as pipes and tunnels. However, the observational data on the seismic soil strain has been limited and fragmentary and the quantitative information on the properties of engineering importance is extremely lacking.

METHOD OF ANALYSIS: The earthquake-induced ground accelerations recorded by the array network are used to calculate the seismic-induced ground strains. The finite element method in three dimensional space has been employed by using a tetrahedron element with a linear shape function.

The general configuration of the array network, with a representative element (P1(-1m) P3(-1m) P4(-1m) C0(-40m)), is shown in Fig.14. Integration of accelerograms to obtain velocities and displacements

were performed in the frequency domain. For various corrections and filterations required during the study, different band-pass filters of cosine tails with different limits were used.

EFFECT OF ELEMENT SIZE: To investigate the effect of element size on calculated soil strain, three elements with sides of approximately 110 m, 30 m, and 5 m were selected. These elements have vertices at points P1(-1m) P3(-1m) P5(-1m) P5(-40m), P1(-1m) P3(-1m) P4(-1m) C0(-40m) and C0(-1m) C3(-1m) C4(-1m) C0(-5m), respectively. Sample calculations were made for Event 1 in Table 4. Some other results have been treated elsewhere.

Strains were evaluated in three specified directions, which coincide with the directions of directly measured relative ground displacements, to examine the accuracy of calculated strains. A portion of enlarged strain time histories in G1 direction (see Fig. 2) calculated in the aforementioned three elements are shown in Fig.15. Figure 16 shows the same portion of time histories, all in G1 direction, of directly measured ground strain, steel pipe strain, and relative motion in a joint of ductile-cast-iron pipe. In this case, the magnitudes of measured strains do not show such a good consistency as shown in Figure 12. However, it may be said that the axial strain of steel pipe is almost the same as that of the surrounding soil.

The strain calculated by the largest element shows the best agreement with the observed pipe strain, and the calculated strain becomes somewhat larger in small elements. It should be noted that a slight incorrect positioning of seismometers has rather significant effect on the calculated strains over the short spans of only 5 m. Further, since relative values are involved in the calculation of strains, a slight difference between characteristics of individual seismometers has a great influence on the accuracy of the calculated strains, especially for very short spans.

Band pass filtration on original accelerogram was found to show strong effect on the evaluated strains. In general, for strong shakings containing high frequency components with low noise-signal ratio, strains can be accurately evaluated by proper filteration even for elements with sides of only 5 m. However, for

earthquakes with dominantly long-period components, the accuracy of the ground strain evaluated in elements with the sides shorter than about 50-100 m is not acceptable. In the latter case, the strain in larger elements evaluated by the use of a broad-banded filter generally gives satisfactory agreement.

EFFECT OF DEPTH: Strains at the depths of -1 m, -10 m and -20 m were evaluated within the array network. In order to eliminate the effects of the other factors, elements of identical horizontal sizes were selected, i.e. P1(-1) P3(-1) P5(-1) P5(-40), P1(-10) P3(-10) P5(-10) P5(-40) and P1(-20) P3(-20) P5(-20) P5(-40). The strains evaluated in these elements are shown in Fig.17. The strain amplitude at deeper layers shows some decrease. A decrease of about 15% at the depth of -10 m was observed, but further reduction at the depth of -20 m was not significant. Higher frequency components of strains clearly diminish at deeper layers as it can be observed through their Fourier spectra shown in Fig. 18.

CHARACTERISTICS OF SEISMIC STRAINS OF SOIL AND PIPE

Past observations have conclusively shown that the soil strain is well represented by the axial strain of buried welded pipe. In most practical purposes, it is more reliable as well as more practical to measure the axial strain of pipe to examine the characteristics of the soil strain itself.

WAVE TYPES AND PIPE STRAIN: Figure 19 shows two typical sets of ground acceleration and pipe strain records. The Naganoken-Seibu Earthquake (Event 3) is known to have excited surface wave in the concerned area as illustrated by the long-period components observed in the latter part of the acceleration record. Although the peak accelerations of this earthquake never exceeded 5 cm/s/s, the pipe strain of about 20×10^{-6} was produced. It is clearly seen that the larger pipe strain in this case is associated with the propogation of surface wave. The Chibaken-Toho-Oki earthquake, on the contrary, occurred at an epicentral distance of 46 km with a focal

depth of 58 km (see Table 4). This implies that the ground motion at Chiba site primarily consisted of body wave, i.e. shear wave propogating almost vertically in the soft surface layers. The pipe strain is seen to become large when the high-frequency shear wave shows large accelerations. The maximum pipe strain was about 50×10^{-6} for the peak acceleration of 330 cm/s/s.

Figure 20 shows the ratios of the maximum axial pipe strains (in 10^{-6}) to the corresponding maximum accelerations (cm/s/s) for the 45 earthquakes which caused either pipe strain greater than 50×10^{-6} or maximum acceleration greater than 10 cm/s/s. It is seen that the ratio is 0.15-0.30 for the cases in which the major incident wave may be considered as shear wave and that the ratio in the case of surface wave propagation is about 4.

It is interesting to note that, only in the case of surface wave propagation, the pipe (=soil) strain waveform shows similarity with the ground (particle) velocity waveform, and that the magnitude of pipe strain roughly agrees with the ratio of the particle velocity to the wave propagation velocity only in the case of surface wave propagation.

PIPE STRAIN CHARACTERISTICS: The waveforms of the axial and bending strains of the welded steel pipe are shown in Fig. 21 for Event 3 and Event 7. Axial strains dominated in the straight portion of the pipe whereas bending strains became large only near the bend of the pipe. However, past observations consistently show that the bending strain right at the corner of the bend is negligibly small. A plausible explanation for this phenomenon is yet to be found.

CLOSING REMARKS

The Chiba Dense Array has been in operation for over six years. However, until the Chibaken-Toho-Oki earthqueake of December 17, 1987, registered the peak acceleration of 300-400 cm/s/s, real strong motions had not been recorded by the array. In-depth analysis of the array data has to be made in the future. Although all of the results presented in this paper are of somewhat

preliminary nature, it may be understood that good array
data can be utilized for a number of scientific and
engineering purposes.

REFERENCES (All in English)

[1] Katayama, T., and N. Sato: Ground Strain Measurement
    by a Very Densely Located Seismometer Array, Proceedings
    of the Sixth Japan Earthquake Engineering Symposium-
    1982, pp. 241-248, Nov., 1982.

[2] Farjoodi, J., T. Katayama, and N. Sato: Evaluation
    of Seismic-Induced Ground Strains by Dense Seismometer
    Array Observation, Proceedings of the 17th JSCE
    Symposium on Earthquake Engineering, pp. 69-72,
    July,1983.

[3] Farjoodi, J., T. Katayama, and N. Sato: Evaluation
    of Ground Strains by Dense Seismometer Array
    Observation, Seisan-Kenkyu, Vol. 35, No. 9, pp. 453-456,
    Sep., 1983.

[4] Katayama, T., J. Farjoodi, and N. Sato: Measurement
    of Seismic Ground Strain by a Dense Seismometer Array,
    Proceedings of the 8th World Conference on Earthquake
    Engineering, Vol. II, pp.207-214, July, 1984.

[5] Farjoodi, J., N. Sato, and T. Katayama: Comparison
    of Ground Strains Evaluated by a Dense Seismograph Array
    with Observed Buried Pipe Strains, Proceedings of the
    39th Annual Conference of the Japan Society of Civil
    Engineers, Vol. 1, pp. 677-678, Oct., 1984.

[6] Farjoodi, J., T. Katayama, and N. Sato: Engineering

Properties of Ground Motion Obtained from Dense
Seismograph Array Data (Part I), <u>Bulletin of the
Earthquake-Resistant Structure Research Center</u>,
Institute of Industrial Science, University of Tokyo,
No. 18, pp. 9-30, Mar., 1985.

[7] Farjoodi, J, T. Katayama, N. Sato: Ground Strain
Characteristics Deduced by Using Dense Seismograph Array
Data, <u>Proceedings of the 18th JSCE Symposium on
Earthquake Engineering</u>, pp. 101-104, July, 1985.

[8] Farjoodi, J.: Evaluation of Engineering Properties
of Earthquake Motion from Dense Seismograph Array Data,
<u>Ph.D. Dissertation</u> submitted to the Department of Civil
Engineering, University of Tokyo, Dec., 1985.

[9] Sato, N., and T. Katayama: Ground Motion of October
4 and November 6, 1985, Earthquakes Recorded by Dense
Seismograph Array, <u>Bulletin of the Earthquake-Resistant
Structure Research Center</u>, Institute of Industrial
Science, University of Tokyo, No. 19, pp. 3-10, Mar.,
1986.

[10]Farjoodi, J., N. Sato, and T. Katayama: Relation
Between Ground Strain and Ground Acceleration, Velocity
and Displacement, <u>Proceedings of the 41st Annual
Conference of the Japan Society of Civil Engineers</u>, Vol.
1, pp. 1033-1034, Nov., 1986.

[11]Farjoodi. J., and T. Katayama: Application of Dense
Seismograph Array Data to Evaluate Engineering
Properties of Strong Ground Motions, <u>Proceedings of the
Seventh Japan Earthquake Engineering Symposium- 1986</u>,
pp. 511-516, Dec., 1986.

[12]Katayama, T., N. Sato, N. Ohbo, M. Kawasaki, and K.
Saito: Ground Shaking Severity Detector by Use of
Spectrum Intensity (SI), <u>Proceedings of the Seventh
Japan Earthquake Engineering Symposium-1986</u>, pp. 373-
378, Dec., 1986.

[13]Katayama, T., and N. Sato: Strong-Motion Records of
the Chibaken-Toho-Oki Earthquake of December 17, 1987,
<u>Bulletin of the Earthquake-Resistant Structure Research
Center</u>, Institute of Industrial Science, University of
Tokyo, No. 21, pp. 25-65, Mar.,1988.

[14]Sato, N., T. Katayama, M. Nakamura, T. Iwamoto, and
N. Ohbo: Observation of Seismic Ground Motion and Buried
Pipe Strain in a Very Dense Seismometer Array,
<u>Proceedings of the 9th World Conference on Earthquake
Engineering</u>, (to be published).

Table 1　Depths of Borehole Seismometers

DEPTH (m)	BOREHOLE														
	C0	C1	C2	C3	C4	P1	P2	P3	P4	P5	P6	P7	P8	P9	P0
1	O	O	O	O	O	O	O	O	O	O	O	O	O	O	O
5.	O	O	O	O	O										
10	O	O	O	O	O	O	O	O	O	O	O				
20	O					O	O	O	O	O	O	O			
40	O									O					

Table 2　Specifications of Borehole Seismometer

Type of Transducer	: Piezo-electric Accelerometer
Sensing Directions	: 2-Horizontal and Vertical
Full Scale Sensitivity	: 1000 cm/s/s
Sensitivity	: 5 mV for 1 cm/s/s
Frequency Range	: 0.1 to 30 Hz
Output Impedance	: 10
Operating Temperature	: -20 to 40 ° C
Transverse Sensitivity	: Max. 3 %
Linearity	: Max. 0.1 %　full scale
Water-proofness	: 10 kg/cm/cm
Required Power	: +6 V D-C
Size of Casing	: φ 65 x 335 mm
Weight	: 2.5 kg

Table 3　Specifications of Digital Recorder

Input Channel	: 64 ch.
Input Signal Voltage	: -5 to 5 V
Input Impedance	: 100 k
Input Filter	: Low-pass (0 to 30 Hz)
A/D Converter	: 12 bits
Sampling Rate	: 200 /s
Pre-event Memory	: 1.5 s
Timer Units	: Month, Day, Hour, Minute and Second
Time Correction	: By N.H.K. Radio Broadcast
Seismic Trigger	: Logical Sum or Product of Arbitrary 3 Channels
Trigger Level	: 0.1 to 10 % full scale
Monitoring	: 8 ch. of D/A Converter (12 bits) for Recording or Playback
Recording Medium	: Digital Magnetic Tape (9 tracks, 1600 bpi)
Quake-proofness	: 0.5 g
Dimensions	: 570(w) x 1500(h) x 400(d) mm
Weight	: 75 kg

Table 4   List of Earthquakes

Event No.	Date		Epicenter	Mag.	Focal Depth	D*	I**	Max. Amp.***	
								Accel.	Strain
1	Feb.	27, 1983	N 35° 56' ,E 140° 9'	6.0	72km	35km	3	55.5	15.5
2	Mar.	6, 1984	N 29° 20' ,E 139° 12'	7.9	452km	705km	4	28.1	10.1
3	Sept.	14, 1984	N 35° 49' ,E 137° 34'	6.8	2km	232km	2	4.4	18.5
4	Oct.	4, 1985	N 35° 52' ,E 140° 10'	6.1	78km	28km	4	82.0	18.8
5	Nov.	6, 1985	N 35° 21' ,E 140° 14'	5.0	63km	32km	3	75.6	14.4
6	June	24, 1986	N 34° 49' ,E 140° 43'	6.5	73km	105km	4	53.5	15.2
7	Dec.	17, 1987	N 35° 21' ,E 140° 29'	6.7	58km	46km	5	326.1	54.2
8	Jan.	5, 1988	N 35° 24' ,E 140° 28'	4.3	43km	41km	2	40.9	12.5
9	Jan.	16, 1988	N 35° 22' ,E 140° 27'	5.2	53km	42km	3	97.9	15.9
10	March 18, 1988		N 35° 40' ,E 139° 39'	6.0	99km	42km	4	59.6	18.1

*   : Epicentral Distance
**   : JMA Intensity at Chiba
*** : Acceleration in cm/s/s and Strain in 10^{-6}

Table 5   Maximum Peak Accelerations (Event 7) (cm/s/s)

Depth / Direction		C0	C1	C2	C3	C4	P1	P2	P3	P4	P5	P6
1m	NS	326	344	375	350	304	303	357	381	308	398	265
	EW	216	206	265	270	268	280	251	294	245	225	225
	UD	122	135	131	136	144	155	147	135	169	124	127
5m	NS	122	123	119	120	126						
	EW	164	154	153	174	174						
	UD	80	79	80	78	94						
10m	NS	132	143	131	126	132	133	134	135	124	110	90
	EW	123	124	124	124	122	135	145	118	123	123	128
	UD	61	58	59	64	67	70	61	63	69	63	56
20m	NS	116					119	140	117	98	90	85
	EW	84					80	77	88	81	82	87
	UD	45					41	47	51	43	50	46
40m	NS	105									101	
	EW	69									98	
	UD	43									36	

Table 6   SI-Values (Event 7)   (cm/s)

Depth / Direction		C0	C1	C2	C3	C4	P1	P2	P3	P4	P5	P6
1m	NS	15	15	15	15	15	16	15	15	16	15	13
	EW	15	15	15	16	16	15	16	15	15	13	14
10m	NS	9	10	9	9	9	10	8	10	9	9	8
	EW	11	11	11	10	11	11	11	11	11	10	11

Table 7   Means, Standard Deviations and Coefficients of Variation of Peak Accelerations and Spectrum Intensities (Event 7)

		NS			EW			UD		
	Depth	(1)	(2)	(3)	(1)	(2)	(3)	(1)	(2)	(3)
Peak Acceleration cm/s/s	1 m	337	38	0.11	250	27	0.11	139	14	0.10
	10 m	126	14	0.11	126	7	0.06	63	4	0.07
Spectrum Intensity cm/s	1 m	15.0	0.7	0.05	15.0	0.9	0.06	--	--	--
	10 m	9.2	0.6	0.06	10.8	0.4	0.04	--	--	--

(1)Mean

(2) Standard Deviation

(3) Coefficient of Variation

DEPTH (m)	SOIL PROFILE	SOIL	N-VALUE 10 20 30 40 50	V_s (m/s)	V_p (m/s)	γ_t (g/cm³)	ν	C (kg/cm²)	E (kg/cm²)
0		SURFACE SOIL							
		LOAM		140	320	1.35	0.381	269	743
5		SANDY CLAY				1.5	0.244	1566	3896
10		CLAYEY SAND		550					
		MEDIUM SAND				1.7		1775	4416
				320			0.481	1775	5257
20		FINE SAND				1.7			
				1670					
30		CLAYEY FINE SAND		420		1.8	0.466	3238	9493
		ORGANIC SILT							
40		FINE SAND							

Point C0

N-VALUE 0 20 40 60

Point P5

N-VALUE 0 20 40 60

Point P6

Fig. 1 Soil Profiles in Three Typical Boreholes

Fig. 2 Layout of the On-Ground Seismometers

Table 8   Maximum Acceleration Amplitude (cm/s/s)

Event No.	Depth	Direction	Borehole						Mean Value	COV*
			P5	P7	P8	P9	PO	CO		
4	-1m	NS	69.5	73.1	79.5	86.9	111.0	82.2	83.7	0.16
		EW	81.8	68.7	72.4	62.0	83.6	58.2	71.1	0.13
	-20m	NS	24.3	25.7	23.2	26.1	30.9	27.8	26.3	0.09
		EW	29.2	27.0	25.0	24.1	25.2	26.6	26.2	0.06
5	-1m	NS	48.7	67.8	64.0	68.5	78.0	70.7	66.3	0.13
		EW	48.2	51.0	52.5	44.2	81.0	75.3	58.7	0.24
	-20m	NS	20.0	22.6	21.0	22.0	21.8	23.3	21.8	0.05
		EW	17.7	16.0	13.6	12.9	17.1	17.9	15.9	0.12

*COV : Coefficient of Variation

Table 9   Means and Covariances of Peak Accelerations
(Weaker Ground Motions)

Date		Y	1982	1983						1984			
		M/D	7/23	2/27	5/21	5/22	8/ 8	10/28	12/30	1/ 1	1/17	2/14	3/ 6
Magnitude			7.0	6.0	5.0	3.7	6.0	5.2	5.4	7.3	5.6	5.4	7.9
Depth(km)			30	72	49	40	22	60	50	388	43	20	460
Epc.D.(km)			178	35	46	34	99	67	55	374	138	93	692
-1m	R	MNS	31.1	59.3	20.3	9.5	18.5	14.7	13.3	26.5	17.3	6.8	29.8
		COV	0.112	0.074	0.084	0.165	0.161	0.066	0.085	0.087	0.192	0.128	0.059
	T	MNS	27.2	46.7	18.2	5.3	16.3	13.7	14.5	24.7	11.9	10.1	23.0
		COV	0.092	0.061	0.136	0.261	0.139	0.083	0.044	0.081	0.046	0.067	0.036
	UD	MNS	12.6	14.6	16.5	23.0	6.2	5.9	5.1	10.7	6.3	2.7	7.7
		COV	0.122	0.102	0.076	0.052	0.142	0.109	0.061	0.144	0.094	0.194	0.100
-5m	R	MNS	16.7	41.4	10.1	3.3	7.6	7.3	6.7	12.6	6.9	3.5	24.7
		COV	0.032	0.024	0.059	0.136	0.045	0.041	0.065	0.039	0.058	0.040	0.021
	T	MNS	18.8	36.8	7.9	1.8	8.5	6.8	7.3	14.9	6.5	6.5	20.8
		COV	0.079	0.026	0.068	0.081	0.028	0.067	0.052	0.076	0.073	0.047	0.028
	UD	MNS	9.6	11.8	8.6	8.5	4.0	3.4	4.4	7.1	4.3	2.1	8.3
		COV	0.155	0.040	0.037	0.045	0.103	0.067	0.036	0.060	0.017	0.150	0.079
-10m	R	MNS	13.7	34.5	8.2	1.6	6.4	5.3	4.9	10.1	5.6	2.9	22.2
		COV	0.052	0.056	0.077	0.066	0.113	0.048	0.046	0.045	0.063	0.084	0.026
	T	MNS	17.2	26.6	5.7	1.4	6.9	5.1	6.2	11.0	5.6	4.5	20.4
		COV	0.064	0.059	0.110	0.193	0.074	0.061	0.034	0.070	0.060	0.059	0.026
	UD	MNS	6.6	9.6	7.6	7.5	3.0	2.7	3.5	5.9	3.2	1.7	6.6
		COV	0.056	0.071	0.080	0.048	0.056	0.164	0.121	0.087	0.074	0.169	0.073
-20m	R	MNS	9.4	23.6	6.3	1.4	4.2	3.7	3.7	8.7	5.7	2.0	18.0
		COV	0.064	0.036	0.067	0.085	0.046	0.037	0.041	0.054	0.061	0.024	0.019
	T	MNS	13.1	20.1	5.1	1.4	4.6	3.9	4.6	7.7	3.8	3.7	18.8
		COV	0.057	0.029	0.060	0.093	0.050	0.059	0.059	0.062	0.037	0.063	0.034
	UD	MNS	5.5	7.5	6.2	7.1	2.6	1.9	2.5	4.3	2.4	1.2	5.9
		COV	0.049	0.094	0.035	0.061	0.117	0.144	0.073	0.170	0.053	0.150	0.056

Fig. 3   Frequency-Response Curves of Seismometer

Rel. Sensitivity

1.02

1.00

0.98

0.96

○ Ref.: Displ.M.

△ Ref.: Vel.M.

□ Ref.: Accel.M.

0.1   0.2 0.3 0.5   1.0   2.0 3.0 5.0   10   20 30   50 (Hz)

Phase

30

20

10

0

-10

Fig. 4   General Layout of Complementary Observation System

○ Borehole Seismometer

I Ground Strain Gauge

▼ Pipe Strain Gauge

□ Rel. Displ. Gauge
   at Joint

N

P2

P3

C2

C0   C1

C3   5m

C4   15m

P1

G3   G2

G1

Anchoring Block

Ductile Iron Pipe

DJ1

SS1   Steel Pipe

P4

DJ2 DJ3 DS1 DJ4

SS2   SS3

90m

DJ5

1m

72 228

300

SS7

DJ7   SS6

SS9

SS5

SS4   SS8   DJ6

30m

a) Schematic Layout of Direct Strain Measurement Equipment

Excavated Soil

Sand

0.6 m

0.7 m

3 m

4 m

1.3 m

Φ0.8 m

1.8 m

b) Details of Direct Strain Detection Transducer

300 cm

CABLE

EXTERNAL PIPE

TRANSDUCER   INTERNAL PIPE

43.5   8.9

PLATE (Φ80cm)

Fig. 5   Direct Ground Strain Measurement System

Fig. 6   Epicenter and JMA Intensity Distribution
         (Event 7)

Fig. 7 Horizontal Motions at Different Depths in Borehole CO
(Event 7)

Fig. 8 NS-Component Accelerograms at 1m from Ground Surface
(Event 7)

Fig. 9   EW-Component Accelerograms at 1m from Ground Surface
(Event 7)

Fig. 10 NS-Component Accelerograms at 10m from Ground Surface
(Event 7)

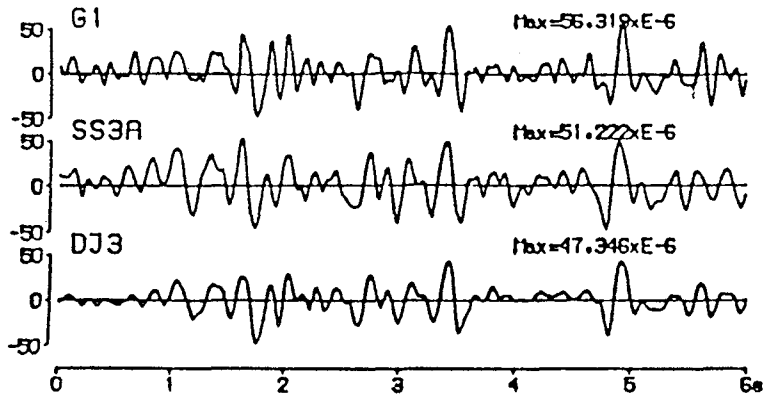Fig. 11 EW-Component Accelerograms at 10m from Ground Surface
(Event 7)

Fig. 12 Soil Strain, Steel Pipe Axial Strain, and Strain Evaluated from DCI Pipe Joint Gauge (Event 7)

Fig. 13 Relation Between SI and Peak Acceleration

Fig. 14 General Configuration Array Network (Element P1(-1m)P3(-1m) P4(-1m)CO(40m))

Fig. 15 Calculated Strain Time Histories in Elements (Event 1)

Fig. 16 Examples of Measured Strains (Event 1)

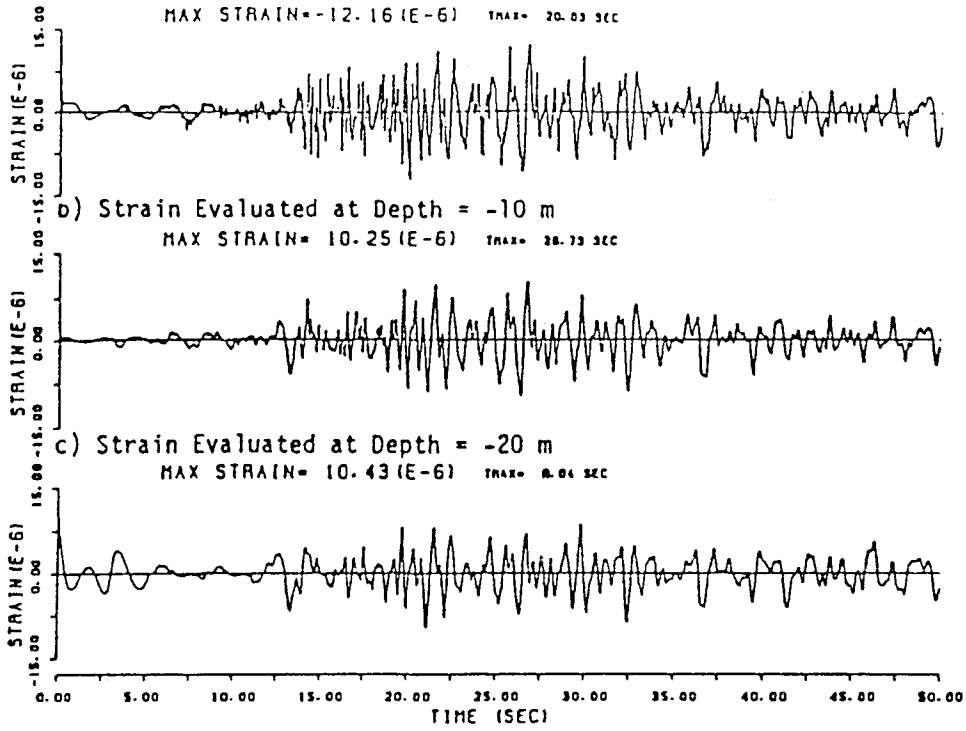a) Strain Evaluated at Depth = -1 m

MAX STRAIN=-12.16(E-6) TMAX= 20.03 SEC

b) Strain Evaluated at Depth = -10 m

MAX STRAIN= 10.25 (E-6) TMAX= 28.73 SEC

c) Strain Evaluated at Depth = -20 m

MAX STRAIN= 10.43 (E-6) TMAX= 8.04 SEC

Fig. 17   Evaluated Strains at Depths -1m, -10m, and -20m
(Event 1)

a) Depth = -1 m

b) Depth = -10 m

Fig. 18   Fourier Spectra of Ground Strain at Depths -1m and -10m
(Event 1)

The Naganoken-Seibu Earthquake (Event No. 3)
Ground Acceleration (cm/s^2)

Pipe Strain (x10^{-6})

The Chibaken-Toho-Oki Earthquake (Event No. 7)
Ground Acceleration (cm/s^2)
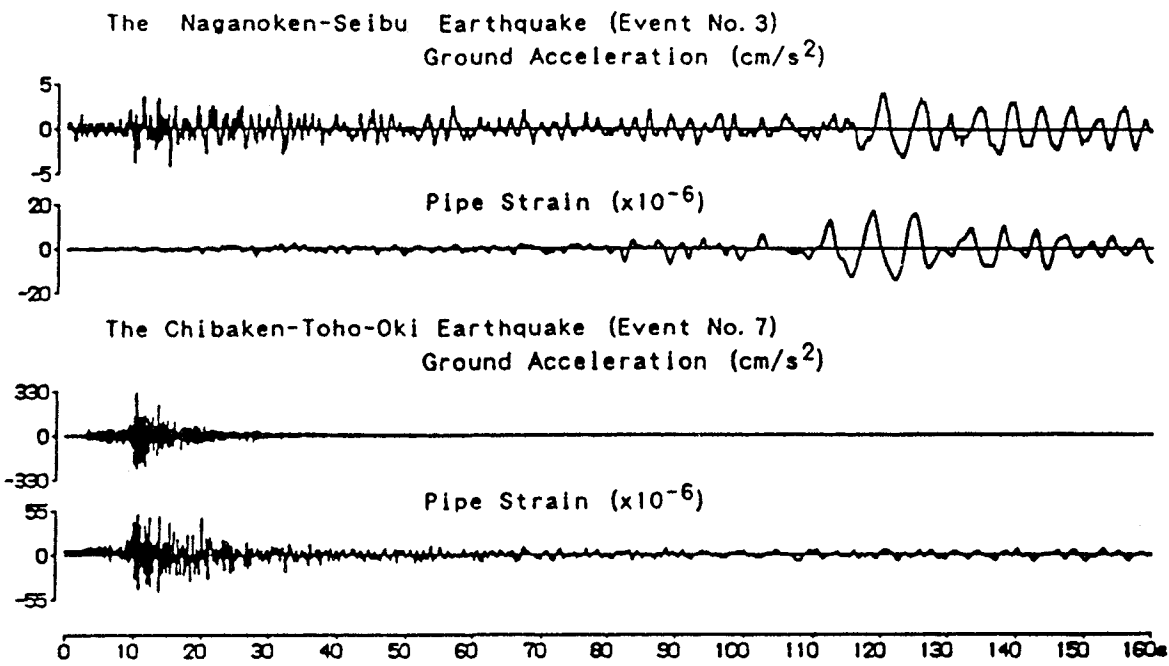
Pipe Strain (x10^{-6})

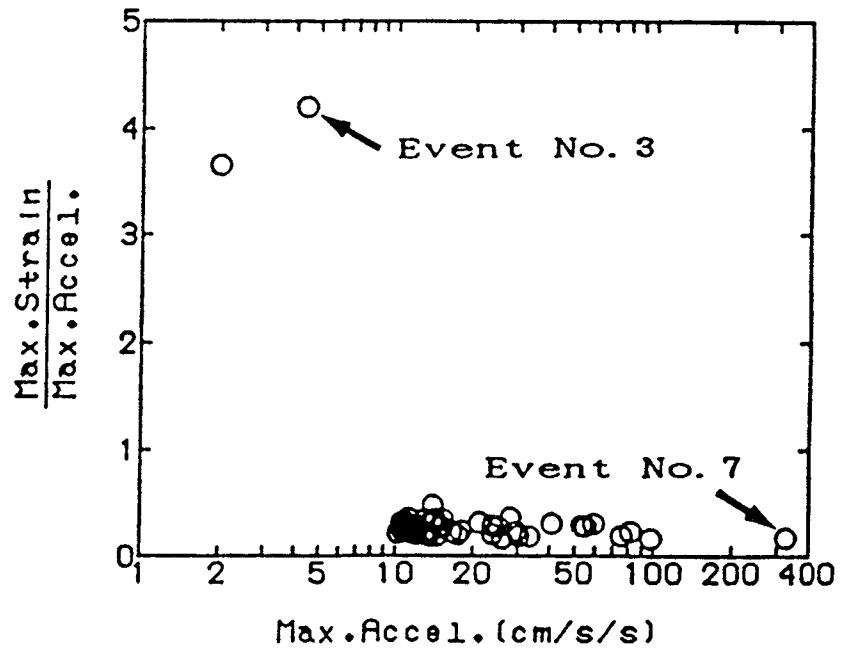Fig. 19   Typical Records of Ground Acceleration and Pipe Strain

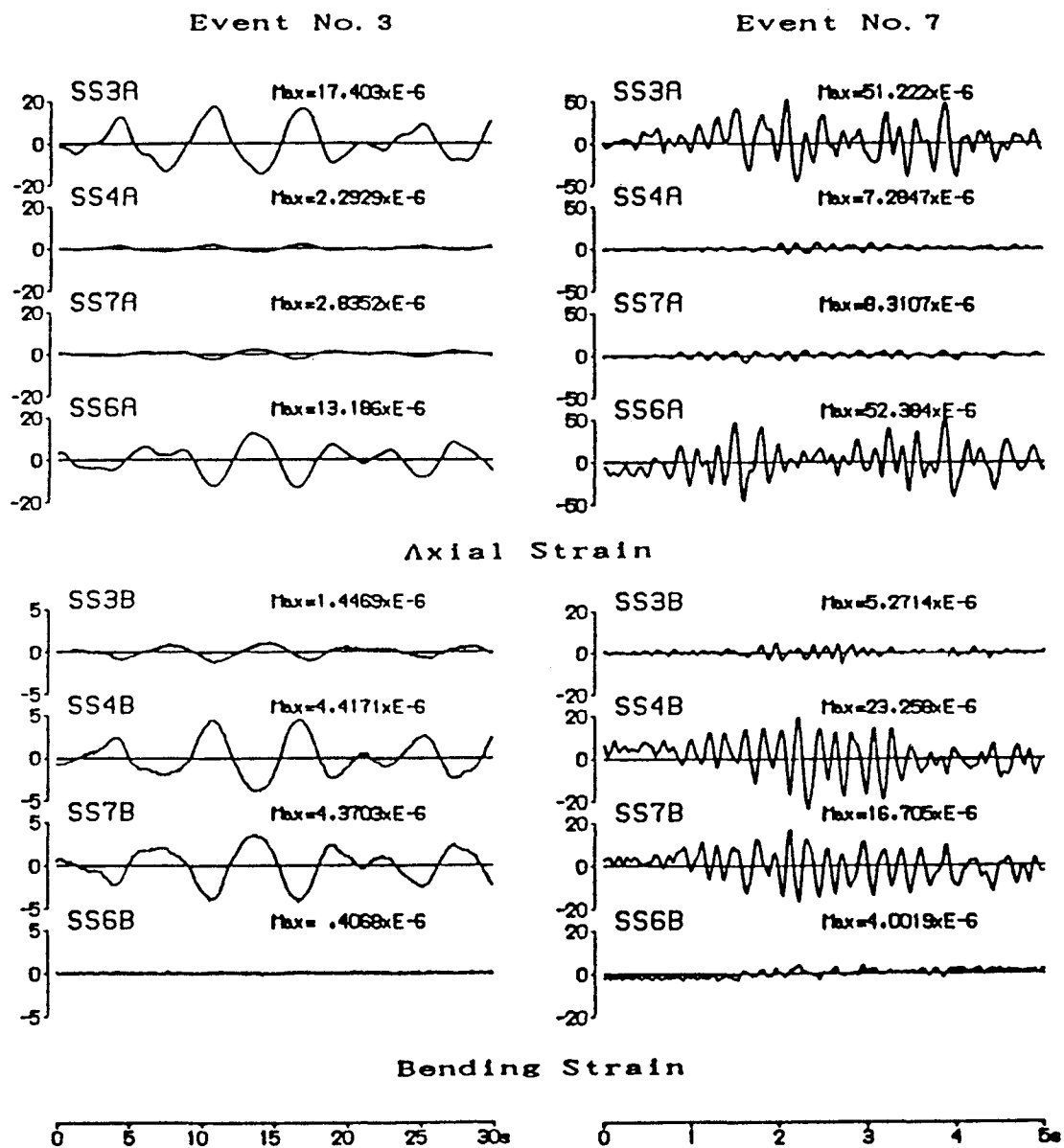Fig. 20   Relation between the Maximum Values of Ground Acceleration and
Pipe Strain

Fig. 21 Records of Axial and Bending Strain (x10⁻⁶)

STRONG-MOTION ARRAY QUESTIONNAIRE

1. Where is your array located and how long has it been operating?

   Imperial Valley, CA - established 1982

   (Array is known as the Wildlife liquefaction array. Array is near town of Calipatria.)

2. Please describe your array, in terms of the type and number of instruments, their spacing, their triggering, their recording means (film, tape, or disc; analog or digital), and their foundation and housing.

   ① 6 pore pressure transducers deployed within a 30-ft diameter circular area at depths from 2.9 to 12.0 m.

   ② 1 downhole triaxial accelerometer at 7.5 m

   ③ 1 surface triaxial accelerometer deployed on a concrete pad

   ④ Recording is by film. (CRA-1)

   ⑤ Triggered at 0.01g.

3. Describe the nature of the data you have obtained, in terms of the number of events recorded, their range of magnitudes, and their distances from the array.

   Significant Records:

   24 Nov 1987 Superstition Hills Earthquake (M_w 6.6, r = 31 km) - Data included surface and downhole acceleration records and pore pressure records for a sand undergoing earthquake-induced liquefaction.

   23 Nov 1987 Elmore Ranch Earthquake (M_w = 6.2, r = 23 km) - Data included surface and downhole acceleration records and pore pressure records for a sand on the threshold of liquefying.

4. What means were used to characterize the site conditions?

   Standard penetration tests
   Cone penetration tests
   Laboratory tests
   Shear wave measurements in situ

STRONG-MOTION ARRAY QUESTIONNAIRE

1. Where is your array located and how long has it been operating?

   Cholame Valley, CA - established 1986

   (Array is known as the Parkfield liquefaction array. Array is about 15km southeast of Parkfield.)

2. Please describe your array, in terms of the type and number of instruments, their spacing, their triggering, their recording means (film, tape, or disc; analog or digital), and their foundation and housing.

   ① 24 pore pressure transducers deployed within either a 15-m diameter circular area or a 9-m by 9-m square.

   ② 4 downhole triaxial accelerometers to a depth of 30-m deployed in the center of the 15-m diameter circular area.

   ③ 1 surface triaxial accelerometer on concrete pad.

   ④ Recording by film (CRA-1) and partially digitally (GEOS)

   ⑤ Film record triggers at 0.01g.

3. Describe the nature of the data you have obtained, in terms of the number of events recorded, their range of magnitudes, and their distances from the array.

   2 triggers of M < 4.0 on San Andreas (< 10km)

4. What means were used to characterize the site conditions?

   Standard penetration ⎫
   Cone penetration tests ⎬ Liquefaction resistance
   Laboratory cyclic loading ⎭
   Shear wave measurements in situ (shear modulus)
   Flat plate dilatometer (in situ stress)
   Slug tests (permeability)

5. If you were to establish a new array, what means would you now use to characterize site conditions?

Same

6. What lessons have been learned

● regarding the operation of the array?

Reliability of pore-pressure transducers is low. Retrievable transducer system for dynamic monitoring is needed.

● regarding ground response to earthquakes?

None yet.

7. Can you comment on the relevance of ambient vibration measurements and forced vibration testing?

Ambient preferred.

8. ADDITIONAL COMMENTS AND ADVICE (please use additional pages if desired)

Archiving and organizing voluminous data that does not warrant publication is a challenge to research scientist. Need long-term institutional commitment.

Thank you!

_____Thomas L. Holzer_____
Name

STRONG-MOTION ARRAY QUESTIONNAIRE

1. Where is your array located and how long has it been operating? PARKFIELD, CA — TURKEY FLAT

    SINCE SPRING 1987

2. Please describe your array, in terms of the type and number of instruments, their spacing, their triggering, their recording means (film, tape, or disc; analog or digital), and their foundation and housing.

    - 4 sites across thin stiff alluvial valley (·S1)

    See attached map for spacing and numbers

    - Contact Tony for instrumentation details

3. Describe the nature of the data you have obtained, in terms of the number of events recorded, their range of magnitudes, and their distances from the array.

    Weak-motion only (33 events)

4. What means were used to characterize the site conditions?

    See attached tables

5. If you were to establish a new array, what means would you now use to characterize site conditions?

Same

6. What lessons have been learned

   x ● regarding the operation of the array? (TONY)

   ● regarding ground response to earthquakes?
   1) 1-D linear model (SHAKE) sensitive to geotechnical input parameters, 2) Difficult to get stable field measurements, from different survey teams, in same borehole.

7. Can you comment on the relevance of ambient vibration measurements and forced vibration testing?

   NO

8. ADDITIONAL COMMENTS AND ADVICE (please use additional pages if desired)
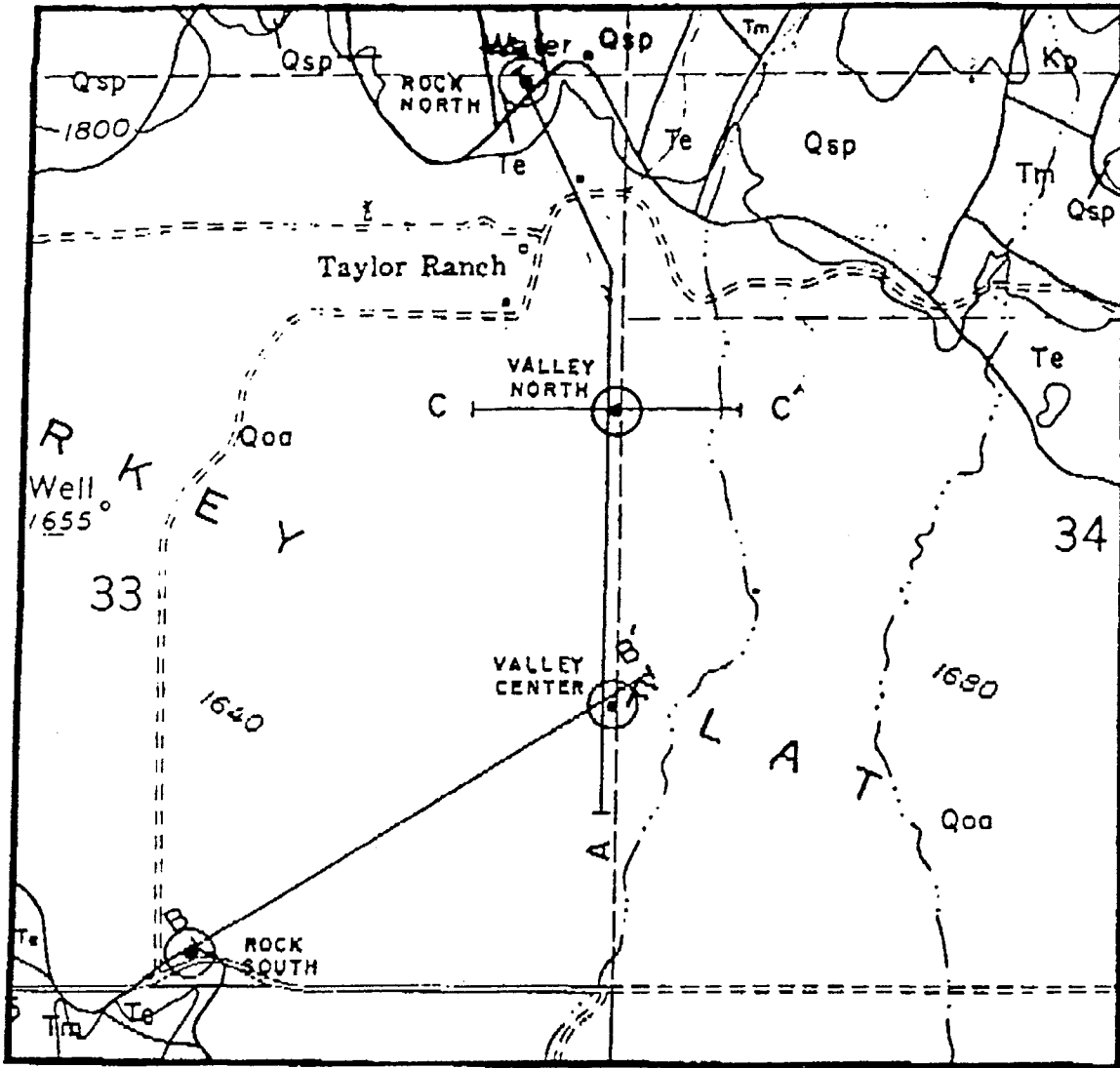
Thank you!

CHUCK REAL
Name

Figure 1. A map of the Turkey Flat Site Effects Test Area showing locations of the four ground motion recording sites, and three lines of profile that correspond to the cross sections shown in figure 2. At these locations, numerous geophysical surveys and laboratory testing of rock and soil samples have been conducted for the purpose of characterizing the test area for analysis of ground response. The remainder of this report describes the site characterization program and its findings in more detail.
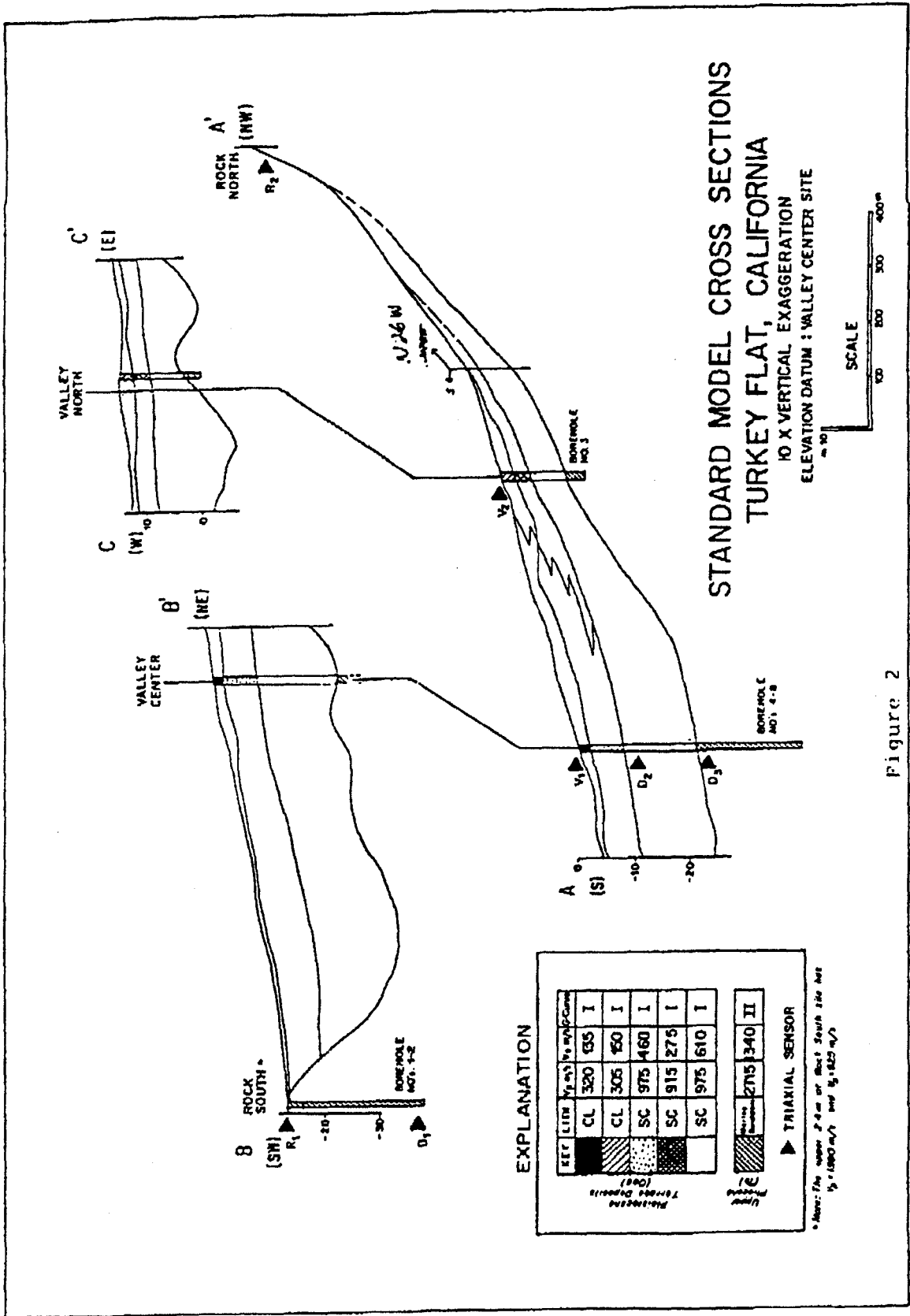
STANDARD MODEL CROSS SECTIONS
TURKEY FLAT, CALIFORNIA
10 X VERTICAL EXAGGERATION
ELEVATION DATUM : VALLEY CENTER SITE

Figure 2

Table 3. Geotechnical field tests.

FIELD TESTS	CDMG	HLA	LCA	QEST	WCC	PDC	OYO	KC
DRILLING AND SAMPLING	■		■		■	■	■	
STANDARD PENETRATION TEST	■		■		■	■		
WATER TABLE DEPTH	■							
CALIPER		■					■	
BOREHOLE DEVIATION	■							
ELECTRICAL							■	
DENSITY (GAMMA-GAMMA)		■						
NATURAL GAMMA		■						
BOREHOLE LATERAL LOAD TEST							■	
DOWNHOLE VP/VS	■		■	■	■		■	
CROSSHOLE VP/VS		■						
SUSPENSION VP/VS							■	
DOWNHOLE Q (P&S)	■			■			■	■
VERTICAL SEISMIC PROFILING							■	
SEISMIC REFLECTION (P&S)							■	
SEISMIC REFRACTION (P&S)	■						■	

CDMG - Calif. Dept. of Conservation
         Division of Mines and Geology
HLA   - Harding Lawson Associates
KC   - Kajima Corporation
LCA   - LeRoy Crandall and Associates

OYO - OYO Corporation
PDC - Pitcher Drilling Co.
QEST - QEST Consultants
WCC - Woodward-Clyde Consultants

Table 4. Geotechnical Laboratory Tests

LABORATORY TESTS	D & M	L C A	O Y O
SOIL CHARACTERISTICS*	■	■	■
CONSOLIDATION TEST		■	
DIRECT SHEAR TEST		■	
DYNAMIC TRIAXIAL TEST	■		
RESONANCE COLUMN TEST			■
DYNAMIC TORSION TEST			■
TRIAXIAL ULTRASONIC WAVE VELOCITY			■

* Grain size, specific gravity, moisture content,
  unit weight, liquid limit, and plastic limit.

D&M - Dames & Moore
LCA - LeRoy Crandall and Associates
OYO - OYO Corporation

STRONG-MOTION ARRAY QUESTIONNAIRE

1. Where is your array located and how long has it been operating? Near Parkfield — Scobie Ranch, Stone Corral. In operation since late Spring 1987; fully operational w/ downhole FBAS since Nov. 1987.

2. Please describe your array, in terms of the type and number of instruments, their spacing, their triggering, their recording means (film, tape, or disc; analog or digital), and their foundation and housing.

21 Kinemetrics PDR-1 recorders, master GOES clock. Records digitally at (selectable) sample rate of 200 samp/sec. Trigger either mechanically from external triaxial mechanical trigger or internally from ratio of long-term/short-term average. Any given instrument triggers entire array. 13 surface and 8 downhole triaxial Kinemetrics FBAS (13⁵ + 23 Surface array has 3 arms (120° angles) of ~120 m length. Downhole array clustered near center with depths of 7.5 - 90 m All recording equipment housed in a single on-site shelter; surfa sensors on concrete pads; downhole sensors in leak-proof, retrievable

Station spacings are variable on each arm to optimize beam steering capability and coherency analysis.

package

3. Describe the nature of the data you have obtained, in terms of the number of events recorded, their range of magnitudes, and their distances from the array.

Array dynamic range is 102 db, 2 G max. Thus far have recorded 2 events from nearby Parkfield segment:

1) 10/23/88 $M = 3$, $z = 9$ km, $r = 9$ km, avg. peak acc at surf ~.002g.
2) 5/27/89 $M = 4$, $z = 10$ km, $r = 8$ km, " " ~.02g.
3) 10/17/89 $M = 7$, $z = 17$ km, $r \cong 200$ km ?

4. What means were used to characterize the site conditions?

Geological mapping, drilling + coring, uphole-downhole P-wave + S-wave profile, P-wave seismic refraction to ~ 150 m depth. Seismic data (travel times) inverted for 2-D velocity for each profile (complete 3-D inversion not done) for P-waves only.

We are considering applying pneumatic shear-wave source to improve shear-wave velocity model. Also interested in Rayleigh wave inversion technique for modeling site on a more regional basis, seismic velocities at

5. **If you were to establish a new array, what means would you now use to characterize site conditions?**

For soil site, additional geotech characterization in form of SPT and triaxial tests would be needed.

(See part 2 of question 4).

Microtremor studies are gaining interest and may be quite useful — access a much broader freq. band than

6. **What lessons have been learned**

o regarding the operation of the array?

False triggers can be minimized by desensitizing surface stations; downhole sensors require offset adjustment of baseline voltage to make use of low-gain (gain-ranged) data - accomplished at output from A/D board; tape recorders malfunction below ~35° ambient temp — introduced propane heater w/ thermostat to instrument shelter; careful engineering and testing is required to assure that multi-station arrays (which are interconnected) work as effectively as single-station counterparts.

o regarding ground response to earthquakes?

Amplitude variation over small dimensions (100 m) is much greater than one might think. Seismic coherency at different sites (Lotung + Parkfield) is remarkably similar (as a function of frequency and station separation).

[left margin note:] Solid state + PC technology ~~is making~~ will make all of this much easier in the future.

7. **Can you comment on the relevance of ambient vibration measurements and forced vibration testing?** not applicable to this site. (You may be interested in modeling of FVT at Lotung done by Anooshehpoor + Brune for Lotung site ½ — supported by EPRI.)

8. **ADDITIONAL COMMENTS AND ADVICE (please use additional pages if desired)** We are in the process of installing, in parallel to our master station at Parkfield, a solid-state "SSA-1 recorder w/ modem for remote access. If we were to start all over today, I would insist on all solid state, with on-site and remote PC accessibility. Additional site characterization may be necessary depending on ~~the~~ how well we can model site response with what we have now.

Thank you!

_____
Name John Schneider
(EPRI/STEPP)

STRONG-MOTION ARRAY QUESTIONNAIRE

1. Where is your array located and how long has it been
   operating?

   The Diablo Canyon Free-field Array is located at PG&E's Diablo
   Canyon Power Plant in central California.
   The array has been in operation since 1987.

2. Please describe your array, in terms of the type and number of
   instruments, their spacing, their triggering, their recording
   means (film, tape, or disc; analog or digital), and their
   foundation and housing.

   Type of instruments: A700 accelerographs by Teledyne/Geotech.
   Number of instruments: 10
   Instrument spacings: 75 feet to over 1000 feet.
   Triggering: Preset threshold triggering.
   Recording means: Solid-state digital recorders.
   Instrument foundation: 20-cm thick concrete pedestal in
                          underground vault.
   Instrument housing: Underground concrete vaults of several
                       feet deep.

3. Describe the nature of the data you have obtained, in terms
   of the number of events recorded, their range of magnitudes,
   and their distances from the array.

   No event has been recorded since the array was installed.

4. What means were used to characterize the site conditions?

   a. Surface geology.
   b. Trenching.
   c. Boring.
   d. Borehole seismic velocity measurements.
   e. Seismic refraction prifiles.
   f. Laboratory tests of rock samples.

5. If you were to establish a new array, what means would you now
   use to characterize site conditions?

   The original investigations of the site conditions were
   already extensive and thorough.

6. What lessons have been learned

   ● regarding the operation of the array?

     Current construction of the solid-state memory recorders is
     not rugged enough for long-term deployment in sultry, humid
     environments, such as underground vaults.

   ● regarding ground response to earthquakes?

No recorded data are available yet.

7. Can you comment on the relevance of ambient vibration measurements and forced vibration testing?

No comment.

8. Additional comments and advice.

No additional comments.

STRONG-MOTION ARRAY QUESTIONNAIRE

1. Where is your array located and how long has it been operating?

   The Diablo Canyon Supplemental Seismic System is located at PG&E's Diablo Canyon Power Plant in central California. The array has been in operation since 1979.

2. Please describe your array, in terms of the type and number of instruments, their spacing, their triggering, their recording means (film, tape, or disc; analog or digital), and their foundation and housing.

   Type of instruments: DCS 302 accelerographs by Terra Technology.

   Number of instruments: 61 channels.

   Array layout: 52 channels record the biaxial or triaxial motions at varios locations of the power plant structures. 9 channels record the triaxial ground motions at three locations around the power plant. All the recorders are at one location.

   Timing and triggering: Common timing and common threshold triggering for all the channels.

   Recording means: digital cassette tapes for all 61 channels. Parallel solid-state recorders for about half of the channels.

   Instrument foundation: 40-cm thick concrete pads poured in place for the three free-field locations.

   Instrument housing: Plywood shelter for the free-field instruments.

3. Describe the nature of the data you have obtained, in terms of the number of events recorded, their range of magnitudes, and their distances from the array.

   Number of events: about 10.

   Magnitude range: 2.4-6.7 M_L.

   Distance range: about 6 to 150 km.

   Focal depth range: all shallow crustal earthquakes.

4. What means were used to characterize the site conditions?

   a. Surface geology.
   b. Trenching.
   c. Boring.
   d. Borehole seismic velocity measurements.
   e. Seismic refraction prifiles.
   f. Laboratory tests of rock samples.

5. If you were to establish a new array, what means would you now use to characterize site conditions?

The original investigations of the site conditions were
already extensive and thorough.

6. What lessons have been learned

   ● regarding the operation of the array?

   Regular checks of the instruments by remote telepone dial-up
   through personal computers are very effective for ensuring
   the system to be always in full operational conditions. In
   case the system is triggerred, the remote telephone dial-up
   circuit provides quick accessibility to the recorded data.

   ● regarding ground response to earthquakes?

   This system provides site-specific ground motion data for
   analyzing structural responses.

7. Can you comment on the relevance of ambient vibration
   measurements and forced vibration testing?

   No comment.

8. Additional comments and advice.

   No additional comments.

Appendix E   ON THE BEHAVIOR OF SOIL DURING EARTHQUAKES: LIQUEFACTION

Φ GEI Consultants, Inc.

ON THE BEHAVIOR OF SOILS
DURING EARTHQUAKES - LIQUEFACTION

by

Dr. Gonzalo Castro

Reprinted from
Soil Dynamics and Liquefaction
A. S. Cakmak, Editor
Elsevier, 1987

ON THE BEHAVIOR OF SOILS DURING EARTHQUAKES - LIQUEFACTION

G. Castro

Geotechnical Engineers Inc., Winchester, MA 01890, USA

INTRODUCTION

The literature on the behavior of soils during earthquakes has dramatically increased in the last 20 years presenting many new ideas, field and laboratory tests, and analytical approaches. It is the purpose of this paper to establish a framework within which one can understand the relationships between the various ideas, the extensive test data, the analytical models, and most importantly the field observations on soil behavior during actual earthquakes. The starting point to create such a framework is to review and classify the phenomena actually observed in the field based upon their physical mechanisms.

A classification of types of soil behavior during earthquakes is proposed based on the presence of "driving" shear stresses in the soils from static loading existing prior to the earthquake. The term "driving" refers to those shear stresses that are required for static equilibrium and, therefore, are available to drive the mass should the soil lose sufficient strength.

The "driving" shear stresses are not the shear stresses resulting from placement or consolidation of the soil, but rather are the minimum shear stresses which are necessary to maintain equilibrium of the soil mass under external or gravity loads (e.g., static foundation loads or weight of sloping ground or embankment). The driving shear stresses correspond to those that one would calculate in a stability analysis.

In a soil deposit with level ground and not supporting any structure, the driving shear stresses are zero. There are shear stresses in the soil due to the fact that $K_o \neq 1$; however, they are not required for equilibrium and may be referred to as "locked-in" shear stresses. As an earthquake shakes the ground, small shear deformations may occur due to the "locked-in" shear stress. However, with very small shear deformations,

the stresses are redistributed and the "locked-in" shear
stresses disappear.

A classification of field observations based on the asso-
ciated mechanism of soil behavior is proposed as follows:

	Soil Behavior	Typical Field Observation
No Driving Shear Stresses	Volume decrease Pore pressure increases	Ground settlement Sand boils and ground settlement
Presence of Driving Shear Stresses	Loss of stability — Liquefaction	Flow slides Sinking of heavy buildings Floating of light structures
	Limited shear dis-tortion (soil mass remains stable)	Slumping of slopes Settlement of buildings Lateral spreading

The paper will describe separately the state of knowledge
concerning the above phenomena, their relationships and dif-
ferences, and recommendations will be presented for their
analysis.

It is important to note at this point that the term
liquefaction is often used to refer to all of the above phenom-
ena, even though, as will be shown in this paper, their phy-
sical mechanisms are quite different. In the subsequent
discussion, the term liquefaction will only be used to describe
the cases in which the soil mass loses stability (e.g., in flow
slides) and will be defined in that context.

PART I — SOIL UNDER ZERO DRIVING SHEAR STRESSES

Soil under zero driving shear stresses is found below level
ground when there are no structures or slopes that apply signi-
ficant shear stresses to the soil. Soil that is located suf-
ficiently deep or far enough away from a structure or slope so
that it does not contribute to its stability will also be
essentially under zero driving shear stress. For example, a
soil layer in the foundation of an embankment is under zero
driving shear stresses if the embankment would be stable, even
if the strength in the soil layer were zero. The relevant soil
behavior under earthquake shaking is volume change, since shear
distortion cannot occur in the absence of shear stresses.
Volume change can occur during shaking in dry soils or it would
be preceded by pore pressure increase and dissipation in satu-
rated soils. Experience has indicated that volume decreases
can be significant for sands and nonplastic silts.

Volume Changes in Sands, Drained Conditions
Volume changes in sand due to controlled cyclic shear strains

-2-

and zero driving shear stress have been investigated by Silver
and Seed (1971) and Youd (1972). Tests on sand were performed
in a simple shear device, and decreases in thickness of the
sample were measured as cyclic shear strains were applied.
These tests show that within each cycle, expansion of the soil
takes place when strained; however, it decreases in volume as
it is unloaded back to the unstrained position. The net result
of a strain cycle is a decrease in volume. It was found that
the decrease in volume for a given number of load cycles
increases with cyclic strain, but it is not a function of con-
fining pressure. It should be noted, however, that the cyclic
stresses required to induce a given cyclic strain, do increase
with confining pressure. Thus, for a given level of cyclic
shear stress, the volume change is a function of confining
pressure. These test results indicate that, to estimate volume
changes in dry sands, cyclic shear strain is a better parameter
to represent the action of the cyclic disturbance than the
corresponding stress. Volume changes were also obtained by
Ishibashi et al using cyclic torsional shear tests on cylindri-
cal hollow specimens of sand. The sand was saturated and
cycling was performed slowly enough to maintain drained con-
ditions.

Fig. 1 – Summary Plot of Volume Decrease of Sands
Under Cyclic Straining

The test results described above are summarized in Fig. 1 in a plot of volume change after ten shear strain cycles versus the amplitude of cyclic strain. It can be seen that different sands show widely different volume changes under the same cyclic strain.
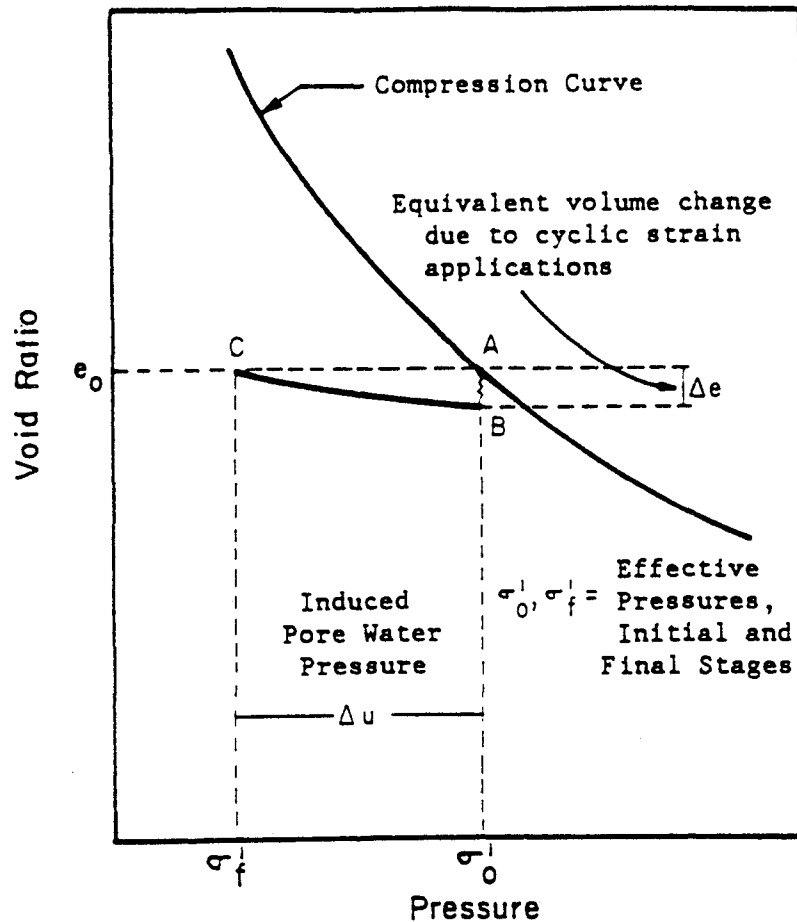
Pore Pressure Increase in Saturated Sands

This section deals with the pore pressure increase in saturated sands that are cyclically loaded under zero driving shear stresses. The subject has been the focus of a large number of laboratory investigations, data collection efforts leading to empirical charts, and development of several mathematical models.

Direct measurements of pore water pressures that developed in a sand deposit were made by Ishihara et al (1981) at a level ground site in Owi Island, Japan during a 1980 earthquake with a peak ground surface acceleration of 0.1 g. In two loose layers of silty fine sand, pore pressure increases were recorded that reached maximum values that were only a small percentage of the effective overburden pressure. No significant surface manifestations of these small pore pressure increases (settlements or sand blows) would be expected and none were observed.

Extensive research has been performed in which laboratory specimens of saturated sand under zero driving shear stress are subjected to either controlled cyclic stresses or strains (e.g., Lee and Seed, 1966; Seed and Lee, 1966; Peacock and Seed, 1968; Finn et al, 1970; Ishihara and Yasuda, 1975; DeAlba et al, 1976; Hedberg, 1977; Ladd, 1977; Ishihara and Yamazaki, 1980; Whitman et al, 1982; Dobry et al, 1982; Chang et al, 1983; Yoshimi et al, 1984). This listing is by no means comprehensive. The types of equipment that have been used are triaxial, simple shear, hollow torsional, shaking table, and centrifuge. Many variables have been investigated, including density of the sand, confining pressure, frequency of loading, shape of load cycle, method of sample preparation, and prior cyclic loading. It is not the purpose of this paper to review in detail the results of these investigations but rather to present the main findings.

The model for pore pressure increase can be represented approximately as shown in Fig. 2. The volume changes that would have occurred under drained conditions are reflected in a pore pressure increase in accordance with the swelling characteristics of the sand skeleton.

As noted in the previous section, the volume change is primarily a function of the magnitude of the cyclic strains. Thus it is reasonable to expect that the pore pressure increase would also be primarily a function of cyclic strains, as has been demonstrated by Dobry (1982). Data from Dobry (National
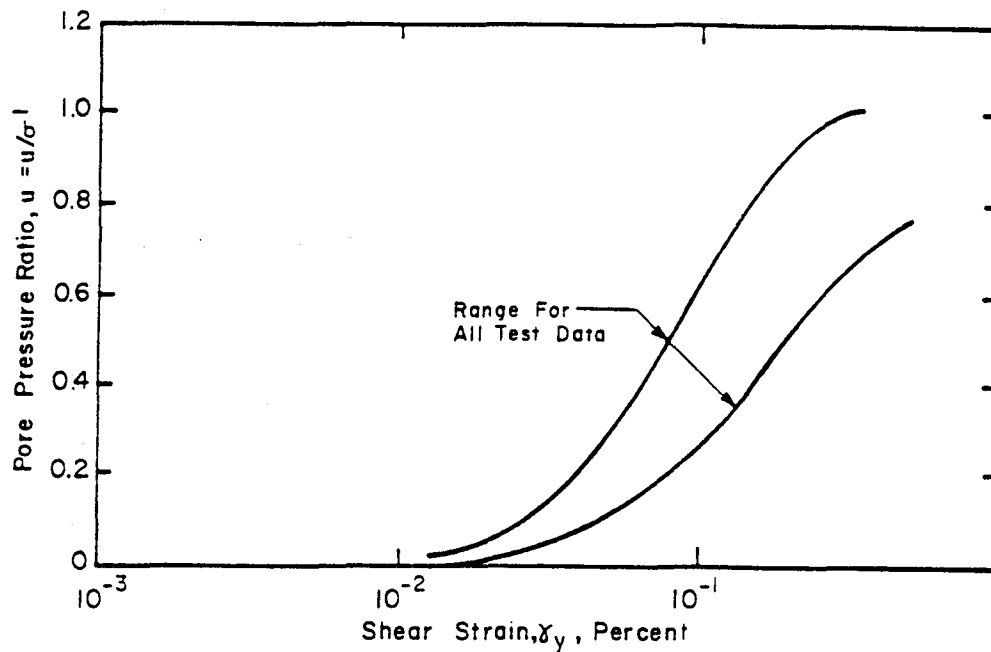
After Seed and Idriss, 1982

Fig. 2 – Schematic Illustration of Mechanism of Pore
Pressure Generation During Cyclic Loading

Research Council, 1985) is presented in Fig. 3 where it can be
seen that the pore pressure increase that develops after 10
cycles of cyclic straining expressed as a fraction of the
consolidation pressure depends mainly on the magnitude of the
cyclic strain and to a much lesser degree on density, type of
sand, initial structure or confining pressure. Furthermore, it
shows that for shear strains below about $2 \times 10^{-2}\%$, there is
practically no pore pressure increase, which lead Dobry to
refer to this strain as "threshold strain."

The cyclic stresses required to produce a given increase
in pore pressure can be viewed as those required to produce the
corresponding magnitude of cyclic strain, as per Fig. 3. It is
found that these cyclic stresses are strongly a function of
density, confining pressure, type of sand, and initial struc-
ture, i.e., the factors that determine the cyclic stresses that
one needs to apply to produce a given cyclic strain.

In controlled cyclic strain tests, the cyclic stresses
decrease when the pore pressure increases, and thus the sand
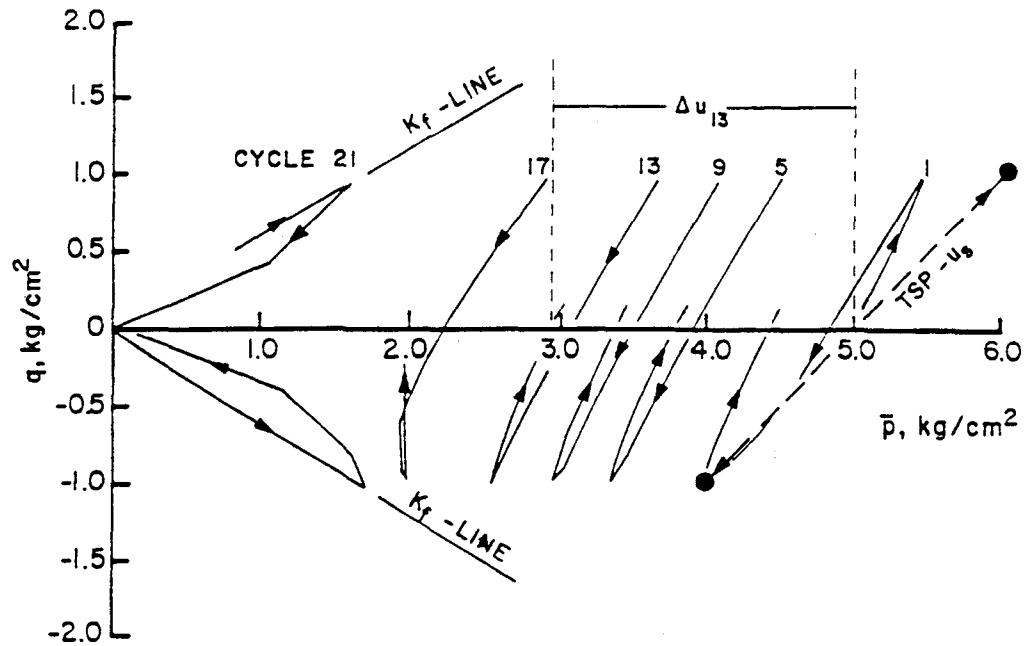softens, particularly when the pore pressure approaches 100% of

-5-

Pore Pressure Ratio, $u = u/\sigma'$

Range For All Test Data

Shear Strain, γ_y, Percent

After Dobry, 1985

Fig. 3 — Summary of Results from Strain-Controlled Cyclic Triaxial Tests on Seven Different Sands, with Different Specimen Preparation Techniques, Densities and Confining Pressures

the initial effective confining pressure. In controlled stress tests, the softening results in increasing strains. When these strains become large, it has been observed that large nonuniformities develop in triaxial as well as in simple shear specimens. Water migrates from one zone of the specimen to another as a result of boundary conditions, which leads to a more deformable specimen (Castro, 1969; Casagrande, 1975; Casagrande and Rendon, 1978; Gilbert, 1984). The laboratory boundary conditions are not representative of those in the field, and thus the large cyclic strains observed in controlled stress cyclic tests may not be representative of field conditions.

The total and effective stress paths for a typical controlled cyclic stress test are shown in Fig. 4. As the pore pressure increases, the stress paths move closer to the origin, and in Cycle 21 and in subsequent cycles, the stress path moves along the envelope starting at or close to the origin. The path moves up along the envelope until the soil develops the resistance that it needs to sustain the applied cyclic load. If the cyclic load were higher, the stress path would move higher along the envelope. (In a subsequent section, it will be shown that the maximum load that can be applied is controlled by the undrained steady state strength of the soil.) The soil is thus able to sustain the load that is applied to it, and therefore, it has not failed, even though the effective stresses momentarily become zero when there is no load applied

After Hedberg, 1977

Fig. 4 — Effective and Total Stress Paths for Cyclic Test on
          Isotropically Consolidated Sand

to the soil, i.e., at the origin in the plot in Fig. 4. The
cyclic strains increase from cycle to cycle in the laboratory
tests. In the context of shaking of level ground, the cyclic
strain in the field cannot grow unimpeded as it can in a
controlled cyclic stress test. In the field, as the soil
softens, the cyclic stresses decrease and the strains become
limited. In an extreme case of softening of a soil layer, the
shaking of the soil below the layer would not be transmitted
through the softened layer, and the soil above would remain
approximately stationary. Thus the maximum shear strain in the
softened layer would be roughly equal to the maximum displace-
ment of the earthquake motion divided by the thickness of the
layer.

    The practical effect of cyclic straining in the soil is
reflected in the type of motion felt at the ground surface
which would influence the response of structures, and in the
reconsolidation of the soil and resulting settlements. When
high pore pressures develop in a sand layer, the resulting
settlements have been observed to be as high as 2 to 3% of the
layer thickness, but usually it is less, see for example
centrifuge test results in Whitman et al (1982).

    Available laboratory data on the compression of sand and
silt after dissipation of pore pressures induced by cyclic
loading are presented in Fig. 5. The correlation of volumetric
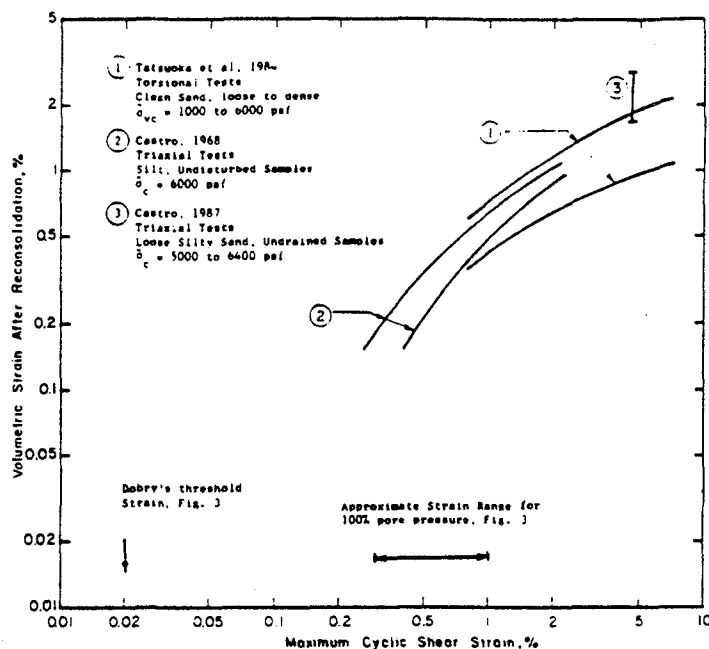strain vs. magnitude of the cyclic strain is a rather wide

-7-

**Fig. 5 — Volume Changes of Sands and Silts due to
Reconsolidation After Cyclic Loading**

band, where for a given soil, the correlation is mainly a function of density. Each set of data corresponds to a different soil, and thus they are not strictly comparable because one would not expect a unique correlation for all sands. A comparison with the data in Fig. 1 indicates higher compression in drained conditions for the same cyclic strain, which seems reasonable based on the fact that drained cyclic straining would be more effective in densifying the sand because straining would be performed under higher effective overburden than under undrained conditions. Note also that the cyclic stresses required to cause the same cycling strains would be higher for drained than for undrained cyclic shear.

The approximate values of Dobry's threshold cyclic strain and the range of cyclic strains for which one can expect to reach 100% pore pressure in ten cycles are also shown in Fig. 5. For undrained tests exceeding these cyclic strains, one can expect that development of specimen nonuniformities would tend to exaggerate the volume changes during reconsolidation of the soils.
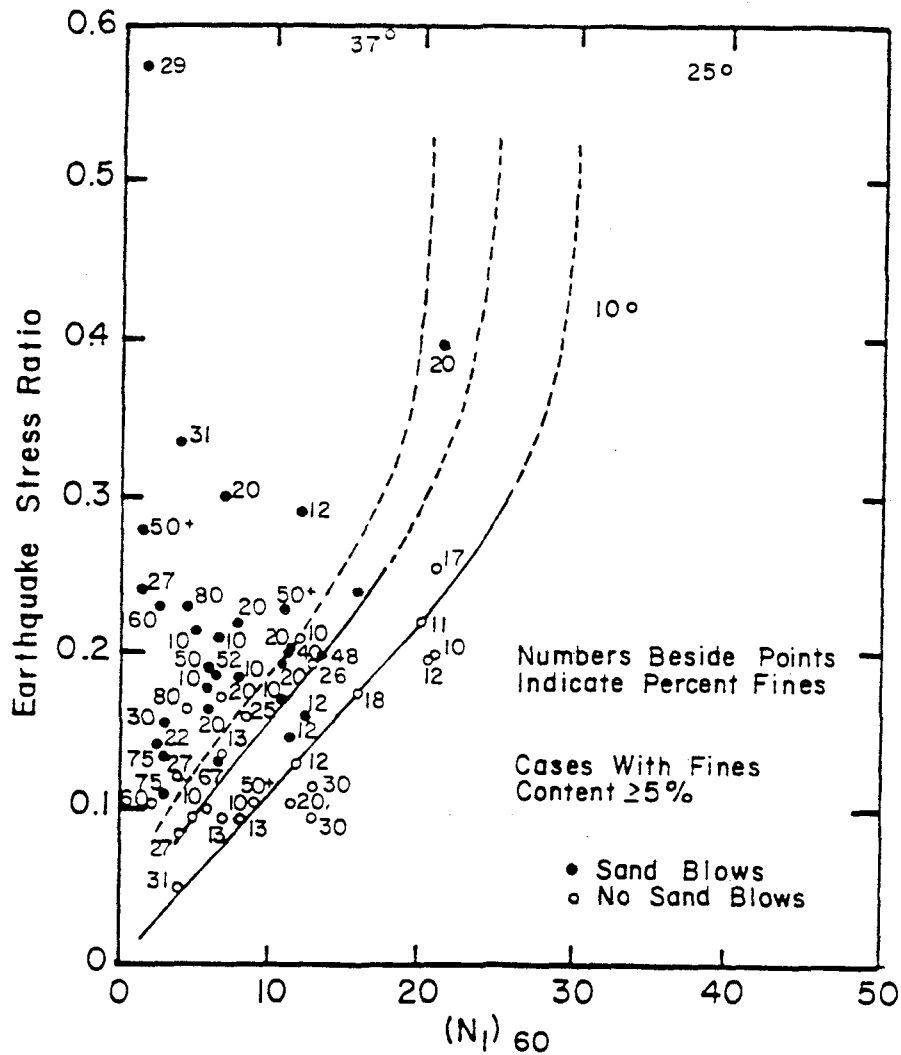
In spite of the limitations discussed above, the chart in Fig. 5 can be used as a rough guide to estimate potential settlements of sandy soils. Better estimates for a particular site can only be made on the basis of site specific investigation and tests. The tests should be performed on high quality samples and can be cyclic triaxial or simple shear tests.

-8-

Perhaps the most widely reported effect of pore pressure increases at depth is the development of sand blows (also referred to as sand boils). Water flow exiting locally at the ground surface brings sand particles with the water creating a pile of sand referred to as a sand volcano. In extreme cases, water has been observed to spout up to heights of 4 ft above ground (Housner, 1958), and the sand volcanoes can be as large as a few feet in diameter. The sand blows are the result of the reconsolidation of sand layers in which pore pressures have been generated.

The reconsolidation process has been the focus of several investigations. Housner (1958) applied Terzaghi's consolidation theory and demonstrated that the large gradients needed to cause sand blows, can develop near the ground surface when a deep layer of soil develops high pore pressures in a uniform soil deposit. Florin and Ivanov (1981) noted that reconsolidation starts from the bottom of the sand layer, and presented a model that predicts the upward movement of the lower boundary of the soil with zero effective stress, which they referred to as the "compaction front." Heidari and James (1982) observed the reconsolidation process in a soil column during a centrifuge test, and concluded that the results agreed with Florin and Ivanov "compaction front" predictions. Whitman et al (1982) showed that a nonlinear consolidation theory is required to model the reconsolidation process because of the large change in effective stress from about zero to its value at the end of reconsolidation.

Sand blows are the result of reconsolidation of a soil layer followed by upward water flow. Therefore, sand blow development is strongly influenced by the stratification and heterogeneity present in natural deposits. They are more likely to occur when the permeability of the soil that undergoes reconsolidation is high relative to the overburden, so that the rate of flow out of the layer is sufficient to create large enough seepage gradients in the overburden, Scott and Zuckerman (1973). Conversely, a silty sand layer that develops pore pressure in an earthquake is not likely to generate sand blows if the overburden is more pervious, such as a clean sand. It should be noted that sand blows and associated sand volcanoes are also observed at the bottom of excavations in sandy soils below the groundwater level and downstream of dams and other water retaining structures. Piping of the sand under large upward exit gradients creates the sand blows. The physical mechanism of the formation of sand volcanoes in these cases is similar to the one that occurs during and after earthquakes, except that the source of the hydraulic gradients is different.

Extensive collections of data on sandy level ground sites subjected to earthquakes have been made by several authors, Whitman (1971), Castro (1975), Seed (1976) and most recently Tokimatsu and Yoshimi (1983) and Seed et al (1984). The data

0.6

•29   37°   25°

0.5

10°

0.4

•20

•31

•20   •12

0.3

•50+

17
•27   80   20   50+
60   10   10   20   10   11
50   52   10   20   40   48   10
10   20   20   26   12
80   20   25   18
30   20   13   12
22   12
75   27   67
75   20   10   12
50+   30
10   20   30
27   13   13   30
31

0.2

0.1

Earthquake Stress Ratio

Numbers Beside Points
Indicate Percent Fines

Cases With Fines
Content ≥5%

• Sand Blows
o No Sand Blows

0

0   10   20   30   40   50

$(N_I)_{60}$

Adapted From Seed et al,1984

Fig. 6 – Empirical Chart Relating the Observation of Sand
Blows During Earthquake to Blowcounts and
Earthquake Stress Ratio

consists of a description of the soil conditions with SPT
information, a measured or estimated peak ground surface acce-
leration, and a classification of sites into those in which
sand blows were observed and those in which they were not.
Note that these charts are often referred to as liquefaction
charts even though they relate chiefly to the observation of
sand blows and not to other phenomena also referred to as
liquefaction, such as flow slides or lateral spreading. A
typical chart is shown in Fig. 6 for sands with percent fines
of 5% or more, where each site is represented by one data
point, i.e., by one value of blowcount normalized to a con-
fining pressure of 1 tsf and a stress ratio that is a function

of peak ground surface acceleration and depth of groundwater level. Also each point shows a value of percent fines. Both the blowcount and the percent fines are the values that the authors felt were representative of the layer in which the larger pore pressures were estimated to have developed. Because of the heterogeneity of natural deposits, the selection of a single representative value of blowcount and of percent fines is based on a considerable amount of judgment. In spite of the simplified representation of soil conditions at each site, several conclusions can be drawn from such a chart, and these are consistent with the physical mechanism of sand blows described earlier:

1) Sand blows are more likely to be observed in soils with low blowcounts, i.e., looser soils in which higher pore pressures would develop for a given earthquake and that also would compress more and thus release more water during reconsolidation.

2) Sand blows are more likely to develop for stronger shaking, which produces larger cyclic strains and thus larger pore pressure increases (see Fig. 3).

3) Other factors being equal, i.e, blowcount and earthquake stress ratio, silty sands are less likely to generate sand blows than clean sands because the rate of reconsolidation is slower, and thus it is less likely to generate sufficiently high gradients in the overlying soils. Note that a different explanation has been offered for the lower likelihood of sand blow development in silty sands (e.g., Seed et al, 1984). It has been suggested that silty sands are less likely to "liquefy" with the term referring to a pore pressure increase of 100%. However, data on shear moduli of sands indicate that a silty sand and a clean sand with the same blowcount do not have consistently different shear moduli (See for example Ohta and Goto, 1986; Seed et al, 1986). Thus, under a given earthquake, the cyclic shear strains in the two soils are likely to be similar, and therefore the pore pressure increases will also be similar as per Fig. 3. Thus it is not warranted to conclude from Fig. 6 that the pore pressure increase in the silty sand would be consistently lower than in a clean sand when compared at the same blowcount. The only conclusion that can be drawn is that the appearance of sand blows is less likely when the sand is silty. In the opinion of the author, the explanation for this observation lies in the lower permeability and thus slower reconsolidation of the silty sands rather than on a lower pore pressure generation.

4) The computation of the earthquake stress ratio is such that a higher number is obtained for higher groundwater levels, which results in a higher likelihood of sand blows. This conclusion is consistent with the fact that for relatively deep groundwater (GW) levels, the dissipation of pore pressures from a layer below the GW level is:

1) less likely to produce sufficient gradients to overcome
the larger effective stresses produced by the full weight
of the soil above the GW level and 2) as the GW level
rises during reconsolidation, the water will first fill
the voids of unsaturated soils above the GW level before a
local quick condition can be induced. Note that placement
of an earth fill over the soil will have an effect similar
to lowering the GW level in that it will inhibit the
development of sand blows through the fill, but it may
actually enhance the possibility of sand blows in the
ground adjacent to the fill as the water seeks the path of
least resistance.

Conclusions

The effect of earthquake shaking for soils not subject to
driving shear stresses, i.e., under level ground, is primarily
the development of volume changes that lead to settlements.
These occur either as a result of immediate compression of dry
soils or as a result of the pore pressure build up and sub-
sequent reconsolidation in saturated soils. The settlements
are not likely to be uniform, and thus they can lead to damage
(e.g., cracked pavements and broken buried pipes). Experience
indicates that significant settlements have been observed only
in sandy soils. Whether sand blows develop or not is a highly
visible issue, but it is not a concern of substantial engi-
neering significance except as a symptom that settlements are
occurring. Thus the main engineering concern is to predict
settlements and not to predict sand blows. It should be noted
that the empirical charts of the type shown in Fig. 6 are
referred to as liquefaction charts with the implication that it
relates to the phenomena of flow slides or lateral spreading
discussed in the next section. Since the chart is based
chiefly on the occurrence of sand blows, whose physical mecha-
nism is very different from that of flow slides or lateral
spreading, the implication that the chart is applicable to
these phenomena is unwarranted, as will be discussed in detail
in Part II of the paper.

The prediction of earthquake-induced settlements in sandy
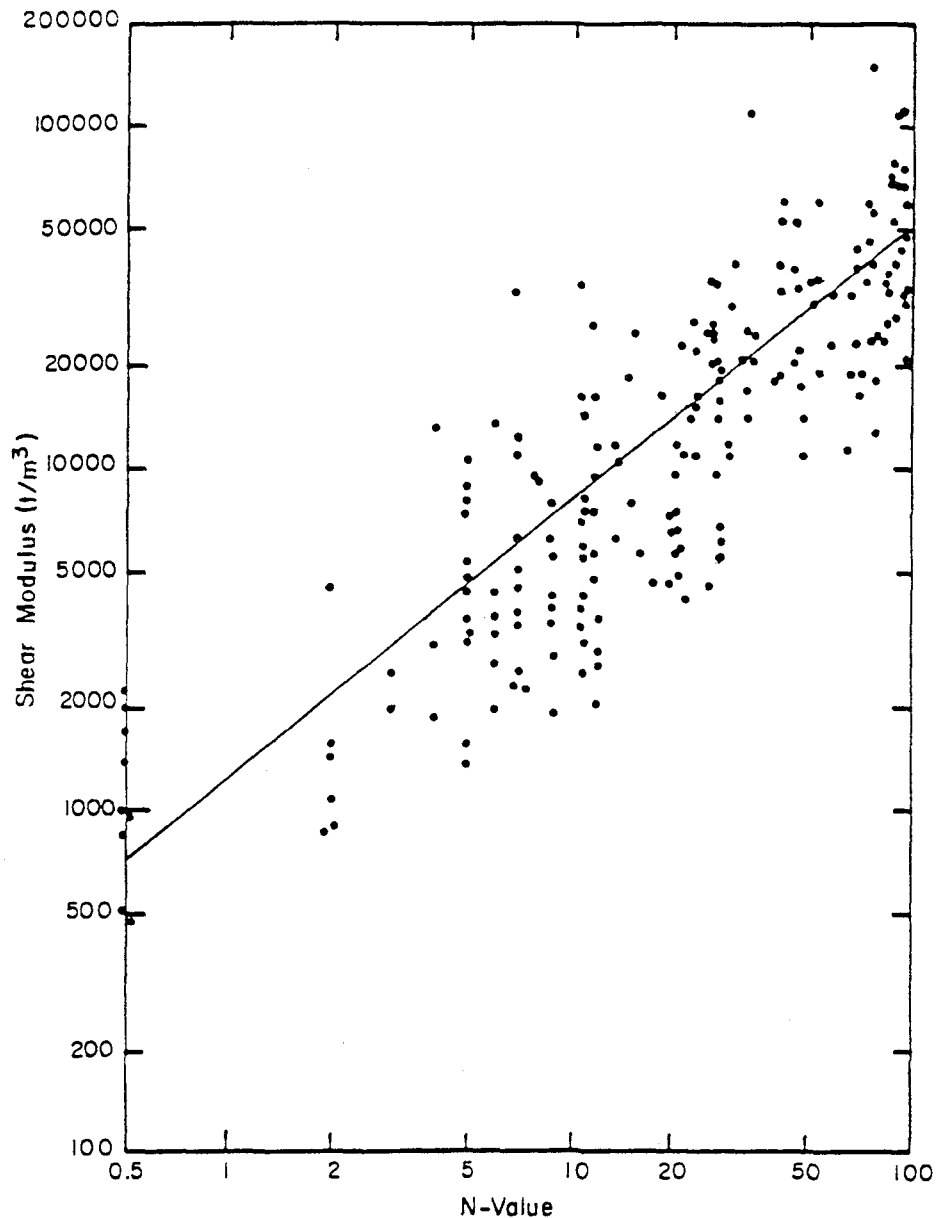soils under level ground involves the following steps:

1) Estimation of the cyclic shear strains γ_y induced by the
earthquake. These can be computed as follows (Dobry et al,
1982):

$$\gamma_y = 0.65 \frac{a_p \times \sigma_o \times r_d}{g \times G_{max} \times (G/G_{max})}$$

a_p = peak horizontal acceleration at the ground surface

g = acceleration of gravity

σ_o = total overburden pressure at depth z

Shear Modulus (t/m^3) vs N-Value

Fig. 7 — Correlation Between Small Strain Shear Modulus and SPT Blowcount

r_d = $r_d(z)$ = stress reduction factor as a function of depth. This factor can be approximated by a linear decrease from 1 at the ground surface to 0.7, at a depth of 90 ft (e.g., Seed, 1976).

G_{max} = shear modulus of the soil at very small cyclic strains, γy = 10^{-4} percent. The best procedure to determine G_{max} is from shear wave velocity measurements using cross hole techniques (see for example Stokoe and Hoar, 1978). Alternatively, a rough estimate of G_{max} can

be obtained from published correlations of G_{max} (or V_s) with Cone Penetration Tests (e.g., Robertson and Campanella, 1983) and with Standard Penetration Tests (e.g., Ohsaki and Iwasaki, 1973; Seed et al, 1986). The Ohsaki and Iwasaki correlation is shown in Fig. 7 which illustrates their proposed average correlation. Index tests such as blowcounts can only give a very rough estimate of G_{max}, as it is apparent from the substantial degree of scatter in the data in Fig. 7. This scatter is typical of all such correlations.

(G/G_{max}) = effective modulus reduction factor of the soil, a function of the cyclic shear strain, γ_y. See, for example, Seed et al (1986).

2) For dry sands, one can estimate compression of the soil using tests of the type performed by Silver and Seed (1971), Youd (1972) or Ishibashi et al, 1985, using undisturbed samples of the soils at the site. Alternatively, one can obtain a rough estimate using the data in Fig. 1.

3) For saturated soils, one can estimate the pore pressure increases in the various zones of the deposit using the chart in Fig. 3. The recompression characteristics can be estimated from published data on recompression properties of sand or it can be obtained from one-dimensional or triaxial compression tests on undisturbed samples from the site in question. Alternatively, a rough estimate can be obtained using the data in Fig. 5.

PART II - SOIL SUBJECT TO DRIVING SHEAR STRESSES

As noted in the introduction to this paper, the driving shear stresses are those required to maintain the soil mass in equilibrium. Driving shear stresses exist, for example, in the soil supporting a heavy building, within an earth embankment and its foundation and beneath natural slopes. Most cases of engineering significance involve the presence of driving shear stresses in the soil. Understanding the behavior of the soil under these stresses and the superimposed earthquake stresses requires a brief review of fundamental aspects of the shear strength of soils in general and of sands in particular.

The stress strain behavior in direct or simple shear of a saturated sand is illustrated schematically in Fig. 8 for four different cases. Drained and undrained behavior are considered for two initial states (i.e., two initial conditions of void ratio and effective normal stress on the failure plane). The two initial states can be considered as loose (State 1) and dense (State 2). In all four cases, after sufficient straining, the state of the soil reaches a point on the steady
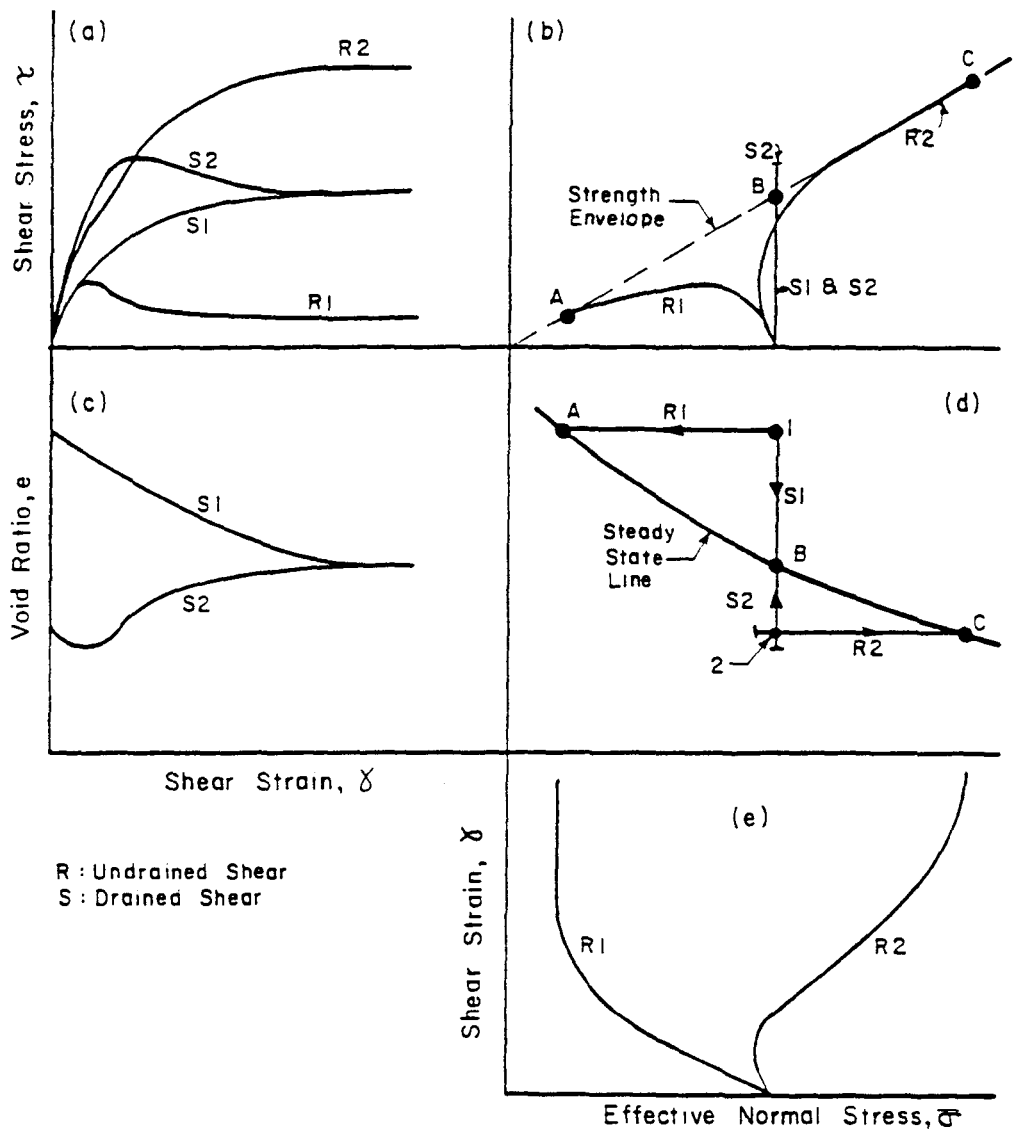
Fig. 8 — Stress-Strain Behavior of a Saturated Sand in
Simple Shear

state line. This line is unique for a given soil and the tests
in Fig. 8 represent only four out of many possible paths that
the soil can follow to reach the steady state line. Regardless
of the path or initial condition, the state of the soil will
reach a point on the steady state line if sufficient unidirec-
tional shear strain is applied. The steady state of defor-
mation for any mass of particles is defined by Poulos (1971,
1981) as "The state in which the mass is continuously deforming
at constant volume, constant normal effective stress, constant
shear stress, and constant velocity. The steady state of
deformation is achieved only after all particle orientation has
reached a statistically steady state condition and after all
particle breakage, if any, is complete so that the shear stress
needed to continue deformation and the velocity of deformation
remains constant."

-15-

Casagrande in 1936 introduced the idea of a critical void ratio at which "a cohesionless soil can undergo any amount of deformation or actual flow without volume change." Casagrande defined the critical void ratio in terms of drained shear and the more general steady state is entirely equivalent to Casagrande's concept. Schofield and Wroth in 1968 defined critical state in a manner that is somewhat different from Casagrande's critical void ratio or steady state. Poulos (1971, 1981) has described the difference between these concepts. Specifically, Schofield in 1985 indicated to the author that for the case R1 in Fig. 8a, he would use in the critical state theory the peak value of τ, while steady state is defined as the minimum value which is reached at large strains.

When considering any path, e.g., R1, the shape of the stress strain curve prior to reaching steady state is a function of the initial structure of the soil; however, its steady state is not, since at steady state the soil is thoroughly remolded and has lost all "memory" of its initial structure. It also follows that the steady state of the sand at the void ratio of state 1 (Fig. 8d) is given by point A in Figs. 8d and 8b regardless of the initial value of the effective normal stress. Or in other words, the undrained steady state strength, designated S_{us}, is only a function of the void ratio of the sand and not of its initial state of stress, nor of the type of undrained loading (monotonic or cyclic), nor of its initial structure, Castro, (1969). At the initial state 1 in Fig. 8d, the soil is said to be contractive because it would tend to decrease in volume as it is sheared and approaches the steady state. If drained, the volume decrease will take place and if undrained the pore pressure will increase.

The steady state line is approximately a straight line or has a slight downward concave shape, when plotted with the void ratio on an arithmetic scale and the effective normal stress on a logarithmic scale. The slope of the line is defined as the change in void ratio for a tenfold change in normal stress (one log cycle). For bulky grained sands, the slope of the line ranges from 0.05 for rounded grains to 0.30 for very angular grains such as for crushed mine tailings (Castro, 1969; Castro et al, 1982; Poulos et al, 1985a). Steeper SSL are obtained for plastic soils with plate shape grains.

The slope of the steady state line for many sands has been shown to be steeper than the slope of the compression curve for the same sand. Thus increased confining pressure would generally cause the state of the sand to be more contractive (or less dilative) in spite of the decrease in void ratio caused by the increased confining pressure. For sands with similar grain shape, the steady state lines are approximately parallel; however, their position in a e vs $\bar{\sigma}$ plot is very sensitive to the gradation of the sand. The scatter in the position of the

lines for various sands is smaller if percent compaction is
plotted instead of void ratio (Castro et al, 1982).

The state diagram in Fig. 8d is plotted in terms of void
ratio and effective normal stress in the failure plane. At
steady state, the soil is at the strength envelope, i.e., the
friction angle is fully mobilized, and therefore the shear
strength at steady state S_s is equal to $\bar{\sigma}_s \tan \varphi_s$ where the
subscript s denotes steady state. The steady state line is
then a line in a three-dimensional space with coordinates of
void ratio (or other density index), effective normal stress in
the failure plane $\bar{\sigma}$ and shear stress in the failure plane, τ.
Other pairs of stress parameters can be chosen instead of $\bar{\sigma}$ and
τ, such as $q = (\sigma_1 - \sigma_3)/2$ and $p = (\bar{\sigma}_1 + \bar{\sigma}_3)/2$; however $\bar{\sigma}$ and
τ in the failure plane are more convenient for the discussion
that follows. The projections of the line in both the e, $\bar{\sigma}$ and
e, τ planes will be used, and even though they are projections
of the line, they will still be referred to as steady state
lines. Note that the projection of the steady state line in
the τ, $\bar{\sigma}$ plane is the steady state strength envelope.

The cases shown in Fig. 8 show undrained loading that con-
sists of a monotonic increase in shear stress. The case of
interest in earthquake engineering is one in which the
undrained loading consists of cyclic loading and is superim-
posed to an initial shear stress. The undrained steady state
strength of the sand, S_{us}, is only a function of its void
ratio, and thus the same value of S_{us} applies whether the soil
is loaded monotonically or cyclically. Test data supporting
this statement have been presented in Castro (1969), Castro
(1975), and Castro et al (1982). The stress strain behavior
under cyclic loading is compared with the behavior under mono-
tonic loading in Fig. 9. Two cases are considered, in one the
undrained steady state strength S_{us} is lower [case 2] and in
the other S_{us} is higher than the driving shear stress τ_d.

The stress strain behavior under cyclic loading for
Case [1] is very similar as under monotonic loading, i.e., the
peak strength is overcome by sufficient straining which is
either caused by a single or by repeated loading. The strain
at which the resistance of the soil starts decreasing towards
S_{us} is about the same in both cases and as noted earlier, S_{us}
is the same, since the void ratio is the same.

In Case [2] cyclic loading causes an accumulation of
strain often accompanied by an increase in pore pressure
(Fig. 9d). The shape of the stress strain curve following
cyclic loading may be different from the monotonic loading case
(Fig. 9c); however, the value of S_{us} is the same.

There are substantial differences in the field behavior
that corresponds to Cases [1] and [2] in Fig. 9 and also in the
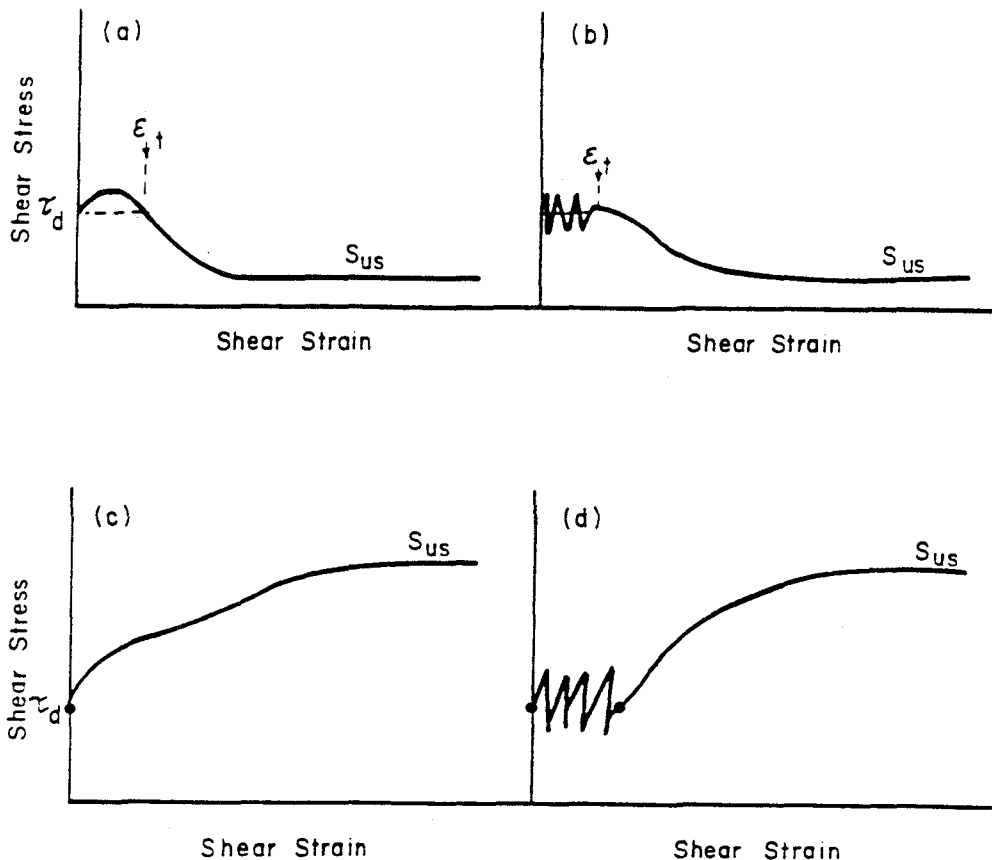method of analysis to predict field behavior. In Case [1] the

Fig. 9 - Monotonic and Cyclic Loading of a Saturated Sand

consequence of cyclic loading is a massive failure, a flow
slide. In Case [2] cyclic loading induces limited deformation
without changing the stable configuration of the soil mass.
These cases will be discussed separately, in the next two sec-
tions of the paper.

Soils Subject to Driving Shear Stresses
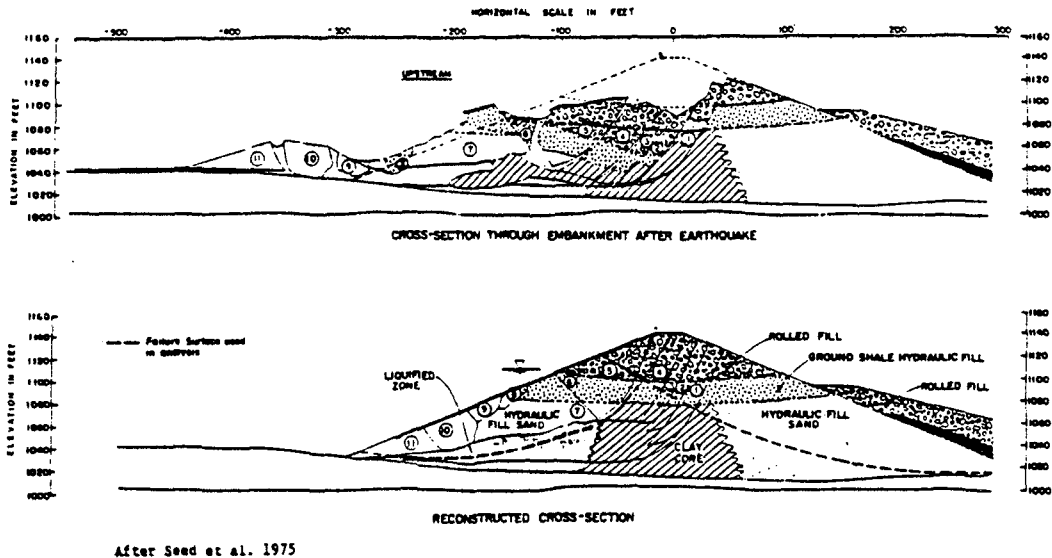Case [1]: Instability and Liquefaction
Flow slides are probably the best example of massive failures
induced by earthquakes, even though they can also be induced by
monotonic loading. In a flow slide the mass spreads out until
the shear stresses acting within the mass become so small that
they are compatible with the reduced shear strength in the
soil. To the author's knowledge, the term liquefaction was
used for the first time by A. Hazen (1920) to explain the
mechanism of the flow failure of the hydraulic-filled Calaveras
Dam in California. The term liquefaction has been associated
with the loss in strength of the soil that causes flow slides.
On the other hand, the term liquefaction was not originally
used for other phenomena that do not involve loss in strength
such as sand blows, e.g., Housner (1958). Only in the last 20
years has the use of the term liquefaction been extended to
other phenomena, such as sand blows or a particular value of

-18-

pore pressure or a particular level of strain, even though no loss in strength is involved in these phenomena. In this paper, the term liquefaction will be used in its original meaning, i.e., to refer to the loss in strength that causes flow slides or other similar phenomena. Liquefaction is thus defined as the phenomena wherein the shear resistance of a mass of soil decreases when subjected to monotonic or cyclic loading at constant volume (undrained loading conditions) so that the mass undergoes very large unidirectional shear strains--it appears to flow--until the shear stresses are as low or lower than the reduced shear resistance. Thus a liquefaction failure requires the presence of driving (static) shear stresses that exceed the reduced shear resistance of the soil. Therefore, a soil is not in itself liquefiable, but it depends on the value of the applied driving shear stresses, i.e., on the configuration of the slope or embankment, or on the shear stresses applied by heavy structures. A soil mass that is liquefiable has driving shear stresses which exceed the potentially reduced shear strength and thus can be considered to be unstable. Since liquefaction failures involve large unidirectional undrained deformations, the relevant shear strength is the undrained steady state strength.

The conditions for a seismically induced liquefaction failure to occur are two, namely, 1) the mass must be unstable in the sense that the driving shear stresses exceed the undrained steady state strength of the soils, $\tau_d > S_{us}$, and 2) the earthquake stresses must be sufficient to trigger the failure, i.e., it must be able to strain the soil sufficiently to overcome the peak strength of the soil as in Fig. 9b (Poulos et al., 1985b).

Perhaps the best known case of a liquefaction slide is the one that occurred in the Lower San Fernando Dam in California in 1971 as the result of an earthquake. This slide has been the subject of considerable interest because it was on the verge of being a major catastrophe. It has been analyzed by Seed et al (1973) and by Castro et al (1985). Additional field and laboratory investigation have been performed recently and the detailed results are presented by Castro et al (1987).

A cross section of the dam after the failure is presented in Fig. 10 along with a reconstructed cross section. The slide occurred in the upstream direction, and the deformations were concentrated in the lower part of the hydraulic fill shell, while the overlying material broke into pieces that "floated" on the shell material that lost strength as a result of the earthquake. The slide apparently occurred about one-half minute after the end of earthquake shaking (Seed, 1979). Thus the earthquake stresses triggered the failure, but only the static (driving) shear stresses caused the massive movements of the slide with a stress strain behavior of the type shown in Fig. 9b.

CROSS-SECTION THROUGH EMBANKMENT AFTER EARTHQUAKE

RECONSTRUCTED CROSS-SECTION

After Seed et al. 1975

Fig. 10 - Lower San Fernando Dam, Section After the Slide and Reconstructed Original Cross Section

The zone designated in Fig. 10 as "liquefied zone" was observed to have developed very large strains throughout the zone, in contrast to the overlying material which broke into pieces but rode over the liquefied zone during the slide. The liquefied zone is roughly triangular with a maximum thickness of about 30 ft and a length of about 150 ft. This large volume of material corresponds to a very silty sand. Since the total duration of the earthquake and subsequent sliding was of less than two minutes, it can be concluded that there was no time for this large mass of soil to change in volume, and therefore, during the failure it strained at its pre-earthquake void ratio. It has been hypothesized (National Research Council, 1985, Whitman, 1985) that earthquake-induced flow slides could develop as a result of water migration to a zone of soil which becomes looser than prior to the earthquake and then causes the failure. There is no known field evidence of such a phenomenon, and as explained above, it could not have occurred in the Lower San Fernando slide. Furthermore, the term flow slide has been used to describe liquefaction failures because the zone responsible for the slide is large, giving the appearance of flow. It is highly unlikely that massive water migration could develop so that large zones could loosen during or immediately after an earthquake. It is conceivable that migration of water could occur through short distances so that only thin layers could loosen. However, if this were the case, flow slides would occur along a thin failure zone, which is not in agreement with field observations.

In the opinion of the author, the loose zones which are responsible for the failure will fail at their pre-earthquake void ratios, and therefore, its relevant strength is the in situ value of S_{us} before the earthquake. Water migration can, however, play a role relative to other stronger zones. Seed (1975) has suggested that such a case occurred in the Lower San Fernando Dam slide. The material at the upstream toe of the dam was relatively dense because it was part of the "starter" dikes built as part of the hydraulic filling method of construction. Thus it is likely that the soil at the toe was dilative. Therefore, initially its undrained strength would exceed its drained strength. As it deformed under the increase in shear stress caused by the loss in strength in the loose zone, it dilated and water was drawn into the soil until its void ratio increased and reached steady state at a higher void ratio than its pre-earthquake value, path S2 in Fig. 8. The potential for water migration into dilative zones must be considered. If the soil is pervious enough so that water migration is possible, one should not rely for stability on shear strengths higher than drained strengths. On the other hand, soils that are contractive will have as a minimum strength the value of S_{us} corresponding to its pre-earthquake void ratio, path R1 in Fig. 13. If there is enough time for a contractive soil to change in volume, it will be a decrease because of its high pore pressure and the result will be that the strength of the loose zone will increase.

A method of analysis for liquefaction slide potential has been presented by Poulos et al (1985). The basic steps in the procedure for an embankment dam are described briefly below:

1) Identify saturated zones in the foundation or embankment soils that are likely to be contractive based on blowcounts or other index tests. Sands and silts are likely to be contractive if the SPT blowcount, normalized to an overburden pressure of one tsf, is lower than 15. Note that the value of 15 is tentative, and it is not likely to be applicable to all sands and silts; however, it is reasonably conservative for preliminary evaluations.

2) Determine the driving shear stresses in potentially contractive sands and silts in the dam or foundation, by means of a stability analysis. Fully mobilized strengths should be assumed in other zones. Strength parameters for dilative zones should be drained unless the soils are considered sufficiently impervious, in which case undrained parameters are appropriate. However, in no case should the undrained strength depend on pore pressures below atmospheric. Generally steady state strengths should be used except for clays of low to moderate sensitivity (large strains at peak) for which peak strains may be used.

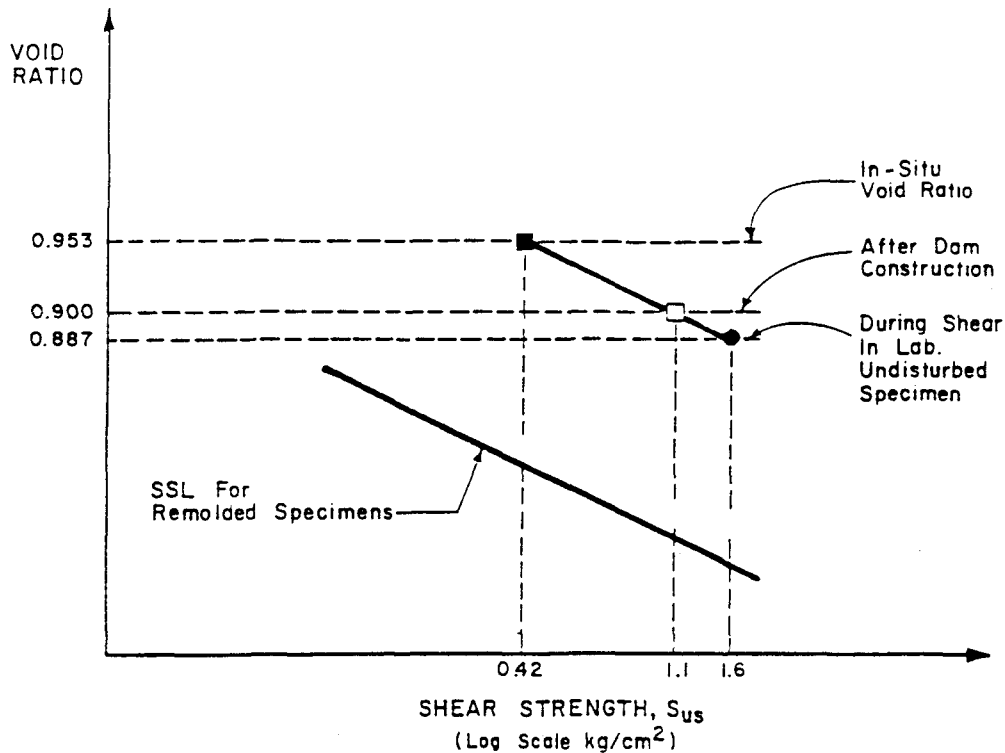3) Determine the undrained steady state strength S_{us} in the potentially critical sands or silts. Values of S_{us}

Fig. 11 — Steady State Diagram Showing Correction of S_{us} for Volume Changes

can be determined on undisturbed samples using laboratory consolidated undrained triaxial tests. The void ratio during shear and S_{us} of the laboratory sample is plotted in Fig. 11. However, the in situ S_{us} is different from the laboratory measured value because void ratio changes take place during sampling and laboratory consolidation and S_{us} is a sensitive function of void ratio. An example of the correction method is shown in Fig. 11 for a sample obtained from the foundation soils for a new dam. A steady state line is obtained on remolded specimens prepared at various void ratios for a representative batch of soil. The steady state line for the undisturbed sample is parallel to the line for the batch sample. Figure 11 shows corrected values of S_{us} for two values of void ratio, for the in situ value at the time of sampling, and for the void ratio after consolidation of the soil under the weight of the dam. It can be seen that the correction applied to the measured S_{us} is substantial, and thus cannot be ignored. Great care must be exercised in monitoring void ratio changes of the samples. For detailed procedures, see Poulos et al, 1985a. As more S_{us} data is obtained, it will be possible to develop empirical correlations for preliminary estimates of S_{us} based on field and laboratory index tests.

4) Compare in situ S_{us} to driving shear stress τ_d. If $\tau_d > S_{us}$, a liquefaction failure is possible, and it must be determined whether a given earthquake can trigger the

failure. If $\tau_d < S_{us}$, a liquefaction failure is not possible. However, deformations may still occur as discussed in the next section.

5) A triggering analysis consists of determining whether the earthquake can cause an accumulation of strain that is sufficient to overcome the peak strength as in Fig. 9b. For details of a procedure for triggering analysis the reader is referred to Poulos et al 1985b.

Soils Subject to Driving Shear Stresses
Case [2]: Limited Deformation of Stable Mass

Cases of limited deformations induced by earthquakes are numerous. Perhaps the most prevalent are those referred to as lateral spreading in which a relatively gentle slope, often with incisions (e.g., rivers or canals) develops downhill movements. The zone of failure can range in size from tens to thousands of feet in the direction of the movement, and the movements themselves can range from a fraction of a foot to several feet. The movements are controlled by the behavior of weak soil layers, typically loose sands or silts. Often the movements occurred as a succession of slide movements starting in the proximity of the relatively steep slopes at the "incisions." Lateral spreading has been observed often as a result of major earthquakes, e.g., during the 1971 San Fernando earthquake (Youd 1971, 1973; Smith and Fallgren, 1973, the 1979 Imperial Valley earthquake (Youd and Bennett, 1983), the 1984 Alaska earthquake (McCulloch and Bonilla, 1970). Structures founded on the soils have been severely damaged, e.g., the Juvenile Hall in the 1971 San Fernando earthquake (Youd, 1973). The strength of the weak layer is reduced by the earthquake to its undrained steady state strength, S_{us}, as in the case of a flow slide. However, the reduced strength of the soil is sufficient to maintain stability, or in other words, the driving shear stresses are smaller than S_{us}. Thus the final stable configuration is similar to the one existing prior to the earthquake.

Other cases of limited deformation have been observed in earth dams, e.g., Hebgen Dam (Sherard et al, 1963); Infiernillo Dam (Resendiz et al, 1982); Coyote Dam (Bureau et al, 1984), and many others. In none of these cases did the deformations endanger the safety of the dams; however, one cannot assume that this will always be the case, since deformation can lead to cracking and in extreme cases to loss of freeboard.

The methods of deformation analysis that are presently available fall into three categories: a) stress analyses methods based on the results of cyclic laboratory tests, originally developed by Seed (1966), b) analyses based on the assumption that deformations are initiated only when the earthquake shear stresses tend to exceed the applicable shear strength of the soil, proposed by Newmark (1965), and c) analy-

tical procedures based on constitutive relationships derived from the results of laboratory cyclic and monotonic tests, e.g., Boukavalas et al, 1984.

The basic elements of the Newmark method, as applied to an embankment dam, are summarized in Fig. 12. For a potential failure wedge of soil, one defines the following:

1) The horizontal force that is required for a factor of safety of one against sliding determined from a pseudostatic stability analysis of a given wedge. The horizontal force is expressed as a fraction of the weight of the wedge and referred to as yield acceleration, N, in units of g (acceleration of gravity).
2) A time history of the acceleration of the "base" over which the wedge would slide during the design earthquake. The peak acceleration is designated as A, in units of g.

If the earthquake accelerations do not exceed the yield accelerations, the Newmark analysis indicates zero deformation. If the earthquake accelerations exceed the yield accelerations at various time intervals, deformations are initiated during those time intervals. The deformations are computed by integrating twice the earthquake minus the yield accelerations for those time intervals when that difference is

Fig. 12 - Principal Elements of Newmark's Method of Deformation Analysis

positive and for sufficient time when the difference is nega-
tive so that the final velocity is zero for each occurrence.
It should be noted that significant displacements (>10 cm)
are obtained only when the peak earthquake acceleration
exceeds the yield acceleration by factors of five or more.
This result is due to the fact that the time intervals when
the yield acceleration is exceeded are generally too short for
the mass of the wedge to move substantially unless the yield
acceleration is greatly exceeded.

Example of a Deformation Analysis

An example of of such an analysis is described below for the
lateral spreading that occurred at a site on Heber Road in the
Imperial Valley in southern California during a 1979 earth-
quake. The 1979 earthquake had a magnitude 6.6 and produced a
22-mile-long (35 km) surface rupture of the Imperial Fault
located about one mile (1.6 km) from the Heber Road site
(Bennett et al, 1981). Extensive investigations have been per-
formed at the Heber Road site by several organizations and have
included SPT borings, cone penetration tests, and shear wave
velocity measurements (Bennett, 1985; Bennett et al, 1981;
Sykora and Stokoe, 1982; Youd, 1985). The analysis described
herein was presented in GEI (1986). A cross section of the
lateral spreading area is presented in Fig. 13. The soil layer
responsible for the movements is Unit A2 consisting of a very
loose silty fine sand with about 20% fines. Cracking was
observed as shown in Fig. 13, and the horizontal displacements
at the road and canal were estimated to be 1.2 m (4 ft) and
2.1 m (7 ft), respectively.

The results of SPT and cone penetration tests in the
critical layer are shown in Fig. 14. From a depth of about 6
to 11 ft, the blowcounts range from 0 to 1 blows/ft and the
cone penetration resistance ranges mostly from about 5 to 15
kg/cm^2 (Bennett, 1985). Note that the blowcounts and cone
penetration resistance were measured after the 1979 earthquake
and thus correspond to a somewhat denser soil than at the time
of the earthquake, since densification of the soil occurred
when it reconsolidated as pore pressures dissipated immediately
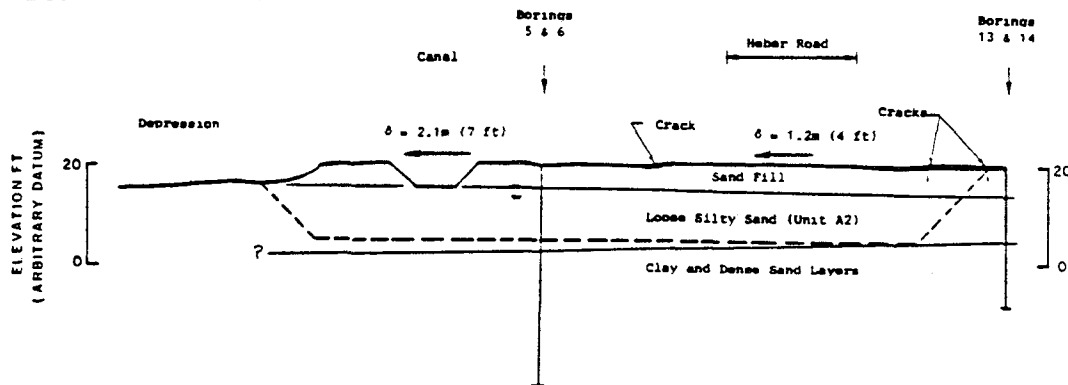after the earthquake.
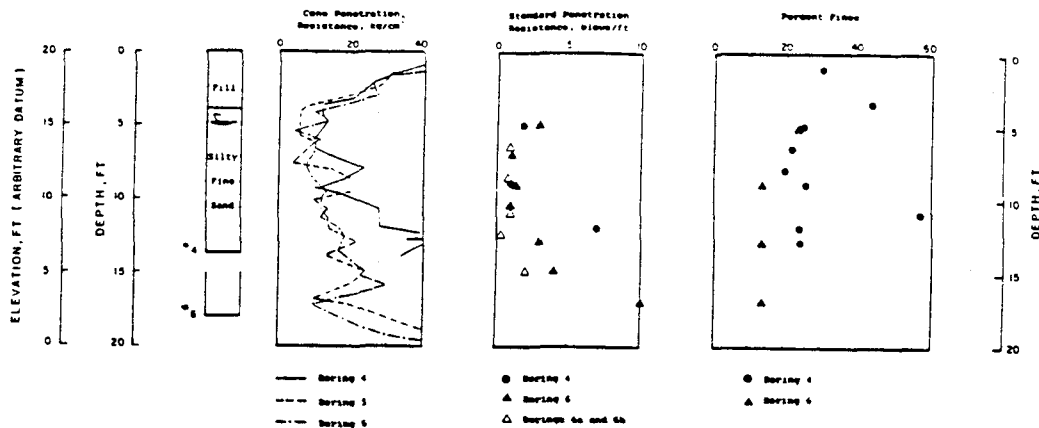

Fig. 13 - Heber Road Site, Cross Section

Fig. 14 - Heber Road Site, Soil Profile

Since the overall ground surface inclination at Heber Road is very gentle, the driving shear stresses in the soils involved are small, with a stability analysis indicating a value of about 40 psf. Because the driving shear stresses were small, the deformed mass was in equilibrium at the end of the earthquake. The mechanism of lateral spreading is one in which deformations of a stable mass accumulate during the earthquake as the soil accumulates strains under the repeated application of earthquake pulses superimposed on the static shear stresses. Thus a Newmark-type of analysis appears to be appropriate, since this type of analysis computes slope movements which are assumed to be initiated when the earthquake accelerations exceed the "yield acceleration" of the soil mass.

The average acceleration of the mass was computed using the program SHAKE with soil moduli obtained from cross hole seismic data by Skyora and Stokoe (1982). The earthquake record used for the analysis was obtained about 3.2 miles (5.2 km) from the southern terminus of the fault rupture at Bonds Corner and has a peak acceleration of 0.8 g. The Heber Road site is 1.0 mile (1.6 km) from the fault, and thus the record used for the analysis may represent somewhat less intense shaking than was actually experienced at Heber Road. The site of the Bonds Corner record is underlain by dense alluvium. In the analysis of the Heber Road site, the earthquake record was applied to the base of the loose sand, i.e., at the top of the denser underlying soil. The resulting acceleration of the mass that moved has a peak value, A, equal to 0.47 g.

The yield acceleration, N, was obtained from pseudostatic stability analyses for a sliding surface along the base of the mass that moved. The yield acceleration is defined as the horizontal acceleration (in units of g) which results in a factor of safety of one in the stability analysis. A sliding surface was selected to be consistent with the location of observed cracks, Fig. 13. The yield accelerations, N, were computed as a function of the yield strength, S_y, in the loose sand layer and are presented in Fig. 15.
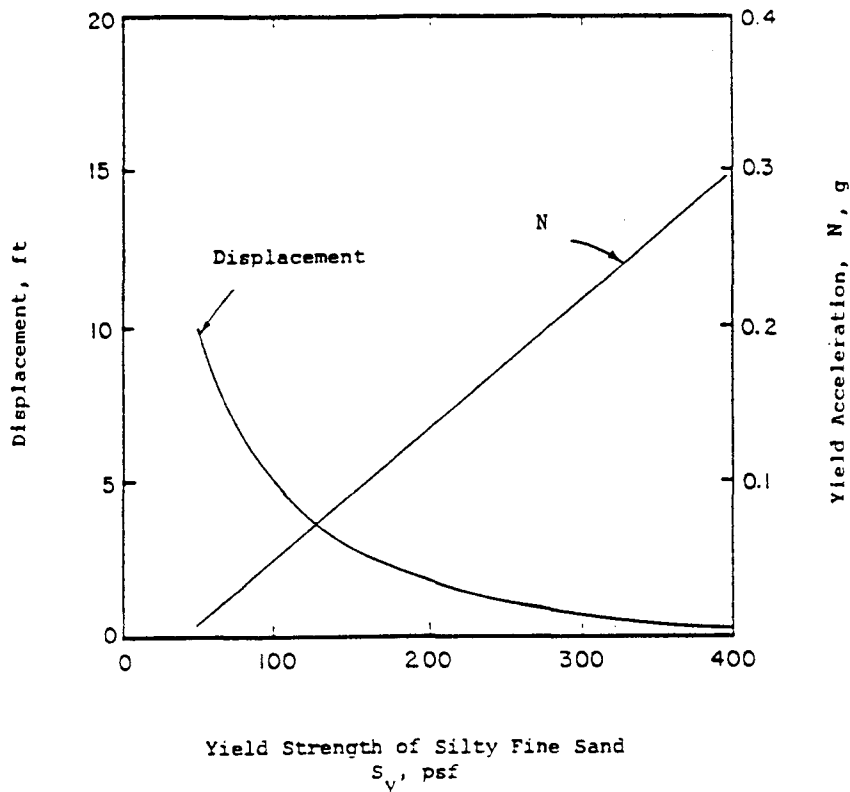
Yield Strength of Silty Fine Sand
S_y, psf

Fig. 15 - Heber Road Site, N vs S_y

The computed displacements for various assumed yield accelerations are shown in Fig. 15. The displacement computed using the Newmark procedure applies to the center of gravity of the moving mass. In the case of Heber Road site, the center of gravity moved about 5.5 ft (the average of the measured displacements at the road and at the canal of 4 and 7 ft, respectively). A displacement of 5.5 ft corresponds to a yield acceleration of 0.05 g and a yield strength of 100 psf, Fig. 15. This very low value of yield strength is consistent with the very loose condition of the soil as indicated by the measured blowcounts (SPT) of 0 to 1 and measured cone penetration resistances (CPT) of about 5 to 15 kg/cm^2. As noted before, the actual SPT and and CPT values at the time of the earthquake were probably even lower.

The Newmark analysis assumes that the soil has a rigid plastic type of behavior as shown by the dashed line in Fig. 16. The actual stress strain behavior is approximately as given by the solid line in Fig. 16. In sands the peak strength typically develops at strains of about 1 percent or less (Poulos, 1971; Castro et al, 1982) and the undrained steady state strength is reached at strains of a few percent. Thus it is reasonable to expect that the yield strength will be approximately equal to the undrained steady state strength (S_{us}) soon after the start of the earthquake, and thus it can be concluded that S_{us} in the silty sand at Heber Road is about

Fig. 16 - Actual and Idealized Stress Strain Behavior of
Silty Sand at Heber Road

equal to 100 psf. Note that the acceleration at the base of
the loose material was about 0.8 g which, if no yielding had
occurred, would have caused a peak shear stress of about 1,400
psf, i.e., much greater than S_{us}. Therefore, substantial
yielding did occur leading to the large displacements that
were observed. It should also be noted that the driving shear
stress of 40 psf is smaller than the backfigured strength of
100 psf, which is consistent with the assumed mechanism of
lateral spreading, i.e., that it is a case of limited (even
though potentially damaging) deformations and not one of
instability and flow (liquefaction) slide. The strength S_{us}
of 100 psf is much smaller than the drained strength which is
about 700 psf, corresponding to the effective normal stress of
about 1,200 psf and a friction angle of 30°. Thus the loose
silty sand is strongly contractive. The effective normal
stress in the sand during yielding at S_{us} is about 14%
(100/700) of the initial effective normal stress in the
failure plane of 700 psf. Thus yielding at S_{us} occurs under
high pore pressures, which is consistent with the observation
of sand blows in the area of the lateral spreading.

Note that if the sand had been dilative rather than
contractive, the yield strength would have been equal to at
least the drained strength. For the Heber Road case, the
drained strength is about 700 psf which corresponds to a yield
acceleration, N, of about 0.5 g from an extrapolation of the
data in Fig. 15. Since the peak acceleration for the overbur-
den is also about 0.5 g, the deformations would have been
negligible. Thus lateral spreading is only observed when
loose contractive sands or silts are present, which yield
under low S_{us} values and corresponding high pore pressures.
These high pore pressures lead to the development of sand

-28-

blows under favorable stratification, see discussion in Part I of this paper.

CONCLUDING REMARKS

Three different aspects of soil behavior under earthquake loading were discussed in this paper, namely, sand blows, flow (liquefaction) slides and lateral spreading. Their physical mechanisms were discussed and methods of investigation were presented that are consistent with the physical mechanisms. The main characteristics of the three phenomena are presented in Fig. 17, which shows the difference between their physical mechanisms.

The soil properties that control the occurrence of sand blows are a) shear modulus, which determines cyclic strain and thus pore pressure increase and b) permeability and compressibility, which control the flow conditions that determine whether sand blows occur.

	Sand Blows Settlements of Level Ground	Flow Slides- Liquefaction	Limited Deformation- Lateral Spreading
Driving Shear Stresses, τ_d	No	Yes	Yes
Undrained Steady State Strength, S_{us}	Not a factor	$\tau_d > S_{us}$	$\tau_d < S_{us}$
Role of Earthquake Stresses, τ_e	Increase pore pressure	Triggers failure	Accumulates deformation if $\tau_e + \tau_d > S_{us}$
Stress Strain Behavior	Not relevant		
Controlling Soil Properties	Shear modulus permeability, compressibility	Undrained Steady State Strength	Undrained Steady State Strength

Fig. 17 - Main Characteristics of Three Induced Earthquake Phenomena

Flow slides and lateral spreading, on the other hand, are controlled by the value of the undrained steady state strength, S_{us}. Flow slides occur only when S_{us} is lower than the driving shear stress, τ_d, while otherwise only limited deformations are possible. Flow slides are triggered by an earthquake when the accumulated deformations are sufficient to overcome the peak strength of the soil. For sands and nonplastic silts, the shear strains needed to trigger the failure are small, typically of about 1%. For plastic clays these strains are very large, and therefore, seismically induced liquefaction failures in plastic clays are unlikely to occur (Poulos et al, 1985b).

-29-

Limited deformations occur when $S_{us} > \tau_d$ and are generally large only when the sum of driving (static) and earthquake shear stresses exceed the yield strength of the soil, S_y. In sands and nonplastic silts, the undrained steady state strength, S_{us}, is reached at low strains and thus the yield strength, S_y is approximately equal to S_{us} whenever significant deformations occur.
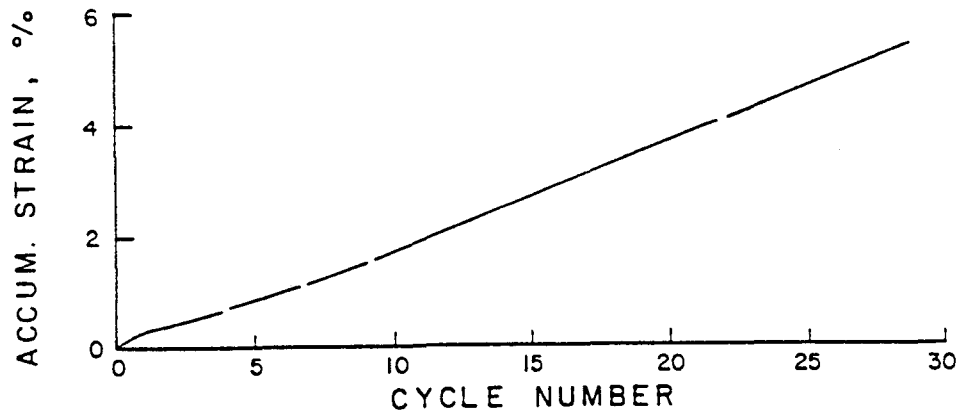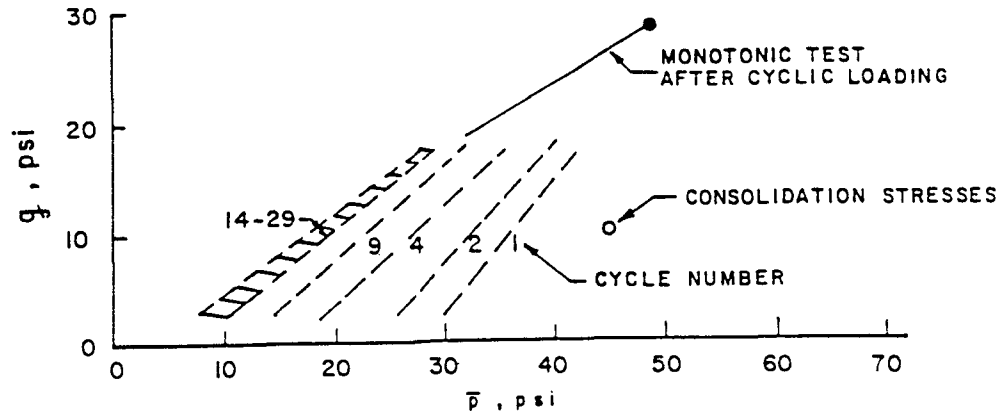

Fig. 18 - Results of Typical Cyclic Triaxial Test on a Medium Dense Silty Sand

The occurrence of sand blows, flow slides, and lateral spreading are associated with high pore pressures in loose contractive sands and silts. The physical significance of the pore pressure increase is, however, quite different for each of these cases. Sand blows develop as the result of water flow caused by the pore pressure increase. In flow slides and lateral spreading cases, S_{us} controls behavior. Pore pressure prior to flow is not relevant to S_{us} nor to deformations. This point is illustrated in Fig. 18 by means of a cyclic load test on a silty sand. The q - p plot shows that the stress path reaches the strength envelope in about cyclic 14, and then from cyclic 14 to 29 it moves up and down along the envelope. The pore pressure that causes the stress path to reach the envelope has been often defined as failure. However, no failure occurs because the strength S_{us} is given by the steady state and it

exceeds the consolidation (static) shear stress. The rate of accumulation of strain per cyclic shows no change after cycle 14, e.g., after the stress path reaches the envelope. Thus a pore pressure increase that causes the soil to reach the strength envelope has no bearing on either the strength of the soil nor the rate of strain accumulation, i.e., the two aspects of behavior that are of engineering significance. The same statement applies to the case in which the pore pressure may reach a value of 100% when the soil is momentarily under zero shear stress.

There has been rapid progress in the last two decades towards a better understanding of the behavior of soils under seismic loading. The author believes that further progress can only be achieved through careful investigations of actual sites and earth structures that have been shaken by earthquakes. Particular attention should be given to the deformations that can occur in earth structures that remain stable during and after the earthquake.

The field observations will provide useful information only to the degree to which one can understand the physical mechanisms behind the observed phenomena. H. Poincare's eloquent advice is relevant to this question.

> "Le savant doit ordonner; on fait la science avec des faits comme une maison avec des pierres; mais une accumulation de faits n'est pas plus une science qu'un tas de pierres n'est une maison."

> (The scientist must organize; science is built with facts just as a house is built with bricks; but an accumulation of facts isn't science, just as a pile of bricks isn't a house.)

REFERENCES

1. Bennett, M. J. (1985) personal communication.
2. Bennett, M. J.; Youd, T, L.; Harp, E. L., and Wieczorek, G. F. (1981) "Subsurface Investigation of Liquefaction, Imperial Valley Earthquake, California, October 15, 1979," U.S. Geological Survey Open File Report 81-502.
3. Bureau, G.; Tepel, R. E.; and Volpe, R. L. (1984) "Performance of Embankment Dams During the Morgan Hill Earthquake of 24 April 1984," USCOLD Newletter, July 1984.
4. Boukavalas, G., Whitman, R. V. and Maw, W. A. (1984) "Permanent Displacement of Sand with Cyclic Loading," Journal of Geotechnical Engineering, ASCE, Vol. 110, No. 11, November.
5. Casagrande, A. (1936) "Characteristics of Cohesionless Soils Affecting the Stability of Slopes and Earth Fills," Journal of the Boston Society of Civil Engineers, reprinted in Contributions to Soil Mechanics, 1925 to 1940, Boston Society of Civil Engineers, Oct. 1940, pp. 257-276.

6. Casagrande, A. (1975) "Liquefaction and Cyclic Deformation in Sands--A Critical Review," **Proceedings of the Fifth Pan American Conference on Soil Mechanics and Foundation Engineering**, Buenos Aires, Argentina; also published as **Harvard Soil Mechanics Series No. 88**, January 1976, Harvard University, Cambridge, Massachusetts.

7. Casagrande, A., and Rendon, F. (1978) "Gyratory Shear Apparatus Design, Testing Procedures, and Test Results on Undrained Sand," Technical Report S-78-15, U.S. Army Corps of Engineers, Waterways Experiment Station, Vicksburg, Mississippi; also published as **Harvard Soil Mechanics Series No. 89**, Harvard University, Cambridge, Massachusetts.

8. Castro, G. (1968) "Laboratory Investigation on Undisturbed Samples of Subsoils for the CONOX Project," Report to Compania de Acero del Pacifico, Harvard University, Cambridge, Massachusetts.

9. Castro, G. (1969) "Liquefaction of Sands," thesis presented to Harvard University in fulfillment of the requirements for the degree of Doctor of Philosophy.

10. Castro, G. (1975) "Liquefaction and Cyclic Mobility of Saturated Sands," **Journal of the Geotechnical Engineering Division**, ASCE 101 (GT6) pp. 551-569.

11. Castro, G.; Poulos, S. J.; France, J. W., and Enos, J. L. (1982) "Liquefaction Induced by Cyclic Loading," Report to National Science Foundation, Geotechnical Engineers Inc., Winchester, Massachusetts.

12. Castro, G.; Poulos, S. J., and Leathers, F. D. (1985) "A Re-examination of the Slide of the Lower San Fernando Dam," **Journal of Geotechnical Engineering**, ASCE 111 (GT9).

13. Castro, G.; Keller, T. O., and Boynton, S. S. (1987) "Re-evaluation of the 1971 Slide in the Lower San Fernando Dam," Report to U.S. Corps of Engineers, in preparation.

14. Chang, C. S.; Kuo, C. L., and Selig, E. T. (1983) "Pore Pressure Development During Cyclic Loading," **Journal of Geotechnical Engineering**, ASCE 109 (1) pp. 103-107.

15. De Alba, P.; Seed, H. B., and Chan, C. K. (1976) "Sand Liquefaction in Large-Scale Simple Shear Tests," **Journal of the Geotechnical Engineering Division**, ASCE 102 (GT9) pp. 909-927.

16. Dobry, R.; Ladd, R. S.; Yokel, F. Y.; Chung, R. M., and Powell, D. (1982) "Prediction of Pore Water Pressure Buildup and Liquefaction of Sands During Earthquakes by the Cyclic Strain Method," **Building Science Series 138**, National Bureau of Standards, U.S. Department of Commerce, U.S. Governmental Printing Office, Washington, D.C.

17. Finn, W. D. L.; Bransby, P. L.; and Pickering, D. J. (1970) "Effect of Strain History on Liquefaction of Sands," **Journal of the Soil Mechanics and Foundations Division, ASCE** 96 (SM6) pp. 1917-1934.

18. Florin, V. A. and Ivanov, P. L. (1961) "Liquefaction of Saturated Sandy Soil," Proc. 5th ICSMFE, Paris.

19. Geotechnical Engineers Inc. (1986) "Seismic Deformation Analysis, Pinopolis West Dam," Report to U.S. Corps of Engineers, April 1986.

20. Gilbert, P. A. (1984) "Investigation of Density Variation in Triaxial Test Specimens of Cohesionless Soil Subjected to Cyclic and Monotonic Loading," Technical Report GL84-10, Department of the Army, U.S. Army Corps of Engineers, Washington, D.C.

21. Hazen, A. (1920), "Hydraulic Fill Dams," **ASCE Transactions**, Vol. 83, pp. 1713-1745.

22. Hedberg, J. (1977) "Cyclic Stress-Strain Behavior of Sand in Offshore Environment," Ph.D. thesis, Department of Civil Engineering, Massachusetts Institute of Technology, Cambridge, Massachusetts.

23. Housner, G. W. (1958) "The Mechanism of Sand Blows," **Bulletin of the Seismological Society of America**, No. 58 pp. 155-161.

24. Ishibashi, I.; Kawamura, M., and Bhatia, S. (1985) "Effect of Initial Shear on Cyclic Behavior of Sand," **Journal of Geotechnical Engineering**, Vol. 111, No. 12, December.

25. Ishihara, K., and Yasuda, S. (1975) "Sand Liquefaction in Hollow Cylinder Torsion Under Irregular Excitation," **Soils and Foundations** 15(1) pp. 45-59.

26. Ishihara, K. and Yamazaki, F. (1980) "Cyclic Simple Shear Tests on Saturated Sand in Multi-Directional Loading," **Soils and Foundations, Japanese Society of Soil Mechanics and Foundation Engineering** 20(1) pp. 45-59.

27. Ishihara, K.; Shimizu, K., and Yamada, Y. (1981) "Pore Water Pressures Measured in Sand Deposits During an Earthquake," **Soils and Foundations**, Vol. 21(4) pp. 85-100.

28. Ishihara, K. (1984) "Post-Earthquake Failure of a Tailings Dam Due to Liquefaction of the Pond Deposit," in **Proceedings of the International Conference on Case Histories in Geotechnical Engineering**, Vol. 3, pp. 1129-1143, University of Missouri, Rolla, Missouri.

29. Ladd, R. S. (1977) "Specimen Preparation and Cyclic Stability of Sands," **Journal of the Geotechnical Engineering Division, ASCE** 103(GT6):535-547.

30. Lee, K. L. and Seed, H. B. (1967) "Cyclic Stress Conditions Causing Liquefaction of Sand," **Journal of the Soil Mechanics and Foundations Division, ASCE**, Vol. 93, No. SM1, pp. 47-70.

31. McCulloch, D. S. and Bonilla, M. G. (1970) "Effects of the Earthquake of March 27, 1964, on the Alaska Railroad," U.S. Geological Survey Prof. Paper 545-D.

32. National Research Council (1985) "Liquefaction of Soils During Earthquakes." National Academy Press, Washington, D.C.

33. Newmark, N. M. (1965) "Effects of Earthquakes on Dams and Embankments," Fifth Rankine Lecture, **Geotechnique**, London, England, Vol. 15, No. 2, pp. 139-159.

34. Ohsaki, Y. and Iwasaki, R. (1973) "On Dynamic Shear Moduli and Poisson's Ratio of Soil Deposits," **Soils and Foundations**, Vol. 13, No. 4, Tokyo, Japan, pp. 61-715.

35. Peacock, W. H. and Seed, H. B. (1968) "Sand Liquefaction Under Cyclic Loading Simple Shear Conditions," Journal of the Soil Mechanics and Foundations Division, ASCE, 94(SM3) pp. 689-708.

36. Poulos, S. J. (1971) "The Stress-Strain Curves of Soils," Geotechnical Engineers Inc., Winchester, Massachusetts, pp. 1-80.

37. Poulos, S. J. (1981) "The Steady State of Deformation," Journal of the Geotechnical Engineering Division, ASCE, Vol. 107, No. GT5, pp. 553-562.

38. Poulos, S. J.; Castro, G., and France, J. W. (1985) "Liquefaction Evaluation Procedure," Journal of Geotechnical Engineering, ASCE 111(6) pp. 772-791.

39. Poulos, S. J.; Robinsky, E. I., and Keller, T. O. (1985b) "Liquefaction Resistance of Thickened Tailings," Journal of Geotechnical Engineering, ASCE, Vol. III, No. 12, December 1985.

40. Resendiz, D.; Romo, M., and Moreno, E. (1982) "El Infiernillo and La Villita Dams: Siesmic Behavior," Journal of The Geotechnical Engineering Division, ASCE, Vol. 108, No. GT1, January 1982.

41. Robertson, P. K. and Campanella, R. G. (1983) "Interpretation of Cone Penetration Tests," Parts I and II, Canadian Geotechnical Journal, Vol. 20, No. 4, 1983, pp. 718-745.

42. Robertson, P. K. and Campanella, R. G. (1985) "Liquefaction Potential of Sands Using the CPT," Journal of Geotechnical Engineering, ASCE 111(GT3):384-403.

43. Schofield, A. N. and Wroth, C. P. (1968) Critical State Soil Mechanics, McGraw-Hill Book Company, New York, New York.

44. Schofield, A. (1985) personal communication.

45. Scott, R. F. Zuckerman, K. A. (1973) "Sand Blows and Liquefaction," in The Great Alaskan Earthquake of 1964—Engineering Volume, Committee on the Alaska Earthquake, Division of Earth Sciences, National Research Council, National Academy of Sciences, Washington, D.C., pp. 179-189.

46. Seed, H. B. (1966) "A Method for Earthquake Resistant Design of Earth Dams," Journal of the Soil Mechanics and Foundation Division, ASCE, Vol. 92, No.SM1, pp. 13-41, January 1966.

47. Seed, H. B. (1976) "Evaluation of Soil Liquefaction Effects on Level Ground During Earthquakes," pp. 1-104 in Liquefaction Problems in Geotechnical Engineering, ASCE Preprint 2752, presented at the ASCE National Convention, Philadelphia, Pennsylvania, ASCE, New York, New York.

48. Seed, H. B.; Wong, R. T.; Idriss, I. M., and Tokimatsu, K. (1986) "Moduli and Damping Factors for Dynamic Analyses of Cohesionless Soils," Journal of Geotechnical Engineering, ASCE, Vol. 112, No. 11, November 1986.

49. Seed, H. B. (1979) "Considerations in the Earthquake-Resistant Design of Earth and Rockfill Dams," *Geotechnique* 29(3) pp. 213-263.

50. Seed, H. B.; Lee, K. L.; Idriss, I. M., and Makdisi, F. I. (1975) "The Slides in the San Fernando Dams During the Earthquake of February 9, 1971," *Journal of the Geotechnical Engineering Division*, ASCE, 101(GT7) pp. 651-688.

51. Seed, H. B.; Tokimatsu, K.; Harder, L. F., and Chung, R. M. (1984) "The Influence of SPT Procedures in Soil Liquefaction Resistance Evaluations," Report No. UBC/EERC-84/15, Earthquake Engineering Research Center, University of California, Berkeley, California.

52. Seed, H. B. and Lee, K. L. (1966) "Liquefaction of Saturated Sands During Cyclic Loading," *Journal of the Soil Mechanics and Foundations Division*, ASCE, Vol. 92, No. SM6, pp. 105-134.

53. Sherard, J. L.; Woodward, R. J.; Gizienski, S. F., and Clevenger, W. A. (1963) *Earth and Earth-Rock Dams*, John Wiley and Sons, Inc.

54. Silver, M. L. and Seed, H. B. (1971) "Volume Changes in Sands During Cyclic Load," *Journal of the Soil Mechanics and Foundations Division*, ASCE, 97(SM9) pp. 1171-1182.

55. Smith, J. L. and Fallgren, R. B. (1973) "Ground Displacement at San Fernando Juvenile Hall and Sylmar Converter Station," *San Fernando, California, Earthquake of February 9, 1971*, U.S. Department of Commerce, National Oceanographic and Atmospheric Administration.

56. Stokoe, K. H. and Hoar, R. J. (1978) "Variables Affecting In-Situ Seismic Measurements," pp. 913-939 in Proceedings of the ASCE Geotechnical Engineering Division Specialty Conference on Earthquake Engineering and Soil Dynamics, Vol. 2, ASCE, New York, New York.

57. Sykora, D. W. and Stokoe, K. H. (1982) "Seismic Investigation of Three Heber Road Sites After the October 15, 1979 Imperial Valley Earthquake," *Geotechnical Engineering Report GR82-24*, University of Texas, Austin.

58. Tatsuoka, F.; Sasaki, T., and Yamada, S. (1984) "Settlement in Saturated Sand Induced by Cyclic Undrained Simple Shear," *Proceedings, 8th World Conference on Earthquake Engineering*, San Francisco, Vol. 3, pp. 95-102, July 1984.

59. Tokimatsu, K. and Yoshimi, Y. (1983) "Empirical Correlation of Soil Liquefaction Based on SPT N-Value and Fines Content," *Soils and Foundations, Japanese Society of Soil Mechanics and Foundation Engineering* 23(4) pp. 56-74.

60. Whitman, R. V. (1971) "Resistance of Soil to Liquefaction and Settlement," *Soils and Foundation*, Vol. 11, No. 4.

61. Whitman, R. V. (1985), "On Liquefaction" Eleventh ICSMFE, San Francisco, August.

62. Yoshimi, Y.; Tokimatsu, K.; Kaneko, O., and Makihara, Y. (1984) "Undrained Cyclic Shear Strength of a Dense Niigata Sand," *Soils and Foundations, Japanese Society of Soil Mechanics and Foundation Engineering* 24(4) pp. 131-145.

63. Yoshimi, Y., Kuwabara, F., and Tokimatsu, K. (1975) "One-Dimensional Volume Change Characteristics of Sands Under Very Low Confining Stresses," Soils and Foundations, Vol. 15, No. 3, September 1975, pp. 51-60.

64. Youd, T. L. (1971) "Landsliding in the Vicinity of the Van Norman Lakes," The San Fernando California Earthquake of February 9, 1971, U.S. Geological Survey Prof. Paper 733, p. 105-109.

65. Youd, T. L. (1972) "Compaction of Sands by Repeated Straining," Journal of the Soil Mechanics and Foundations Division, ASCE 98(SM7) pp. 709-725.

66. Youd, T. L. (1973) "Ground Movements in the Van Norman Lake Vicinity," San Fernando, California Earthquake of February 9, 1971, U.S. Department of Commerce, National Oceanographic and Atmospheric Administration.

67. Youd, T. L. and Bennett, M. J. (1983) "Liquefaction Sites, Imperial Valley, California," Journal of Geotechnical Engineering, ASCE, Vol. 109, No. 3, March.

68. Youd, T. L. (1985) personal communication.

U.S. DEPARTMENT OF COMMERCE
Technology Administration
National Technical Information Service
Springfield, VA 22161   (703) 487-4650